Organic Iron-binding ligands
in the Arctic, Antarctic, and sub-tropical regions

Indah Ardiningsih

Members of the reading committee:

Prof. dr. A.G.J. (Anita) Buma, University of Groningen

Dr. H. Whitby, University of Liverpool

Dr. K. Soetaert, NIOZ Royal Netherlands Institute for Sea Research

Dr. L. M. Laglera, Universitat de les Illes Balears

Prof. dr. J. B. M. Middelburg, Utrecht University

Cover design Indah Ardiningsih

Printed by ProefschriftMaken

ISBN: 978-90-6266-602-7

USES Series: 235

Organic Iron-binding ligands in the Arctic, Antarctic and subtropical regions

Ligan organik pengikat besi di kawasan laut Arktik, laut Antartika dan laut daerah subtropis

(dengan ringkasan bahasa Indonesia)

Organische ijzerbindende liganden in de arctische, antarctische en subtropische gebieden

(met een samenvatting in het Nederlands)

Proefschrift

ter verkrijging van de graad van doctor aan de
Universiteit Utrecht
op gezag van de
rector magnificus, prof.dr. H.R.B.M. Kummeling,
ingevolge het besluit van het college voor promoties
in het openbaar te verdedigen op
vrijdag 3 september 2021 des morgens te 10.15 uur

door

Indah Ardiningsih

geboren op 26 juli 1988
te Pasuruan, Indonesië

Promotor:

Prof. dr. G.J. Reichart

Copromotoren:

Dr. R. Middag
Dr. L.J.A Gerringa

This thesis was (partly) made possible with financial support from Indonesia Endowment Fund for Education (LPDP).

Contents

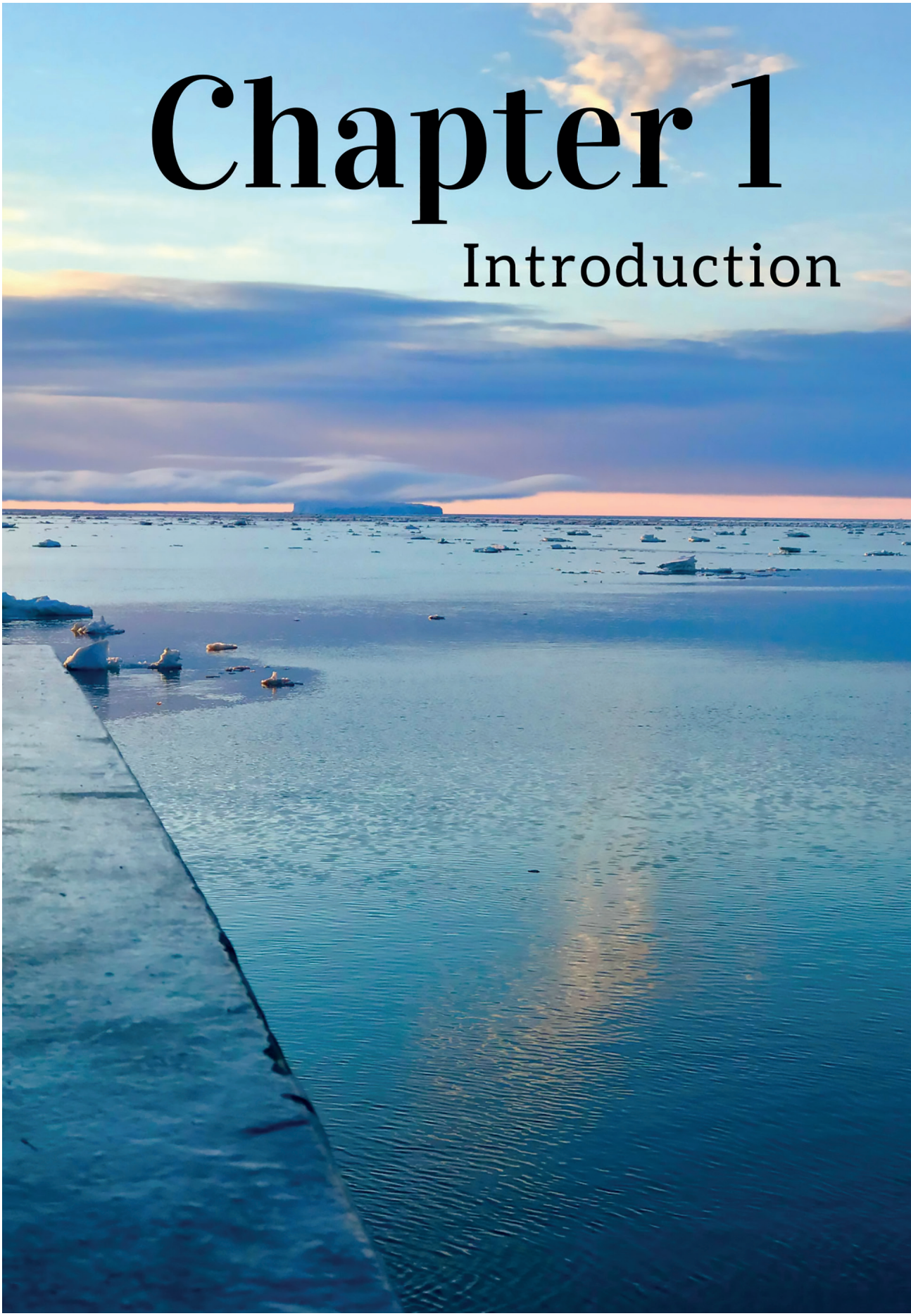

Chapter 1

Introduction

1. Introduction

1.1 Iron (Fe) in the marine environment

Global climate change has a profound influence on the environment, and hence also has substantial influence on trace metal cycling in the ocean. Some of these trace metals are essential micronutrients for marine life and influence the dynamics of the marine ecosystem. One of this bio-essential trace is iron (Fe). This micronutrient plays an essential role in multiple metabolic pathways within phytoplankton cells (Sunda, 2012; Sunda et al., 1995; Timmermans et al., 2005), including photosynthesis, respiration, and nitrogen fixation (Geider et al., 1994). Dissolved-Fe (DFe) is present at trace levels in seawater since it has low solubility (Millero, 1998; Turner et al., 2001) and there are limited sources of Fe to open ocean. As a result, Fe can become a limiting micronutrient for marine primary producers (de Baar, 1990; Martin et al., 1988; Rijkenberg et al., 2018). Limitation by Fe has widely been observed in high-nutrient low chlorophyll (HNLC) regions such as the Southern Ocean, an area where relatively low phytoplankton biomass is found despite ample availability of major nutrients (de Baar, 1990; Kinsey et al., 2016; Klunder et al., 2011; Schoffman et al., 2016). Seasonal Fe limitation has also been reported elsewhere (i.e (Moore et al., 2013; Nielsdóttir et al., 2009; Ryan-Keogh et al., 2018; Sedwick et al., 2000), including in the north Atlantic Ocean (Achterberg et al., 2018; Hopwood et al., 2018).

In seawater, Fe is present in dissolved and particulate fractions (Boyd, 2013; Wu et al., 2001). The DFe fraction is operationally defined as passing a 0.2- or 0.4-µm filter (0.2-µm filter was used for filtration in this study), whereas the particulate (PFe) fraction is >0.4-µm. The DFe fraction consists of inorganic complexes and organic complexed-Fe and can be further divided into colloidal Fe (>0.02 µm to <0.2 µm) and soluble Fe (<0.02m). As water ages, the soluble Fe can be converted into colloidal Fe. Coalescence of colloidal Fe can lead to the formation of PFe, and vice versa, the release of DFe is also possible from the breakdown of PFe

fraction. The process involving physical transformation of the DFe fraction into the PFe fraction is known as scavenging, which involves adsorption and aggregation (Boyd et al., 2010b). The scavenging process results in the formation of PFe fraction, this fraction is less bioavailable.

Concentrations of DFe in the ocean are strongly dependent on the balance between supply and removal processes including chemical, physical and biological processes in the marine environment. Multiple sources of Fe contribute to the global DFe concentration in the open ocean, such as from atmospheric dust deposition, coastal and shallow reductive dissolution, hydrothermal fluxes and sea ice and glaciers. The major removal pathways are biological uptake, scavenging and sedimentation (Boyd, 2013; Boyd and Ellwood, 2010b; Boyle et al., 1977; Bruland et al., 2014). In summary, the biogeochemical cycle of Fe in the ocean involves a complex interaction between Fe input, biological uptake, scavenging, remineralization and sedimentation. Each of these aspects in the Fe biogeochemical cycle are influenced by natural Fe-binding organic ligands since more than 99% of the DFe in seawater is strongly bound by organic ligands (Boye et al., 2001; Gledhill et al., 2012; van den Berg, 1995).

The presence of organic ligands – a mixture of organic molecules with a high affinity to Fe – enhances the solubility of Fe in seawater (Gledhill et al., 1994; Liu et al., 2002; Millero, 1998). This idea complements the model by Millero (1998) that calculated the solubility of Fe(III) in seawater as a function of pH. Fe(III) solubility is increased by up to 32 – 65% at pH 8.1 when the formation of Fe-organic complexes is considered in the model (Kuma et al., 1996). Field measurements (e.g. (Ardiningsih et al., 2020; Laglera et al., 2009; Lannuzel et al., 2015; Rue et al., 1997), experimental studies (e.g. (Buck et al., 2010; Laglera et al., 2019b) and modelling effort (e.g. (Völker et al., 2015) over the last two decades have demonstrated that organic ligands determine the threshold of DFe concentrations in seawater, pointing out the importance of organic ligands in maintaining Fe in the dissolved fraction in seawater (e.g. (Hunter et al., 2007; Johnson et al., 1997; Lauderdale et al., 2020; Lohan et al., 2015). In this thesis the dissolved fraction will be studied and discussed in relation to the presence of dissolved organic ligands.

1.2 DFe speciation in seawater

The speciation of DFe comprises the different chemical species of DFe existing in seawater. DFe can exist in two different oxidation states, Fe(II) or Fe(III), as free metal ions or complexed with inorganic or organic ligands. In seawater under oxic conditions and natural pH, the solubility of DFe is determined by Fe(III) as the dominant species (Liu and Millero, 2002; Millero, 1998). The inorganic Fe species denotes the inorganic complexation of Fe which is dominated by the hydroxide complexes (i.e. $[Fe(OH)]^{2+}$, $[Fe(OH)_2]^{+}$, $[Fe(OH)_3]^{0}$, $[Fe(OH)_4]^{-}$) at normal seawater pH of ~8.0 – 8.1 under oxic conditions (Byrne et al., 1988; Hudson et al., 1992; Millero et al., 1995). Thermodynamic models predict that main inorganic DFe species at seawater pH is in the form of $[Fe(OH)_3]^{0}$, which is prone to undergo further hydrolysis and subsequent precipitation (Millero et al., 1995).

The organic DFe speciation refers to the chelation of DFe with organic molecules. Due to the strong affinity of Fe for natural occurring organic ligands, Fe forms strong Fe-ligand complexes in seawater, increasing the Fe solubility and the residence time of DFe (Gerringa et al., 2015). Increasing residence times enable the potential transport of Fe as DFe (Boye et al., 2001; Rijkenberg et al., 2008a) and increases the potential availability for uptake by planktonic assemblages. Understanding the processes controlling the dynamics of natural organic ligands is of fundamental importance toward a better understanding of biogeochemical cycle of Fe in the ocean.

1.3 Dissolved organic Fe-binding ligands

1.3.1 Sources and sinks of Fe-binding ligands

Studies into the organic complexation of Fe showed the tight coupling between DFe and its organic complexes (e.g (Boyd, 2013; Boye et al., 2006; Buck et al., 2007a; Gerringa et al., 2015; Kleint, 2016), suggesting

that sources of Fe-binding ligands are linked to most Fe sources (Bennett et al., 2008). The organic ligands in seawater either have a marine or terrestrial origin. The organic ligands with marine origin come from *in situ* biological activities. These biological-sourced ligands include ligands actively produced by marine microbes as a strategy to get Fe (i.e. siderophores; e.g. (Soria-Dengg et al., 2001; Velasquez et al., 2016), and also passively generated by microbial degradation of organic matter (Decho et al., 2017), cell excretion (Hassler et al., 2011), grazing (Laglera et al., 2019b; Sato et al., 2007) and viral lysis (Slagter et al., 2016) (i.e. polysaccharides). Lithogenic inputs found within the boundary region between land and sea (i.e coastal seas and estuaries) often supply ligands from terrestrial origin (Batchelli et al., 2010; Buck and Bruland, 2007a; Buck et al., 2007b; Bundy et al., 2015; Gerringa et al., 2007; Kondo et al., 2007; Laglera and van den Berg, 2009). Bottom sediment resuspension (Buck and Bruland, 2007a; Bundy et al., 2014) and hydrothermal vents (Bennett et al., 2008; Hawkes et al., 2013; Kleint et al., 2016; Sander et al., 2011b) are also reported to supply ligands. High concentrations of organic ligands up to μM level have been observed in a hydrothermal vent field, suggesting a source of Fe-binding ligands near the hydrothermal vent field (Kleint et al., 2016). Downwind of dry land areas, dust deposition is an important source of Fe for the open ocean and dust might also be responsible for the supply of Fe-binding ligands in surface water, promoting dust-Fe solubility (Fitzsimmons et al., 2015; Paris et al., 2013). In the Antarctic and Arctic Oceans melt of land-ice (i.e glaciers) and sea-ice (Genovese et al., 2018; Lannuzel et al., 2015) is an additional source of organic ligands.

The concentration of Fe-binding ligands in seawater is a result of the dynamics of supply and loss (Figure 1-1). Loss of organic ligands is related to degradation and downward export fluxes of organic carbon, i.e. aggregation and sinking with particles (Gledhill and Buck, 2012). Remineralization is thought to be a removal pathway of organic ligands too, since concentrations of organic ligands tend to decrease with depth (*e.g.* (Buck et al., 2015; Gerringa et al., 2015). In contrast, viral lysis (Poorvin et al., 2011; Slagter et al., 2016) and grazing (Laglera et al.,

2019b; Sato et al., 2007) in the ocean interior are sources of organic ligands in the water column (Figure 1-1). The chemical transformation of ligands due to solar irradiance or mediated by biological activities can result in both supply and loss of ligands to the water column, hence called internal recycling of organic ligands. Photochemical degradation of organic ligands, for example, can cause loss of Fe-binding ligands, decreasing the total ligand concentration in surface water. Photochemistry can also result in the chemical transformation of a strong ligand into a weaker ligand (Barbeau et al., 2001; Hassler et al., 2020). The biologically mediated internal recycling is illustrated by the production of a weaker ligand in remineralization experiments (Boyd and Ellwood, 2010b; Bundy et al., 2016; Hunter and Boyd, 2007; Velasquez et al., 2016). Furthermore, weaker ligands exist predominantly deeper in the water column. These ligands are typically formed by microbial remineralization or as breakdown products of stronger ligands (Boyd and Ellwood, 2010b; Buck et al., 2015; Hunter and Boyd, 2007).

1.3.2 Properties of Fe-binding organic ligands

Dissolved organic Fe-binding ligands are part of dissolved organic matter (DOM) and are still poorly characterized (Gledhill and Buck, 2012; Gledhill and van den Berg, 1994; Hassler et al., 2017; Rue et al., 1995), known as ‘a ligand soup’. Characterization of organic ligands in seawater is quite challenging, since these ligands are of unknown composition, of diverse chemical nature and are typically present at low concentrations. However, the current knowledge on the identity of ligands defines a broad range of Fe-binding ligands from low molecular weight (i.e. siderophores) up to macromolecular compounds (i.e. so-called humic substances and polysaccharides) with the characteristics of ligands often being defined by their origin. The different ligand types are explained each in more detail below.

The low molecular-weight compounds include siderophores or siderophore-like compounds (Boiteau et al., 2016; Boiteau et al., 2019; Macrellis et al., 2001; Mawji et al., 2008; Velasquez et al., 2016).

Siderophores are small organic molecules synthesized by certain heterotrophic bacteria (e.g., cyano-bacteria) as part of an Fe acquisition mechanism (Butler, 2005; De Serrano et al., 2016; Mawji et al., 2008). The siderophore ligands are thought to represent the strongest Fe-binding ligand group (Butler, 2005; Mawji et al., 2008), although they are often present at picomolar level and thus their contribution to the total ligand pool being rather limited (Boiteau et al., 2019; Bundy et al., 2018).

Humic substances (HS) and HS-like substances, represent a large component of the Fe-binding ligand pool. HS ligands occur throughout the ocean (Batchelli et al., 2010; Krachler et al., 2015; Laglera et al., 2019a; Laglera and van den Berg, 2009; Slagter et al., 2019; Su et al., 2018), and have been shown to comprise a large fraction of the Fe-binding ligand pool in the water column (Whitby et al., 2020). HS-like compounds have also been shown to provide the Fe-binding ligands in biologically refractory deep ocean dissolved organic matter (Hassler et al., 2020). In fact, HS ligands are typically derived from degradation of terrestrial organic matter (e.g. (Dulaquais et al., 2018; Krachler et al., 2015; Laglera et al., 2007), although marine HS (HS-like) can be produced *in situ* by microbial decomposition, remineralization and grazing (Laglera et al., 2019b; Sato et al., 2007; Whitby et al., 2020). The HS ligands with a strong terrestrial component mainly occur in the ocean-coastal margin and near estuaries (Batchelli et al., 2010; Buck and Bruland, 2007a; Gerringa et al., 2007; Laglera et al., 2007; Laglera et al., 2019a; Slagter et al., 2017).

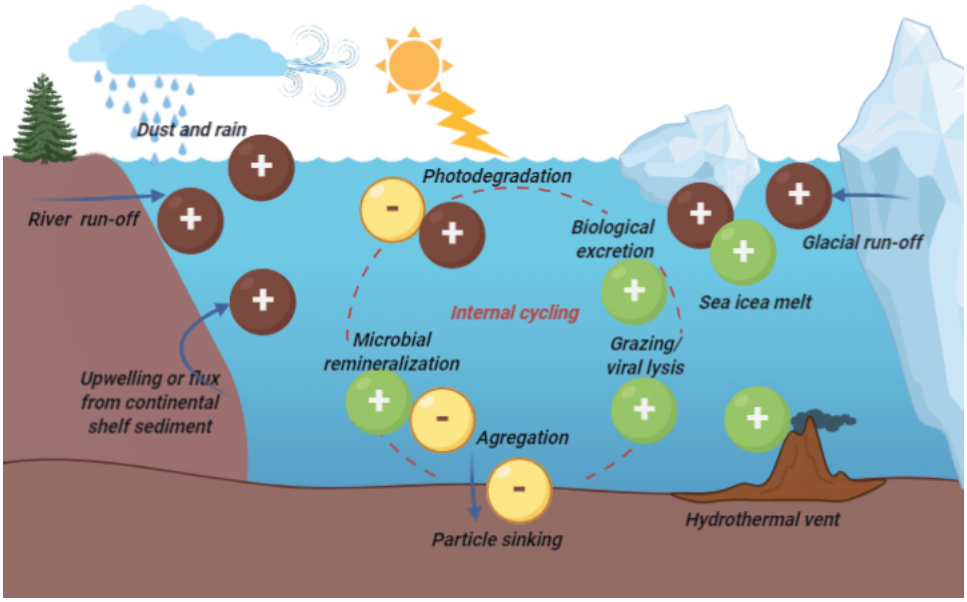

Figure 1-1. Schematic diagram of the major sources and sinks of Fe-binding ligands in the marine environment. The (+) symbol in a circle represents the supply of organic ligands, where the brown circle indicates lithogenic sources and the green circle indicates biological sources. A removal pathway is represented by the (-) symbol in a yellow circle. The red dashed-line circle indicates the internal cycle of Fe-binding ligands in the water column. Diagram is adapted from Hassler et al. (2017).

Polysaccharide macromolecules are the most abundant component of marine dissolved organic carbon (DOC), which can be a significant contributor to the ligand pool (Benner et al., 1992; Zigah et al., 2017). Exo-polymeric substances (EPS), are polysaccharide macromolecules excreted by marine microbes (Decho and Gutierrez, 2017; Hoagland et al., 1993). EPS can occur in high concentrations in surface water (Decho and Gutierrez, 2017; Hassler et al., 2011; Norman et al., 2015) and have the potential to outcompete siderophores and HS ligands for Fe-complexation, although they are considered to be short-lived reactive compounds (Norman et al., 2015; Pakulski et al., 1994). Furthermore, the melting of ice-bergs and sea-ice have been reported to release substantial amounts of organic ligands that were attributed to EPS ligands (Genovese et al., 2018; Lannuzel et al., 2015; Norman et al., 2015).

2. Analytical methods

Studies of (organic) Fe speciation in the marine environment commonly rely on an electrochemical technique: competitive ligand exchange-adsorptive cathodic stripping voltammetry (CLE-AdCSV). This technique determines the characteristics of Fe-binding properties, such as total ligand concentrations (L_t) and the average conditional stability constant of the bulk ligand pool ($K^{cond}_{Fe'L}$). The term 'conditional' is used to indicate the dependency on the conditional nature of seawater (i.e., ionic strength, salinity, pH, etc). The value of $K^{cond}_{Fe'L}$ represents the binding strength of Fe-ligand complexes. Organic Fe-binding ligands are operationally classified, by the $K^{cond}_{Fe'L}$ value. In case that more ligands classes are distinguished based on $K^{cond}_{Fe'L}$, these classes are denoted by L*i*, in which *i*=1 for the strongest ligand class, and *i*=2, 3, … and so on for the progressively weaker ligand classes.

In addition, mass-spectrometry techniques have been developed to identify the chemical structure of Fe-binding ligands simultaneously (Boiteau et al., 2013; Boiteau et al., 2015; Velasquez et al., 2011). Both electrochemical and mass-spectrometry approaches result in a similar portrayal of the organic ligands, which consist of a highly heterogenic pool of biomolecules with strong to progressively weaker Fe-binding strengths.

The CLE-AdCSV technique involves competition of Fe between a known added ligand (AL) and natural organic ligands. The AL competes with the natural ligands and forms an electroactive complex, Fe(AL)x that can be measured at the surface of a hanging mercury drop electrode. The determination of [L_t] and $K^{cond}_{Fe'L}$ is accomplished by titrating a sample with Fe to saturate the natural organic ligands present. The measured electrical signal from each titration point is used to calculate [L_t] and $K^{cond}_{Fe'L}$ simultaneously by applying the Langmuir isotherm, either using a linear or non-linear transformation. The obtained [L_t] is reported in nM equivalents of Fe (nM eq. Fe) and the value of $K^{cond}_{Fe'L}$ in M^{-1}, is expressed as its log value, log $K^{cond}_{Fe'L}$.

The CLE-AdCSV is the most common technique to analyze organic Fe speciation in seawater. There are four well-established CLE-AdCSV methods for DFe speciation in seawater. These methods use different ALs and titration conditions (pH, concentration of AL and equilibration time). The ALs used are 2-(2-thiazolylazo)-p-cresol (TAC), salicylaldoxime (SA), 1-nitroso-2-napthol (NN) and 2,3-dihydroxynaphthalen (DHN). The CLE- AdCSV methods using (2-thiazolylazo)-p-cresol (TAC) and salicylaldoxime (SA) as AL are the most widely used in the CLE-AdCSV analysis (Abualhaija et al., 2014; Buck and Bruland, 2007a; Croot et al., 2000).

The CLE AdCSV method is a relatively simple method, giving at least a good estimate of binding sites of molecules that keep Fe dissolved and potentially bioavailable. No sample treatment such as concentrating, or removal of salt is necessary. However, it should be noted that the method has its limitations when interpretating the data. The determination of [L_t] and $K_{Fe'L}^{cond}$ from the CLE-AdCSV analysis is quite challenging, of the application of the above-mentioned different AL's, may result in different speciation data. Yet, the majority of insight into the sources, sinks, and biogeochemical cycle of natural ligands in marine system is based on the Fe-binding characteristics of the ligands obtained from CLE-AdCSV analysis.

2.1 The assumptions and limitations of voltammetric method

The voltammetric technique is an indirect approach to study DFe speciation in seawater with some underlying assumptions, notably for interpretation of the data obtained from CLE-AdCSV titration. Thus, despite being the most used method, CLE-AdCSV has some limitations (e.g.,(Apte et al., 1988; Gerringa et al., 2014; Hudson et al., 2003; Laglera et al., 2015; Pizeta et al., 2015). Several limitations of the CLE-AdCSV are summarized briefly below:

1. The assumption that ligands chelate DFe in 1:1 coordination is unlikely to become fulfilled in a natural sample, since a wide range

of organic matter present in seawater likely includes ligands with multidentate binding coordination. To overcome this drawback, the obtained [L_t] is reported in nM equivalents of Fe (nM eq. Fe) thus reflecting ligand sites of all ligands present in sample, instead of absolute concentration of ligand molecules expressed in nM (Gerringa et al., 2014; Gledhill and Buck, 2012).

2. It is assumed that Fe binds to organic ligands reversibly, and thus, is exchangeable by competition with AL. The inclusion of inert Fe, $DFe_{inert,}$ can lead to an overestimation of [L_t]. Further, inter-dependency between the determination of [L_t] and log $K_{Fe'L}^{cond}$ could lead to analytical bias, where log $K_{Fe'L}^{cond}$ can be shifted towards higher stabilities when it is calculated using an overestimated [L_t] (Gerringa et al., 2014; Hudson et al., 2003; Miller et al., 1997). This bias is unknown and difficult to determine, and this causes an unknown error.
3. Different AL and analytical conditions (such as pH, equilibration time, and AL concentrations) result in different speciation data. For example, TAC as AL, may interact with humic-ligand binding sites, which could lead to the inaccurate detection of total ligand concentrations present in the sample (Laglera et al., 2011). Presently we are to evaluate the application of different AL's in CLE-AdCSV using model ligands (Gerringa et al., in review). Overestimation of [L_t] can arise from the lack of equilibration time when using a relatively high SA concentration (25 µM) with short equilibration time (15 minutes; Buck and Bruland (2007a). Moreover, the calibration of AL, such as the determination of AL's stability constant, is also propagated several uncertainties, causing subtle yet important differences in the detection window between AL's (Laglera and Filella, 2015).

3. The thesis contents

In this thesis the presence, solubility and potential bioavailability of Fe is studied and discussed in relation to the organic speciation of Fe. It describes organic Fe speciation in the laboratory to get insight in specific

processes of ligand formation (Chapter 2). But foremost it describes organic complexation in the field, in subtropical (Chapter 3), Arctic (Chapters 4 and 5) and Antarctic (Chapter 6) regions. Regional oceanographic processes affect the organic ligand production and influence the potential transport of DFe bound to organic ligands along with global circulation. The study area in Fram strait is crucial in the thermohaline circulation that transports ocean water around the globe, often referred to as the global ocean conveyor belt (Figure 1-2). As part of this system, a deep current transports cold and salty water from the Arctic Ocean southward via Fram Strait. This cold and salty water eventually reaches the HNLC region in the Southern Ocean. Here, water flows eastward with the Antarctic Circumpolar Current (ACC). Water masses originating from the ACC subsequently flow northward and move into the lower latitude oceans, including the Pacific Ocean, passing the subtropical region around New Zealand, where shelf processes could be sources or sinks of ligands that affect local ecosystems. As the water travels through the ocean, the mixing between the deep and cold water with overlying warmer water brings nutrients to the surface. Such upwelling also influences ligand production in surface waters. Moreover, the Arctic and Antarctic regions are subject to rapid environmental changes (i.e., changing sea-ice extent) due to climate change. In this study, organic DFe speciation was determined in the high latitude ocean to broaden our knowledge on the role of Fe-binding ligands on the biogeochemical cycle of Fe in the area where Fe limitation can occur. Additionally, a coastal low latitude region was studied to assess the cycling of Fe-binding ligands in a region dominated by recycling as well as the potential for transport to the open ocean.

Chapter 2 shows the results of laboratory experiments investigating the production of Fe-binding organic ligands by marine microbes. The production of Fe-binding ligands is investigated by co-culturing phytoplankton and bacteria. Seawater used for the cultures was taken offshore from the Otago peninsula (New Zealand), an area where subtropical and subantarctic water are encountered. The study aims to

understand how phytoplankton and bacteria interact to achieve the most efficient Fe acquisition when Fe resources are sparse.

Chapter 3 describes the organic Fe speciation that was investigated in the Hauraki Gulf, located to the northwest of Auckland, the fastest growing metropolitan city of New Zealand (Figure 1-2). The Hauraki Gulf is a semi-enclosed sea experiencing seasonal oligotrophic conditions. The area provides an ideal setting to study DFe speciation in a highly variable system. The seasonal changes in physical water circulation in this shelf sea trigger a shift in the community composition of the ecosystem. Such changes of the microbial ecosystem can have a profound effect on the DFe speciation.

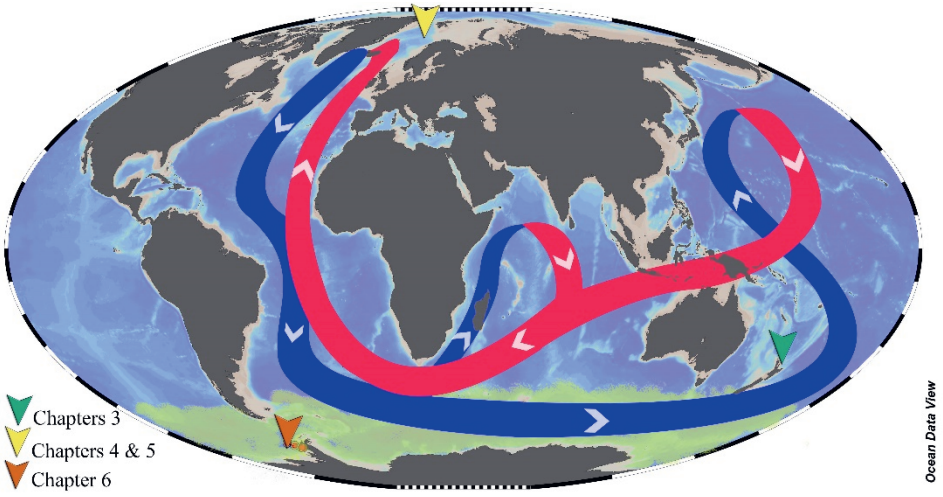

Figure 1-2. Schematic diagram of the global ocean conveyor belt with study areas indicated by green (Chapter 3), yellow (Chapters 4 & 5) and brown (Chapter 6) arrows. The green shade around Antarctica indicates the approximate area of the High Nutrient Low Chlorophyll (HNLC) region. The blue path depicts the cold and salty deep current, whereas the red path depicts warm and shallow current. The arrows in the blue and red paths indicate its flow direction, where it should be noted this is a very simplified representation of a complex system.

Chapters 4 and 5 describe the organic DFe speciation that was investigated in Fram Strait, a deep-sea strait located in the Arctic between Greenland and Svalbard, where water mass and heat exchange occur between the Arctic Ocean and the Atlantic Ocean (Figure 1-2). To examine

the impact of local sources of Fe-binding ligands, DFe speciation was determined in the northeast Greenland shelf region. This DFe speciation study was conducted with the CLE-AdCSV technique using TAC as the AL. Given that various ligand sources existed, comprising a ligand pool with high heterogeneity, including HS, the area is of particular interest to conduct a comparison study on the different analytical CLE-AdCSV procedures using different ALs. The same samples were measured using CLE-AdCSV with different AL's (Chapter 5) to investigate the influence of the used AL's on the outcomes of DFe speciation studies.

Organic DFe speciation was also investigated in the Bellingshausen Sea located adjacent to the western Antarctic Peninsula (WAP) in the Southern Ocean, the largest HNLC area where Fe limitation is widely observed (Chapter 6, Figure 1-2). The waters of the WAP region are known to have a natural gradient with an Fe-rich area in the shelf sea and an Fe-poor area in the open ocean, where the shelf area was still partly ice-covered during sampling in early spring season. In between the shelf sea and open ocean, a number of oceanographic fronts existed. The waters of the WAP region act as a natural laboratory to study organic DFe speciation in Fe-rich to Fe-poor environments from an ice-covered shelf area to an ice-free open ocean. The presence of fronts in this area is also of particular interest, since the physical water circulation could be an important aspect influencing the distribution of DFe and its organic ligands.

The main findings and their implications for the role of organic ligands in the Fe biogeochemical cycle, as well as recommendation s for the future research, are summarized in a synthesis (Chapter 7).

Chapter 2

The interaction between marine bacteria and diatom, *Pseudo-nitzschia sp.*, under different iron scenarios

Indah Ardiningsih, Evelyn Armstrong, Linn Hoffmann, Federico Baltar, Loes J. A. Gerringa, Rob Middag, Sylvia G. Sander

Abstract

Phytoplankton are the most abundant primary producers in the oceans, and diatoms often dominate the marine phytoplankton assemblage. Phytoplankton and heterotopic bacteria coexist in the marine environment and actively engage in a specific way that influences the nutrient and carbon cycles in the marine environment. Iron (Fe) is an essential micronutrient for primary producers. Despite its importance, it is present at trace level in the ocean as it is rather insoluble at the pH of seawater. However, organic iron-binding is acknowledged to enhance Fe solubility in seawater. Diatom and bacteria have developed mutualistic interactions for Fe acquisition. However, very limited knowledge is available about how phytoplankton and bacteria interact to achieve the most efficient Fe acquisition when there is a lack of Fe resources. We developed an approach to reveal the influence of marine bacteria in diatom cultures of *Pseudo-nitzschia* sp. We used a dialysis membrane to physically separate the diatoms from marine bacteria to test whether direct cell contact between bacteria and diatoms is necessary for chemical signalling. Our results showed that bacteria and diatoms might interact chemically, in which the presence of bacteria is able to enhance phytoplankton growth even without direct physical contact. The different Fe treatments used did not have a measurable effect on the growth of phytoplankton, yet affected phytoplankton physiological performance (Fv/Fm) and yielded biomass (Chl-*a*/cell). The low-Fe treatments resulted in Fv/Fm < 0.25, indicating that phytoplankton was experiencing physiological stress. Consequentially, chl-*a*/cell ratios in low-Fe treatments were often lower compared to those in higher-iron treatments. Dissolved iron (DFe) drawn down was observed as the incubation progressed along with macronutrients (PO_4 and Si) utilization. Since Fe was sufficient for phytoplankton growth, the production of strong Fe-binding ligands was not likely stimulated as the incubation progressed. Otherwise, ligands may have been degraded as the incubation progressed. The initial [L_t] varied between 2.26 ± 0.3 and 8.69 ± 0.2 nmol/L eq. Fe, and at the end of incubation ranged between 2.62 ± 0.1 and 6.07 ± 0.1 nmol/L eq. Fe. The values of conditional binding constant (log $K^{cond}_{Fe'L}$) ranged from 10.8±0.2 to 12.3±0.2. Based on the value of log $K^{cond}_{Fe'L}$, the detected ligands in our experiment were potentially a degradation product of stronger ligands, or microbial exudates.

1. Introduction

Phytoplankton are the most abundant primary producers in the ocean and responsible for up to 50% of the global primary production (Field et al., 1998; Moore et al., 2013; Paul et al., 2009; Poulson-Ellestad et al., 2014). Marine heterotopic bacteria contribute to the organic carbon biomass transfer in the ocean through their secondary production (Ducklow et al., 2000). Phytoplankton and heterotopic bacteria coexist in the marine environment. They interact in a specific way creating a microbial loop which involves micronutrients (e.g., iron), vitamins (e.g., cobalamin) and nutrients (e.g., nitrogen) (Amin et al., 2012b). Through photosynthesis, inorganic carbon is fixed into organic carbon by marine phytoplankton. A large fraction of the fixed organic carbon is directly utilized by bacteria to obtain energy by respiring it, contributing to major CO_2 release in the ocean (Amin et al., 2012b; Baltar et al., 2015). Otherwise, organic carbon is taken up by bacteria to synthesize new organic carbon biomass, which flows to the higher trophic levels, moving organic carbon from one pool to another (Longnecker et al., 2015). Thus, the interaction between phytoplankton and bacteria influences nutrient and carbon cycles in the marine environment (Hans-Peter et al., 2007; Poulson-Ellestad et al., 2014). Diatoms often dominate the marine phytoplankton assemblage, and are ecologically essential as they are recognized to be a key player on primary productivity in high nutrient and coastal waters (Nelson et al., 1995).

Iron (Fe) is an essential micronutrient for primary producers. By possessing the ability to transfer electrons, this element plays a crucial role in photosynthesis, respiration, and nitrogen fixation (e.g.,(Geider and La Roche, 1994; Morel et al., 2003). However, Fe solubility is depending on its redox state. The reduced state of iron, Fe(II), is highly soluble, while the oxidized form, Fe(III), is rather insoluble at the pH of seawater, largely precipitates, and sinks out of the photic zone. Unfortunately, the latter is the predominant redox state at the pH of seawater, thus it is present at low concentrations and often becomes a limiting micro-nutrient (Boyd and Ellwood, 2010b). In the marine system, the solubility of Fe is enhanced by

the presence of organic Fe-binding ligands. Organic ligands chelate Fe, keeping Fe in dissolved form as Fe-ligand complexes, and enhancing the pool of dissolved-Fe (DFe) for marine microbes (Boyd and Ellwood, 2010b; Boye et al., 2001; Bruland et al., 1991).

Organic Fe-binding ligands are classified by their binding strength into three large groups (Gledhill and Buck, 2012; Hassler et al., 2017). These three large groups include (1) siderophores (Mawji et al., 2008; Velasquez et al., 2016; Vraspir et al., 2009); (2) humic substances, HS (Laglera and van den Berg, 2009; Su et al., 2015; Tani et al., 2003; Whitby et al., 2020) and marine humic substances (HS-like substances); and (3) biologically excreted substances such as polysaccharides or exopolymeric substances, EPS (Hassler et al., 2011). Even though this classification is very broad, knowledge is progressing rapidly through application of advanced techniques and instrumentation (Boiteau et al., 2013; Boiteau et al., 2019; Velasquez et al., 2011). Siderophores are of particular interest as they are biologically produced ligands with strong affinity for Fe. Siderophores are small organic molecules synthesized by certain heterotrophic bacteria (e.g., cyano-bacteria) as part of an adaptation strategy for Fe acquisition (Butler, 2005; De Serrano et al., 2016). Siderophores solubilize Fe and regulate Fe uptake by marine microbes. They are therefore known as a ferric ion (Fe^{3+}) specific transport compounds and are important compounds for bacterial Fe acquisition in seawater (De Serrano et al., 2016; Hopkinson et al., 2009).

The association between phytoplankton and bacteria is beneficial for both communities. While phytoplankton supply the organic carbon for bacteria, bacteria can fulfil needs of phytoplankton, such as producing vitamins, fixing nitrogen and producing siderophores (Amin et al., 2012b). Previous work showed that siderophores are produced by marine heterotrophic bacteria (Granger et al., 1999), but not by phytoplankton. In fact, phytoplankton also excrete organic exudates to promote Fe uptake, but are predicted to have a weaker affinity to Fe compared to siderophores (Karen et al., 1999; Norman et al., 2015). Thus, it is hypothesized that phytoplankton also benefit from siderophores produced by bacteria to

obtain Fe. Indeed, a mutualistic symbiosis is formed via excretion of small molecules that permit communication between phytoplankton and bacteria (Fuqua et al., 2002), allowing an association to be established and triggering phytoplankton blooms (Amin et al., 2012b). However, very limited knowledge is available to understand how phytoplankton and bacteria function together to achieve the most efficient iron acquisition under limiting iron resources. It is also still unknown whether such association is mediated chemically or if cell contact is needed.

Understanding the bacteria and phytoplankton interaction is important to improve our knowledge of marine biogeochemical cycles. In the present study, we focus on the interaction between phytoplankton and bacteria under iron deplete and replete conditions. We developed an approach to reveal the influence of marine bacteria in diatom cultures of *Pseudo-nitzschia* sp. Our main research focus was to determine how a natural bacteria community affects phytoplankton performance under iron-limiting conditions, in subantarctic seawater, for example by the production of Fe-binding organic ligands. We used a dialysis membrane to physically separate the diatoms from marine bacteria to test whether direct cell contact between bacteria and diatoms is necessary for chemical signalling. This study aims to provide information on the potentially essential role of bacteria in phytoplankton nutrient acquisition.

2. Methods

2.1 Seawater sampling for incubation media

The incubation media used in this work was collected from surface (10-25m) seawater about 60km southeast of the Otago Peninsula shoreline (45.836°S and 171.541°W), New Zealand (Figure 2-1). The detailed hydrographic setting is described elsewhere (Sander et al., 2015; Sutton, 2003). The *in-situ* seawater temperature was 12.4°C and salinity 34.3. The sampling was carried out during Austral summer in February 2017 onboard the research vessel Polaris, using a trace metal clean sampler system.

Surface seawater was filtered on board with two different pre-cleaned membrane filters integrated into a pumping system, a 0.8µm membrane filter and a 0.1µm membrane filter. The 0.8µm filtration excluded natural phytoplankton, but not the natural bacteria communities. The 0.1µm filtered water is assumed to be 'sterile' without the natural bacteria and phytoplankton, and will be addressed as sterile water here. The filtered seawater was stored in rigorously acid cleaned and Milli-Q conditioned 20L carboys and transported to the laboratory.

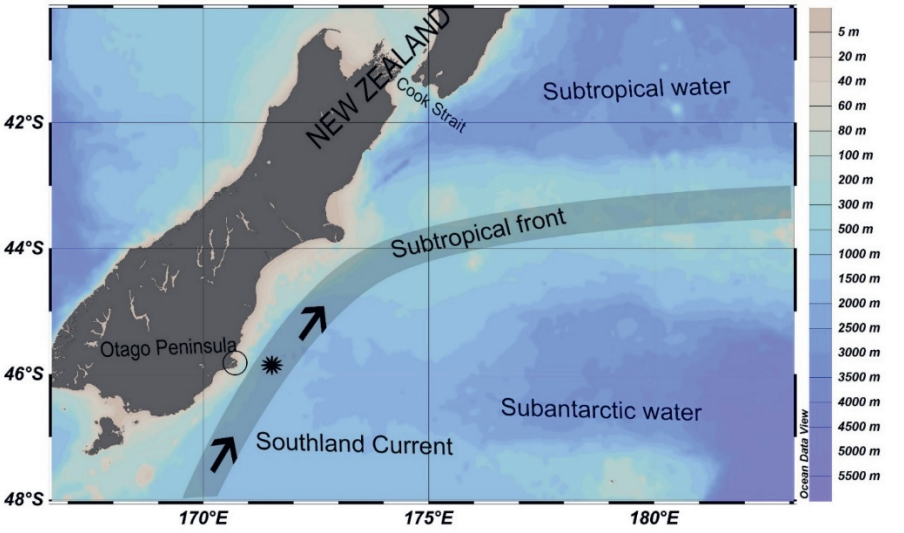

Figure 1-1. Seawater sampling location, marked with (*) in the map. Hydrological setting of the map adapted from Sander et al, 2015 and based on Sutton, 2003.

2.2 Incubation set-up

Acid cleaned 2.7L polycarbonate bottles stored with 10% HCl, were rinsed with Milli-Q water before use, and filled with the incubation water. Three different incubation waters were used as the growth media (Figure 2-2): A) 2L of 0.1µm membrane filtered seawater, addressed as 0.1µm-filtered seawater; B) a mixture of 1.75L of 0.1µm-fultered seawater and 0.25L of 0.8µm membrane filtered seawater, addressed as mixed seawater;

C) 1.75L of 0.1µm-filtered seawater, with 0.25L 0.8µm filtered seawater inside the dialysis tubing, addressed as C*.

The incubations were prepared in quadruplicate for each type of medium and a low and high-Fe treatment (Figure 2-2). Macronutrients were added into each bottle: 30µM nitrate (NO_3), 30 µM silicate (Si) and 2 µM phosphate (PO_4). While there was no Fe added to the low-Fe treatment, 4 nmol/L of Fe (as $FeCl_3$) was added to high-Fe treatment. For the culture with the dialysis bag, macronutrients and Fe were added to the culture outside the dialysis bag, C, but not inside the dialysis bag, C*. Thus, in total 24 incubation bottles were incubated at 11ºC under white-fluorescent light, 60 µE m^{-2} s^{-1}. The cultures were incubated on 12 hours:12 hours light to dark cycle. Please note that incubations A and B also contained a dialysis bag, similar to C, but here the dialysis bag was not filled. This is to avoid artefacts due to the physical presence of the dialysis bag material.

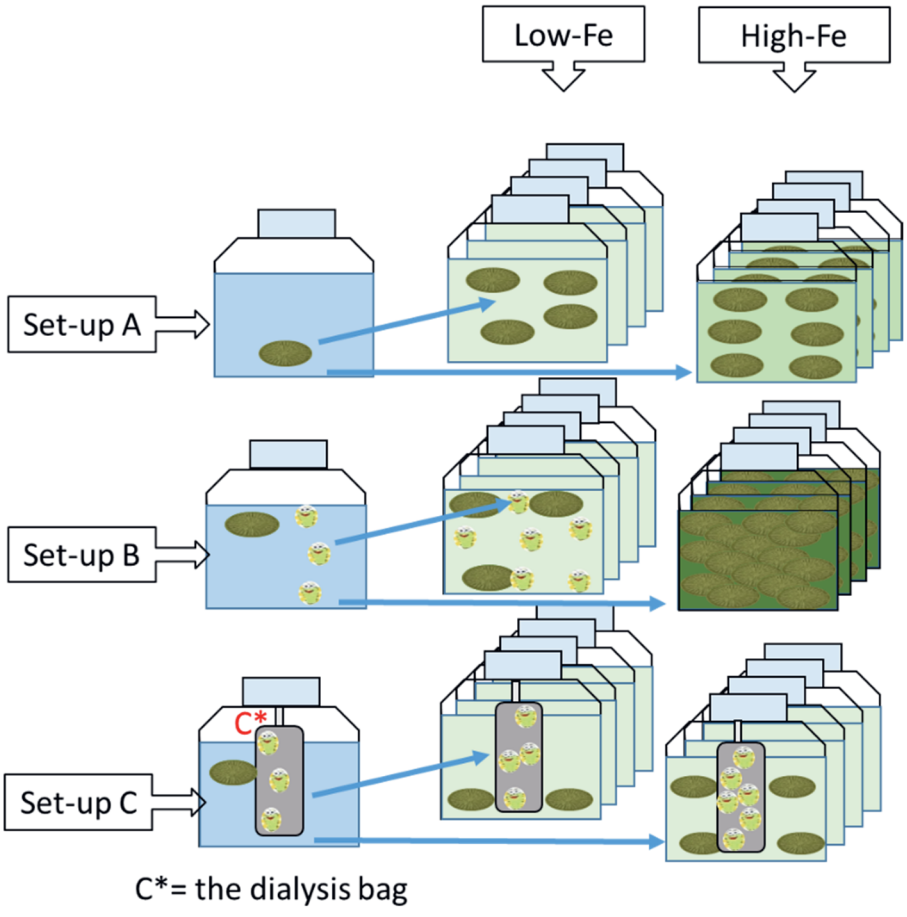

Figure 1-2. Schematic diagram showing different treatments in incubation setup. No Fe was added to the low-Fe treatments (left), and 4 nmolL^{-1} of Fe (as $FeCl_3$) was added to high-Fe treatment (right). The A bottles contain 0.1µm-filtered seawater with added diatoms, and assumed to be very low in bacteria. A mixture of seawater in the B bottles contains both bacteria and phytoplankton. The C bottles also contain a mixture of seawater, but separated by a dialysis tube: outside the tube, the seawater contained diatom, whereas bacteria were present inside the dialysis tubing (C).*

A subantarctic diatom species, *Pseudo-nitzschia sp.*, was chosen as a representative phytoplankton species and approximately 10 cells/mL of culture were added into the incubation medium. Cellulose membrane dialysis tubing (pore size 10 kDa, Sigma Aldrich) was used to physically

separate co-cultures in set-up C (Figure 2-2). The tubes were cut into sections of approximately 31 cm and clamps (dialysis tubing closures, sigma-aldrich) were used to close both ends of this dialysis tubing. The clamps were acid-cleaned and the tubes were pre-cleaned as recommended by the manufacturer. Briefly, the tubes were soaked with a 0.3% (w/v) solution of sodium sulfide at 80°C for 1 minute, then rinsed with Milli-Q water (60°C) for 2 minutes, followed by acidification with a 0.2% (v/v) solution of sulfuric acid. These treatments were done to remove the sulfuric compounds that may remain in the tubing from the manufacturing processes. Finally, the tubes were rinsed with warm (60°C) and room temperature Milli-Q water to remove the acid. The pre-cleaned tubes and acid-cleaned clamps were rinsed and boiled with 80°C Milli-Q water for sterilization and stored in 0.2% quartz distilled HCl until use.

2.3 Sampling from the cultures

Sub-samples were collected for each treatment on the first day of incubation by sampling a bottle for each treatment immediately after set-up was completed, to provide measurements of a suit of parameters at the beginning of the incubation (t_0): major nutrients, DFe, Fe-binding ligands, cell counts, dissolved organic carbon (DOC) and photosynthetic capacity. The remaining triplicate bottles of each type (18 bottles in total) were incubated at the incubation conditions mentioned above. During the incubation, subsamples for diatom and bacterial cell counts were taken periodically from one bottle of each experimental set-up to monitor growth. The same bottle was sampled at each time point. Since the culture inside the dialysis tubes is not accessible for day-to-day sampling in a trace metal clean manner, subsamples for the cell growth were only taken from the outer cultures in set-up C. The experiments lasted 20 days for set-ups A and B (the end of experiment, t_{end}) and 19 days for set-up C. Only at t_{end}, it was possible to take subsamples of the culture inside the dialysis tubing. At t0 and t_{end}, the cultures were filtered through 0.2µm polycarbonate membrane filters. All work was done in a laminar flow bench, and trace metal clean techniques were used throughout the experiments and sampling.

2.4 Analytical methods

2.4.1 Nutrients, dissolved organic carbon (DOC), Chlorophyll-a (chl-*a*), cell counts and photosynthesis capacity (Fv/Fm) analysis

Samples for macronutrients were stored frozen in acid-washed vials at -20ºC until analysis. The thawed samples were analyzed colorimetrically for dissolved silicate, phosphate and the sum of nitrate and nitrite (NO_x) using flow-injection analysis on a Lachat Auto-analyzer as described by (Parsons, 1984). For the analysis of DOC, 30mL aliquots were transferred into acid-cleaned and pre-combusted (450ºC for 4 h) borosilicate glass vials, then acidified to pH 2 using concentrated quarts-distilled hydrochloric acid (1% v/v). The DOC concentrations were measured by high temperature combustion using a Shimadzu total organic carbon (TOC) analyser (Cauwet, 1994). Cells for biogenic silicate analysis were collected on 0.4 µm polycarbonate filters before the filters were washed with artificial seawater and stored frozen until analysis. Analysis was carried out following the methods of Nelson et al. (1995).

Samples for diatom cell counting were taken every 2-3 days and immediately measured by flow cytometry using an Accuri C6 Flow Cytometer (Becton Dickinson), and were analyzed for 1 to 4 minutes depending on cell density at a flow rate of 65 µl/min. Cell identification was triggered on chlorophyll fluorescence (FL3) and the threshold was set to 1000 on FL3. The growth rates of phytoplankton were calculated based on the slope of natural logarithm of cell counts during exponential growth versus incubation time (Wood, 2005). For the bacteria cells, 10 mL subsamples were preserved with glutaraldehyde (0.5% v/v) for 15–30 min and frozen in liquid nitrogen before being stored at -20ºC prior to cell enumeration. Upon thawing, samples were enumerated after DAPI (40,6-diamidino-2-phenylindole) staining by epifluorescence microscopy (Porter et al., 1980) and samples were measured by flow cytometry. Chlorophyll-*a* (Chl-*a*) was determined fluorometrically from acetone

extracts as described by (Welschmeyer, 1994). The photosynthetic efficiency of phytoplankton (F_v/F_m) was measured with a Fast Repetition Rate Fluorometer (Chelsea Instruments).

The standard deviation reported here was calculated from the average values of triplicate bottles. Statistical analyses were done with SPSS software included analysis of variance (ANOVA) and significant differences were determined and reported with an error level of 5% or $p \leq 0.05$.

2.4.2 Dissolved iron analyses

Samples for DFe analysis were collected in acid-cleaned LDPE bottles and acidified to pH 1.8 with concentrated quarts-distilled hydrochloric acid (final concentration 0.024 M HCl). The acidified samples were stored at 4ºC prior to analysis. Sub-samples were pre-concentrated using an automated seaFAST system (SC-4 DX seaFAST pico; ESI). The pre-concentrated samples were analyzed using high-resolution inductively coupled plasma mass spectrometry (HR-ICP-MS, Thermo Fisher Element XR), with quantification via standard additions. The average overall method blank (seaFAST & ICP-MS) concentration, determined by measuring acidified ultrapure water as a sample, was 0.09±0.04 nmol/L (n = 6). Reference materials were measured to check accuracy and reproducibility of DFe analysis. The reference materials are including SAFe D1 and GEOTRACES coastal surface seawater (GSC) and an in-house reference seawater sample. The analysis of reference materials was in good agreement with consensus values, for SAFe D1 0.724 nmol/L (consensus value 0.69 ± 0.04 nmol/L).

2.4.3 Iron-binding ligand analysis

For Fe-binding ligand analysis, at least 125 mL filtered sample was collected into acid-cleaned narrow mouth LDPE bottles that had been rinsed at least three times with sample prior to filling. Samples were stored at -20ºC and defrosted before analysis. The total Fe-binding ligand concentration ($[L_t]$) and conditional stability constant ($K_{Fe'L}^{cond}$), was

determined by competitive ligand exchange - cathodic stripping voltammetry (CLE-CSV) with Salicylaldoxime (SA, Acros Organics) as competing ligands (Rue and Bruland, 1995;Abualhaija and van den Berg, 2014). The voltammetric instruments consisted of a BioAnalytical System (BASi) controlled growth mercury electrode (static drop setting, size 11) coupled with an Epsilon-2 (BASi) electrochemical analyzer (Buck et al., 2007). This voltammetric system was controlled by computer using ECDsoft as an interface software.

For Fe-binding ligand determination, the thawed samples were shaken, and sub-sampled aliquots of 10 mL were distributed to eleven lidded Teflon vials (Nalgene). Vials were rinsed with using ultrapure water (18.2 MΩ, Milli-Q element system, Merch Millipore – addressed as MQ water hereafter) and at least twice conditioned prior to use with known Fe(III) standard and SA concentrations added into buffered seawater. The Teflon vials were marked and always used for the same Fe(III) concentration added and only rinsed with MQ water in between sample measurement in order to keep them conditioned. For the measurement, the sample was buffered to a pH of 8.2 with 0.1 M ammonium-borate buffer. The Fe(III) standard solution was added in different concentrations to the 11 vials into final concentrations 0 (twice, i.e. no Fe(III) standard addition); 0.5; 1; 1.5; 2; 3; 4; 5; 6; 8; 10 nmol/L Fe. Then, SA was added to a final concentration of 5 µM. The solutions in the Teflon vials were allowed to equilibrate for at least 8 hours before measurement (Abualhaija and van den Berg, 2014) or typically overnight. For each sample, duplicate scans were done with a deposition time of 90 s, starting with the lowest added Fe(III) and subsequent increasing Fe concentrations, without rinsing the measuring cell. The measuring cell was rinsed with MQ water and blanks were scanned in between samples to avoid carry over.

The data obtained by CLE-CSV was interpreted for [L_t] and $K^{cond}_{Fe'L}$, with [L_t] reported in nanomole equivalent of Fe (nmol/L eq. Fe) and the $K^{cond}_{Fe'L}$ value reported as log-10 value (log $K^{cond}_{Fe'L}$) with respect to inorganic iron (Fe′). The data were plotted into a one-ligand model using non-linear

regression of the Langmuir isotherm with freely available software R as described by Gerringa et al. (2014). Details regarding the theory on the calculation of the ligand's parameters can be found elsewhere (Gledhill and Buck, 2012; Pizeta et al., 2015; Sander et al., 2011a; van den Berg, 1982).

3. Results

3.1 Biological response

The initial bacterial abundance was scarce, the cells count ranged from $2.6x10^5$ to $6.8x10^5$ per mL and increased at least an order of magnitude over the course of the incubation period, 19 days for set-up C and 20 days for set-up A and B. Although theoretically the seawater in set-up A and C do not contain natural bacteria, a low bacterial abundance was found in setup A (2.6 to $3.0x10^5$ /mL) and C (2.7 to $3.4x10^5$ /mL). The initial bacterial biomass inside the dialysis bag (C* in the incubation set-up, Figure 2-1) was not counted directly. However, since C* contained the same filtered seawater as B, where C* has 1/8 the volume of B, it is assumed that C* has 8 times the number of bacteria at the beginning of the incubation. The highest increase in bacteria cells per milliliter seems to have happened in C* at t_{end}, $1.1x10^7$/mL (Table 2-1). At the end of incubation, the bacteria cells count in B for both treatments ($3.6x10^6$/mL to $3.5x10^6$/mL) was higher than in A ($1.7x10^6$/mL and 1.3 $x10^6$/mL), since 1/8 of medium contained bacteria at the start for treatment B.

Table 1-1. Bacteria and diatom cell counts and growth rate of diatoms. Standard deviation (SD) in bacteria cells is calculated from the triplicate treatment in different bottles, thereby there is no SD for bacteria cell counts at t_0.

Setup	Treatment	time	day	Bacteria ($x10^5$) (cells/mL)	Diatom (cells/mL)	diatom growth rate per day
A	Low-Fe	t_0	0	2.6	6.19	0.32 ± 0.09
		t_{end}	20	17.4±1.7	(19.9±5.0) $x10^3$	
	High-Fe	t_0	0	3.0	10.3	0.36 ± 0.16
		t_{end}	20	12.9±5.2	(20.6 ± 6.2) $x10^3$	

B	Low-Fe	t_0	0	6.8	72.2	0.40 ± 0.21
		t_{end}	20	36.0±10	(22.4 ± 8.5) x10^3	
	High-Fe	t_0	0	3.0	30.9	0.50 ± 0.13
		t_{end}	20	34.8±6.5	(26.3 ± 1.9) x10^3	
C	Low-Fe	t_0	0	2.7	51.5	0.52 ± 0.10
		t_{end}	19	17.3±3.6	(26.0 ± 3.9) x10^3	
	High-Fe	t_0	0	3.4	30.9	0.56 ± 0.03
		t_{end}	19	18.8±5.9	(39.1 ± 6.0) x10^3	
C*	Low-Fe	t_0	0	54.4	0	NA
		t_{end}	19	86.3±60	6.04	
	High-Fe	t_0	0	54.4	0	NA
		t_{end}	19	110.4±23	0.31	

The diatoms were growing up to 3 orders of magnitude during the incubation period in set-up A, B and C. The growth rates of diatoms increased from set-up A to set-up C, in which the lowest growth rate was observed in the low-Fe treatment in set-up A (0.32 ± 0.09; Table 2-1), and the highest one found in the high-Fe treatment in set-up C (0.56 ± 0.03 per day; Table 2-1). In results, the diatom cell number at the end of the experiment was highest in the high-Fe treatment in set-up C, 39.1 ± 6.0 x10^3 cells/mL. The growth rates of diatoms in the three different set-ups showed that addition of Fe did not influence the growth rate significantly (ANOVA, $F_{5,18}$=1.75, p<0.174), except in set-up B where the growth rates of *Pseudo-nitzschia sp.* were significantly higher (ANOVA, $F_{2,21}$=4.75, p<0.021).

Addition of Fe did affect the photosynthetic performance (Fv/Fm) of the diatoms. The lowest value (0.17) was observed in the low-Fe treatment in set-up C, while the highest value (0.34) was detected in the high-Fe treatment in set-up B (Figure 3a). The measured Fv/Fm in the low-Fe treatments was consistently lower relative to the high-Fe treatment (ANOVA, $F_{5,18}$=25.846, p<0.001) and significantly different among A, B, C, and C* (ANOVA, $F_{2,21}$=11.592, p<0.001).

The average chl-*a*/cell was 2.82x10^7 µg/L with the lowest value (2.2 x10^7 µg/L) observed in the low-Fe treatment in set-up B, while the highest

value (3.6 x10^7 µg/L) was detected in the high-Fe treatment in set-up C (Figure 3b). The Chl-*a*/cell in the low-Fe treatments was always lower compared to the high-Fe treatments (Figure 3b) and the difference is significant overall (ANOVA, $F_{5,12}$=4.935, p<0.011), as well as among the set-ups A, B and C (ANOVA, $F_{5,12}$=6.745, p<0.008). Interestingly, a relatively higher Chl-*a*/cell and diatom growth rate were observed in set-up C, but the Fv/Fm in this set-up was low compared to set-up A and B.

3.2 Major nutrients and dissolved organic carbon (DOC)

The dissolved major nutrients silicate (Si), phosphate (PO_4) and sum of nitrate and nitrite (NO_x) were measured at the beginning and at the end of incubation. The major nutrient concentrations declined during the incubation experiment (Figure 4). However, a slight increase in NO_x was observed in the high-Fe treatment in setup B and in C*, but also in both NOx and Si low-Fe C*. At t_0, PO_4 ranged from 2.33 to 3.25µmol/L; NO_x ranged from 37.9 to 203 µmol/L and Si ranged 97.81 to 161.63µmol/L. Both PO_4 and Si concentrations were never depleted in any of the treatments. The maximum PO_4 drawdown was observed in the high-Fe treatment in set-up B, from 3.25±0.2 µmol/L to 1.70±0.2µmol/L. For Si, the high-Fe treatment in set-up A showed the largest decline, from 161.63±12.0µmol/ L to 83.0±4.1µmol/ L. The Si concentration declined during the incubation, the exception to this was the low-Fe treatment inside the dialysis bag, C*, where the Si concentration slightly increased over time, from 97.8 to 112.7±0.2µmol/ L.

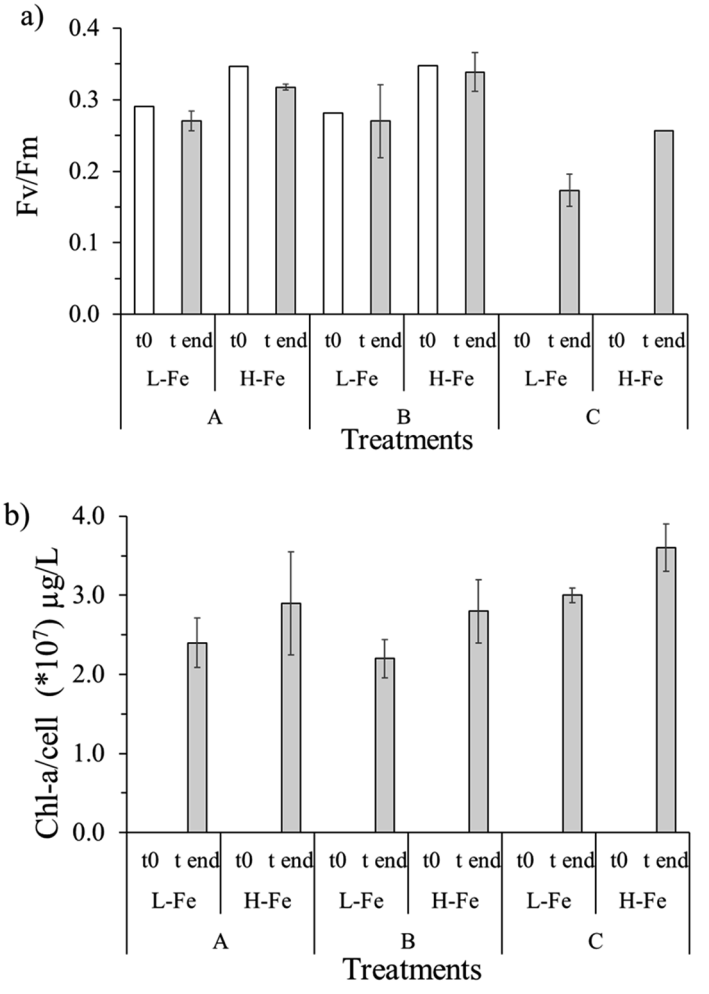

Figure 1-3. The photosynthetic performance (Fv/Fm) of diatoms (a) and chlorophyll-a (b) under different Fe treatments; low-Fe treatment (L-Fe) and high-Fe treatment (H-Fe). The start of incubation is denoted as t_0, and the end of the incubation period is denoted as t_{end}.

The DOC concentrations declined during the incubation time in both low-Fe and high-Fe treatments in A and B (Figure 2-5). The DOC concentrations in C and C* were almost equal and declined slightly over time except for the high-Fe treatment in C, where DOC increased. The

DOC concentrations at t_0 varied between 3.12±0.9 and 8.30±1.2mg/L, and at t_{end} between 2.23±0.9 and 4.23±0.8mg/L.

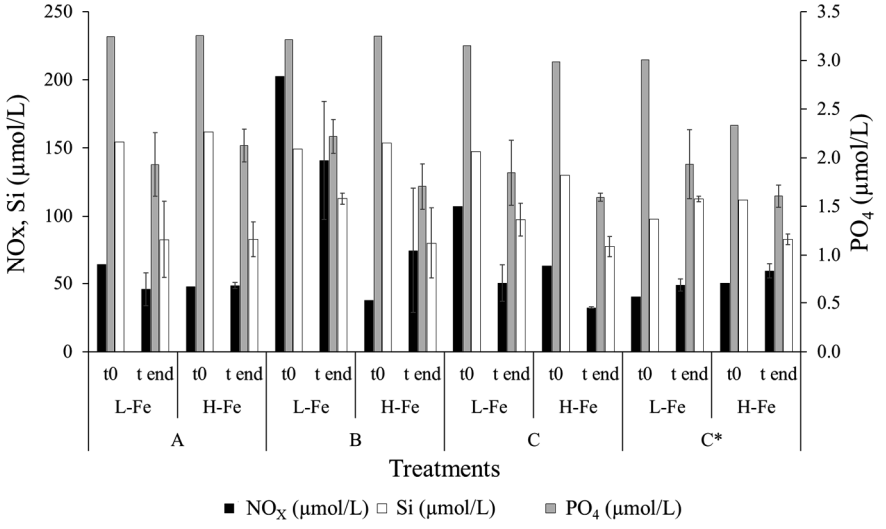

Figure 1-4. Concentration of Nitrate (NOx), silicate and phosphate (PO4) at the initial (t_0) and the end (t_{end}) of the incubation period for both low-Fe treatments (L-Fe) and high-Fe treatments (H-Fe).

3.3 Dissolved Fe and total dissolved Fe-binding ligands

The initial DFe concentrations in the low-Fe treatment ranged between 2.01 and 2.95 nmol/L. The Fe addition in the high-Fe treatments resulted in initial DFe concentrations between 1.64 and 4.68 nmol/L (Figure 2-5a), in which the lowest DFe belonged to the culture inside the dialysis bag, C*, where Fe was added into the culture outside the bag, C, not C*. In general, DFe declined during the incubation. At t_{end}, DFe concentrations ranged from 0.81 to 1.49 nmol/L in the low Fe-treatments, and from 1.15 to 1.59nmol/L in the high-Fe treatments. The DFe drawn down was greater in the high-Fe treatment compare to low-Fe treatment. Among A, B and C, the greatest DFe decrease was observed in the high-Fe treatments in B. Inside the dialysis bag, C*, only small changes in DFe were detected in the high-Fe treatment where initially DFe concentration was already low, 1.64±0.02 nmol/L and decreased to 1.59±0.20 nmol/L at the end of incubation (Figure 2-5b).

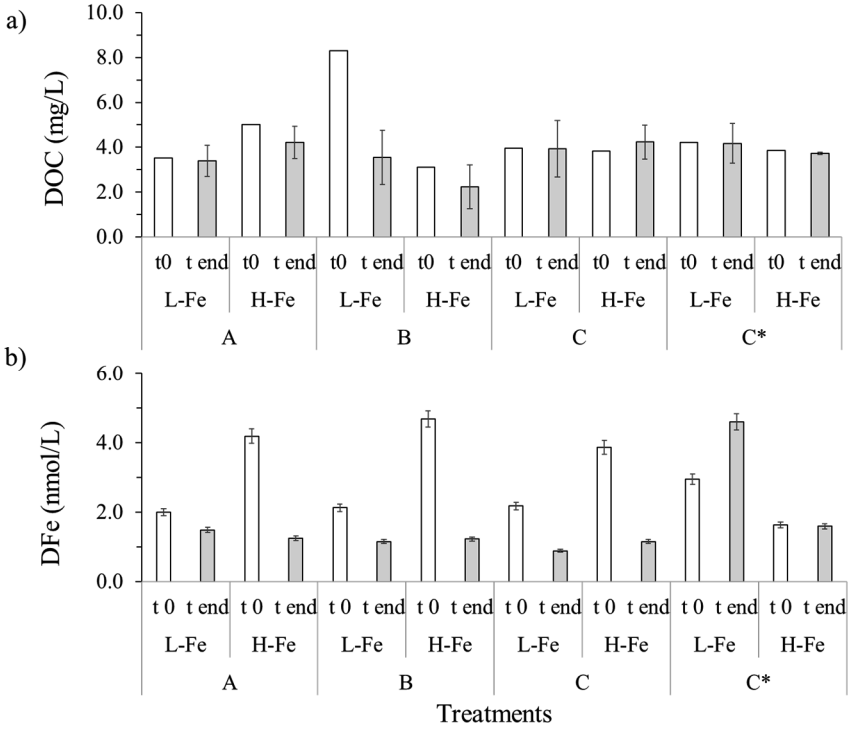

Figure 1-5. Dissolved organic carbon (DOC) concentration (a) and dissolved Fe (DFe) concentration (b) under different Fe treatments. Abbreviations as in Figure 2-3.

During the incubation, [L_t] decreased in both low-Fe and high-Fe treatments, with the exception of the low-Fe treatment of C and C* (Figure 2-6a). The initial [L_t] varied between 2.96 ± 0.3 and 8.99 ± 0.2 nmol/L eq. Fe, and at the end of incubation ranged between 2.62 ± 0.1 and 6.07 ± 0.1 nmol/L eq. Fe. A larger decline was seen in the high-Fe treatment relative to the low-Fe treatment among set-up A, B, C and C*. In the low-Fe treatment of C and C*, L_t increased from 2.96 ± 0.34 to 4.56 ± 0.16 eq. nmol/L Fe, and from 5.09 ± 0.12 to 6.07 ± 0.16 eq. nmol/L Fe, respectively (Figure 2-6a).

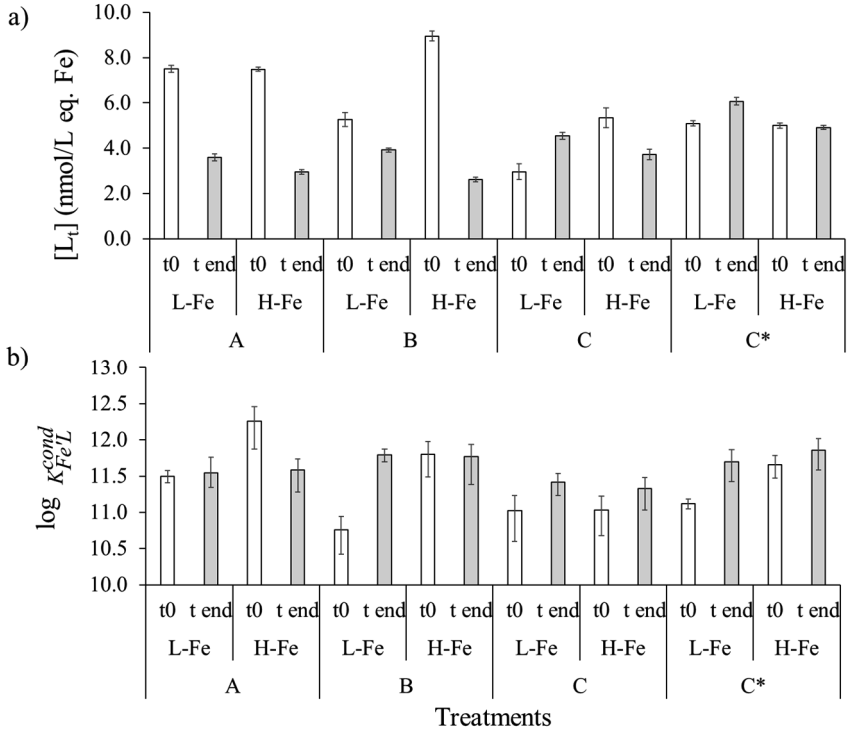

Figure 1-6. Total Fe-binding ligand concentration (a) and conditional stability constant (log $K^{cond}_{Fe'L}$ b) in different Fe treatments. Abbreviations as in Figure 2-3.

The log $K^{cond}_{Fe'L}$ value represents the average strength of the Fe-binding ligand complexes in a specific medium. In this experiment, one ligand class was modelled and yielded log values between 10.8±0.2 and 12.3±0.2 (Figure 2-6b), with 11.5±0.1 and 11.6±0.1 as average and median values, respectively. The log $K^{cond}_{Fe'L}$ values remained relatively constant throughout the experiment without significant changes during the incubation.

4. Discussion

4.1 Microbial activity

This experiment was performed to examine the interaction between natural bacteria and phytoplankton in sub-Antarctic water. The different Fe treatments aimed to observe the response of this microbial community to different Fe scenarios. The initial incubation condition t_0 for the non-Fe addition cultures (low-Fe treatment) served as baseline. As intended, in most cases in our study, the initial bacteria and phytoplankton counts were low to avoid plateauing off too fast (visible in bacteria and diatom cells numbers in Table 2-1).

While the initial bacteria and cells numbers in A and C were comparable in the beginning and at the end of incubation, the bacteria number at t_{end} followed the trend C, A<B<C*. Set-up B was prepared with mixed seawater, and the growth rate of phytoplankton in this culture was slightly higher than in A. This indicates that the co-culture might positively influence the growth of phytoplankton. Additionally, the presence of natural bacteria in the dialysis bag, C*, seems to have significantly enhanced the phytoplankton growth in C relative to A. This result showed that the presence of natural bacteria indeed enhanced the growth of phytoplankton. Since the dialysis tubing let the bacterial exudates (i.e. siderophores) pass through but not the bacteria, the results also indicated that bacteria and phytoplankton might interact chemically and direct contact between bacteria and phytoplankton might not be required to enhance the growth of phytoplankton. Bacteria and diatom have been reported to interact in a specific area called the pychosphere, a region that extends outward from a single eukaryote or a cell colony. However, chemical signalling may also occur between bacteria and diatoms without physical contact, as also indicated by the current results. For instance, both bacteria and phytoplankton secreted lipid based and hydrophobic molecules (e.g. acyl homoserine lactones), as an auto-inducer to start chemical signaling that permit communication between specific taxa of

diatoms and bacteria (Fuqua and Greenberg, 2002). This chemical signal is allowing an association to be established thereby forming a mutualistic symbiosis (Amin et al., 2012a). However, further study is needed to resolve the detailed of microbial interaction via chemical exudation such metabolomics and/or proteomic analysis (Longnecker et al., 2015; Poulson-Ellestad et al., 2014) combined with the evaluation of specific growth rate of particular diatom and bacteria. Overall, our results indicate chemicals produced by the bacteria enhance growth of phytoplankton, while the physical contact is somewhat counterproductive.

In this study, macronutrients (PO_4, NOx and Si) were measured to assess the influence of these nutrients on the growth between treatments and/or among each incubation set-up. Since macronutrients were added to all bottles in the initial incubation, the initial cultures were not macronutrient limited. In addition, the lowest initial DFe concentration was 2.01±0.1 nmol/L, indicating that DFe background in the initial state of our incubations was not reflecting an Fe-limited environment. Hence, the effect of Fe limitation on phytoplankton growth with minimum bacteria interference (set-up A) could not be evaluated. Moreover, the different Fe treatments did not seem to have a measurable effect on the growth of phytoplankton, although the high-Fe treatment resulted in slightly higher cell number in set up A, B and C (Table 2-1).

However, the different Fe treatment seemed to affect phytoplankton physiological performance. The yield of photochemical quantum efficiency (Fv/Fm) indicates a physiological phase of *in-situ* phytoplankton populations. The measured Fv/Fm in this experiment was relatively low in the Fe-depleted treatments compared to treatments with Fe added. In general, the value of Fv/Fm <0.25, indicates that phytoplankton were experiencing physiological stress (McKay et al., 2005). A reduction in Fv/Fm due to lack of Fe has been reported in several studies (Suggett et al., 2009; Timmermans et al., 2005; Tsilinsky et al., 2018), which is also visible in our experiment. Consequentially, chl-*a*/cell ratios observed in low-Fe treatments were often lower compared to those in higher-Fe treatments (Figure 2-3b). The shortage of a micronutrient, such as Fe, is the dominant factor affecting the potential photochemical

reaction efficiency of photosystem II (Tsilinsky and Finenko, 2018), and can affect the photosynthetic performance of phytoplankton and/or the yielded biomass (Viljoen et al., 2018). Even though Fe is not in the chl-*a* itself, the chl-*a* biosynthesis pathway requires Fe. Thereby, Fe insufficiency may simply reduce the chl-*a* synthesis rate or the cell numbers (biomass), and vice versa (Xing et al., 2007).

Diatom-bacteria interaction also affects the DOC dynamics in the cultures. A study on the dissolved organic matter released in cultures of the marine diatom *Thalassiosira rotula* and natural bacteria reported that DOC concentrations typically decrease when phytoplankton and natural bacteria were present in the same medium, notably when bacterial numbers were high (Hans-Peter and Meinhard, 2007). This is in agreement with our result for set-up B, where mixed seawater was used as the culture medium. The DOC concentration sharply declined over time, indicating an *in-situ* DOC utilization by the presence of bacteria in the medium. In contrast, in the absence of bacteria, the DOC concentration was reported to continuously increase, reflecting less or no DOC removal and decomposition by bacteria (Hans-Peter and Meinhard, 2007). Since the seawater medium used in A and C set-up was intended to exclude natural bacteria, the DOC concentration theoretically is supposed to increase over time. However, in fact bacteria were present in both media and thus the DOC decreased or stayed relatively constant as the incubation progressed.

4.2 Dissolved iron and major nutrients

In our experiment, DFe declined as the incubation progressed. This result agrees with previous incubation experiment conducted (e.g., (Adly et al., 2015); Buck et al. (2010). Our results showed that the DFe drawdown is mostly concurrent with a decline in PO_4 and Si (King et al., 2012; Viljoen et al., 2018). Additionally, Viljoen et al. (2018) reported that during chl-*a* synthesis phytoplankton require Fe that is used for electron transport in addition to macronutrients that are needed for chlorophyll production. Despite the fact that 4 nmol/L of DFe was added to make an

Fe-enriched environment, the measured DFe concentration was less. Most likely, part of this DFe loss is bottle wall adsorption during the incubation. Such a wall adsorption effect is well known (e.g. Fischer et al. (2007)), where polycarbonate bottles have a relatively low affinity to Fe, but absorb Fe nonetheless. Even though bottles were conditioned by filling the bottles with the culture medium seawater followed by three times rinsing with the same water, apparently the wall adsorption effect should not be neglected. Besides wall adsorption, precipitation of DFe as particulate Fe onto cell surfaces or other particles in the incubation plays a role too.

Previous work from Hutchins et al. (1998) reported that diatoms tend to consume silicic acid and nitrate equally when ample Fe is available, ~2nmol/L or above (Bruland et al., 1991; Sunda and Huntsman, 1995). Diatoms have an absolute requirement for Si to build their outer cell wall, known as diatom frustules (Kröger and Poulsen, 2008). This explains the relatively large Si decline observed in the high-Fe treatment of A in which there was relatively little interference of natural bacteria. In the low-Fe treatment inside the dialysis bag, C*, Si concentration was slightly enhanced from t_0 to t_{end}, but not in C. This occurrence could be either the dialysis bag did not allow Si to pass, or it is measurement error or contamination of Si inside dialysis bag. In case the dialysis bag did not allow Si to pass, the se-tup is completely compromised given the idea of physical separation but chemical equilibrium. Moreover, the silica regeneration through dissolution of diatom silica was reported in earlier study (Bidle et al., 1999).

The PO_4 concentrations consistently decreased in all set-ups whether in low- or high-Fe treatments since both diatom and bacteria assimilate PO_4. These microbes interact competitively to obtain PO_4, and a field study conducted by Thingstad et al. (1993) showed that bacteria can outcompete diatom in assimilating PO_4 especially at low ambient PO_4 concentration. This explains our result of maximum PO_4 drawdown found in the high-Fe treatment of B, where both bacteria and diatom were present in the same medium.

4.3 Fe-binding ligand

There have been several studies addressing the linkage between ligand pools and phytoplankton growth (Buck et al., 2010; King et al., 2012; Mawji et al., 2011) through incubation experiments. Most of these studies started with macronutrients or Fe limitation. In this study, phytoplankton did not appear to be Fe-limited nor macronutrient-limited. Our results suggest that with the ambient DFe concentration in our medium, the production of strong Fe-binding ligands was not stimulated as the incubation progressed. Actually, ligands appear to have been degraded as the incubation progressed as the total Fe-binding ligands concentration declined in the incubation experiment (Figure 2-5b). The exception to this was the low-Fe treatment in C, and possibly the production of Fe-binding ligands was activated in response to the alteration of ambient DFe concentrations at t_{end}, 0.89 nmol/L in C. However, in low-Fe treatment in C*, concentration of organic ligands was slightly increased although DFe concentration was increased from 3.27 to 4.6 nmol/L. Siderophore-type Fe-binding ligands are typically produced as a microbial strategy designed to minimize diffusive loss while facilitating Fe acquisition (Boiteau et al., 2016). Adly et al. (2015) reported that ambient DFe levels of about 2-3 nmol/L can already trigger the production of Fe-binding ligands. Additionally, the field study also showed that siderophores-type ligands, ferrioxamines and amphibactins, are produced at coastal Fe concentration, 2.9±1.4 and 2.2±0.1 nmol/L (Gledhill et al., 2004) , thus the relatively high Fe levels in our experiment do not preclude siderophore production. Such siderophore production would be expected to increase the overall binding strength of the ligand pool, unless concurrent degradation of ligands masks this signal.

The log $K^{cond}_{Fe'L}$ ranged from 10.8±0.2 to 12.3±0.2. Excluding the maximum and minimum values which were observed only once, the log $K^{cond}_{Fe'L}$ values become relatively stable throughout the incubation experiment in the range of 11.0 to 11.8. These values fall into a weaker ligand class than the siderophores or siderophore-like ligand class (log

$K_{Fe'L}^{cond}$ > 12; Rue and Bruland, 1995). Lower log $K_{Fe'L}^{cond}$ in this study compared to log $K_{Fe'L}^{cond}$ of typical siderophores-like Fe-binding ligands may indicate that ligands have undergone chemical alteration and/or were passively generated following the stationary phase of microbial growth. Ligands may be released from cell lysis or as an excretion product such as domoic acid and transparent exopolymer substances (TEP) or exopolymeric substances (EPS). As reported by Norman et al. (2015), EPS ligands released by bacteria and phytoplankton primarily have weak affinity to Fe, log $K_{Fe'L}^{cond}$ in the ranged of 11.2 to 11.9, but in some cases affinity can be as those of siderophores, log $K_{Fe'L}^{cond}\geq$ 12. These EPS are released by microbes for many different functions, and EPS occur up to micromolar levels, particularly when chl-*a* is high. Because of its abundance, EPS are considered as a significant contributor to the ligand pool, thus potentially dominate the ligand pool (Hassler et al., 2017). Given that log $K_{Fe'L}^{cond}$ mostly in the range of 11.0 to 11.8, it is possible that organic ligands measured in this study are dominated by EPS rather than siderophores.

5. Conclusion

Our results showed that chemicals produced by bacteria enhance growth of phytoplankton, while the physical contact is somewhat counterproductive. Although the different Fe treatments did not seem to have a measurable effect on the growth of phytoplankton, the phytoplankton physiological performance (Fv/Fm) and Chl-*a*/cell ratio where affected. In the low Fe treatments, phytoplankton was experiencing physiological stress with a low chl-*a*/cell relative to the high-Fe treatments. Our results suggest that with the ambient DFe concentration in the medium, the production of strong Fe-binding ligands was not stimulated as the incubation progressed. Rather, ligands may be degraded over time as [L_t] declined from t_0 to t_{end} with log $K_{Fe'L}^{cond}$ values lower than the log $K_{Fe'L}^{cond}$ of siderophores, the strong Fe-binding ligands. Organic ligands detected in this experiment are likely mainly the degradation product of stronger

ligands, or microbial exudates classified as polysaccharides predominant compounds.

Chapter 3

Organic Fe speciation in the Hauraki Gulf, New Zealand

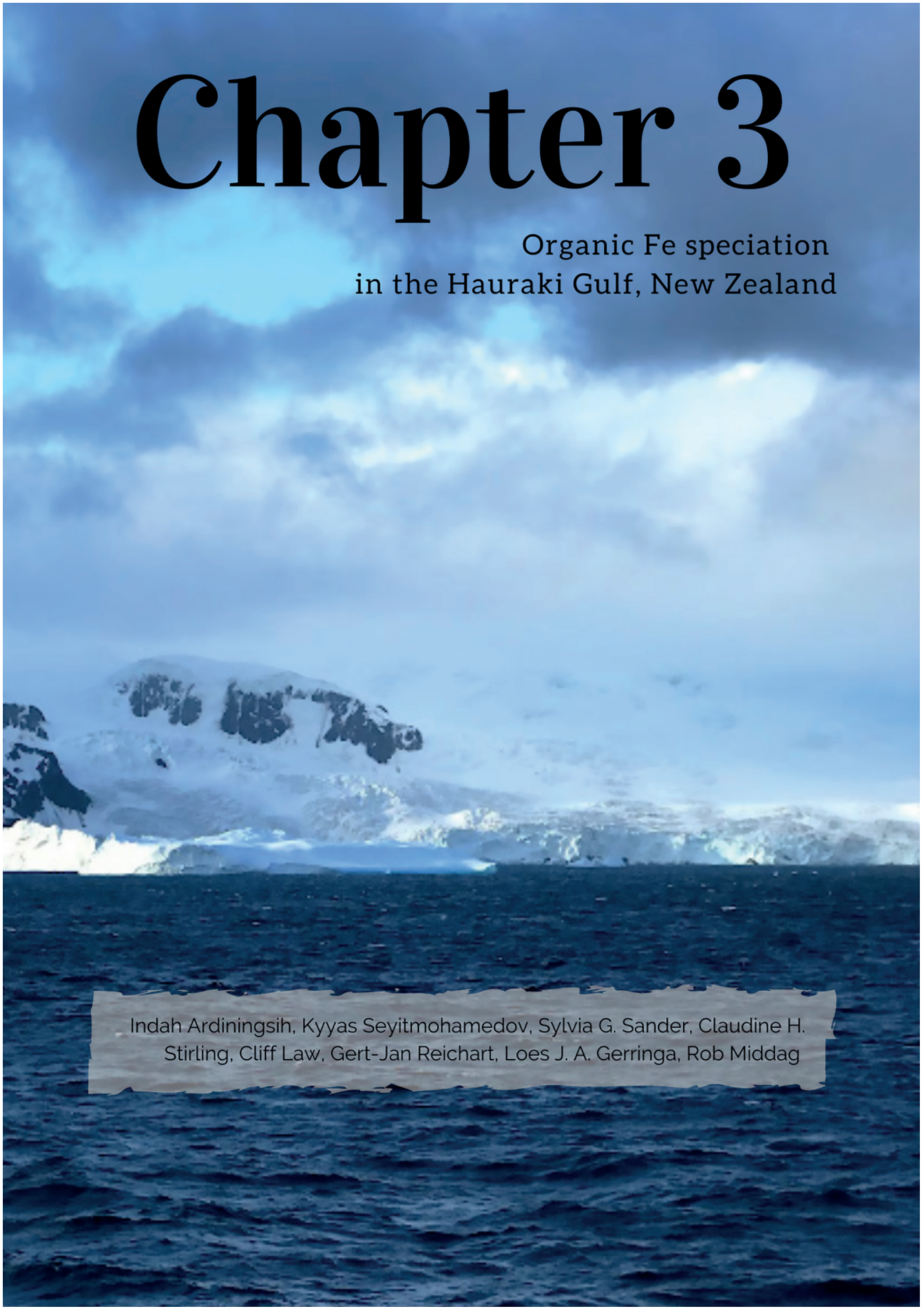

Indah Ardiningsih, Kyyas Seyitmohamedov, Sylvia G. Sander, Claudine H. Stirling, Cliff Law, Gert-Jan Reichart, Loes J. A. Gerringa, Rob Middag

Abstract

The marine biogeochemical cycling of Fe involves complex interactions between physico-chemical and biological processes. Organic ligands influence these interactions by chelating Fe, forming organic Fe species. These organic Fe species govern the dissolved-Fe (DFe) concentration in seawater. The net input and characteristics of Fe-binding ligands are influenced not only by global ocean circulation, but also regional water circulation that can be variable between seasons and years. Here we present results of organic Fe speciation along a transect from the shelf to the open ocean in the Hauraki Gulf in the north-east of the North Island of New Zealand across two consecutive years in the austral spring, 2015 and 2016. The shelf region is subjected to cross-shelf mixing and inter-annual variability with seasonal intrusion of oligotrophic water, which influences the Fe speciation. An electrochemical approach, competitive ligand exchange - adsorptive cathodic stripping voltammetry (CLE-AdCSV) using SA (5μM) was applied. Total ligand concentration ([L_t]) ranged from 0.69 to 7.53 nM eq. Fe in 2015, and from 0.95 to 5.23 nM eq. Fe in 2016. The high [Lt] (~2.5 to 7.5 nM eq. Fe) on the shelf during both years can be explained by the various ligand sources in the shelf region, including heterotrophic production, fluvial input, and remineralization processes. At the shelf break, [L_t] was still relatively high (~1.0 – 5.6 nM eq. Fe) during both years, possibly due to biological activity following a decline of the phytoplankton bloom. From the shelf-break to the open ocean, surface [L_t] decreased (~0.6 – 2.7 nM eq. Fe) along with decreased primary production. The passive generation of ligands via bacterial remineralization of organic matter appears to be a ligand source in deep water (>500m) from the shelf break towards the open ocean. The largest variation in excess ligand concentration, [L´] (~0.5 – 5 nM eq. Fe) was observed in surface water. The varying extent of the intrusion of the East Auckland Current (EAUC) onto the shelf, influences the net supply and removal of DFe and organic ligands, resulting in most variation and a high [L_t]/DFe ratio in the surface waters. The presence of organic ligands enables DFe to exist in high concentrations in the shelf region, implying there is potential for the export of DFe from the shelf to the open ocean. Our results suggest that remineralization processes are important for ligand production in a seasonally oligotrophic shelf region and the nearby open ocean. This finding points out the potential importance of remineralization processes for ligand production in similar oceanographic setting.

1. Introduction

Since the Fe hypothesis of J. Martin (Martin, 1990; Martin and Fitzwater, 1988) emerged, Fe has gained particular attention as an essential micronutrient that can limit phytoplankton growth in marine ecosystems (e.g.(de Baar, 1990; Hutchins and Bruland, 1998; Lelong et al., 2013). The limited availability of Fe in the open ocean is not only due to the limited supply of Fe, but also the low solubility of Fe with respect to (oxy)hydroxides in seawater (Liu and Millero, 2002; Millero, 1998). Complexation of Fe with organic ligands elevates the Fe solubility in seawater considerably (e.g., (Hunter and Boyd, 2007; Kuma et al., 1996). Dissolved Fe (DFe) bound to organic ligands appears to be bioavailable for primary producers or at least complexation with organic ligands increases the residence time of DFe (Hassler et al., 2015; Lis et al., 2015; Maldonado et al., 1999; Poorvin et al., 2011; Rijkenberg et al., 2008a). Organic Fe-binding ligands are ubiquitous in sea water (Hunter and Boyd, 2007) and play a significant role in the Fe biogeochemical cycle in the marine environment (Boyd and Ellwood, 2010b; Hunter and Boyd, 2007). Nevertheless, many aspects governing ligand distributions, sources and sinks are still poorly understood.

A research expedition to the Hauraki Gulf, located to the northeast of the North Island of New Zealand, was undertaken to study the trace metal speciation in this area in two consecutive years during Autumn (in May 2015 and in April 2016; Figure 3-1). This Hauraki Gulf is a semi-enclosed sea located downstream of the metropolitan city of Auckland, with over 1.6 million people the largest and fastest growing city in New Zealand. The increased anthropogenic input of metals to the ocean (Zeldis et al., 1999; Zeldis, 2004) due to industrialization, urbanization and agriculture, can influence primary productivity, and trace metal speciation (Aguirre et al., 2016; Boxberg, 2017; Seyitmuhammedov et al., in review; Zitoun, 2019), including Fe. Moreover, cross-shelf mixing processes can spread nutrients and other terrigenous materials over the continental shelf area, supporting the productive shelf ecosystem (Zeldis et al., 2004). The shelf area of the Hauraki Gulf is reported to have high primary production in the

austral spring, followed by secondary production over late spring and summer (Zeldis et al., 2015) as oligotrophic water seasonally encroaches into the shelf area (Sharples, 1997; Zeldis et al., 2004). The physicochemical conditions over the shelf are strongly affected by the physical shelf-circulation that is governed by seasonal wind-forced upwelling and downwelling dynamics (Zeldis et al., 2004). Such physical forcing has profound effects on the shelf ecosystem, making the shelf area sensitive to seasonal variability (Greig, 1990; Sharples et al., 2019). Seasonal variability influences phytoplankton assemblages, cell size and net biomass production over the shelf and adjacent areas (Baltar et al., 2018; Chang et al., 2003; Gall et al., 2011). Moreover, the shift from primary to secondary producer-dominated microbial assemblages associated with the seasonal transition, can lead to the production of dissolved organic carbon (DOC). A fraction of the marine DOC pool can form complexes with Fe, such that a fraction of DOC constitutes the Fe-binding ligand pool.

The organic ligand pool consists of a heterogenous mixture of organic compounds which have strong to progressively weaker affinity to chelate Fe (Hunter and Boyd, 2007; Macrellis et al., 2001). Little is known about the origin of ligands, but some mechanisms have been identified, such as active production of Fe-binding ligands as an Fe acquisition mechanism by marine microbes, including zooplankton and phytoplankton (Butler, 2005; Mawji et al., 2008). Direct microbial excretion of polysaccharides, such as exo-polymeric substances (EPS), also contribute to the organic ligand pool (e.g. Decho and Gutierrez (2017). Additionally, the remineralization of marine particulate matter has been found to produce Fe-binding ligands (Boyd et al., 2010a). Passive generation of organic ligands, resulting in e.g., humic substances (HS), has been reported to originate from degradation of organic matter, grazing and viral lysis (Laglera et al., 2019b; Poorvin et al., 2011; Sato et al., 2007; Slagter et al., 2016; Whitby et al., 2020). The HS ligands can be produced in the ocean, or in the terrestrial domain after which they are supplied to the ocean via riverine input.

The bulk concentrations and conditional stability constants of Fe-binding ligands can be determined with an electrochemical technique, competitive ligand exchange (CLE) – adsorptive cathodic striping voltammetry (AdCSV). With the CLE-AdCSV method, the total concentration ([L_t]) and average conditional binding ($K^{cond}_{Fe'L}$) of Fe-binding organic ligands can be obtained. Conditional stability constants of Fe-ligand complexes define the 'binding strength' of ligands at seawater conditions, and are usually given as its log values, i.e., log $K^{cond}_{Fe'L}$. The 'ability' of ligands to chelate Fe is defined by its side reaction coefficient, $\alpha_{Fe'L}$. The $\alpha_{Fe'L}$ ($K^{cond}_{Fe'L}$ *[L′]) is also known as the complexation capacity of ligands, which determines the competing strength of natural ligands to bind Fe versus adsorption on particles or precipitation as oxyhydroxides (Gledhill et al., 2017). Consequently, $\alpha_{Fe'L}$ defines the threshold of DFe present in the water column (Gledhill and Gerringa, 2017; Hudson et al., 2003). Concentrations of DFe that exceed the complexation capacity of natural ligands will potentially be transferred into particulate form (Achterberg et al., 2018). The importance of organic ligands in maintaining DFe levels in seawater has been shown in Fe speciation studies conducted at a global (e.g (Buck et al., 2017; Gerringa et al., 2015) and regional scale (e.g. (Kondo et al., 2007; Mahmood et al., 2015). Local processes, such as riverine input and shallow sediment resuspension, influence the supply and removal of organic ligands, and thus organic Fe speciation. Cross-shelf exchange in the current study region, intrusion of low-nutrient oceanic (oligotrophic) water onto the shelf, and other regional oceanographic processes during the seasonal transition, can have considerable influence on the characteristics of Fe-binding organic ligands. However, Fe speciation studies in such environmental circumstances are scarce.

To address these limitations, an Fe speciation study was conducted in the Hauraki Gulf, which serves as a natural laboratory to study Fe speciation in an area subjected to distinct temporal variability. Such Fe speciation data provides an important addition to the global dataset on Fe speciation, since regional processes influence the global cycle and are exemplary for other similar settings. Here we present results for Fe-

binding ligands and DFe from expeditions in the austral autumn of 2015 and 2016 along a transect from the shelf to the open ocean in the Hauraki Gulf. This study reports initial observations of sources and characteristics of Fe-binding ligands in this region. The results of this study reveal the importance of bacterial remineralization for the supply of ligands in subsurface water, and the impact of seasonal intrusion of oligotrophic ocean water into the shelf region, on the concentration of excess ligands that are not bound to Fe. The initial findings presented here represent a starting point to examine inter-annual variability of DFe speciation and to further study Fe cycling in this region. Furthermore, the observations of this study provide insight into the Fe cycle in this region that is dominated by heterotrophic production and/or affected by seasonal oligotrophic conditions.

2. Material and methods

2.1 Sample collection

Seawater samples were collected on-board *RV Tangaroa* during two cruises in the Hauraki Gulf, north-eastern New Zealand, in the austral autumn in two consecutive years (May 5 – 20th, 2015 and May 10 – 31st, 2016). Water column samples were collected as full depth profiles from 5 stations along a cross-shelf transect (CS; Figure 3-1) from the shelf (stations CS2 and CS7), across the shelf-break (station CS14) to the open ocean (stations CS19 and CS25).

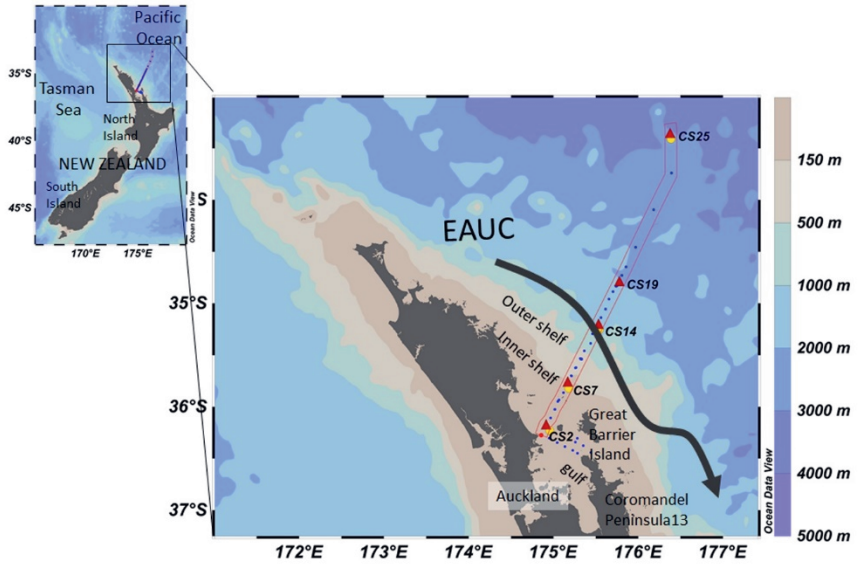

Figure 2-1. Map of the Hauraki Gulf with sampling stations. The red rectangle indicates the cross-shelf transect. The sampling stations during the 2015 campaign are indicated by red triangles, and the re-visited stations during the 2016 campaign are indicated by yellow dots. The arrow indicates the direction of the main current, the East Auckland Current (EAUC).

Samples for DFe and Fe-binding ligands were collected in 10-L Teflon coated Niskin samplers (General Oceanics Inc.) for the 2015 cruise. At the beginning of the 2015 cruise, the trace-metal-clean rosette malfunctioned. Therefore, the Niskin samplers were deployed instead using a manual messenger system attached to a Dyneema rope. The messenger system consisted of up to 5 Niskin samplers and 5 coated messenger weights. The rope was marked at regular depth intervals with colored tape. For the 2016 cruise, 12-L Teflon coated PVC GO-FLO bottles (General Oceanics Inc.) were used for sample collection of DFe and Fe-binding ligands. GO-FLO bottles were mounted on an autonomous trace metal clean rosette frame (General Oceanics model 1018). Sampling was done following standard sampling procedures for trace metals (Cutter et al., 2012). Immediately after recovery, the Niskin samplers (2015 cruise) or GO-FLO bottles (2016 cruise) were carried into a trace metal clean sampling-container, where sub-sampling and filtration was done under HEPA (High Efficiency Particulate Air) filtered air. Samples were filtered under N_2 pressure (~ 0.5

bar) using 0.2 μm filters (Sartrobran-300, Sartorius) connected to acid-cleaned polytetrafluoroethylene (PTFE) tubing.

Filtered samples were collected into acid-cleaned low-density polyethylene (LDPE, Nalgene) 500mL bottles for ligand samples and 60mL bottles for DFe samples. Before use, the LDPE sample bottles were pre-cleaned following a three-step cleaning protocols for trace element sample bottles (Middag et al., 2009). Filtered water for DFe analysis was acidified using concentrated hydrochloric acid (HCl) that had been purified using sub-boiling quartz distillation to give a final concentration of 0.024 M HCl (pH ~1.8), and then stored at room temperature until the analysis in the laboratories at NIOZ and the University of Otago (Dunedin, New Zealand). Filtered samples for Fe-binding ligand analysis were immediately stored at -20ºC and kept frozen during transport to the laboratory at the University of Otago.

Samples for chlorophyll-*a* (chl-*a*), DOC and macronutrients (NO_3 and Si) were collected using a regular 12 x 10L SBE 32 CTD rosette water sampler, and were filtered onboard through Whatman GF.F filters using a low vacuum (<200 mmHg). Samples for macronutrients were analyzed on-board, whereas samples for the analysis of chl-*a* were stored in 1.5 mL cryovials at -80°C until analysis in the laboratory at the National Institute of Water and Atmospheric Research (NIWA, Wellington, New Zealand). Samples for DOC analysis were acidified to pH = 2, and stored at 4ºC in pre-combusted glass tubes until analysis in the laboratory at NIWA. Hydrographic data at higher resolution was obtained from the regular CTD rosette sampler at 70 stations in 2015 and at 149 stations in 2016 along the CS transect.

2.2 Sample analysis

2.2.1 Analysis of dissolved-Fe (DFe)

Analysis of DFe for 2015 samples was conducted at the Royal Netherlands Institute for Sea Research (NIOZ, Texel, the Netherlands).

The DFe samples were pre-concentrated using an automatic SeaFAST system (SC-4 DX SeaFAST pico; ESI), and subsequently analyzed using High-Resolution Sector Field Inductively Coupled Plasma-Mass Spectrometry (HR-SF-ICP-MS; Thermo Fisher Element XR) with quantification via standard additions (Seyitmuhammedov et al., in review).

Analysis of DFe for 2016 samples was done at the Trace Metal Center of the University of Otago. Similarly, samples were analyzed using HR-SF-ICP-MS (Amtek Ltd Nu Attom) after pre-concentration using a SeaFAST system (Seyitmuhammedov et al., in review). For both years, measurement accuracy and reproducibility were monitored regularly by measuring standard reference materials (SAFe D1; GEOTRACES South Pacific (GSP) seawater) and values were within the range of the consensus values (SI Table 3-1). Results for in-house standards gave a method precision of ±2%. The average concentration of the overall method blank (SeaFAST and ICP-MS) was 0.05±0.02 nM, determined by treating ultrapure water as a sample. The detailed procedure for DFe (and other trace metals) analysis is described elsewhere (Seyitmuhammedov et al., in review).

2.2.2 Analysis of Fe-binding ligands

The CLE-AdCSV with the added ligand salicylaldoxime (SA) was used to determine the total concentrations ($[L_t]$) and conditional stability constant ($\log K_{Fe'L}^{cond}$) of Fe-binding organic ligands (Abualhaija and van den Berg, 2014; Abualhaija et al., 2015). Sample analysis was conducted on a voltammetric system which consisted of a BioAnalytical System (BASi) controlled growth mercury electrode equipped with an Epsilon 2 analyzer (BASi), and connected to an ECDsoft interface software. The electrodes in the voltammetric stand included a standard Hg drop working electrode, a platinum wire counter electrode and a double-junction Ag/AgCl reference electrode (3M KCl).

Prior to analysis, the frozen samples were brought to room temperature. Sub-samples of 10mL were pipetted into 14 Teflon (Fluorinated Ethylene Propylene, FEP; Savillex) vials that had been

conditioned to the planned Fe and SA concentration. Aliquots were buffered to a final pH = 8.2 with an ammonium-borate (Merck) buffer 0.1 M (final concentration 5mM), and titrated with Fe additions (0; 0.5; 0.1; 1.5; 2.0; 2.5; 3.0; 4.0; 5.0; 6.0; 8.0; 10 nM Fe – 0 and 10 nM additions were done twice). The competing ligand SA was added at a final concentration of 5 μM. After at least 8 hours (or typically overnight) of equilibration, the sample aliquots were sequentially transferred to a voltammetric cell and analyzed by AdCSV in duplicate scans at a deposition time of 90s (Table 3-1).

Table 2-1. Operating conditions of the CLE-AdCSV analysis for Fe speciation measurements

Operation condition	***the SA method***
mode	differential pulse
purge time	none
Deposition potential	0 V
deposition time	90 s
quiet time	10 s
Initial potential	-0.15 V
Final potential	-0.75 V
step potential	-0.006 V
Modulation amplitude	-0.03 V
scan rate	30 mVs^{-1}
pulse period	0.2 s
pulse amplitude	0.03 V
pulse width	0.005 s

The results were interpreted by fitting the data into a non-linear Langmuir model to obtain [L_t] and $K^{cond}_{Fe'L}$. Using the Langmuir model, the following assumptions need to be fulfilled: (1) equilibrium exists between all Fe(III) species, (2) the binding sites between Fe and natural ligands are in 1:1 coordination, and (3) the binding between Fe and natural ligands is reversible (Gerringa et al., 2014; Gledhill and Buck, 2012). The detailed theory on the calculation is described elsewhere (Gerringa et al., 2014).

The side reaction coefficient of SA defines the center of the detection window of the method (D_{SA}). The D_{SA} is given by the product of the concentration of SA and the conditional binding constant of SA. The conditional binding constant of SA was calculated with respect to inorganic Fe (Fe′), thus the inorganic Fe side reaction coefficient ($\alpha_{Fe'}$) was used to transform the conditional binding constant of SA with respect to Fe^{3+} ($K^{cond}_{Fe^{3+}(SA)}$) into the constant with respect to Fe′ ($K^{cond}_{Fe'(SA)}$). Using the hydrolysis constants of Liu et al. (1999) at salinity=36 and at pH of the analysis (pH=8.2), the logarithm of $\alpha_{Fe'}$ was determined to be 10.4 (Gerringa et al., in review), which is slightly different from the commonly used literature value of log $\alpha_{Fe'} = 10$ (Abualhaija and van den Berg, 2014; Hudson et al., 1992). The conditional binding constant of SA was calculated to be 5.94 (as logarithmic value, log $K^{cond}_{Fe'(SA)}$ = 5.94 or log $K^{cond}_{Fe^{3+}(SA)}$= 16.34), whereas Abualhaija and van den Berg (2014) obtained log $K^{cond}_{Fe'(SA)}$ = 6.5 or log $K^{cond}_{Fe^{3+}(SA)}$= 16.5. The resulting D_{SA} was 4.36 (log D_{SA} = 0.6; after Gerringa et al., in review) and the range of the detection window is approximately an order of magnitude above and below log D (log D = 0.6±1) (Apte et al., 1988; Laglera and Filella, 2015).

The Langmuir model was fitted using the R software package (Gerringa et al., 2014). A one ligand model showed the best fit to the data. The [L_t] is expressed in nM eq. Fe. The concentration of natural ligands not bound to Fe ([L′], excess ligands) was calculated based on the values of DFe, [L_t] and log $K^{cond}_{Fe'L}$. The $\alpha_{Fe'L}$ is defined as the product of [L′] and $K^{cond}_{Fe'L}$, via

$$K^{cond}_{Fe'L} = [FeL]/[Fe']*[L'] \quad (1)$$

$$\alpha_{Fe'L} = [FeL]/[Fe'] = K^{cond}_{Fe'L} *[L'] \quad (2)$$

where [Fe′] represents the inorganic Fe concentration. Furthermore, $\alpha_{Fe'L}$ represents the complexation capacity of ligands and is present as its logarithmic value, log $\alpha_{Fe'L}$ (Gledhill and Gerringa, 2017).

2.2.3 Analysis and calculation of other parameters

Chl-*a* was extracted from the GF/F filters using 90% acetone and the resulting extracts were analyzed using spectrofluorometry standard methods (A*10200H). DOC was determined using a high temperature catalytic oxidation total organic carbon analyzer (standard method: APHA5310B). The macronutrients NO_3 and silicate were analyzed with an Astoria Analyzer. Apparent Oxygen Utilization (AOU) is generated from the freeware Ocean Data View (ODV, Schlitzer (2018), where AOU is based on the difference between the calculated dissolved oxygen concentration assuming saturation and the actual observed oxygen concentration (from a sensor on the CTD).

3. Results

3.1 Hydrography of the study area

The detailed water circulation in the Hauraki Gulf region is described elsewhere (Chiswell et al., 2015; Greig, 1990; Sharples, 1997; Zeldis et al., 2004). Briefly, the surface water circulation in the Hauraki Gulf and adjacent shelf-slope system is predominantly controlled by the highly variable south eastward flowing East Auckland Current (EAUC). Seasonal upwelling over the shelf occurs in spring to early summer, and seasonal downwelling occurs in late summer. The periodic upwelling is crucial for the introduction of nutrient-rich water onto the shelf (CS2, CS7) (Chang et al., 2003; Zeldis, 2004).

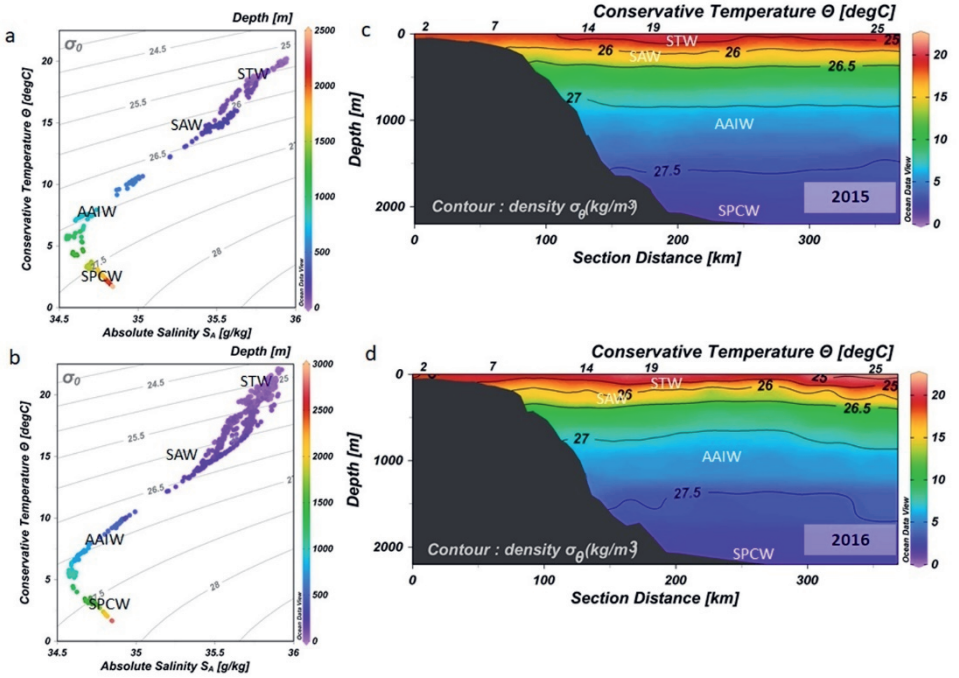

Figure 2-2. Hydrographic properties: Absolute salinity (S_A) vs. conservative temperature (Θ) with isopycnals and depth (m) in color scale (a) 2015 and (b) 2016. The distribution of Θ from (c) 2015 and (d) 2016, including isopycnals. The positions of the various water masses are indicated. The values of Θ and S_A were generated by ODV software from CTD data. Subtropical Water=STW, the Sub-Antarctic Water =SAW, the Antarctic Intermediate Water=AAIW, South Pacific Central Water =SPCW. Station numbers are indicated on top of the transects.

In this study, water masses were identified by plotting the conservative temperature (Θ) versus the absolute salinity (S_A; Figure 3-2a and 3-2b) (Tomczak et al., 2003), and definitions from Chiswell et al. (2015) were used. During the 2015 expedition, warm (16 – 20ºC) and high S_A >35.4 g/kg Subtropical Water (STW) occurred in the surface layer of all stations (Figures 3-2c and 3-2d). Near the shelf break (CS14) and toward the ocean (CS19 and CS25), Sub-Antarctic Water (SAW) was found underneath the STW. The SAW is relatively cold (Θ = 10 - 15ºC) and less saline (S_A 35 - 35.4 g/kg) compared to STW. Antarctic Intermediate Water (AAIW, S_A = 34.3 - 34.6 g/kg; σ >27.1 kg/m^3) was observed between 500 and 1300 m depth. Deeper than 1300 m, the South Pacific Central Water (SPCW) was

found, particularly at stations CS19 and CS25, which is characterized by $\Theta < 2^{o}C$. The hydrographic properties during both expeditions in 2015 and in 2016 were similar (Figures 3-2a and 3-2b).

3.2 Organic Fe speciation

On the shelf (CS2 and CS7), [L_t] and DFe were higher relative to the continental shelf break area (CS14) and the ocean (CS19 and CS25) in both years (Figures 3a-3f). For the 2015 expedition, [L_t] ranged from 0.69 to 7.53 nM eq. Fe and DFe ranged from 0.15 to 8.49 nM (Figures 3a - 3c). For the 2016 expedition, [L_t] ranged from 0.95 to 5.23 nM eq. Fe and DFe ranged from 0.12 to 2.51 nM eq. Fe (Figures 3d - 3f).

3.2.1 The shelf stations

At stations CS2 and CS7, for both years, [L_t] and DFe concentrations were higher near the sediment compared to surface samples (Figures 3-3a and 3b). In the 2015 samples, the maximum concentrations were especially high closest to the coast (CS2; [L_t] = 7.53 nM eq. Fe and DFe = 8.49 nM; Figures 3-3a) and DFe exceeded [L_t]. Concentrations decreased away from the shore. At station CS7, surface DFe concentrations were always lower than ~0.6 nM with [L_t] of 1.29 nM eq. Fe. In the 2016 samples, elevated [L_t] (3.45 nM eq. Fe) and DFe (2.51 nM) were also found at the deepest sampled depth at CS2 (Figure 3-3b). Further from the shore (CS7), surface DFe was always lower than 0.5 nM, and only increased close to the sediments, reaching up to 2.5 nM. Here, [L_t] remained high between 2.08 and 5.23 nM eq. Fe.

3.2.2 The station near the shelf-break

At the station near the continental shelf break, CS14, [L_t] ranged from 1.00 – 5.65 nM eq. Fe for both years (Figures 3-3c and 3-3d). In contrast to the shelf, the highest [L_t] was found in surface water at 20-30 m depth (2015: [L_t] = 5.65 nM eq. Fe; 2016: [L_t] = 4.15 nM eq. Fe), where DFe remained relatively low (0.12 – 0.99 nM; Figures 3-3e and 3-3f). For both

years, the concentration of DFe increased with depth and the surface concentration in 2016 was lower than for 2015 (DFe <0.2 nM versus 0.3 – 0.5 nM; Figure 3-3f).

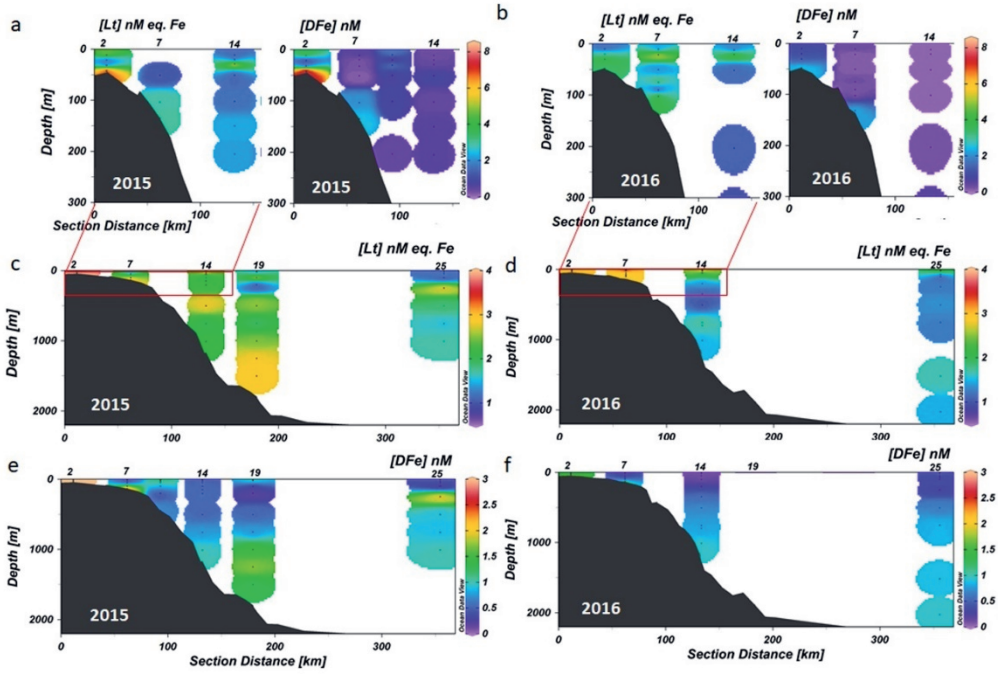

Figure 2-3. The distribution of total Fe-binding ligand [L_t] and dissolved-Fe (DFe) from both expeditions. DFe data is from Seyitmuhammedov et al. (in review) ; 2015 (a, c, e) and 2016 (b, d, f). Figures a and b are enlargements with respect to depth of c and d and e and f, respectively. Please note the scale difference between panels a, b and c, d, e and f. Station numbers are indicated on top of the transects.

3.2.3 The open ocean stations

In 2015, CS19 was sampled as a full depth station, whereas CS25 was only sampled from the surface to 1000 m depth. In 2016, ligand samples were only analyzed at station CS25. During the 2015 sampling campaign, [L_t] and DFe showed an increase with depth and reached highest values close to the seafloor at CS19 ([L_t] = 2.84 nM eq. Fe; DFe =1.71 nM). During the 2016 sampling campaign, relatively high [L_t] (1.33 – 2.60 nM eq. Fe) was observed at the station furthest from the coast (CS25). DFe was low near

the surface (0.14 – 0.70 nM) and increased towards the seafloor. With depth, [L_t] persisted at 1.3 – 1.6 nM eq. Fe (Figure 3-3b and 3-3d).

3.2.4 Organic ligand details

During the 2015 sampling campaign, [L´] varied from 0.48 to 5.19 nM eq. Fe (1.22±0.84 nM eq. Fe; N=34; Figure 3-4a), and during the 2016 sampling campaign [L´] varied from 0.49 to 5.09 nM eq. Fe (1.59±1.11 nM eq. Fe; N=24; Figure 3-4b). For both years, the highest variation of [L´] was found in STW. In 2015, [L´] in SAW was highly variable (~0.5 to 2 nM eq. of Fe) and reached 1.5 nM eq. Fe in deep water (SPCW; only one point). However, during 2016, in SAW as well as the deep waters, AAIW and SPCW, [L´] was relatively constant at about ~0.5 to 1 nM eq. of Fe. The ratio of [L_t]/DFe indicates the saturation state of ligands with Fe. Ligands are undersaturated when the ratio is above 1 and generally, in STW, ligands were less saturated than in deeper water masses (Figures 3-4c and 3-4d).

The log $K^{cond}_{Fe'L}$ and log $\alpha_{Fe'L}$ ranged over two orders of magnitude for both years, log $K^{cond}_{Fe'L}$ = 9.7 to 11. 8 (2015: 10.7±0.5; N=34; Figure 3-5a, and 2016: 10.5±0.5; N=24; Figure 3-5b) as did log $\alpha_{Fe'L}$ = 0.6 to 2.7 (2015: 1.6±0.5; N=34; Figure 3-5c and 2016: 1.3±0.4; N=24; Figure 3-5d). There was no distinct trend of log $K^{cond}_{Fe'L}$ and log $\alpha_{Fe'L}$ between water masses, or along the transect from the shore to the open ocean.

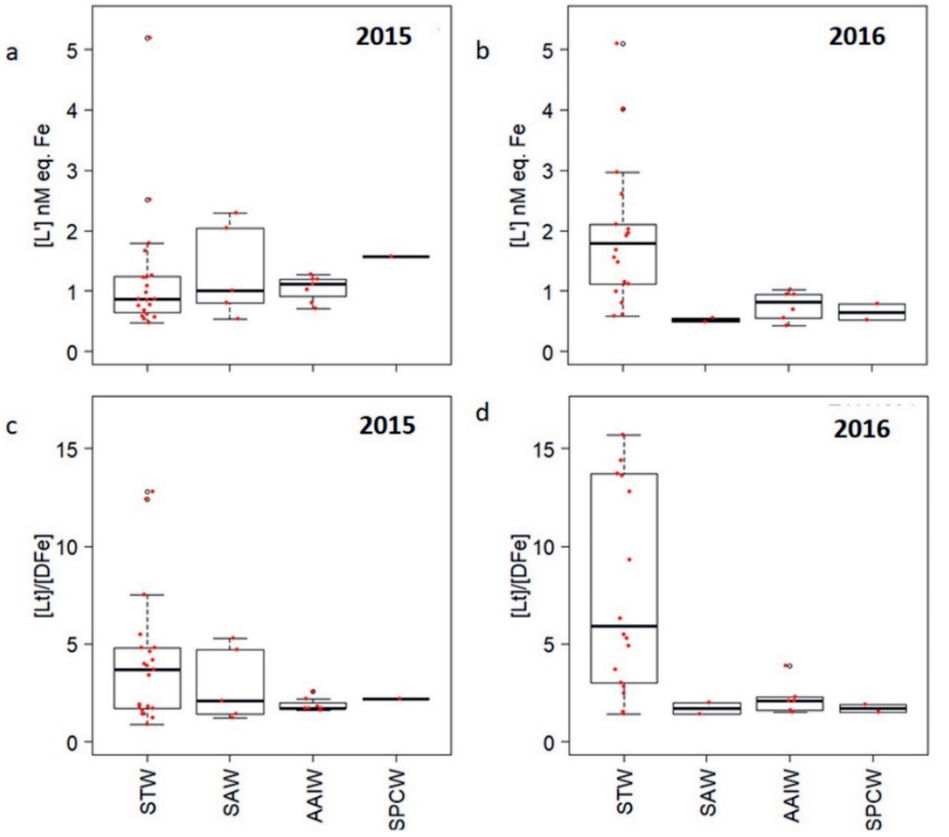

*Figure 2-4. Boxplot of (a, b) excess ligand concentrations [L´] and (c, d) the ratio of total Fe-binding ligand [L_t] over dissolved-Fe (DFe) categorized by water mass. The boxplots on the left are from the 2015 sampling campaign and the 2016 sampling campaign on the right. The water mass abbreviation as in Figure 3-2. The box contains the first and third quartiles, the whiskers are the range of data excluding any outliers. The thick horizontal lines in the boxes indicate the median value and the circles indicate the outliers that are 1.5 * interquartile range from the box.*

4. Discussion

A distinction between ligand groups could not be made in this study, and log $K_{Fe'L}^{cond}$ values varied within our detection window near the upper boundary (log D_{SA} = 0.6±1; 2015: log $\alpha_{Fe'L}$ = 1.6±0.5 and 2016: 1.3±0.4 ; Figures 3-5c and 3-5d). A large uncertainty in log $K_{Fe'L}^{cond}$ is inherent to the applied method and hampers the distinction between ligand groups and

direct comparison of the log $K_{Fe'L}^{cond}$ value among studies of organic ligands (Gerringa et al., (in review); Gledhill and Gerringa (2017).

4.1 The sources of organic Fe-binding ligands

Generally, DFe is predominantly present as organic Fe-ligand complexes in coastal seas and estuaries (e.g.(Buck and Bruland, 2007a; Buck et al., 2007b; Bundy et al., 2015; Laglera et al., 2011; Su et al., 2015)), shelves (Sander et al., 2015) and the open ocean (e.g.(Kondo et al., 2007; Rue and Bruland, 1995)). In this study, [L_t] and DFe concentrations appeared to decrease from the shelf, across the shelf-break and into the open ocean in both sampling years (Figures 3-3c – 3-3f), and in 2016, a significant correlation between S_A and [L_t] (R^2=0.17; F(1,26)=5.46; p=0.02, coef. correlation r = 0.41) and between S_A and DFe (R^2=0.19; F(1,40)=9.65; p<0.01, coef. correlation r = -0.44) was observed. Given that S_A typically increases from near shore region to the open ocean, the positive correlation between S_A and [L_t] can be an indication of sources of organic ligands from the neritic zone (i.e. shallow shelf sea), whereas the negative correlation is indicative of sources of DFe from land (i.e fluvial discharge) (Aguilar-Islas et al., 2016; Buck and Bruland, 2007a; Hunter and Boyd, 2007; Lippiatt et al., 2010; Seyitmuhammedov et al., in review; Zitoun, 2019), as discussed in more detail below.

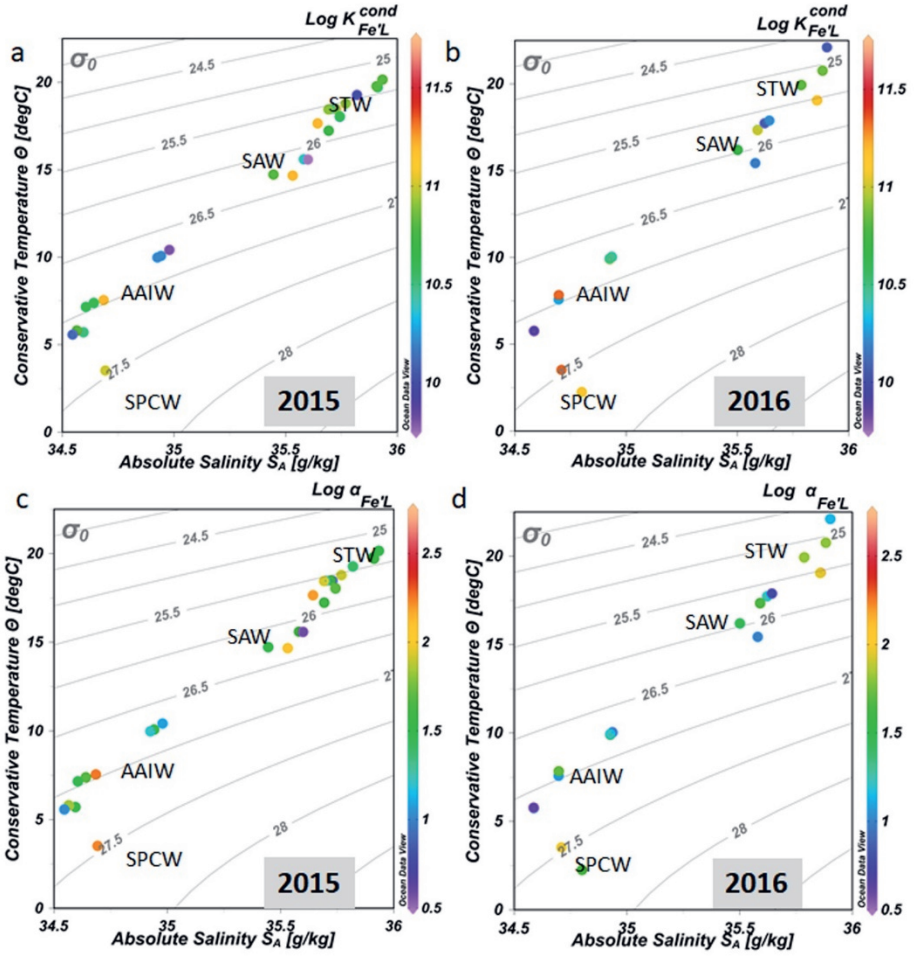

Figure 2-5. Θ-S_A diagrams with log $K^{cond}_{Fe'L}$ in color scale (a, b) and log $\alpha_{Fe'L}$ in color scale (c,d) for both expeditions (a, c from the 2015 sampling campaign; b, d from the 2016 sampling campaign).

4.1.1 The shelf area

At the shelf stations, [L_t] was higher than 1 nM eq. Fe over the entire water column (Figure 3-3a). Although the vertical profiles from both sampling years showed that deeper samples had higher [L_t] than surface samples, surface [L_t] was still relatively high (>1 nM eq. Fe). High microbial activity in the euphotic zone, is thought to be responsible for

high concentrations of organic ligands (>1 nM eq. Fe) in surface water (e.g. (Gledhill and Buck, 2012; Hunter and Boyd, 2007), and hence [L_t] is often associated with fluorescence and chl-*a*. The fluorescence data (Figures 3-6a and 3-6b) indeed indicates that the shelf region (CS2 and CS7) was productive during both sampling periods with relatively high chl-*a* (Figures 3-6c and 3-6d). Also, a higher [L_t]/DFe ratio in STW compared to deeper water masses was observed (Figure 3-4b and 3-4c), suggesting that uptake of Fe concurred with the production of Fe-binding organic ligands (e.g. Buck et al. (2007b). Such phytoplankton-sourced ligands are expected to contribute to the ligand pool, however, a significant correlation between [L_t] and fluorescence (R^2=0.19; F(1,26)=6.23; p=0.02) was only observed in 2016 but not in 2015. Although the relatively high [L_t] (1 – 2 nM eq. Fe) in STW still coincided with high fluorescence, the lack of a significant correlation between [L_t] and chl-*a* in 2015 suggests that phytoplankton did not appear to be the main source of ligands. The ligand pool in surface water of this shelf sea consisted of heterogenous organic molecules that were not only derived from phytoplankton sources, but also , could have other sources, such as from riverine discharge (e.g.(Buck et al., 2007b). There was no significant correlation between [L_t] and DOC in either year, although Seyitmuhammedov (2020) suggested that direct fluvial discharge was important in controlling the DFe distribution in the shelf region, particularly during the 2016 campaign. Assuming that riverine input also supplies organic ligands (e.g.(Buck et al., 2007b), the fluvial discharge can contribute to the ligand pool on the shelf, in addition to ligands produced *in situ*.

Based on annual observations of the water circulation in the Hauraki Gulf and the shelf sea (Sharples, 1997; Zeldis et al., 2004), a south-westerly wind direction favors the shoreward progression of the EAUC (Sharples and Zeldis, 2019; Zeldis, 2004), leading to intrusion of oligotrophic, low-macronutrient STW into the shelf area (Figure 3-7a and 3-7b). In such oligotrophic water, organic matter produced by primary producers is re-mineralized by heterotrophic prokaryotes throughout the water column (e.g. (Boyd et al., 2010a; Calleja et al., 2019; Ibisanmi et al., 2011). This microbial remineralization forms a second source of organic

ligands in addition to primary production (Burkhardt et al., 2014). Supply of Fe-binding ligands and DFe from the shelf-sediment is also expected, as was confirmed by the increase of [L_t] and DFe towards the shelf-sediments in both sampling years (Figures 3-3a and 3-3b). Given that the inner shelf area is relatively shallow (~50 m), it is also possible that sediment resuspension followed by mixing due to upwelling (Sharples and Zeldis, 2019) resulted in a flux of ligands and DFe into the overlying water column. The sediment resuspension and remineralization processes, are both possible sources of Fe-binding ligands in the subsurface and bottom layers of the water column of the shelf area, as was also observed for copper-binding ligands (Zitoun, 2019). The high concentration of organic ligands can keep Fe in the dissolved form, making it possible for DFe to be present in much higher concentrations over the shelf compared to open ocean regions (Seyitmuhammedov et al., in review). The high Fe and organic ligand concentrations in this shelf sea highlight the potential for transport of DFe from the shelf to the open ocean. Since Fe bound to organic ligands stays in solution longer, organic complexation increases the possibility of Fe-ligand complexes to be transported further away from its sources (Gerringa et al., 2015). Thus, the supply of DFe from shelf regions, specifically shelf sediments, could be an important factor in global Fe cycling as suggested previously (Shi et al., 2019). We postulate that supply of Fe from shelf regions to the open ocean is intimately linked to the dynamics of ligand production where notably microbial remineralization might play an important role (see section below).

4.1.2 Near the shelf break

In both years, maximum [L_t] (2015: 5.65 nM eq. Fe; 2016: 4.15 nM eq. Fe) was found near the surface at 20-30 m (Figures 3-3b and 3-3c) near the shelf break. Below this maximum until ~200m depth, [L_t] remained high (>1.5 nM eq. Fe), whereas fluorescence (Figure 3-6a and 3-6b), chl-*a* concentration (0.1 mg/m^3; Figures 3-6c and 3-6d) and DFe (0.1 – 0.8 nM) were low. The elevated [L_t] at low DFe with low biomass could be indicative of the remnants of a prior bloom. The consumption of phytoplankton by grazers as well as cell lysis and viral lysis can increase

total ligand concentrations (Laglera et al., 2019b; Poorvin et al., 2011; Sato et al., 2007; Slagter et al., 2016), whereas DFe could be taken up again relatively quickly within a day followed by export down the water column in particulate form. Polysaccharides are an important component of the Fe-binding ligand pool, and are expected to be released into the water column, either as polysaccharides or EPS (Decho and Gutierrez, 2017; Hassler et al., 2011), through exudation processes, cell lysis or viral lysis (Poorvin et al., 2011; Slagter et al., 2016) following the collapse of phytoplankton blooms. The collapse of a bloom in the area is also indicated by a lack of correlation between chl-*a* and DOC (Zitoun, 2019), which suggests non-planktonic sourced DOC at the time of sampling. The fact that DOC was slightly elevated in the upper 100m of the water column near the shelf break (CS14; Figure 3-6e and 3-6f), implies that productivity here is related to heterotrophic production instead of autotrophic (i.e phytoplankton) production. Overall, (post-)bloom microbial processes can be sources of Fe-binding ligands, and thus are a plausible explanation for the surface [L_t] maximum at low chl-*a* and DFe at station CS14 in this study.

High DOC concentrations existed in surface water on the shelf and across the continental shelf-break (Figure 3-5f), where [L_t] was relatively higher in 2016 compared to in 2015. In late summer, stratification usually intensifies (Zeldis, 2004) and the combined effect of strong stratification and hydrodynamic changes (i.e downwelling dominance, sea surface temperature) during the seasonal transition, has a substantial effect on the chemical characteristics and thus biological structure (i.e. microbial community composition) in the Hauraki gulf region (Chang et al., 2003; Zeldis, 2004). These changes favor dinoflagellates and pico-phytoplankton over larger diatoms and shift the marine ecosystem from autotrophy to heterotrophy (Baltar et al., 2018; Chang et al., 2003; Zeldis, 2004). The ecosystem shift into heterotrophy is followed by an increase of the bacterial assimilation of organic matter (Baltar et al., 2018), supplying organic ligands (Laglera et al., 2019b). In the deeper water column, advection of water along the slope and/or export of ligands from the shelf towards the open ocean seems to supply ligands at mid-depth near the

continental slope (CS14). The trend towards more positive values of AOU (Figures 3-7c and 3-7d) indicates oxygen consumption by heterotrophic processes (Robinson, 2019) and that bacterial remineralization occurred in the water column, potentially leading to the release of DFe (Seyitmuhammedov et al., in review), and passive generation of organic ligands (Zitoun, 2019). Indeed, both [L_t] and DFe at the station near the shelf-break (CS14) during both years increased with increasing depth, most likely due to remineralization processes. Prior studies of shelf regions that are subject to seasonal oligotrophic conditions are limited. Typically, oligotrophic ocean regions are heterotrophic with little remineralization (Duarte et al., 2013; Marañón et al., 2003), however, our data suggests that remineralization could be an important process for ligand production in seasonally oligotrophic continental-shelf water.

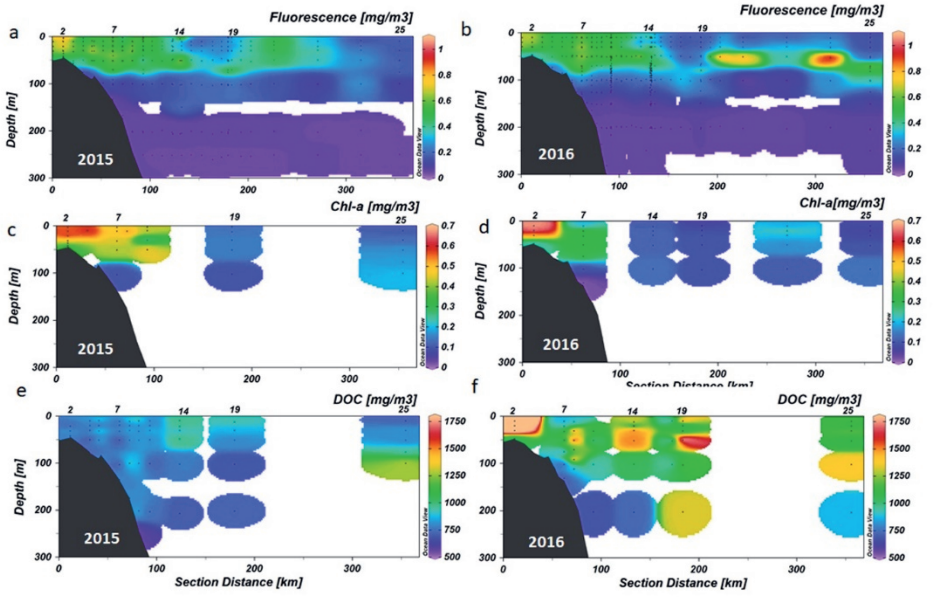

Figure 2-6. The distribution of fluorescence (a, b), chlorophyll-a (c, d) and dissolved-organic carbon (e, f) in the upper 300m depth for both expeditions; the 2015 sampling campaign on the left and the 2016 sampling campaign on the right. Station numbers are indicated on top of the transects.

4.1.3 Open ocean

From the shelf-break further into the open ocean, surface [L_t] decreased. Based on fluorescence (Figures 3-6a and 3-6b), less primary productivity occurred in this region relative to the shelf area at the time of sampling, with low chl-*a* at CS19 and CS25 (Figures 3-6c and 3-6d). However, the DOC concentrations were relatively high, particularly in the upper 100m of the water column during the 2016 sampling period (Figure 3-6f). As detailed above, elevated surface DOC indicates the dominance of heterotrophic production. Moreover, incubation experiments, conducted during the same expedition (Baltar et al., 2018), revealed that hydrocarbon-degrading bacteria were present in the open ocean of this study region. Towards the deep ocean, remineralization is also apparent as more positive AOU values (Figures 3-7a and 3-7b) and higher levels of nitrate (Figures 3-7c – 3-7d). However, some remineralization in the open ocean did not occur locally, but during the lifetime of the water mass (i.e., between its formation and transport to the study location), and therefore, AOU values and the nitrate levels do not necessarily represent local remineralization at the particular sampling location. Nevertheless, the high DOC levels that coincided with the presence of hydrocarbon-degrading bacteria at our sampling location suggest that local remineralization also plays a role in the production of organic ligands, but the exact fraction produced locally is impossible to distinguish. Any DFe released from remineralization benefits the hydrocarbon-degrading bacteria, which in deep water, appeared to be a key competitor in a trace metal addition remineralization experiment (Baltar et al., 2018). As such, hydrocarbon-degrading bacteria could play an important role in both ligand production as well as Fe cycling. In addition to ligand production in the water column, the continental slope sediments seem to supply ligands, as an increase in [L_t] near the slope sediment at CS19 was observed, particularly in 2015. Our data, combined with the results of the incubation experiments from the same expeditions, suggest that heterotrophic production could be a major source of Fe-binding ligands in the open ocean area where notably

local remineralization processes could provide a considerable contribution.

4.2 Organic Fe-binding ligands characteristics

The largest variation of log $K_{Fe'L}^{cond}$ was observed in STW in both years, and is likely explained by the various possible sources of ligands in surface water (Gledhill and Buck, 2012), as discussed above. Furthermore, removal of DFe from surface water can occur via biological uptake (Buck and Bruland, 2007a; Gledhill and Buck, 2012), and at the same time, organic ligands are often passively released. Such production of ligands coinciding with biological uptake of DFe results in a high ratio for $[L_t]$/DFe in surface water (Figures 3-4c and 3-4d). The high $[L_t]$/DFe ratio is particularly apparent in STW during the 2016 campaign, which is most likely related to high surface primary production and more prominent intrusion of EAUC in 2016 (Figures 3-2c and 3-2d). The profound EAUC intrusion presumably resulted in dominance of low DFe oceanic water over the shelf (Figure 3-3b; (Seyitmuhammedov, 2020), whereas the input of Fe from anthropogenic sources from industrialization, urbanization and agriculture (Aguirre et al., 2016; Boxberg, 2017) maintained high primary production near shore. $[L_t]$ was also maintained at relatively high concentrations, most likely due to a combination of *in situ* production and fluvial input of ligands. The primary production and profound intrusion of EAUC, therefore, resulted in a high ratio of $[L_t]$/DFe in STW during the 2016 campaign.

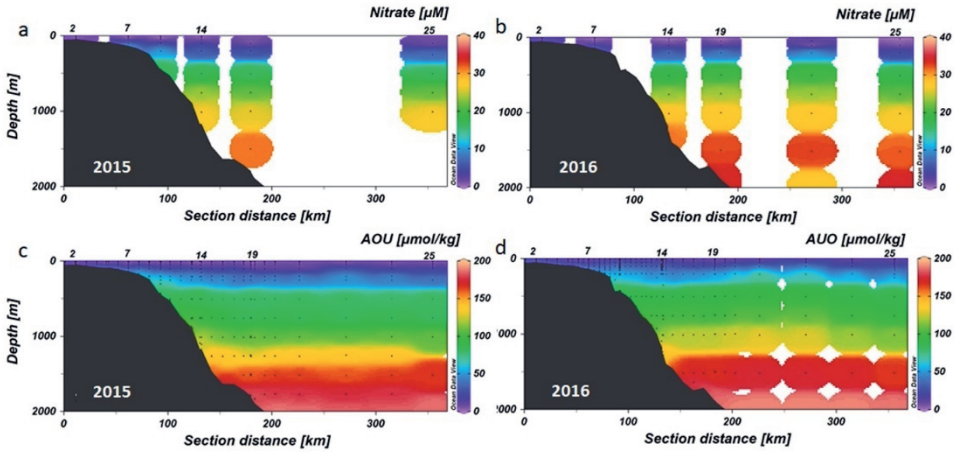

Figure 2-7. The distribution of nitrate a, b) and Apparent Oxygen Utilization (AOU in c, d). AOu was calculated using the ODV software (Schlitzer, 2018) based on oxygen concentration, temperature, salinity and depth from CTD sensor data. Station numbers are indicated on top of the transects.

Numerous processes in surface water involving Fe supply and removal influence [L´], and hence, most variation in [L´] was observed in STW (Figures 3-4a and 3-4b). Besides *in situ* production of organic ligands, fluvial input from shore is another possible ligand source for surface waters (Zitoun, 2019), as well as trace metals such as Fe (Seyitmuhammedov et al., in review). The release of Fe from an anthropogenic source could fill the binding sites of organic ligands, decreasing [L´] in surface waters in the shelf area closest to land. Atmospheric input of Fe was reported after dust deposition events in the open ocean (Rijkenberg et al., 2008b), but it does not seem to supply organic ligands, and thus has less effect on [L_t]. Input of Fe from atmospheric deposition was also suggested during our expeditions (Seyitmuhammedov et al., in review). Such Fe input without a coinciding ligand source could thus also have contributed to the decrease in [L´] in STW, since dissolution of aeolian Fe could fill the available binding sites of ligands (Wagener et al., 2008), [L´] as a buffer to bind additional input of Fe. Therefore, changes in [L´] can be a good indicator to observe Fe input in the absence of a coinciding ligand source or input of ligands in the absence of an Fe source. For example, in subsurface SAW waters, [L´] was

within a similar range as in STW during 2015 (Figure 3-4a). In contrast, [L´] in SAW during 2016 only displayed small variation within a range similar to deeper water masses (Figure 3-4b). The differing variability of [L´] in SAW between sampling years is possibly related to a varying extent of cross-shelf water mixing, which affects the distribution and concentration of both [L_t] and DFe.

Typically, [L´] decreases with depth (Buck et al., 2017; Slagter et al., 2017; Thuróczy et al., 2011b), as observed in the 2016 campaign (Figure 3-4b). However, some local exceptions instead show an increase of [L_t] in the water column near the seafloor (Buck et al., 2017; Gerringa et al., 2015), and an increase in [L_t] near the bottom sediments can coincide with an increase in [L´], which is similar to our results, with elevated [L´] near the bottom in SPCW in 2015. Previous work (Buck et al., 2017; Gerringa et al., 2015) showed that such an exception, an [L_t] maxima associated with an increase in [L´] near the seafloor, is likely associated with hydrothermal vent input. However, the variation of [L´] in the SPCW between years in this study is difficult to explain without higher data resolution (*i.e* more data points in the deep water) or without direct evidence for the influence of hydrothermal vent input in this particular region. Therefore, the varying [L´] in the SPCW between years remains unresolved.

The commonly observed decrease in [L´] with depth is consistent with more saturated ligands that are usually found in the deep waters (Gerringa et al., 2015; Thuróczy et al., 2011b), which could be related to refractory DOC at depth (Hassler et al., 2020; Laglera et al., 2019a; Whitby et al., 2020) due to particle scavenging (Slagter et al., 2017; Thuróczy et al., 2011b). These ligands, as a refractory component of the deep ocean DOC pool, are expected to have a relatively long residence time within years (Gerringa et al., 2015). Therefore, DFe bound to such organic ligands can be subjected to long range transport, as was previously suggested for Fe and ligands transported with North Atlantic deep water (Gerringa et al., 2015). We postulate that with such relatively long residence times, DFe-ligand complexes are not only found in the deep water of the open ocean, but also occur in the shelf sea of the Hauraki Gulf, and thus support the

shelf to open ocean DFe export. Notably, in our data, there was no distinct trend of the complexation capacity of ligands between water masses, or along the transect from the shore to the open ocean, and log $\alpha_{Fe'L}$ values remained high by the same order of magnitude (Figure 3-5c and 3-5d) in both years. This result implies that a portion of organic Fe-binding ligands are associated with the more stable refractory DOC and such ligands are found throughout the water column, maintaining a high complexation capacity for Fe (Hassler et al., 2020). These ligands likely play a critical role to maintain the ocean DFe inventory, as previously suggested (Whitby et al., 2020).

To summarize, the supply of organic ligands involves the complex interplay between fluvial discharge, autotrophic (i.e phytoplankton) and heterotrophic production, as well as sediment resuspension over the shelf and continental slope. As observed in other ocean regions, surface sources are dominated by biological activity, with potential additional input of ligands from fluvial discharge on the shelf. Towards the open ocean, heterotrophic production via organic matter remineralization was more apparent. The local hydrological processes, which vary between years, also play a role in ligand characteristics. The varying extent of oceanic water intrusion to the shelf between years affects the distribution and concentration of DFe and [Lt], influencing [L´] in surface water. In order to gain a better understanding of the seasonal variability of DFe speciation, higher temporal resolution data of DFe speciation is required, particularly in the season when remineralization is at its peak.

5. Conclusions

Numerous ligand sources over the shelf, including surface biological activity, fluvial discharge, input from sediments and remineralization, resulted in high [L_t] (2.08 to 5.23 nM eq. Fe) in the Hauraki Gulf region. Elevated [L_t] enabled DFe to persist on the shelf, increasing the feasibility for DFe export from the shelf region to the open ocean. Despite the oligotrophic conditions during the austral autumn sampling period, the surface waters of the Hauraki Gulf region are considered to be productive

and support (heterotrophic) microbial processes. As a result, large variations in [L´] and the [L_t]/DFe ratio were observed in STW. Near the shelf break, the collapse of a previous phytoplankton bloom was probably responsible for relatively high [L_t] (CS14; 1.00 – 5.65 nM eq. Fe). The relatively high DOC concentrations (>500 mg/m^3) due to heterotrophic activities, and the increase in AOU in deeper water (>500 m depth) at CS14 suggests that remineralization of organic matter could be an important process for the production of ligands in seasonally oligotrophic shelf regions. In the open ocean, remineralization seemed to be a major source of organic Fe-binding ligands where local remineralization could be an important contributor.

The intrusion of oceanic water onto the shelf affects the distribution and concentration of both [L_t] and DFe, indirectly affecting [L´] in surface water. Changes in [L´] could be a good indicator to observe differences in Fe input, if DFe input does not coincide with any ligand sources. Organic ligands in the deep-water masses could be associated with a refractory component of the deep ocean DOC pool. The complexation capacity of organic ligands, log $\alpha_{Fe'L}$, remains relatively high throughout the water column. Such a relatively high log $\alpha_{Fe'L}$ implies that organic ligands with a high complexation capacity for Fe are able to maintain DFe at high levels over the water column.

The elevated concentrations of both ligands and Fe imply there is potential for offshore transport of dissolved Fe to the open ocean where Fe can be an important driver of primary productivity. Further research is required to determine if such transport regularly occurs, how far it reaches into the open ocean, and if it affects open ocean primary productivity, but shelf regions dominated by remineralization and associated ligand production could play a more important role in organic ligand production than previously recognized.

Supplementary

Supplementary Table 2-1. Results for DFe analyses of reference materials. The consensus values of May 2013 were obtained from http://www.geotraces.org/ (data was accessed in June 2020).

Analysis of DFe	Reference Material	Consensus value	Reported value
2015 samples	SAFe D1 186	0.69± 0.04 nM	0.72± 0.08 nM (n = 3)
	SAFe D1 23	0.69± 0.04 nM	0.68± 0.02 nM (n = 3)
	GSP 239	0.15± 0.04 nM	0.15± 0.09 nM (n=13)
2016 samples	SAFe D1-262	0.69± 0.04 nM	0.73 ± 0.02 nM (n = 6)

Acknowledgments

The authors would like to thank NIWA, NIWA Vessels Management, RV *Tangaroa* officers, crew members and all the participants on both expeditions. This project was funded by the New Zealand Ministry of Business, Innovation and Employment (MBIE) to NIWA's Strategic Science Investment Fund (SSIF) for the "Ocean Flows and Productivity" programme in NIWA's Coasts & Oceans Centre. IA is funded by Indonesia endowment fund for education (LPDP) and KS is funded by a University of Otago PhD Scholarship. Measurements of DFe concentration at NIOZ were funded by the department of Ocean Systems, and analyses of DFe at the University of Otago were funded by NIWA (Core Funded Project Contracts COOF1902 and COOF2002).

Chapter 4

Natural Fe-binding organic ligands in Fram Strait and over the northeast Greenland shelf

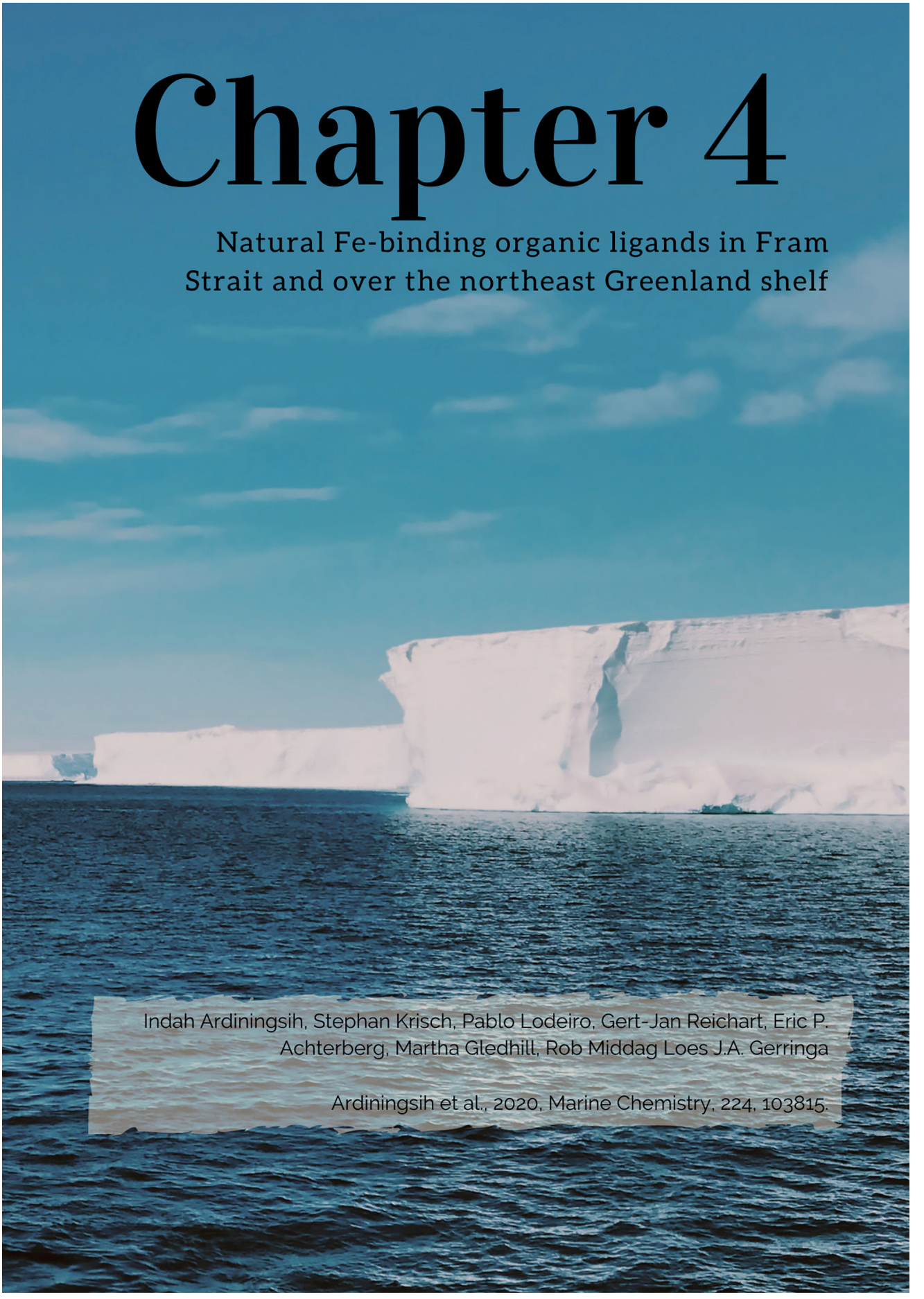

Indah Ardiningsih, Stephan Krisch, Pablo Lodeiro, Gert-Jan Reichart, Eric P. Achterberg, Martha Gledhill, Rob Middag Loes J.A. Gerringa

Ardiningsih et al., 2020, Marine Chemistry, 224, 103815.

Abstract

There is a paucity of data on Fe-binding ligands in the Arctic Ocean. Here we investigate the distribution and chemical properties of natural Fe-binding ligands in Fram Strait and over the northeast Greenland shelf, shedding light on their potential sources and transport. Our results indicate that the main sources of organic ligands to surface waters of Fram Strait included primary productivity and supply from the Arctic Ocean. We calculated the mean total Fe-binding ligand concentration, [L_t], in Polar Surface Water from the western Fram Strait to be 1.65±0.4 nM eq. Fe. This value is in between reported values for the Arctic and North Atlantic Oceans, confirming reports of north to south decreases in [L_t] from the Arctic Ocean. The differences between ligand sources in different biogeochemical provinces, resulted in distinctive ligand properties and distributions that are reflected in [L_t], binding strength (log $K^{cond}_{Fe'L}$) and competing strength (log $\alpha_{Fe'L}$) of ligands. Higher [L_t] was present near the Nioghalvfjerdsfjorden (79N) Glacier terminus and in the Westwind Trough (median of [L_t] = 2.17 nM eq. Fe; log $K^{cond}_{Fe'L}$ = 12.3; log $\alpha_{Fe'L}$ = 3.4) than in the Norske Trough (median of [L_t] = 1.89 nM eq. Fe; log $K^{cond}_{Fe'L}$ = 12.8; log $\alpha_{Fe'L}$ = 3.8) and in Fram Strait (median of [L_t] = 1.38 nM eq. Fe; log $K^{cond}_{Fe'L}$ = 13; log $\alpha_{Fe'L}$= 3.9). However, organic ligands near the 79N Glacier terminus and in the Westwind Trough were weaker, and therefore less reactive than organic ligands in the Norske Trough and in Fram Strait. These weaker ligands, although more abundant than in the Fram Strait, reduce overall Fe solubility in waters transported from the 79N Glacier to Fram Strait. The lower ligand binding strength in the outflow results in a higher inorganic Fe concentration, [Fe′], which is more prone to precipitation and/or scavenging than Fe complexed with stronger ligands. Ongoing changes in the Arctic and sub-Arctic Oceans will influence both terrestrially derived and *in-situ* produced Fe-binding ligands, and therefore will have consequences for Fe solubility and availability to microbial populations and Fe cycling in Fram Strait.

1. Introduction

The Arctic region is undergoing rapid environmental changes (Gascard et al., 2008; IPCC, 2014), including permafrost (Schuur et al., 2015) and ice-sheet melt (Ekwurzel et al., 2001). The environmental alteration induced by climate changes will influence the biogeochemical cycle of many elements, including iron (Fe), an important micronutrient regulating the dynamics of primary productivity (Boyd et al., 2000; de Baar, 1990; Martin and Fitzwater, 1988; Rijkenberg et al., 2018).In the shelf-dominated Arctic Ocean, the Polar Surface Water (PSW) is strongly influenced by runoff from Eurasian rivers with waters reaching the central basin via the Transpolar Drift (TPD)) (Gascard et al., 2008; Gordienko et al., 1969), and lateral transport over the shelf areas. The runoff introduces organic matter, fluvial sediment, and other terrigenous materials (Ekwurzel et al., 2001; Klunder et al., 2012; Measures, 1999). These materials contribute organic ligands of terrestrial origin, mainly humics humics (Laglera et al., 2019a; Slagter et al., 2019). The organic ligands stabilize Fe in the dissolved form, and prevent Fe from precipitating (Kuma et al., 1996; Millero et al., 2002) thereby enabling a substantial amount of dissolved-Fe (DFe) to be present in PSW (Klunder et al., 2012; Rijkenberg et al., 2018; Slagter et al., 2017). Determining the complexation of Fe with organic ligands is, thus, a crucial component of Fe biogeochemistry. The PSW, enriched in DFe bound to terrestrially derived organic ligands as well as ligands produced in the Arctic Ocean, can be transported out of the central Arctic via Fram Strait (Laukert et al., 2017; Slagter et al., 2019), a main gateway for heat and water mass exchange between the Arctic Ocean and the Nordic Seas (Greenland Sea, Norwegian Sea and Iceland Sea) (Rudels et al., 2005; Rudels et al., 2015). In the vicinity of Fram Strait, the Nioghalvfjerdsfjorden (79N) Glacier terminates on the northeast Greenland shelf, where the Norske Trough and Westwind Trough are located. The ongoing changes in the Arctic and sub-Arctic Oceans will influence the sources of Fe-binding organic ligands, and therefore have consequences for DFe supply and transport, particularly in Fram Strait. However, there is a paucity of data to

comprehensively assess the effect of global climate change on the biogeochemical cycle of DFe as well as associated feedback mechanisms.

Iron is present at sub-nanomolar levels in oceanic water due to its low solubility and low supply rate (Liu and Millero, 2002), limiting primary productivity in approximately one third of the global ocean (Boyd et al., 2000; de Baar, 1990; Martin and Fitzwater, 1988; Rijkenberg et al., 2018). In seawater, DFe can exist in two different oxidation states, Fe(II) and Fe(III). The Fe(III) oxidation state dominates the chemical speciation of DFe around pH 8 in oxygenated waters, forming Fe oxy-hydroxides (Kuma et al., 1996). At the natural seawater pH, Fe oxy-hydroxides tend to undergo further hydrolysis, and are thus prone to precipitation. However, organic complexation by Fe-binding ligands shifts the equilibrium reaction away from Fe hydrolysis (Kuma et al., 1996; Millero et al., 2002), governing Fe solubility in seawater (Gledhill and Buck, 2012; Hunter and Boyd, 2007). Despite its importance in determining Fe solubility, Fe-binding ligand data is scarce, notably in ice-covered Arctic and subarctic regions.

To date, only a few studies have looked at Fe-binding ligands in the subarctic and Arctic Ocean. Thuróczy et al. (2011) presented the first dataset on Fe fractionation and organic chelation in the central Arctic. Recently, the terrestrial influence on organic ligands in surface waters of the Arctic Ocean was investigated (Slagter et al., 2017). The high concentrations of DFe (up to 4.4 nM) in PSW (Klunder et al., 2012; Rijkenberg et al., 2018) facilitated by complexation with enhanced concentrations of organic ligands (Slagter et al., 2017). This surface DFe enhancement was a clear indication of a riverine contribution in the flow path of the TPD in the Arctic Ocean. The DFe and Fe-binding ligand concentrations were up to 4.5 and 1.7 times higher inside than outside the flow of the TPD, respectively, and ligands from terrestrial origin dominated the total ligand pool in the TPD (Laglera et al., 2019a). This indicates a transport of organic Fe-binding ligands via the TPD (Slagter et al., 2019), and these ligands are likely transported out of the Arctic Ocean towards Fram Strait.

The concentrations and conditional stability constants ($K_{Fe'L}^{cond}$) of Fe-binding ligands in seawater are typically determined by the electrochemical technique known as competitive ligand equilibration (CLE) – adsorptive cathodic stripping voltammetry (AdCSV). This technique is based on the competitive equilibrium between an added known ligand and natural ligands present in seawater (Abualhaija and van den Berg, 2014; Croot and Johansson, 2000; Gledhill and van den Berg, 1994; Rue and Bruland, 1995; van den Berg, 2006). A distribution of conditional stability constants is commonly used to classify Fe-binding ligand groups (Gledhill and Buck, 2012), although the boundaries between the groups are still indistinct and probably more gradual than first assumed. In short, three key groups are acknowledged, (i) strong Fe-binding siderophores (Mawji et al., 2008; Velasquez et al., 2016; Vraspir and Butler, 2009), (ii) relatively weak Fe-binding humic substances (Bundy et al., 2014; Laglera and van den Berg, 2009), and (iii) relatively weak Fe-binding microbially-excreted sugars such as polysaccharides or exopolymeric substances (Hassler et al., 2011). Siderophores are defined as low-molecular-weight organic compounds (<1kDa) secreted by prokaryotes as part of an Fe-uptake system (Mawji et al., 2008; Vraspir and Butler, 2009). Humic substances (HS) typically come from the degradation of organic matter; they have a strong terrestrial component in the Arctic and are substantially resistant to degradation (Calace et al., 2001; Laglera et al., 2019b; Laglera and van den Berg, 2009). However, marine HS can also be produced *in situ* by bacterial remineralization of biogenic particles (Burkhardt et al., 2014) and grazing (Decho and Gutierrez, 2017; Laglera et al., 2019b). Exopolymeric substances (EPS) are relatively labile macromolecules excreted by microbial cells during all life cycles of phytoplankton growth (Decho and Gutierrez, 2017). During an extreme bloom and following its termination, EPS can dominate from 1% to 50% of the dissolved organic carbon (DOC) pool (Orellana et al., 2003) and together with HS, can be a significant contributor of colloidal organic ligands (Batchelli et al., 2010; Hassler et al., 2011). As microbial exudates, EPS are expected to be produced abundantly up to micromolar levels in surface waters, also at the base of sea ice (Lannuzel et al., 2015), showing the potential to outcompete the stronger ligand group (Hassler et

al., 2011). The classification of weak and strong ligand groups based on these three groups is challenging. For example, Slagter et al. (2019) concluded that HS, thought to be a weaker ligand group, can also contain relatively strong ligands (log $K_{Fe'L}^{cond}$ 11.5 – 12.6), whereas Norman et al. (2015) demonstrated that EPS could have strong binding stability constants as well (log $K_{Fe'L}^{cond}$ >12).

This study focuses on the distribution and chemical properties of natural Fe-binding ligands in Fram Strait and over the northeast Greenland shelf. Concentrations of dissolved and total dissolvable Fe of the same expedition (Krisch et al., 2021) are here combined with the distribution and chemical properties of natural Fe-binding ligands in Fram Strait and over the northeast Greenland shelf (77°N – 81°N and 20°W – 20°E), shedding light on their potential sources and transport and further elucidate the cycling of both Fe and Fe-binding ligands in the rapidly changing Fram Strait region.

2. Material and methods

2.1 Sampling

Samples were obtained during GEOTRACES expedition GN05 (PS100) on the German research vessel Polarstern during summer 2016. Seawater samples for trace metals and ligands were sampled between 22nd July and 1st September. Details about the cruise track, ice-cover and hydrographic data can be found in the expedition report (Kanzow, 2017).

A total of 10 stations were sampled as full depth profiles, 8 - 12 ligand samples per station in Fram Strait and 5 - 7 samples per station over the shelf. Conductivity, temperature, depth (CTD), oxygen and turbidity profiles were obtained using a titanium Seabird SBE 911plus on a trace metal clean rosette frame. The frame was equipped with 24 x 12 L Go-Flo bottles (Ocean Test Equipment) and seawater was collected following the sampling procedures as described by (Cutter, 2010). Across Fram Strait,

samples were collected from 4 different stations (1, 7, 14 and 26). Station 1 was located on the eastern side of Fram Strait close to the Svalbard archipelago, while stations 7, 14 and 26 were located towards the western side of Fram Strait (Figure 4-1). The northeast Greenland shelf section consisted of 6 stations covering the Norske-Westwind trough system, 3 stations were sampled in the Norske Trough (17, 18, and 19) and 1 station (11) was sampled in the Westwind Trough (Figure 4-1). In addition, 2 more stations (21 and 22) were sampled in front of the largest glacier of northeast Greenland, the 79N Glacier (Schaffer et al., 2017). Station 21 was located ~20 km away from the glacier front, and station 22 was located in front of the floating glacier ice-tongue.

Immediately after recovery of the CTD rosette, the Go-Flo bottles were carried into a trace metal clean sampling-container where sub-sampling and filtration was performed under N_2 overpressure (~0.2 Bar) using 0.2 µm filters (Acropack 0.8/0.2 µm cartridge filter, Pall). The samples for dissolved Fe analysis were collected in low density polyethylene bottles (LDPE, 125 mL, Nalgene) immediately acidified to pH 1.8 using ultraclean HCl (Romil Suprapure) on board as described elsewhere (Krisch et al., 2021).

Samples for Fe-binding ligand analysis were collected into acid-cleaned 1000 mL LDPE bottles, immediately stored at -20°C after sampling, and transported to the NIOZ laboratory for analysis. Prior to analysis, samples were thawed in the dark and sub-samples were taken to determine DFe present in the ligand sample bottles for calculation of total Fe-binding ligand concentrations. Therefore approximately 50 mL was collected into 60 mL pre-cleaned LDPE bottles and acidified to pH ~1.8 using concentrated ultrapure hydrochloric acid into final concentration ~0.024 µM (0.2% v/v; Seastar chemicals). The acidified samples were stored at room temperature prior to analysis.

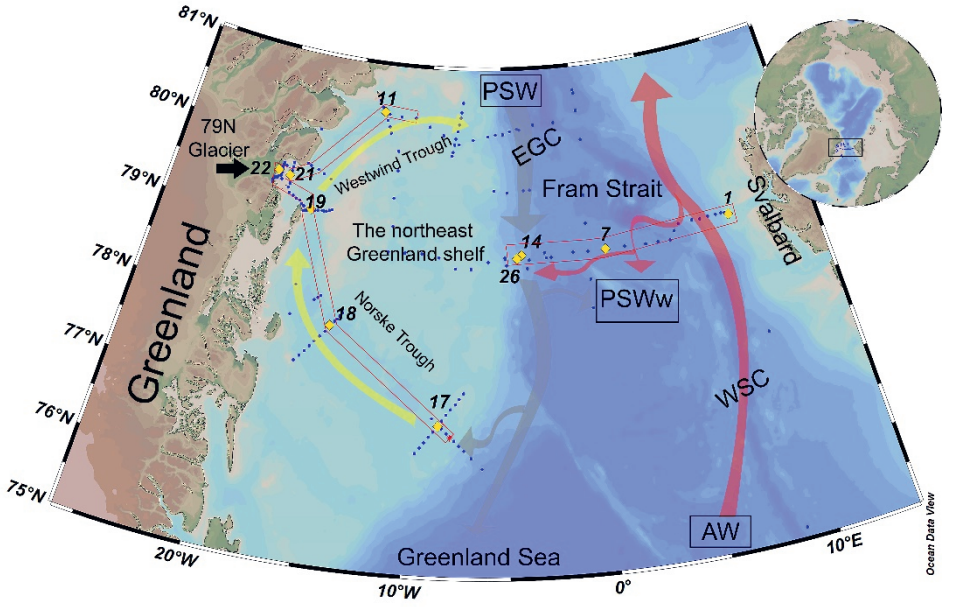

Figure 3-1. Map of the study area with schematic currents. The yellow marks indicate the station positions in this study sampled by a trace metal clean CTD Rosette sampling system. The blue dots indicate the stations sampled by a large CTD sampling system. The Fram Strait transect consists of stations 1, 7, 14 and 26. The northeast Greenland shelf transect consist of stations 17, 18 and 19 in the Norske Trough, stations 21 and 22 near the 79N Glacier terminus, and station 11 in the Westwind Trough. The West-Spitsbergen Current (WSC, indicated by red arrows) brings warm Atlantic Water (AW) into the Arctic Ocean. The southward flowing East Greenland (EGC, grey arrows) carries part of the recirculated WSC as well as outflow Polar Surface Water (PSW) from the Arctic Ocean. The yellow arrows indicate the anti-cyclonic circulation through the trough system. This figure is adapted from Schaffer et al., (2017) and based on Bourke et al., (1987).

2.2 Material handling

Before use, sample bottles were cleaned following three-step cleaning procedure for trace element sample bottles (Cutter, 2010; Middag et al., 2009). All chemicals were prepared using ultrapure water (18.2 MΩ cm, Milli-Q element system, Merck Millipore) and handling performed in an

ISO class 7 ultra-clean laboratory with ISO class 5 workspaces. Outside the ultraclean environment, samples were handled in a laminar flood hood (ISO class 5, interflow and AirClean systems).

2.3 Iron analysis

Analysis of DFe was done twice, at GEOMAR, Kiel (Krisch et al., 2021) in samples acidified immediately shipboard, and in subsamples taken from the ligand samples at NIOZ, Texel. In the laboratory at GEOMAR, DFe concentrations were measured by isotope dilution high-resolution inductively coupled plasma-mass spectrometry (HR-ICP-MS, Thermo Fisher Element XR) after pre-concentration (Rapp et al., 2017). The detailed procedure for DFe determination described elsewhere (Krisch et al., 2021).

For calculation of [L_t] values, we used the DFe measured from the same bottles as the ligand samples. The DFe samples were pre-concentrated using an automated SeaFAST system (SC-4 DX SeaFAST pico; ESI), and analyzed by HR-ICP-MS (Thermo Fisher Element XR) with quantification via standard additions. Accuracy and reproducibility were checked by regular measurements of reference material SAFe D1 (#169) and in-house standards. Results for DFe analyses of reference materials were within the range of May 2013 consensus values (SI Table 4-1). The average overall method blank (SeaFAST & ICP-MS) concentration, determined by measuring acidified ultrapure water as a sample, was 55±7 pM. Dissolved-Fe concentrations measured from the ligand bottles were approximately 15% (n = 69) lower than DFe measured from immediately acidified samples as also found by Gerringa et al. (2014)

2.4 Fe-binding ligands analysis (TAC Method)

The CLE-AdCSV technique using 2-(2-thiazolylazo)-p-cresol (TAC, Alfa Aesar) was employed to determine the total Fe-binding ligand concentrations, [L_t] and K'_{FeL} (Croot and Johansson, 2000).

A Hanging Mercury Drop Electrode stand (VA663 Metrohm), connected to a PC via an interface (IME663) to control the potentiostat (μAutolab III, Metrohm Autolab B.V.) was used. The electrodes in the voltammetric stand included a standard Hg drop working electrode, a glassy carbon counter electrode and a double-junction Ag/AgCl reference electrode (3M KCl). For the titration, 10 mL subsample aliquots were distributed into the pre-conditioned Teflon (30 mL Savillex) vials, and buffered to a final pH of 8.05 with MnO_2-cleaned borate-ammonium (Merck) buffer (final concentration 5 mM). An Fe standard working solution was added to the sample vials, resulting into final concentrations of 0 (twice, no Fe addition); 0.2; 0.4; 0.6; 0.8; 1; 1.2; 1.5; 2; 2.5; 3; 4; 6; 8 (twice) nM of Fe. The purpose of double measurement of the no Fe additions was to be absolutely sure this measurement was not influenced by an unconditioned cell. Based on our experience, a small error of the measurement of the highest addition of the titration has large an effect on the result. Therefore, these points were done twice and the ones that gave the best fit were used for the calculation. After Fe additions, TAC was added to each vial at a final concentration of 10 μM. The content in the vials was allowed to equilibrate for at least 8 hours before analysis or typically overnight (Croot and Johansson, 2000). For analysis, the voltammetric scans were in the differential-pulse mode, with a modification from the original procedure (Croot and Johansson, 2000) as previously reported by Slagter et al. (2017). For each sample, two duplicate scans were done at a deposition time of 140s.

2.5 Fe speciation calculations

The data obtained by CLE-AdCSV was interpreted for the ligand parameters, $[L_t]$ and $K^{cond}_{Fe'L}$ The data were fitted by a Langmuir model using non-linear regression using the software package R (R Development Core Team, 2011) as described by (Gerringa et al., 2014). A one-ligand model was applied, assuming a single ligand group existed. This model fitted the data well (SD < 2%; SD of the fitted data from the Langmuir model). The total Fe-binding ligand concentration, $[L_t]$, is reported in nM equivalents

of Fe (nM eq. Fe) and $K_{Fe'L}^{cond}$ values are reported as a common logarithm to base 10 value (log $K_{Fe'L}^{cond}$) with respect to inorganic Fe (Fe′). The prime symbol (′) is used to denote the fraction not bound by L. For the purpose of this paper, we define log $K_{Fe'L}^{cond}$ as the binding strength of ligands.

The values of [L_t] and log $K_{Fe'L}^{cond}$ were combined with DFe, measured at GEOMAR to derive concentrations of inorganic Fe, [Fe′]. The Fe′ species are predominantly Fe-hydroxides, and at a fixed pH of 8.05, [Fe′] can be calculated (Hudson et al., 1992; Liu and Millero, 2002). The calculation of the ligand parameters is described elsewhere (Gerringa et al., 2014; Ružić, 1982; van den Berg, 1982).

The center of detection window (D) determines which ligand groups, with respect to their conditional binding strength, can be determined. D is defined as the product of the concentration of TAC and the conditional stability constant of $Fe(TAC)_2$, $\beta'_{Fe'(TAC)2}$.

$$D_{TAC} = [TAC]^2 \times \beta'_{Fe'(TAC)2}$$

The inorganic side reaction coefficient of Fe ($\alpha_{Fe'}$) of $10^{10.31}$, as determined using Visual MINTEQ software (Gustafsson, 2012), was used to transform the $\beta'_{Fe'(TAC)2}$ after Croot and Johansson (2000) with respect to Fe^{3+}, into the one with respect to Fe′. Hence, $\beta'_{Fe'(TAC)2} = 10^{12.1}$ was used, resulting in log D_{TAC} = 2.1. The range of the detection window is assumed to be one order above and below log D_{TAC} (Apte et al., 1988).

The side reaction coefficient $\alpha_{Fe'L}$ reflects the ability of ligands to compete for Fe with other ligands and particles. We define $\alpha_{Fe'L}$ here as the competing strength of ligands, expressed as a logarithmic value, log $\alpha_{Fe'L}$. The saturation state of ligands is indicated by the ratio of [L_t]/[DFe]. Assuming that other competing metals can be neglected, ligands are undersaturated when [L_t]/[DFe] >1, whereas [L_t]/[DFe] ≤1 indicate that the ligands are close to saturation (Thuróczy et al., 2010). Statistical analysis of a t-test was performed using the software package R.

3. Results

3.1 Hydrography

The hydrographic features of Fram Strait have been described in detail elsewhere (Beszczynska-Möller et al., 2012; Laukert et al., 2017; Richter et al., 2018; Rudels et al., 2005; Swift et al., 1981) and are summarized briefly in this study. Water masses were identified using conservative temperature (Θ in ^{o}C) and absolute salinity (S_A in g/kg) plots following definitions by Tomczak and Godfrey (2003). The data of Θ and S_A were derived from the CTD data using Ocean Data View (Schlitzer, 2018).

The relatively warm Atlantic Water (AW) flows northward, carried by the West Spitsbergen Current (WSC) at depths shallower than ~500 m at station 1 (Figure 4-2a). In Fram Strait, about half of AW recirculates back southward, and the other half continues northward into the Arctic Ocean, where it is cooled and freshened, forming Arctic Atlantic Water (AAW) in the process (Bourke et al., 1987; Laukert et al., 2017). The AAW is modified by Pacific-origin water and a large amount of terrestrial runoff in the central Arctic before exiting back through Fram Strait. This modified AAW flows out of the Arctic Ocean along with PSW. These water masses flow southward carried by the East Greenland Current (EGC) (Laukert et al., 2017; Richter et al., 2018; Rudels et al., 2005) in western Fram Strait (at stations 14 and 26; Figure 4-2a). The western and middle Fram Strait section is substantially affected by the southward flowing Recirculating-Atlantic Water (RAW). The mixing product of RAW (~200 to ~500 m) and PSW (upper ~300 m), known as warmer PSW (PSWw) (Rudels et al., 2005; Swift and Aagaard, 1981), was observed in surface waters in between the EGC and WSC at station 7 (Figure 4-2a). On both sides of Fram Strait, Atlantic Intermediate Water (AIW) (Bourke et al., 1987; Rudels et al., 2005) was present at ~500 to ~900 m depth, and Norwegian Sea Deep Water (NSDW) (Laukert et al., 2017; Swift and Aagaard, 1981) was present below 1000 m. In this study, AIW and NSDW are categorized as deep waters.

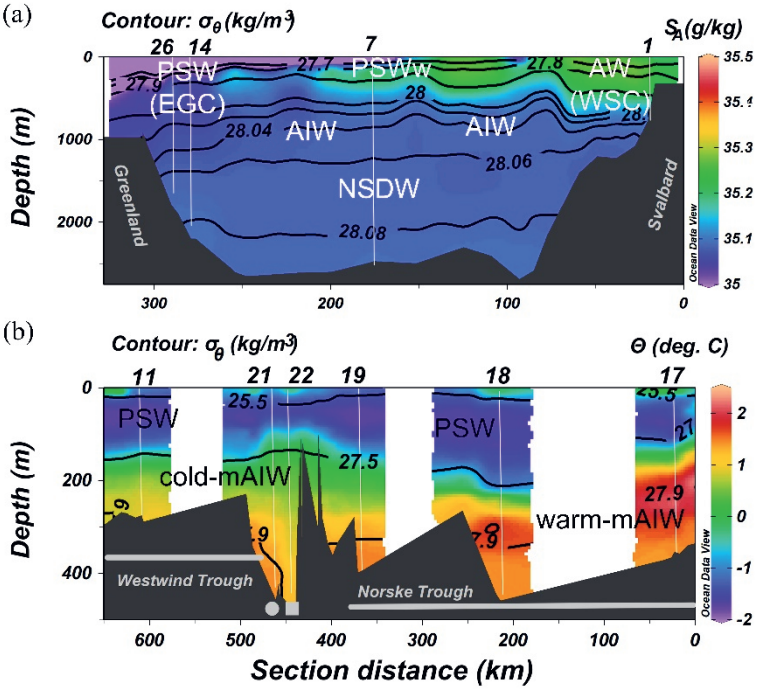

Figure 3-2. The distribution of absolute salinity (S_A), conservative temperature (Θ) and potential density (σ_θ) along the transects with the various water masses indicated. (a): Absolute salinity with potential density as contours in the Fram Strait transect; (b): conservative temperature with potential density as contours along the northeast Greenland shelf transect. The square symbol indicates the station (22) in front of the glacier terminus, and the dot symbol indicates the station (21) at ~20 km distance from the glacier terminus.

Along the northeast Greenland shelf transect, the bathymetry is characterized by the Norske-Westwind Trough system (Figure 4-1), that features a deep sill in the Norske Trough and a shallow sill in the Westwind Trough (Schaffer et al., 2017). Along this transect, the surface circulation in the C-shaped trough system carried PSW into the Norske-Westwind Trough system in the upper 150-200 m (Bourke et al., 1987; Schaffer et al., 2017). The PSW layer, modified-AIW (mAIW) was found deeper than ~200-250 m (Figure 4-2b). For the purpose of this study, mAIW is differentiated as warm-mAIW in the Norske Trough and cold-mAIW in the Westwind Trough based on (Schaffer et al., 2017).

3.2 Dissolved-Fe and Fe-binding ligands

Here we present DFe profiles (Figures 4-3a and 4-3b) from stations for which Fe-binding ligand samples were also taken. Higher resolution DFe profiles from GEOTRACES expedition GN05 are reported by (Krisch et al., 2021).

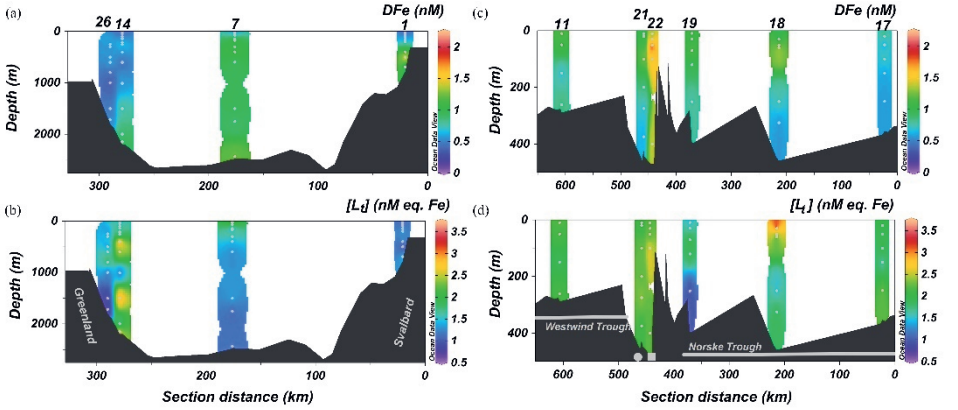

Figure 3-3. The distribution of dissolved Fe (DFe, data from Krisch et al. (2021) and total Fe-binding ligand concentrations ([L_t]) of both transects; the Fram Strait transect on the left and the northeast Greenland shelf transect on the right. DFe concentrations (a,c) and [L_t] (b,d). Along the northeast Greenland shelf transect, the square symbol indicates the station in front of the glacier terminus, and the dot symbol indicates the station at ~20 km distance from the glacier terminus.

3.2.1 The Fram Strait transect

DFe concentrations in Fram Strait were in the range of 0.28-1.64 nM. Concentrations of DFe in Fram Strait were low in surface waters (median AW = 0.59 nM, PSWw = 0.76 nM, PSW = 0.48 nM) and increased towards the seafloor to 1.28 nM. On the eastern side, a maximum in DFe was present at ~500 m (1.64 nM). This elevated DFe decreased horizontally westward from station 1 in the east to stations 14 and 26 in the west to concentrations of 0.37 nM (Figure 4-3a).

In Fram Strait, [L_t] ranged from 0.79 to 3.00 nM eq. Fe (median AW = 1.20 nM eq. Fe, PSWw = 1.77 nM eq. Fe, PSW = 1.78 nM eq. Fe, deep waters=1.36 nM eq. Fe; SI Table 4-2). At stations on the western side (14 and 26), [L_t] was generally higher than at stations in the east and central Fram Strait (1 and 7; Figure 4-3b). The ratio [L_t]/[DFe] varied between 0.5 and 5.4 (Figure 4-4a). In the central and eastern regions (stations 1 and 7), the ratio decreased below 250 m, whereas it remained high on the western side of Fram Strait (stations 14 and 26). The ligands were saturated with Fe ([L_t]/[DFe] < 1) at 500 m depth at station 1 and nearly saturated near the sea floor.

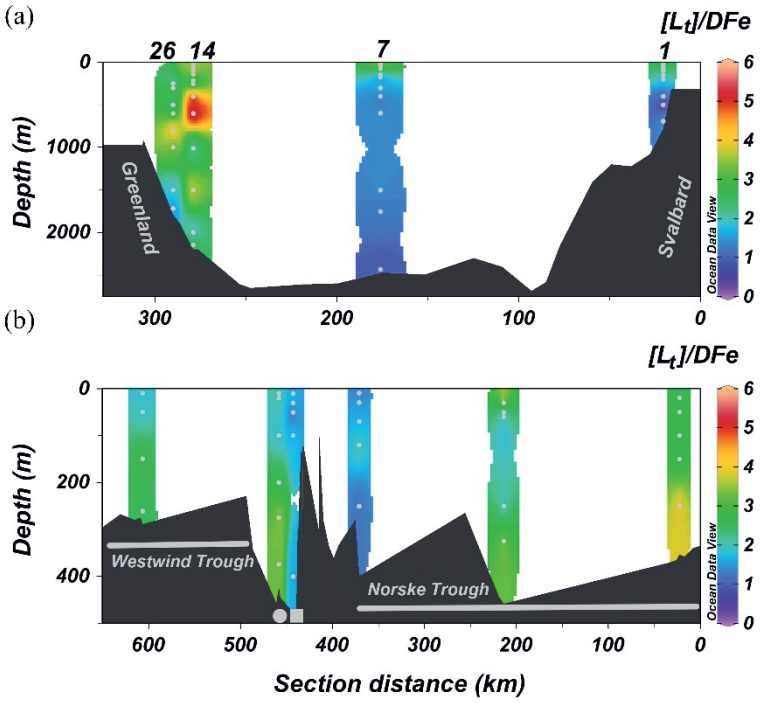

Figure 3-4. The distribution of ligand saturation ([L_t]/DFe) of both transects; the Fram Strait transect (a) and the northeast Greenland shelf transect (b). Along the northeast Greenland shelf transect, the square symbol indicates the station in front of the glacier terminus, and the dot symbol indicates the station at ~20 km distance from the glacier terminus.

Whilst [L_t] in surface waters of Fram Strait generally increased from AW (median=1.20 nM eq. Fe) in the east to PSW (median=1.77 nM eq. Fe) in the west (Figures 4-3b and 4-5a), the median of [Fe′] in Fram Strait

was relatively uniform at 0.05 – 0.15 pM (Figure 4-5b), apart from the two samples where organic ligands were saturated with Fe.

A considerable variation was observed in log $K^{cond}_{Fe'L}$ values (Figure 4-6a) that ranged from 11.8 to 13.9 (median AW = 13.3, PSWw = 12.9, PSW = 12.4, deep waters = 13.0; Figure 4-6a). The values of log $\alpha_{Fe'L}$ (Figure 4-6b) varied between 1.3 and 4.7 (median AW=4.0, PSWw=3.7, PSW=3.4, deep waters=3.9; Figure 4-6b). The highest log $\alpha_{Fe'L}$ value falls more than 2 orders of magnitude above the log D_{TAC} and thus the highest log $K^{cond}_{Fe'L}$ could not be estimated accurately. Since the ligands were saturated with DFe at 500 m depth at station 1, the calculated $\alpha_{Fe'L}$ does not represent the actual value of ligand competing strength and thus this data point was not used for calculations.

3.2.2 The northeast Greenland shelf transect

Concentrations of DFe ranged from 0.58 to 1.45 nM in PSW (median DFe = 0.92 nM) and 0.55 to 0.78 nM in warm-mAIW (median DFe = 0.68 nM) in the Norske Trough (Figure 4-3c). Near the 79N Glacier terminus and Westwind Trough, DFe concentrations ranged from 0.71 to 2.10 nM (median DFe = 1.16 nM) in PSW and 0.63 to 1.38 nM in cold-mAIW (median DFe = 0.77 nM). The highest DFe concentration (2.10 nM) was found in PSW at 30 m depth in front of the glacier terminus (station 22).

In the Norske Trough, [L_t] varied from 1.41 to 3.60 nM eq. Fe in PSW and 0.97 to 2.26 nM eq. Fe in warm-mAIW, whereas near the glacier terminus and Westwind Trough, [L_t] ranged from 1.88 to 2.64 nM eq. Fe in PSW and 2.08 to 2.38 in cold-mAIW (Figure 3d, SI Table 4-2). On average, [L_t] was slightly higher at stations near the glacier terminus (stations 21 and 22) than in the Norske Trough, although the highest [Lt] existed in PSW in the Norske Through (station 18) with values up to 3.60 nM eq. Fe at 30 m depth. The ratio of [L_t]/[DFe] ranged between 1 and 4.4 (Figure 4-4b), indicating that Fe-binding ligands along the northeast Greenland shelf transect were undersaturated. Near the seafloor at station

19 (Norske Through) and at 50 m depth at station 22 (glacier terminus), nearly saturated ligands were observed.

Generally, organic ligands were present at higher concentrations in PSW and mAIW near the glacier terminus and Westwind Trough than in the Norske Trough and Fram Strait (Figure 4-5a). High concentrations of [Fe′] were found in PSW and cold-mAIW in front of the floating glacier ice-tongue (Figure 4-5b), where the organic ligands were nearly saturated (at station 22; Figure 4-4b). Excluding high [Fe′] concentrations in samples where organic ligands were nearly saturated, the median of [Fe′] in PSW and mAIW was lower in the Norske Trough (0.16 and 0.13 pM) than the Westwind Trough and near the glacier terminus (0.41 and 0.33 pM) (Figure 4-5b).

The log $K^{cond}_{Fe'L}$ ranged from 12.4–13.2 in the Norske Trough (median PSW=12.7, warm-mAIW=12.9; Figure 4-6a). Near the glacier terminus and in the Westwind Trough, the log $K^{cond}_{Fe'L}$ ranged from 12.0 – 12.9 (median PSW and cold-mAIW=12.3, warm-mAIW=12.9; Figure 4-6a). The log $K^{cond}_{Fe'L}$ in the northeast Greenland shelf waters were on average lower than in Fram Strait (Figure 4-6a). The median values of log $\alpha_{Fe'L}$ in PSW and warm-mAIW in the Norske Trough were 3.9 and 3.7, respectively. In the Westwind Trough and in front of glacier terminus, the median values of log $\alpha_{Fe'L}$ were 3.5 in PSW and 3.4 in cold-mAIW. In general, variation in log $\alpha_{Fe'L}$ values over the northeast Greenland shelf were less than in Fram Strait (Figure 4-6b).

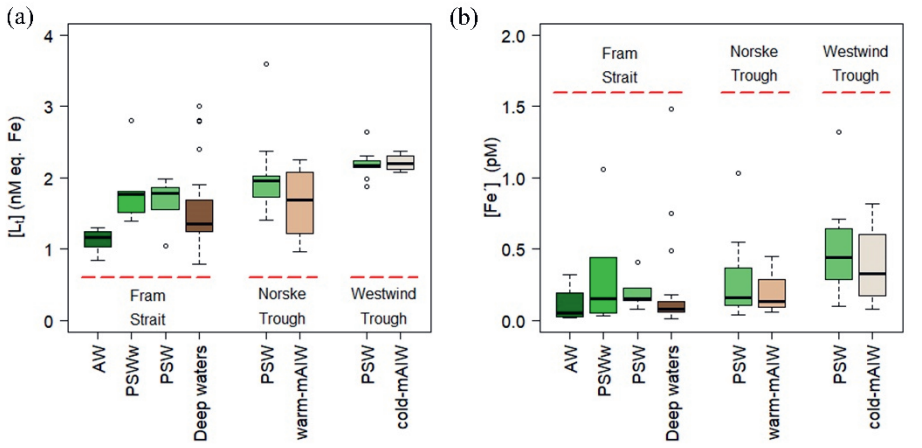

Figure 3-5. Boxplots of the concentrations of (a) total organic Fe-binding ligands, [L_t], and (b) inorganic iron, [Fe´], from all stations in Fram Strait and over the northeast Greenland shelf (the Norske Trough and Westwind Trough), categorized by water mass. Indicated are the median value by a thick horizontal line, the box contains the first and third quartiles, the whiskers are the range of data excluding the outliers. The circles indicate the outliers being 1.5 interquartile range from the box (Teetor, 2011).*

4. Discussion

The applied method using TAC was reported to underestimate [L_t] due to an interaction of TAC with HS binding sites (Laglera et al., 2011; Slagter et al., 2019). However, this method did reveal HS involvement in the ligand pool in different environments (Batchelli et al., 2010; Dulaquais et al., 2018), even in the TPD flow path, where the HS ligands were the dominant group (Slagter et al., 2017). Slagter et al. (2019) compared two CLE-AdCSV techniques, TAC and salicylaldoxime (SA) in the Arctic Ocean and concluded that an offset in [L_t] between the methods existed. Yet, the increase in [L_t] due to HS ligands in the TPD was the same for both methods. Thus in our study, we assume that HS is detectable by the TAC method, although [L_t] might be underestimated.

4.1 Comparison to previous studies

Natural ligand measurements have not previously been reported for Fram Strait, but data is available for adjacent areas, notably the Northern Atlantic (Buck et al., 2015; Gerringa et al., 2015; Mohamed et al., 2011) and Arctic Ocean (Slagter et al., 2017; Thuróczy et al., 2011a). studies conducted by Thuróczy et al. (2011), Gerringa et al. (2015) and Slagter et al. (2017) used the same analytical method and data processing technique as in this study, allowing a direct comparison. The here reported [L_t] in Fram Strait (median PSW = 1.78 nM eq. Fe, PSWw = 1.77 nM eq. Fe, SI Table 4-2) is comparable to the median [L_t] (1.61 nM eq. Fe) outside the TPD flow path (Slagter et al., 2017), but slightly higher than [L_t] reported by Gerringa et al. (2015) for the region between 60 and 33°N in the north west Atlantic Ocean where the median [L_t] was 1.2 nM eq. Fe (N=8) and reached up to 3.3 nM eq. Fe (SI Figure 4-2). The median [L_t] in PSW in the western Fram Strait (1.78 nM eq. Fe) and in the northeast Greenland shelf waters (1.96 and 2.17 nM eq. Fe, SI Table 4-2; surface shelf waters = 2.06 nM eq. Fe; SI Figure 4-2) was comparable to the median [L_t] (2.02 nM eq. Fe) reported by Thuróczy et al. (2011) for the Arctic Ocean, but lower than the average [L_t] (2.79±0.92, N=19) inside the TPD flow path (Slagter et al., 2017). The elevated [L_t] in the TPD has been related to HS ligands from fluvial input as well as interaction between sea-ice and sediment (Slagter et al., 2017 and references therein). Gerringa et al. (2015) hypothesized that the Arctic is a source of ligands, largely of humic origin, to the North Atlantic and that [L_t] decreases over time and distance during advection to the south with North Atlantic Deep Water. The current data in Fram Strait indeed confirmed the Arctic can be a source of ligands, likely of humic origin, to regions to the south.

We found high [L_t] up to 3.6 nM eq. Fe in the sea-ice covered PSW in the Norske Trough (station 18). Antarctic sea ice is known to be a source of ligands, probably due to EPS excretion at the bottom of the sea ice by diatoms. According to Lannuzel et al. (2015), abundant sea ice diatoms were responsible for relatively high [L_t] in under-ice seawater (4.9 to 9.6 nM eq. Fe; log $K^{cond}_{Fe'L}$ ~11 to 13 measured with 1-nitroso-2-napthol),

indicating that EPS could increase [L_t] in seawater with sea-ice coverage. As far as we know, no ligand data of Arctic Sea ice is available, but the high [L_t] in the sea-ice covered in the Norske Trough, was only slightly lower than the [L_t] reported by Lannuzel et al. (2015) and had comparable relatively high log $K^{cond}_{Fe'L}$ (12.4 - 12.8). As detailed in the introduction, EPS were considered to be part of the weak ligand group (Buck et al., 2016; Bundy et al., 2014; Hassler et al., 2011; Hassler et al., 2017; Laglera and van den Berg, 2009), but Norman et al. (2015) demonstrated that EPS could have strong conditional stability constants (log $K^{cond}_{Fe'L}$ >12), hence could contribute to the strong ligands detected in surface waters, especially in regions with sea-ice coverage (Krembs et al., 2002; Lannuzel et al., 2015; Lin et al., 2012). Thus we suggest that the high [L_t] in sea-ice covered Norske Trough is possibly due to EPS.

4.2 Organic ligand sources in Fram Strait

A considerable variation in log $K^{cond}_{Fe'L}$ values (median AW = 13.3, PSWw = 12.9, PSW = 12.4; Figure 4-6a), suggests varying contributions of relatively strong and weak ligand groups to the overall ligand pool. The Fe-binding ligands in surface waters of Fram Strait were dominated by a strong ligand group as apparent from the relatively high log $K^{cond}_{Fe'L}$ (>12; Figure 4-6a). Despite seasonal NO_3 depletion (Hopwood et al., 2018), this area is productive (Cherkasheva et al., 2014; Smith Jr. et al., 1987). Primary productivity is a known source of organic ligands in surface waters as high ligand concentrations are often associated with high chlorophyll-*a* concentrations (Boye et al., 2001; Gledhill and Buck, 2012; Hunter and Boyd, 2007; Rue and Bruland, 1995; van den Berg, 1995). Besides releasing EPS, marine bacteria (*Alteromonas sp*.) can also synthesize siderophores during a bloom (Hogle et al., 2016). Additionally, following the decline of a phytoplankton bloom, excessive production of EPS can occur (Decho and Gutierrez, 2017). A high weekly average of chlorophyll-*a* concentrations was observed using the MODIS satellite (https://giovanni.gsfc.nasa.gov/giovanni/), which indicates the presence of

a phytoplankton bloom in June and July. Our sampling time in Fram Strait (end of July to early August, 2016) coincided with the post-bloom period and therefore it seems likely that bloom-associated ligands are responsible for the relatively high concentration of strong ligands in surface waters of Fram Strait.

The surface ligand concentration (Figure 4-5a) on the western side of Fram strait (median PSW=1.78 nM eq. Fe) as well as further into central Fram Strait (median PSWw = 1.77 nM eq. Fe) was somewhat higher than in eastern Fram Strait (median AW = 1.20 nM eq. Fe). Lateral transport of TPD-carried HS ligands from the Arctic (Laglera et al., 2019a; Slagter et al., 2019), likely formed an additional ligand source to surface waters of the western Fram Strait, where PSW flows south with the EGC in the upper ~150 m (Laukert et al., 2017; Richter et al., 2018). This implies both the phytoplankton bloom and TPD may play a role in the surface composition and distribution of ligands in Fram Strait. Atmospheric input does not seem to influence ligand concentrations, Rijkenberg et al. (2008a) and Wagener et al. (2008) have shown that there is no input of aeolian Fe-binding ligands during dust deposition events, but dissolution of Fe from the dust does depend on the Fe-binding ligands present in seawater.

The organic ligands in Fram Strait were almost saturated near the seafloor (Figure 4-4a), notably in the region with elevated DFe concentrations (station 7). The western Fram Strait (stations 14 and 26) had relatively high, but variably distributed [L_t] over the water column (Figure 4-3b, SI Figure 4-1). Slope sediments can serve as a source of ligands to the deeper part of the water column (Buck and Bruland, 2007a), however this does not seem to be the case for the station nearest to the slope (station 26), in contrast to the station further into Fram Strait (station 14). Possibly the water transport along the shelf break and interaction with the slope is not constant with time and place. Eddies exist at the shelf break and can reach deep enough to propagate subsurface waters (i.e AIW) toward the inner shelf (Schaffer et al., 2017; Topp et al., 1997). In addition, here at this latitude (79^{o}N) the core of the southward flowing RAW mixes with the PSW, and thus substantially contribute to the EGC (Richter et al., 2018). Water transport driven by eddies and RAW intrusion to the EGC

may explain the variably distributed [L_t] in the upper (~500m) water column, however, the elevated concentrations in the deeper part of station 14 remain unexplained.

4.3 Organic ligand sources over the northeast Greenland shelf

In this section, the transect over the northeast Greenland shelf will be discussed in the direction of the general circulation, starting at the southern inlet and going along the Norske Trough towards the 79N Glacier and back towards Fram Strait via the Westwind Trough. The water masses from Fram Strait are propagated toward the inner shelf at the southern inlet (station 17), potentially by eddies, while undergoing pronounced mixing at the shelf edge. Eddy stirring and tidal mixing seem to be persistent features in the Norske Trough inlet (Bourke et al., 1987; Budéus et al., 1997; Schaffer et al., 2017). The balance between release and removal of organic ligands, along with physical water mass mixing (Budéus et al., 1997), is likely responsible for the fairly constant [L_t] observed in the water column at station 17 (Figure 4-3d).

The relatively high concentrations of strong organic ligands (up to 3.60 nM eq. Fe, log $K^{cond}_{Fe'L}$ 12.4-12.8) observed in PSW in the Norske Trough were most likely related to an earlier bloom, generating marine HS and EPS ligand groups with relatively strong affinity for Fe. The macro-nutrients (NO_3, PO_4, Si; data not shown) at this location were depleted and DFe was low (Figure 4-3d), indicative of a prior bloom. Consistently the chlorophyll-*a* concentration was low at the time of sampling (unpublished data), whereas higher concentrations were observed via satellite in the period prior to sampling (https://giovanni.gsfc.nasa.gov/giovanni/). Sato et al. (2007) showed a relation between increasing [L_t] and decreasing chlorophyll-*a* due to zooplankton grazing, and Laglera et al. (2019b) measured an increase in strong organic ligands as a consequence of grazing. This demonstrated that declining blooms can indeed contribute strong organic ligands and increase [L_t] as we observed in our study region.

Additionally, black sea-ice with entrapped sediment was spotted during sampling at this location and the melting of black sea-ice can release HS ligands (Genovese et al., 2018) in addition to ligands released from grazing (Decho and Gutierrez, 2017; Laglera et al., 2019b). Also, we cannot eliminate the possible contribution of EPS, either produced *in situ* by sea-ice diatoms (Lannuzel et al., 2015) or released by phytoplankton cells after bloom termination (Decho and Gutierrez, 2017). Recent studies pointed out that HS and EPS can have strong Fe-binding sites Fe (Laglera et al., 2019b; Lannuzel et al., 2015; Norman et al., 2015; Slagter et al., 2019). Therefore, the presence of HS and EPS can contribute to the pool of relatively strong ligands with elevated [L_t] in PSW in the Norske Trough.

The ligand-rich PSW in the Norske Trough did not seem to be a significant contributor of organic ligands to either the glacier front or the glacier outflow. Probably ligands produced in the Norske Trough did not yet reach the glacier front. In addition, newly produced ligands associated with primary productivity over the shelf, such as at station 18, are likely to be partially lost due to photodegradation (Barbeau et al., 2001; Powell et al., 2003), aggregation and sinking (Cullen et al., 2006) during transport. Either way, a high ligand concentration, such as in the surface waters of Norske Trough, was not observed at the glacier terminus (at stations 21 and 22). At the 79N Glacier terminus, the 80-120 m thick ice-front is limiting direct entry of PSW into the glacier cavity, and at depths of ~80-270 m, water flows eastward away from the glacier front and into the trough system (Schaffer et al., 2017). As warm-mAIW in the Norske Trough has a relatively low [L_t], notably at station 19 on the northern end of the Norske Trough, ligands in the glacier outflow are thus likely produced in the glacier cavity itself. In general, meltwater is relatively poor in DOC compared to coastal seawater, but this DOC may be highly available to bacteria (Paulsen et al., 2017). Hence, the relatively high [L_t] over the entire water column near the 79N Glacier terminus (Figure 4-3d), could be associated with bacterial remineralization or byproducts of organic matter degradation (Gledhill and Buck, 2012; Gordienko and Laktionov, 1969; Hunter and Boyd, 2007). These ligands would be transported into the Westwind Trough, following the anti-cyclonic water

circulation of the Norske-Westwind Trough system (Schaffer et al., 2017; Topp and Johnson, 1997). The median of log $K^{cond}_{Fe'L}$, both in the PSW and mAIW near the glacier terminus (stations 21 and 22) and Westwind Trough (station 11) were somewhat lower (Figure 4-6a) than in the Norske Trough (median log $K^{cond}_{Fe'L}$ =12.3 versus 12.7 and 12.9). This indicates that different ligand sources shift the characteristics of the overall ligand pool or the ligand pool has undergone physical, chemical or biologically-induced structural alterations during transport, e.g. through photo- or microbial degradation. Although ligands were present at higher concentrations (Figures 4-3d and 4-5a), these organic ligands were weaker than in the Norske Trough (Figure 4-6a). Primary productivity likely dominated the organic ligand sources in the Norske Trough, which may have led to a ligand pool with a relatively high conditional stability constant. In contrast, near the glacier terminus and in Westwind Trough, bacterial remineralization most likely was the dominant ligand source, resulting in more, but overall weaker ligands.

Near the glacier terminus and in Westwind Trough, [Fe′] was relatively high compared to Norske Trough and Fram Strait (Figure 4-5b). The glacier acts as a source of Fe and organic-ligand bound Fe, thereby facilitating glacial-Fe transport. However, at the glacier terminus, Fe was prone to precipitation and/or scavenging as [Fe′] was enhanced (Figure 4-5b) and the competing strength of the ligands (log $\alpha_{Fe'L}$) was relatively low (Figure 4-6b). It should be noted here that the complexation of Fe by organic ligands is an equilibrium reaction between complexed Fe and [Fe′], where [Fe′] is not only determined by competing strength, but also by the scavenging intensity and precipitation reactions. Thus, the ligands can effectively release Fe if their competing strength is relatively low and they are outcompeted by scavenging and precipitation processes as shown in the deep Makarov Basin (Slagter et al., 2017; Thuróczy et al., 2011a). Availability of [L_t] is thus not a guarantee for complexing (additional) DFe, as it is the overall equilibration between excess ligands, scavenging sites and precipitation that governs the fate of DFe.

4.4 Biogeochemical provinces of organic ligands

This study distinguished three biogeochemical provinces with respect to Fe-binding ligands, based on the influence of different sources of ligands, and hence ligand properties and distribution. The biogeochemical provinces include (1) Fram Strait, (2) Norske Trough and (3) near the glacier terminus and Westwind Trough. The different ligand properties and distribution are reflected in the differences in [L_t] (Figure 4-5a), log $K^{cond}_{Fe'L}$ (Figure 4-6a) and log $\alpha_{Fe'L}$ (Figure 4-6b).

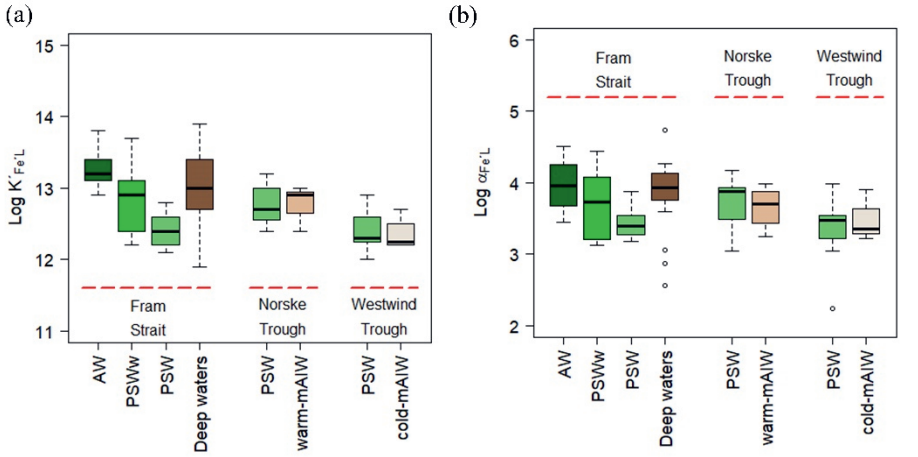

Figure 3-6. Boxplots of the conditional stability constants (binding strength), log $K^{cond}_{Fe'L}$ (a) and side reaction coefficients (competing strength), log $\alpha_{Fe'L}$ (b) from all stations in Fram Strait and over the northeast Greenland shelf (the Norske Trough and Westwind Trough), categorized by water mass. The detail explanation of the boxplot is as described in Figure 4-5.

As described above, in the northward flowing AW of the eastern Fram Strait, strong organic ligands derived from phytoplankton blooms are suggested to dominate the ligand pool. Whereas in the western Fram Strait in southward flowing PSW, part of the ligands probably originated from the Arctic Ocean and partly consists of HS ligands carried by the TPD (Slagter et al., 2017). The average log $K^{cond}_{Fe'L}$ is significantly higher (SI Table 4-3) in the AW flow (mean log $K^{cond}_{Fe'L}$ = 13.3±0.3 (1 SD); SI Table 4-2), compared to the PSW flow in western Fram Strait where the influence

of Arctic waters resulted in lower log $K^{cond}_{Fe'L}$ values (the mean of log $K^{cond}_{Fe'L}$ 12.4±0.3 (1 SD); SI Table 4-2). The range in log $K^{cond}_{Fe'L}$ is relatively broad (Figure 4-6a), implying that different ligand sources supply ligands with various chemical properties, thus different affinity to bind Fe.

As detailed, organic ligands were present at higher concentrations near the glacier terminus and Westwind Trough than in the Norske Trough and Fram Strait (Figures 4-3b and 4-5a), but the ligands near the glacier terminus and Westwind Trough had a lower affinity for binding Fe (Figure 4-6a) and a lower competing strength, log $\alpha_{Fe'L}$ (Figure 4-6b). (Krisch et al., 2021) observed that glacial-derived Fe transfer through the Westwind Trough was low because of a net transfer of Fe from the colloidal (thus part of DFe) to the particulate phase with subsequent settling out of the water column, an important removal process in the Fe cycle (Wu et al., 2001). Although organic ligands exist in both the soluble and colloidal fractions (Boye et al., 2010; Fitzsimmons et al., 2015; Thuróczy et al., 2011a), part of the colloidal Fe fraction is inert, and not exchangeable (Cullen et al., 2006) and might contribute to coagulation and aggregation and disappearance of Fe. We did not separate soluble and colloidal fractions, but we do demonstrate that the ligands in the glacier outflow and Westwind Trough were relatively weak with a lower competing strength (Figures 4-6a and 4-6b). This results in a relatively high [Fe′] which in turn allow loss of DFe via precipitation and/or scavenging, consistent with the loss of colloidal Fe observed by (Krisch et al., 2021).

Global warming causes rapid environmental changes in the Arctic and sub-Arctic Oceans (Gascard et al., 2008; IPCC, 2014) to which Fram Strait belong (Ekwurzel et al., 2001; Schuur et al., 2015). These changes may alter the properties and distribution of organic Fe-binding ligands. Melting of sea-ice influences biological activity (Arrigo et al., 2008b; Meier et al., 2014) and without considering possible nutrient depletion, this may increase the release of strong organic ligands. An increased competing strength of organic ligands enhances the ability of ligands to stabilize additional Fe input, potentially increasing the DFe export from Greenland towards the open ocean if the timing and location of DFe input coincides

with the presence of these ligands. Not much is known about Fe limitation in the Nordic Seas, although potential Fe limitation was reported for the Nansen Basin of the Arctic Ocean (Rijkenberg et al., 2018). Also the Iceland Basin in the North Atlantic experiences seasonal Fe limitation (Hopwood et al., 2018; Mohamed et al., 2011; Nielsdóttir et al., 2009; Ryan-Keogh et al., 2013). Enhanced transport of ligand bound Fe from the Arctic may thus have a profound effect on primary productivity in the high-latitude North Atlantic. However, such changes must also be considered alongside other physical/chemical perturbations in the region as a result of ongoing changes such as the increase in freshwater discharge around Greenland. The complex interplay between Fe and ligand sources versus scavenging and coagulation will need to be better constrained to enable accurate predictions of changes in the biogeochemical cycle of Fe in the globally important northern high latitudes, as well as elsewhere.

5. Conclusions

This study provides a connection between the previous reports on organic Fe-binding ligands in the Arctic Ocean and North Atlantic Ocean, as well as insight into the competing strength of organic Fe-binding ligands that regulate DFe transport from a Greenland glacier. Our results indicate that the Fe-binding ligands in surface waters of Fram Strait originate from microbial activity with addition from southward-flowing TPD transported terrestrial ligands on the western side of Fram Strait. Given that the [L_t] in western Fram Strait is intermediate to the higher concentrations reported for the Arctic and the lower concentrations reported for the North Atlantic, this confirms the decreasing [L_t] southward from the Arctic Ocean.

In the Norske Trough, the remnant from an earlier bloom was likely the main source of organic Fe-binding ligands in surface waters, as the contribution of ligands can be substantial at the base of sea-ice. The elevated [L_t] at stations near the 79N Glacier terminus is probably associated with remineralization of glacially-derived organic matter. Our data shows that even though significantly higher concentrations of organic ligands were present at the vicinity of 79N Glacier terminus and in the

Westwind Trough (outflow) than in the Norske Trough (inflow), the organic ligands are weaker and therefore can compete less efficiently with scavenging processes and precipitation. Especially close to the glacier, ligands have a weaker affinity for binding Fe. We show that transport of Fe in the glacial outflow is potentially regulated by ligands as has been anticipated from comparisons of particulate and dissolved Fe distributions in several systems worldwide. Additionally, our results reveal the underlying mechanism where the lower ligand binding strength and consequently higher [Fe′] (rather than a low concentration of ligands) result in more precipitation of Fe-oxyhydroxides or/and scavenging. Thereby only a small part of the glacial DFe will be transported over the shelf into the ocean. Different sources supply ligands with various chemical properties, resulting in distinctive properties of the ligand pool among regions.

Rapid environmental changes due to global warming will cause increased river runoff and glacial melt into the Arctic Ocean, increasing gross Fe supply into the Arctic basin. However, it is the combination of availability and binding strength of organic ligands that regulate DFe transport and distribution in Fram Strait region. Thus, to understand the consequences of global warming in the Arctic and sub-Arctic Oceans for the biogeochemical cycle of Fe, the changes in the biogeochemical cycle of the ligands need to be understood as well. Especially glacial systems will need to be investigated further to determine if there is strong temporal variability in the concentration and competing strength of Fe-binding ligands or if large differences exist between different glaciers.

Supplementary Information (SI)

SI Table 3-1. Values for dissolved-Fe analyses of reference materials. The consensus values were obtained from http://www.geotraces.org/.

	Reference Material	Consensus value	Reported value
Entire PS100/GN05 trace metal samples analyses at GEOMAR	SAFe S (#273)	0.093 ± 0.008 nM	0.101 ± 0.016 nM (n = 10)
	GSP (#144, #192)	0.27 ± 0.05 nM	0.28 ± 0.07 nM (n = 11)
Dissolved-Fe samples from ligand bottles analyses at NIOZ	SAFe D1 (#169)	0.67 ± 0.04 nM	0.718 ± 0.024 nM (n = 3)

SI Table 3-2. The summary of ligand data grouped by water mass.

Province	Water mass		$[L_t]$ (nM eq. Fe)	log $K^{cond}_{Fe'L}$	[Fe′] (pM)	log $\alpha_{Fe'L}$	$[L_t]$/DFe
Fram Strait	AW	Mean	1.15	13.3	0.08	3.5	2.0
		SD	0.18	0.3	0.11	1.5	1.0
		N	8	8	7	8	8
		Median	1.20	13.3	0.05	4.0	2.0
	PSWw	Mean	1.84	12.9	0.31	3.7	2.4
		SD	0.50	0.6	0.39	0.5	1.2
		N	6	6	6	6	6
		Median	1.77	12.9	0.15	3.7	2.2
	PSW	Mean	1.63	12.6	0.18	3.6	3.1
		SD	0.33	0.5	0.13	0.4	1.0
		N	6	6	6	6	6
		Median	1.67	12.5	0.14	3.5	2.8
	deep waters	Mean	1.59	13.0	0.21	3.7	2.5
		SD	0.65	0.6	0.36	0.8	1.3
		N	20	20	19	20	20
		Median	1.36	13.0	0.08	3.9	2.1
Norske Trough	PSW	Mean	2.03	12.8	0.28	3.7	2.3
		SD	0.58	0.3	0.30	0.4	0.9
		N	11	11	11	11	11
		median	1.96	12.7	0.16	3.9	2.0
	warm-mAIW	Mean	1.65	12.8	0.11	3.7	2.6
		SD	0.55	0.3	0.04	0.3	1.3
		N	4	4	3	4	4
		Median	1.68	12.9	0.13	3.7	2.6
Westwind Trough	PSW	Mean	2.19	12.4	0.48	3.3	1.9
		SD	0.19	0.3	0.34	0.4	0.4
		N	11	11	10	11	11
		Median	2.17	12.3	0.41	3.5	1.9
	cold-mAIW	Mean	2.21	12.4	0.39	3.5	2.7
		SD	0.13	0.2	0.31	0.3	0.8
		N	4	4	4	4	4
		Median	2.20	12.3	0.33	3.4	2.9

*SI Table 3-3. T-test statistics summary. The significance levels are p<0.005***, p<0.01**, p<0.05* and p<0.1.*

		Parameters	P-value	
Fram Strait	AW vs PSW	$[L_t]$	0.03	*
		$\log K'^{cond}_{Fe'L}$	**0.0009**	***
		$\log \alpha_{Fe'L}$	>0.1	
	AW vs PSWw	$[L_t]$	0.015	*
		$\log K'^{cond}_{Fe'L}$	>0.1	
		$\log \alpha_{Fe'L}$	>0.1	
Northeast Greenland shelf	PSW in the Norske Trough vs. PSW in the Westwind Trough	$[L_t]$	0.008	**
		$\log K'^{cond}_{Fe'L}$	0.009	**
		$\log \alpha_{Fe'L}$	0.032	*
	mAIW in the Norske Trough vs. mAIW in the Westwind Trough	$[L_t]$	0.095	
		$\log K'^{cond}_{Fe'L}$	0.042	*
		$\log \alpha_{Fe'L}$	>0.1	

Note: the bold emphasis is mentioned in the discussion, and the others are provided as reference.

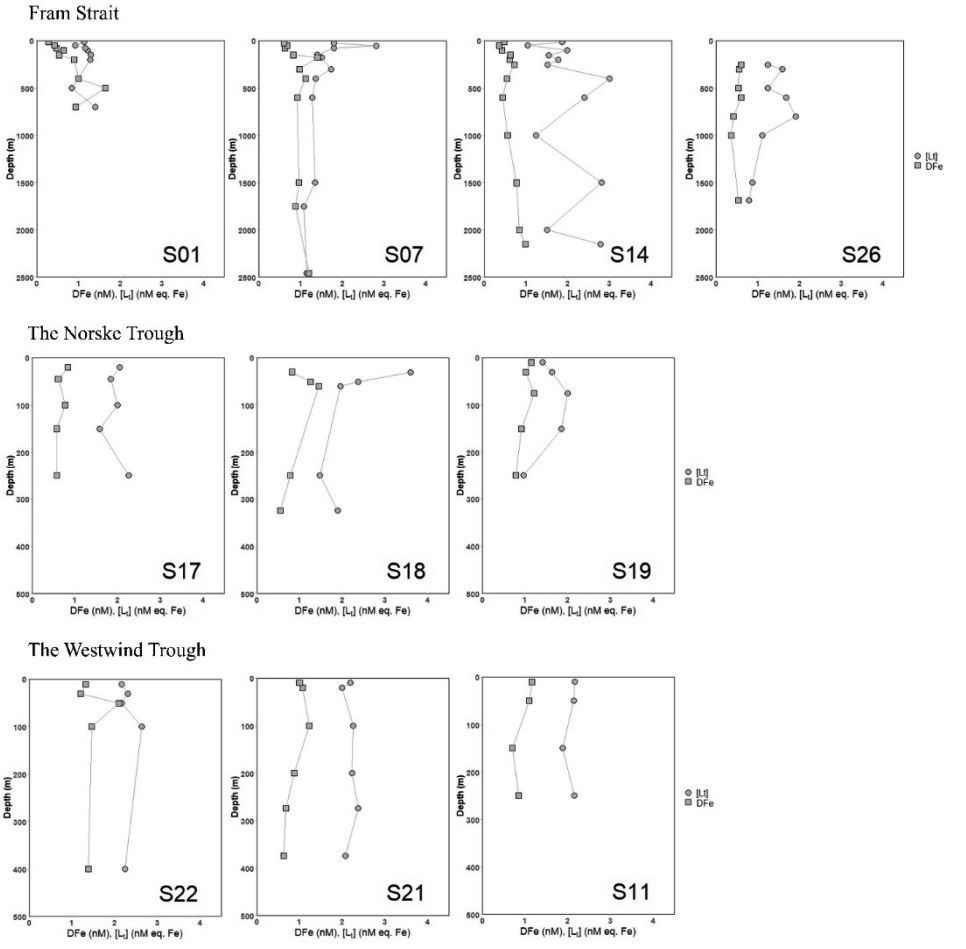

SI Figure 3-1. The depth profiles of dissolved-Fe (DFe) and total ligand concentrations [L_t] for each station in Fram Strait and over the northeast Greenland shelf. Station numbers are indicated at the bottom right of each figure. Figures are made using the software package R.

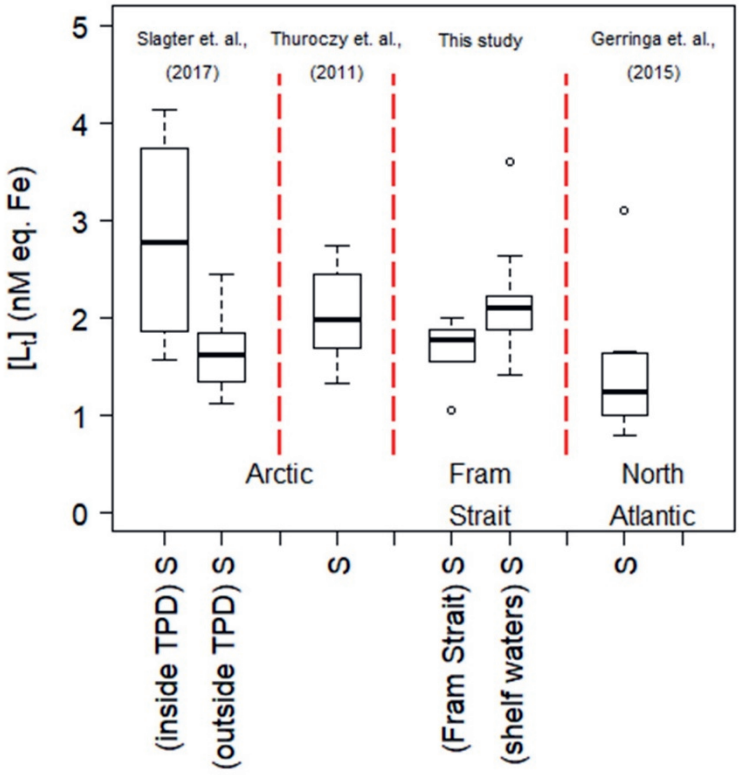

SI Figure 3-2. Boxplots of the total Fe-binding ligand concentrations, [L_t], from existing studies in the Arctic Ocean (Slagter et al., 2017; Thuróczy et al., 2011) and the North Atlantic Ocean (Gerringa et al., 2014). The letter "S" refers to surface data. Surface samples from Slagter et al., (2017) were selected from Polar Surface Water (PSW) at stations inside (81, 87, 91, 96) and outside (50, 64 and 69) the Transpolar Drift (TPD), based on the TPD definition as described in the original paper of Slagter et al., (2017). Surface samples from Thuróczy et al, (2011) were taken from upper 200m at stations in Makarov and Amundsen Basin. Surface samples from Gerringa et al., (2014) were taken from upper 200m at stations 2 and 5 in the North Atlantic Ocean.

Acknowledgments

Authors would like to thank Captain Schwarze and his crew of the RV Polarstern, as well as chief scientist Torsten Kanzow, for their effort and support during sample collection. Patrick Laan is acknowledged for analyzing DFe for Fe-binding ligands calculation. We thank anonymous reviewers for their comments that improved the manuscript considerably. IA was financed by Indonesia Endowment Fund for Education (LPDP), and SK was financed by GEOMAR and the German Research Foundation (DFG award number AC 217/1-1 to E. P. A). Figures 1 to 4 are made using the software Ocean Data View 5.1.7 (Schlitzer, 2018). Figures 5 and 6 are made using the software package R version 3.4.2. Data can be accessed online at https://doi.org/10.25850/nioz/7b.b.u.

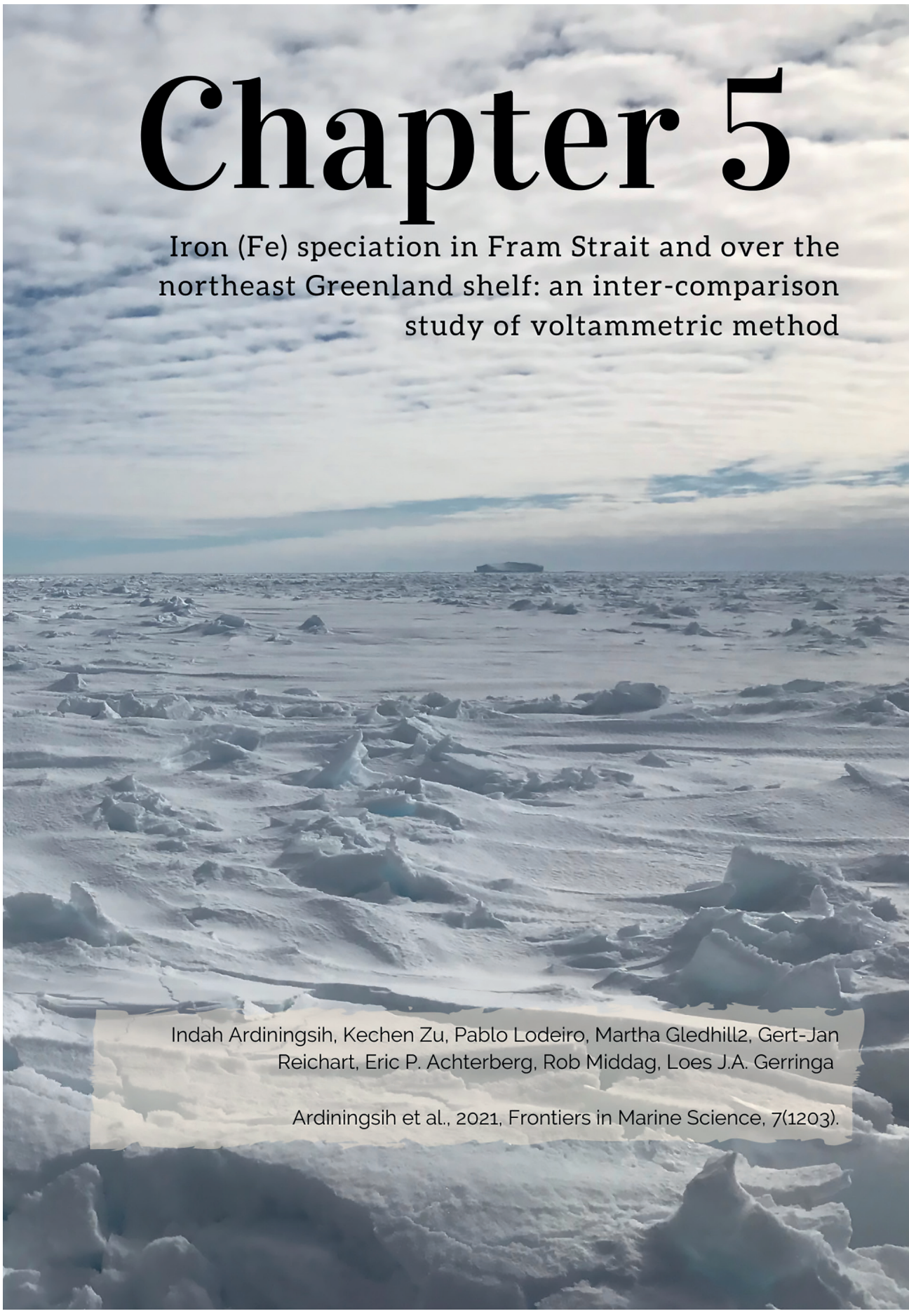

Chapter 5

Iron (Fe) speciation in Fram Strait and over the northeast Greenland shelf: an inter-comparison study of voltammetric method

Indah Ardiningsih, Kechen Zu, Pablo Lodeiro, Martha Gledhill2, Gert-Jan Reichart, Eric P. Achterberg, Rob Middag, Loes J.A. Gerringa

Ardiningsih et al., 2021, Frontiers in Marine Science, 7(1203).

Abstract

Competitive ligand exchange – adsorptive cathodic stripping voltammetry (CLE-AdCSV) is a widely used technique to determine dissolved iron (Fe) speciation in seawater and involves competition for Fe of a known added ligand (AL) with natural organic ligands. Three different ALs were used, 2-(2-thiazolylazo)-p-cresol (TAC), salicylaldoxime (SA) and 1-nitroso-2-napthol (NN). The total ligand concentrations ($[L_t]$) and conditional stability constants ($\log K^{cond}_{Fe'L}$) obtained using the different ALs are compared. The comparison was done on seawater samples from Fram Strait and northeast Greenland shelf region, including the Norske Trough, Nioghalvfjerdsfjorden (79N) Glacier front and Westwind Trough. Data interpretation using a one-ligand model resulted in $[L_t]_{SA}$ (2.72 ± 0.99 nM eq Fe) > $[L_t]_{TAC}$ (1.77 ± 0.57 nM eq Fe) > $[L_t]_{NN}$ (1.57 ± 0.58 nM eq Fe); with the mean of $\log K^{cond}_{Fe'L}$ being the highest for TAC ($\log K^{cond}_{Fe'L\,(TAC)}$ = 12.8 ± 0.5), followed by SA ($\log K^{cond}_{Fe'L\,(SA)}$ = 10.9 ± 0.4) and NN ($\log K^{cond}_{Fe'L\ (NN)}$ = 10.1 ± 0.6). These differences are only partly explained by the detection windows employed and are probably due to uncertainties propagated from the calibration and the heterogeneity of the natural organic ligands. An almost constant ratio of $[L_t]_{TAC}/[L_t]_{SA}$ = 0.5 - 0.6 was obtained in samples over the shelf, potentially related to contributions of humic acid-type ligands. In contrast, in Fram Strait $[L_t]_{TAC}/[L_t]_{SA}$ varied considerably from 0.6 to 1, indicating the influence of other ligand types, which seemed to be detected to a different extent by the TAC and SA methods. Our results show that even though the SA, TAC and NN methods have different detection windows, the results of the one ligand model captured a similar trend in $[L_t]$, increasing from Fram Strait to the Norske Trough to the Westwind Trough. Application of a two-ligand model confirms a previous suggestion that in Polar Surface Water and in water masses over the shelf, two ligand groups existed, a relatively strong and relatively weak ligand group. The relatively weak ligand group contributed less to the total complexation capacity; hence it could only keep part of Fe released from the 79N Glacier in the dissolved phase.

1. Introduction

Organic Fe-binding ligands allow dissolved Fe (DFe) to be present at concentrations above the inorganic solubility of Fe in seawater, increase the residence time of DFe and enable DFe to be transported by ocean currents (Boyd and Ellwood, 2010b; Gerringa et al., 2015; Hunter and Boyd, 2007; van den Berg, 1995). Despite their importance, not much is known about the origin, loss and residence time of these organic substances (Gerringa et al., 2015; Gledhill and Buck, 2012; Hassler et al., 2017). Whilst more information is becoming available on specific molecules that bind Fe (Boiteau et al., 2016; Mawji et al., 2011) and the acid-base properties of marine dissolved organic matter (Lodeiro et al., 2020), the bulk of the ligands is of unknown identity and is described in terms of broad groups such as siderophores, humic acids and polysaccharides (Bundy et al., 2016; Dulaquais et al., 2018; Gledhill and Buck, 2012; Hassler et al., 2017; Laglera et al., 2011; Laglera et al., 2019a; Whitby et al., 2020).

The concentration and conditional binding strength of the bulk ligands in seawater are typically determined with an electrochemical technique, using the competitive ligand exchange–adsorptive cathodic stripping voltammetry (CLE-AdCSV), where the conditional binding strength is used to infer a broad ligand group. In this technique, a sample aliquot is titrated with Fe to saturate natural Fe-binding ligands. A well-characterized competing ligand, the added ligand (AL), competes with the natural ligands, and forms an electroactive complex $Fe(AL)_x$ that can be deposited at 0 V or a negative potential on a hanging mercury drop. The Fe in the $Fe(AL)_x$ complex is reduced during a potential scan towards more negative potentials (cathodic stripping), and the electrical reduction current is recorded. At each titration point, the electrical signal recorded in nano-Ampere (nA) is converted into a concentration in nM equivalents of Fe (nM eq. Fe). Using the Langmuir isotherm, the data is fitted with non-linear regression to calculate the ligand concentration $[L_t]$ and conditional binding strength expressed as a log value of the conditional stability

constant, log $K_{Fe'L}^{cond}$ (Gerringa et al., 2014; Hudson et al., 2003; Omanović et al., 2015).

There are four CLE-AdCSV methods to determine DFe speciation that use different ALs and titration conditions (pH, concentration of AL and equilibration time). The commonly used ALs for DFe speciation study are 2-(2-thiazolylazo)-p-cresol (TAC), salicylaldoxime (SA), 1-nitroso-2-napthol (NN) and 2,3-dihydroxynaphthalen (DHN). The different conditional stability constants and concentrations of each AL will result in different analytical detection windows (Apte et al., 1988; Pizeta et al., 2015; van den Berg, 2006). The center of the detection window (D), expressed in logarithmic form (log D), is defined as the product of the concentration of AL, [AL], and the conditional stability constant of the formed $Fe(AL)_x$ complex. The detection window determines which Fe-binding organic ligands can be detected. It is assumed that ligands with a complexation capacity (product of their conditional stability constant and concentration of ligands not bound to Fe) in the range of one order of magnitude above and below D, the detection window (Dw), can be measured (Apte et al., 1988; Filella et al., 2000; Hudson et al., 2003; Pizeta et al., 2015; van den Berg et al., 1990). However, it has also been shown that the complexation capacity of detected natural ligands is often above the assumed upper limit of Dw (Buck et al., 2017; Bundy et al., 2014; Gerringa et al., 2015).

The pioneering study on the CLE-AdCSV method for DFe speciation in seawater was conducted by Gledhill and van den Berg (1994) using NN as a competing ligand (log D ~2.1 at [NN] = 1 µM and pH 6.9). Later this method was adapted to pH 8 by van den Berg (1995) and Boye et al. (2001). Croot and Johansson (2000) introduced TAC as competing ligand (log D = 2.4 at [TAC] = 10 µM and pH = 8.05). The use of SA as competing ligand ([SA]= 27.5 µM, log D = 1.8 at pH = 8.0) was first introduced by Rue and Bruland (1995) using a short equilibration time of 15 to 20 minutes. Buck et al. (2007b) modified the method using a pH of 8.2 and a final concentration of SA of 25 µM (log D = 1.9). Abualhaija and van den Berg (2014) modified the SA method by purging with air instead of

nitrogen which has improved the sensitivity considerably. After concluding that the $Fe(SA)_2$ was actually not the electro-active complex as previously assumed, but rather FeSA, they used a lower SA concentration of 5 µM to prevent loss of sensitivity by formation of $Fe(SA)_2$. These adaptions enabled an equilibration time of at least 8 hours (or overnight) after SA addition, similar to other methods. These changes including the use of a lower SA concentration (5 µM) decreased the center detection window by a factor of 4 (log D = 1.2).

Until recently, methods with TAC or SA as competing AL were the most widely used CLE-AdCSV techniques for DFe speciation in open ocean water, although methods with NN or DHN are also used. Comparisons of the techniques have been restricted to the methods using TAC and SA (Buck et al., 2012, 2016; Slagter et al, 2019). Buck et al. (2016) showed comparable concentrations of ligands (log $K_{Fe'L}^{cond}$ = 12 - 13) obtained with TAC ([TAC] = 10 µM; log D = 2.4) and ligands belonging to the strong ligand group obtained with 25 µM SA ([SA] = 25 µM; log D = 1.8). An additional weaker ligand group was detected using the SA method, whereas the TAC method detected only one ligand group. The detection of two ligand groups using SA is common (Buck et al., 2017; Bundy et al., 2016; Rue and Bruland, 1995; Rue and Bruland, 1997), whereas using TAC, these are seldom detected (Gerringa et al., 2019; Nolting et al., 1998).

Laglera et al. (2011) showed that Suwannee River Fulvic Acid (SRFA), a model Humic substance (HS), cannot be detected using TAC or NN as AL. Slagter et al. (2019) however, showed that TAC detected part of HS, and revealed the role of HS in the Fe-binding ligand pool in the Transpolar Polar Drift (TPD) flow path (Slagter et al., 2019). Using NN, Boye et al. (2001) showed that a longer deposition time was required to obtain acceptable sensitivities for detecting ambient HS concentrations, however, an interference peak appeared. Although such a drawback can be solved by subtracting the interference peak from the scan (Boye at al., 2001), Laglera et al. (2011) reported that the analysis time can take 5 to 10 fold longer as a consequence of the increase in the deposition time.

In addition, using 25 µM SA with a short equilibration time could lead to an overestimation of [L_t] (Slagter et al., 2019; Gerringa et al., in review). As complexes of Fe and natural ligand groups have different dissociation rates, the complexes with fast dissociation rate are detected using 25 µM SA. However, a certain number of complexes with slow dissociation rates are not fully outcompeted by SA in such a short time period, and hence, are determined as being strong ligands. Thus, the use of 25 µM SA with a 15 minutes equilibration time might be too short for natural ligands, SA and Fe to reach equilibrium, even though a stable CSV signal is obtained (Laglera and Filella, 2015).

As described above, it is apparent that there are quite some analytical issues for each method to determine Fe-binding organic ligands, warranting further study. Moreover, previously conducted inter-comparison studies (Buck et al., 2016; Buck et al., 2012) suggested the use of multiple methods to obtain different detection windows and detect a wider spectrum of organic ligands in natural seawaters. Therefore, a comparison of the different detection windows and the ligands they detect can be very useful to assess the overall composition and concentration of organic Fe-binding ligands.

In the Fram Strait and on the northeast Greenland shelf, water mass and heat exchange occurs between the Arctic Ocean and Norwegian Sea. From results from the same expedition where our samples were taken we know that probably phytoplankton is limited by Fe and N in Fram strait. These deficiencies have geographical east west gradients with N being more deficient in the west near Greenland and Fe in the east (Krisch et al., 2020). This region provides an ideal hydrographic setting for comparing different CLE-AdCSV methods with different ALs. As Ardiningsih et al. (2020) showed, there is a difference in ligand properties ([L_t] and log $K^{cond}_{Fe'L}$) between three biogeochemical provinces in this area; (1) Fram Strait, (2) Norske Trough and (3) Nioghalvfjerdsfjorden (79N) Glacier terminus, and Westwind Trough. The suspected inflow of relatively weak ligands from the Arctic Ocean with the Polar Surface Water (PSW) in the western Fram Strait results in higher ligand concentrations with lower

binding strength in comparison to the eastern side of Fram Strait. Concentrations of organic ligands in the vicinity of the 79N Glacier terminus were high, but those ligands were relatively weak compared to organic ligands in Fram Strait and Norske Trough. In addition, it appears that the characteristics of organic ligands control the glacial DFe export from the northeast Greenland continental shelf to the Fram Strait (Ardiningsih et al., 2020; Krisch et al., 2020). Therefore, it is of interest to study whether the different methods will give the same information on ligand presence and environmental Fe transport in this region.

Here we present results for DFe speciation from selected stations of the PS100 GEOTRACES expedition GN05 in Fram Strait and the northeast Greenland shelf. We focus on different CLE-AdCSV methodologies that cover a 63 fold range in D values. The CLE-AdCSV methods in this study include a method using 5 µM SA with overnight equilibration (Abualhaija and van den Berg, 2014) and a method using 10 µM TAC (Croot and Johansson, 2000). Additionally, a method with the AL NN (2 µM (Boye et al., 2001)) was used for a subset of the samples. Unfortunately, we could not add the fourth method using DHN as AL to this study because of lack of sample volume and technical reasons. Since different pH conditions are used for the three methods, we calculated inorganic side reaction coefficients for Fe ($\alpha_{Fe'}$, fraction of Fe that forms inorganic hydroxide complexes) using the constants of Liu and Millero (1999) and this resulted in the following log D values of 0.6 for SA and 2.4 for NN and TAC.

2. Material and methods

All reagents were prepared using ultrapure water (18.2 MΩ cm, Milli-Q element system, Merck Millipore). The DFe samples were acidified with ultraclean hydrochloric acid (onboard, Romil Suprapure; subsample from ligand bottles: Seastar chemical). The AL stock solutions were prepared by dissolving high purity AL (TAC: Alfa Aesar; SA: Acros Organics, Fisher Scientific, 98% purity; NN: Sigma Aldric) into three times-distilled methanol. Sample handling was performed in an ultra-clean environment

(ultra-clean laboratory class 100). Outside the ultra-clean environment, samples were handled in a laminar flood hood (ISO class 5, interflow and AirClean systems).

2.1 Sample collection

Samples were collected during GEOTRACES expedition (GN05) from July 22nd to September 1st, 2016. Water column samples were collected in 24 x 12 L GO-FLO (Ocean Test Equipment) bottles mounted on a trace metal clean rosette frame equipped with a titanium Seabird SBE 911plus. Sampling and sample-handling were done following GEOTRACES sampling procedures for trace elements ((Cutter, 2010). The detailed sample collection for DFe was reported by Kanzow (2017); (Krisch et al., 2020), and for dissolved Fe-binding organic ligands by Ardiningsih et al. (2020). Right after recovery of the trace metal clean rosette and the GO-FLO bottles were carried into a trace metal clean container for filtration. Samples were collected into pre-cleaned LDPE bottles (high density polyethylene, Nalgene; volume 1000mL for ligand and 125mL for DFe samples). The bottles were rigorously rinsed before use to avoid contaminations from storage material following GEOTRACES protocols (Cutter, 2010; Middag et al., 2009).

Seawater samples were collected from 10 full depth stations representing different regions in Fram Strait and the northeast Greenland shelf (Figure 5-1). Across Fram Strait, sampling sites include an eastern (station 1), middle (station 7) and western (stations 14 and 26) station. On the shelf, stations covered the Norske Trough (stations 17, 18, 19), Westwind Trough (station 11) and the vicinity of the 79N Glacier terminus (stations 21 and 22). Station 21 was located in the bay (about 20 km from 79N Glacier terminus) and station 22 was located at the glacial front.

2.2 DFe and Fe-binding ligand analysis

Seawater samples for Fe speciation analysis were immediately stored at -20ºC without acidification, since pH affects the partitioning of Fe among its different species. In un-acidified samples however, bottle wall adsorption can cause Fe loss (Fischer et al., 2007; Jensen et al., 2020). The analysis of DFe was undertaken using two different subsamples, one immediately acidified onboard (Krisch et al., 2021) and a subsample taken from the ligand samples (Ardiningsih et al. (2020) and available at doi:10.25850/nioz/7b.b.u). DFe was determined in acidified samples, by isotope dilution high-resolution inductively coupled plasma-mass spectrometry (HR-ICP-MS, Thermo Fisher Element XR) after pre-concentration (Rapp et al., 2017), the detailed procedure is described elsewhere (Krisch et al., 2020). Subsamples for a second DFe determination from the ligand bottles, was analyzed using HR-ICP-MS (Thermo Fisher Element XR) after pre-concentration using an automated SeaFAST system (SC-4 DX SeaFAST pico; ESI), and the quantification was done via standard additions. The procedure is described in detail in Ardiningsih et al. (2020). DFe obtained from ligand samples was approximately 15% lower than DFe obtained from immediately acidified samples, as also found by others (Gerringa et al., 2019; Gerringa et al., 2016). DFe from ligand samples was used for the calculation of [L_t] and log $K^{cond}_{Fe'L}$. The results of the determination in samples immediately acidified onboard and in subsamples taken from the ligand is attributed to either adsorption of Fe on the ligand bottle wall and possibly, even though we worked in laminar flow benches, contamination subsample from the ligand bottle, since this bottle was handled several times for the different applications.

In order to extrapolate DFe speciation to ambient DFe concentrations, DFe from the immediately acidified samples, [L_t] and log $K^{cond}_{Fe'L}$ were used to calculate the excess ligand concentrations [L´] (i.e. concentration of ligands not bound to Fe). The [L´] was subsequently used to calculate the side reaction coefficient of the ligands ($\alpha_{Fe'L}$), which is the product of log $K^{cond}_{Fe'L}$ and [L´]. The side reactions coefficient describes the effective

affinity of a ligand for Fe, and takes into account the concentrations of the metal, the ligand and other competing cations thus describing the effective affinity between the natural ligands and Fe. The three different ALs used in the voltammetric methods (TAC, SA and NN) in this study will be indicated in subscript letters after the ligand parameters, e. g. $[L_t]_{TAC}$ or log $K^{cond}_{Fe'L\,(TAC)}$.

2.2.1 TAC method

The analytical procedure of the here used TAC method is based on Croot and Johansson (2000), with modifications after Slagter et al. (2017). The method is described in detail by Ardiningsih et al. (2020) and uses a Hg drop electrode stand (VA663 Metrohm, Switzerland) connected to a μAutolab voltammeter and Nova 1.9 (Metrohm Autolab B.V., the Netherlands) as the software user-interface. The titrations were done at pH 8.05 using 5 mM ammonium-borate buffer in the presence of 10 μM TAC and left to equilibrate for at least 8 hours or overnight before voltammetric analysis. For each sample, duplicate scans were undertaken at a deposition time of 140 s, starting with the lowest added Fe(III) aliquot and working towards the highest added Fe(III) concentration. The Fe additions were 0; 0.2; 0.4; 0.6; 0.8; 1.0; 1.2; 1.5; 2.0; 2.5; 3.0; 4.0; 6.0; 8.0 nM, where the no Fe addition and the highest Fe addition vials were prepared in duplicate and both were analyzed. The limit of detection (LOD) was 0.016 nM eq. Fe, obtained as three times the noise in the scan.

2.2.2 SA Method

The SA method follows the protocol by (Abualhaija and van den Berg, 2014) with a low SA concentration (5 μM) and overnight (8 hours) equilibration, but using the BioAnalytical System (BASi) controlled growth mercury electrode coupled with an Epsilon ε2 (BASi) electrochemical analyzer (Buck et al., 2015). The voltammetry system was controlled by a computer using BASi Epsilon-EC as the interface software, and ECDsoft was used to quantify the peak height of the voltammetric scan.

Teflon vials (Fluorinated Ethylene Propylene (FEP), Savillex) were conditioned at least three times with seawater amended with buffer, DFe addition and SA. The first conditioning solution was changed immediately after rigorous shaking, followed by the next addition of conditioning solution, whereas the last conditioning solution was left at least for 8 hours. The samples were buffered to a final pH of 8.2 with 5 mM of a boric acid-ammonium buffer. The titration consisted of 14 sub-sampled aliquots with Fe(III) standard additions of 0 to 3.0 nM with 0.5 nM intervals followed by concentrations of 4.0, 5.0, 6.0, 8.0 and 10 nM. The no addition and the highest addition were prepared in duplicate and both were analyzed. The chemical blank is measured in between samples to avoid carry over. For each sample, duplicate scans were done in a Teflon vial as voltammetric cell with a deposition time of 90 s. The LOD was 0.12 nM eq. Fe, obtained as three times the noise of our lowest standard (0.5 nM) in the scan.

2.2.3 NN Method

The analytical procedure for the NN method followed (Boye et al., 2001) and was adapted from the original NN method (Gledhill and van den Berg, 1994; Yokoi et al., 1992). Voltammetric analysis was performed using a mercury drop electrode stand model VA663 (Metrohm, Switzerland) connected to a μAutolab voltammeter (Metrohm Autolab B.V., the Netherlands).

Sample aliquots of 10 mL were buffered to pH 8.0 with 4-(2-Hydroxyethyl) piperazine-1-ethanesulfonic acid (HEPES; final concentration 0.01 M) and a final concentration of 2 μM NN was added. The addition of Fe (III) standards ranged from 0 to 10 nM with increments of 0.5 nM from 0 to 4.5 nM, followed by concentrations of 6.0; 8.0 and 10 nM. The sample mixtures were left to equilibrate overnight (≥12 h). The voltammetric scans were done in duplicate for each sample with a deposition time of 240 s. The LOD for the detection of $FeNN_3$, calculated using three times standard deviation of our lowest standard (0.5 nM)/slope is 0.13 nM eq. Fe for samples analyzed using the conditions used in this study.

2.3 Calculation of speciation parameters

We define the side reaction coefficient describing the effective affinity of Fe binding to AL as D, in order to prevent confusion with the side reaction coefficient of the natural ligands. It is the product of log $K'_{Fe'(AL)_x}$ and [AL], and calculated as (Table 5-1).

$D = [AL] \times K'_{Fe'(AL)}$ or $D = [AL]^x \times \beta'_{Fe'(AL)_x}$

The 'upper' limit of the detection window (Dw) is defined by the precision and detection limit of the analytical method (Laglera and Filella, 2015), whilst in an internally calibrated system, the lower limit is set by the assumption that all the weak ligand sites have been titrated within the range of added Fe concentrations, which can in practice be restricted by the linear range of the technique (Hudson et al., 2003). For this study, we assumed that the width of the Dw is one order of magnitude above and below the center of detection window, D, as conventionally assumed in the literature (Apte et al., 1988; Hudson et al., 2003; Pizeta et al., 2015; van den Berg et al., 1990).

The inorganic Fe side reaction coefficient ($\alpha_{Fe'}$) is used to transform the conditional stability constant of AL with respect to Fe^{3+} into the one with respect to Fe′ (log $K^{cond}_{Fe'L}$). As the buffer pH differed between the methods, the pH of analysis was slightly different for each AL, thus the value of $\alpha_{Fe'}$ is different for each pH (Table 1). Ardiningsih et al. (2020) used the value of $\alpha_{Fe'}$ derived from Visual MINTEQ software (Gustafsson, 2012) with the ionic strength (I) is being calculated along with the determination of $\alpha_{Fe'}$. In this study, the values of $\alpha_{Fe'}$ were calculated based on the solubility products of the Fe-hydroxides at the fixed pH of analysis and I = 0.7 (Liu and Millero, 1999). As a result of different $\alpha_{Fe'}$ values compared to previous results obtained with the TAC method, the resulted value of log $K^{cond}_{Fe'L}$ and log $\alpha_{Fe'L}$ in this study are 0.1 higher than the results of TAC method reported by Ardiningsih et al. (2020).

Table 4-1. Summary of the formed $Fe(AL)_x$ complexes and the detection window of each voltammetric methods.

$Fe(AL)_x$	pH	Log $\alpha_{Fe'}$	Log $K'_{Fe'(AL)}$	Log $\beta'_{Fe'(AL)_x}$	$D_{(AL)}=\alpha_{Fe'AL}$	Log D	Ref.
$Fe(NN)_3$	8.00	9.8	-	19.5	253	2.4	Avendano et al., (2016)
$Fe(TAC)_2$	8.05	9.9	-	12.44	275	2.4	(Gerringa et al., in review)
FeSA	8.20	10.4	5.94	-	4.4	0.6	(Gerringa et al., in review)

A non-linear model of the Langmuir isotherm (Gerringa et al., 2014) was used to interpret the ligand parameters, as described for the data obtained with the TAC method by Ardiningsih et al. (2020). A one- and two-ligand model was applied to the data, and the ligand parameters calculated were $[L_t]$, log $K^{cond}_{Fe'L}$ and log $\alpha_{Fe'L}$. In case of two ligand groups, the relatively strong ligand group was denoted with 1, the relative weak group with 2, as follows: $[L_1]_{TAC}$, and $[L_2]_{TAC}$, or log $K'_{1(TAC)}$ and log $K'_{2(TAC)}$. The sum of the concentration of $[L_1]$ and $[L_2]$ from the two-ligand model will be denoted as $\sum L$. The absolute difference between $[L_t]$ values derived with two different method is referred to as $\delta[L_t]$ (i.e. $\delta[L_t]_{SA\text{-}TAC}$ is the absolute difference between $[L_t]_{SA}$ and $[L_t]_{TAC}$). Two ligand groups could not be resolved for the NN method. The mean sensitivity (S) obtained for the samples with the different methods were S = 3.97 ± 0.70 (N=70) for the TAC method, S = 76.4 ± 23.0 (N=69) for the SA method, and for the NN method S = 0.93 ± 0.17 (N=15).

3. Results

3.1 Hydrography

The water mass distribution and circulation are described elsewhere in detail (Beszczynska-Möller et al., 2012; Laukert et al., 2017; Richter et al., 2018; Rudels et al., 2005; Rudels et al., 2015). The selected stations in this

study represent the main hydrographic features present in Fram Strait and on the northeast Greenland continental shelf (Figure 5-1; more details in Ardiningsih et al., 2020). Warm and saline (Temperature >2ºC and Salinity>35; Rudels et al., 2005; Laukert et al., 2017). Atlantic Water (AW) is present at depths shallower than ~500 m in our stations. Cold and less saline (Temperature ≤ 0ºC and Salinity <34.5; Rudels et al., 2005) PSW is present on the western side (stations 14, 26) in the upper ~300 m. AW recirculates in the upper 200 m in the central Fram Strait, forming warmer Polar Surface Water (PSWw) (Swift and Aagaard, 1981). At about 500 to 900 m depth on both sides of Fram Strait, Atlantic Intermediate Water (AIW) (Rudels et al., 2005) exists above the Norwegian Sea Deep Water (NSDW) (Swift and Aagaard, 1981). In this study, AIW and NSWD are referred to as deep waters.

The Norske-Westwind Trough system is situated on the Northeast Greenland shelf (Figure 5-1). The surface water, PSW, follows this circulation flowing along the Norske Trough to the bay of the 79N Glacier and thereafter continues into the Westwind Trough. Deeper than 200 m, modified-AIW (mAIW) enters the Norske-Westwind Trough system, modified by physical mixing before being propagated toward the inner shelf (Schaffer et al., 2017; Topp and Johnson, 1997). The shallow sill in the Norske Trough restricts the flow of mAIW, causing the mAIW in the Norske Trough was 1ºC warmer than mAIW in the Westwind Trough (Schaffer et al., 2017), therefore in this study, it is referred to as warm-mAIW and cold-mAIW, respectively.

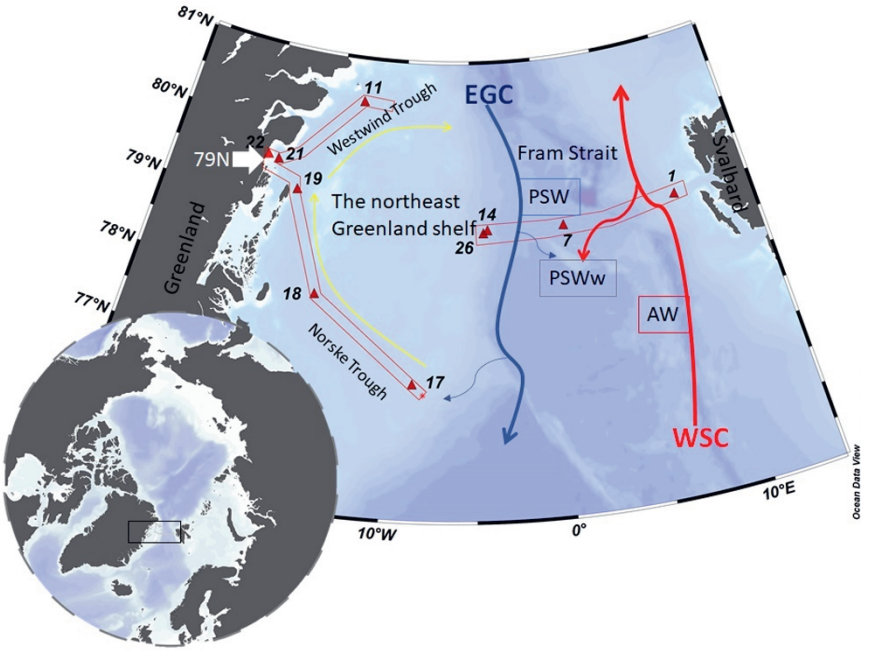

Figure 4-1. Map of the study area and schematic currents in Fram Strait. The black square indicates the sampling location, and stations are indicated by red triangles. The West-Spitsbergen Current (WSC, red arrows) brings warm Atlantic Water (AW) into the Arctic Ocean. The southward flowing East Greenland (EGC, grey arrows) carries part of the recirculated WSC as well as outflow waters from the Arctic Ocean. The anti-cyclonic circulation through the Norske – Westwind Trough system is indicated by yellow arrows. These schematic currents are simplified from Schaffer et al. (2017) and based on Bourke et al. (1987). Figure was made using the software Ocean Data View (Schlitzer, 2018).

3.2 Fe speciation using a one-ligand model

Total ligand concentration, [L_t], is calculated for each method and grouped based on the water masses existing in the different biogeochemical provinces (Figure 5-2). We observed similar trends for [L_t]$_{TAC}$, [L_t]$_{SA}$ and [L_t]$_{NN}$ in various waters (Figures 5-2a , 5-2b and 5-2c; the number of samples for each water masses is given in Table 2), with an increase in the median [L_t] from Fram Strait to the Norske Trough and

highest values at the glacier front and in Westwind Trough. The absolute values of [L_t] derived via the three different methods differed considerably. The $[L_t]_{SA}$ (median=2.82 nM eq. Fe) was highest followed by $[L_t]_{TAC}$ (median=1.79 nM eq. Fe) and $[L_t]_{NN}$ (median=0.96 nM eq. Fe). In Fram Strait, the ratio of $[L_t]_{TAC}$ /$[L_t]_{SA}$ varied between 0.6 to 1, however, on the shelf, this ratio was nearly constant at approximately 0.6 (median, Figure 5-3a). The ratio of $[L_t]_{NN}$ /$[L_t]_{SA}$ was 0.2 – 0.5 in Fram Strait and 0.2 – 0.8 over the shelf (Figure 5-3b).

For individual voltammetric methods, the variation in log $K^{cond}_{Fe'L}$ values reached up to two orders of magnitude between samples (Figures 5-4a, 5-4b and 5-4c). The variation in log $K^{cond}_{Fe'L}$ values in Fram Strait was larger than on the shelf. The most constant but lowest log $K^{cond}_{Fe'L}$ values were observed in Westwind Trough. The value of log $K^{cond}_{Fe'L}$ was highest for TAC, log $K^{cond}_{Fe'L\,(TAC)}$ (median = 12.8), followed by log $K^{cond}_{Fe'L\,(SA)}$ (median = 10.9) and log $K^{cond}_{Fe'L\,(NN)}$ (median=10.1; SI Figure 5-1a). The differences in log $K^{cond}_{Fe'L}$ values between the methods are significant ($p<0.05$; SI Figure 5-1a). For NN, median log $K^{cond}_{Fe'L\,(NN)}$ values were significantly lower and ranged from 9.8 to 11.0 (Figure 5-4c; Table 5-2). For the determination of log $K^{cond}_{Fe'L}$, the curved part is essential. In the non-linear transformation of the Langmuir isotherm, log $K^{cond}_{Fe'L}$ is derived by dividing the tangent of the curve at the lowest determined Fe concentration by the total ligand concentration. However, because ligand concentrations are typically ca. 1 nM eq. Fe in excess of the dissolved Fe concentration, an inability to detect the first titration point and a lower number of points in the curved part of the titration will mean that the tangent of the curve at the first detectable Fe concentration will be considerably lower than the tangent that would have been observed at the ambient DFe concentration and this will lead to an underestimation in log $K^{cond}_{Fe'L}$ (e.g. for a samples with 0.5 nM DFe and a ligand concentration of 1.5 nM eq. Fe , 66 % of the ligands are titrated already at the first titration point of DFe+0.5 nM added). Thus, this difference likely arises because the peak with 0 Fe addition was usually not detected, which compromises the estimate of log $K^{cond}_{Fe'L\,(NN)}$.

Furthermore, for some samples the titration curves were nearly linear and the difference between the determined $FeNN_3$ concentration and the expected Fe concentration was too low to detect so that values of log $K^{cond}_{Fe'L\,(NN)}$ and log $\alpha_{Fe'L(NN)}$ could not be estimated.

A relatively wide range in log $\alpha_{Fe'L}$ for both TAC and SA methods was observed in Fram Strait, whereas on the shelf, log $\alpha_{Fe'L}$ decreased with depth. The median log $\alpha_{Fe'L(TAC)}$ (3.8) was highest compared to log $\alpha_{Fe'L(SA)}$ (2.3) and log $\alpha_{Fe'L(NN)}$ (0.6) (SI Figure 5-1b). The values of log $\alpha_{Fe'L(TAC)}$ and log $\alpha_{Fe'L(SA)}$ fell within and on the upper limit of log Dw (Figures 5-4d and 5-4e), whereas the values of log $\alpha_{Fe'L(NN)}$ mostly fell below the lower limit of log Dw (Figure 5-4f).

3.3 Fe speciation using a two-ligand model

For both the TAC and SA methods, two ligand groups could be resolved in some of the samples, mostly the shelf samples (Figures 5-5a and 5-5b). Only 10% (4 out of 39) of samples from the Fram Strait could be resolved for two ligands using the TAC and SA methods, therefore, it is not possible to make a statistical comparison of the results of TAC and SA in the Fram Strait using the two-ligand model. On the shelf two ligands could be resolved for about 26% (8 out of 30) of the samples using TAC and 77% (24 out of 31) of the samples using the SA method.

Using the TAC method, $[L_1]_{TAC}$, ranged from 0.48 to 2.66 nM eq. Fe (Figures 5-5a and 5-5b) with values of log $K'_{1(TAC)}$ between 11.6 and 14 (Figures 5-6a and 5-6b). In comparison, $[L_2]_{TAC}$ varied between 0.30 to 3.10 nM eq. Fe with log $K'_{2(TAC)}$ between 11.1 and 11.7. The values of log $\alpha_{2(TAC)}$ and log $\alpha_{1(TAC)}$ were mostly within log Dw for TAC, with an exceptions some log $\alpha_{1(TAC)}$ values were higher than the upper limit of log Dw (Figure 5-6c and 5-6d).

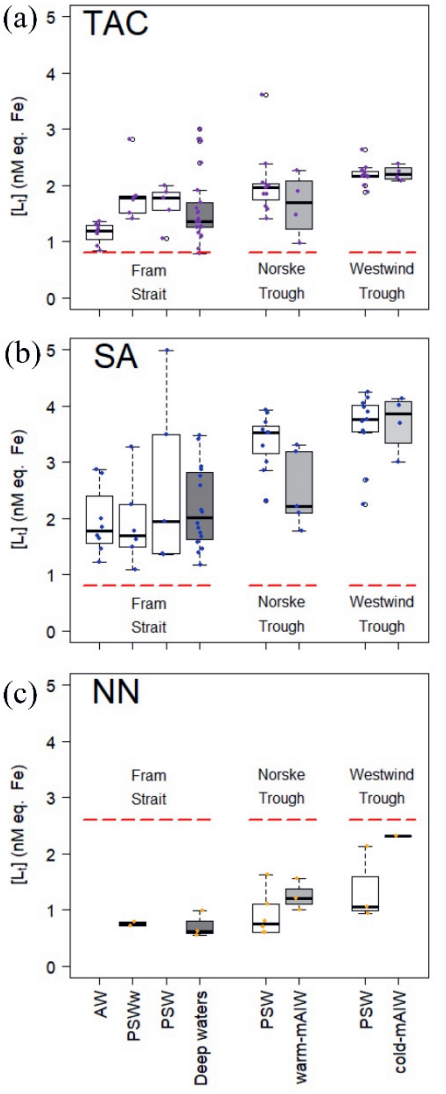

Figure 4-2. Boxplot of ligand concentrations, [L_t], in nM eq. Fe from three different applications of added ligands (a) TAC, (b) SA, and (c) NN, as fitted (non-linear) by a one-ligand model using the Langmuir isotherm. The data is grouped by the biogeochemical provinces as described by Ardiningsih et al. (2020). A thick horizontal line indicates the median, the box contains the first to third quartiles, the whiskers are the range of data excluding the outliers and the circles indicate the outliers being 1.5 interquartile range from the box (Teetor, 2011). Figures were made using the software package R.*

Using the SA method, $[L_1]_{SA}$ ranged from 0.82 to 3.87 nM eq. Fe and $[L_2]_{SA}$ from 0.08 to 3.43 nM eq. Fe. The values of log $K'_{1(SA)}$ ranged from 11.3 to 13.8 and log $K'_{2(SA)}$ from 10.5 to 11.2. Similar values of log $\alpha_{1\,(SA)}$ were higher than log Dw, and log $\alpha_{2\,(SA)}$ values fell within log Dw (Figure 5-5b).

4. Discussion

In the below discussion the ligand parameters (log $K^{cond}_{Fe'L}$, log $\alpha_{Fe'L}$ and $[L_t]$) derived from each method are related to Dw of the three ALs. Using different Dw, the 'target ligand pool' shifts, and it is thus appealing to use the different Dw to distinguish different fractions of binding sites. However, the precision of the Dw, its value and thus the conditional stability constant of AL ($K'_{Fe'AL}$ or $\beta'_{Fe'AL}$) with Fe must be considered. In order to properly evaluate $K'_{Fe'AL}$ or $\beta'_{Fe'AL}$, we must therefore consider uncertainties in the determination of $K'_{Fe'AL}$ or $\beta'_{Fe'AL}$. For example, ionic strength, the side reaction coefficients of the calibration ligand and the pH of the analysis could lead to subtle but important differences in Dw (Gledhill et al., 2015; Laglera and Filella, 2015; Ye et al., 2020).

The calibration of the competing AL is done by comparing the well-defined log α value of calibrating ligand, such as EDTA and diethylenetriaminepentaacetic acid (DTPA) with D. The corrections for ionic strength, the choice of the calibrating ligand side reactions and differences in pH have consequences for the resulting $K'_{Fe'AL}$ and/or $\beta'_{Fe'AL}$. Errors obtained during the derivation of D for the methods applied here range from < log 0.1 to log 0.9 (Abualhaija and van den Berg, 2014; Croot and Johansson, 2000; Gledhill and van den Berg, 1994; Rue and Bruland, 1995). From unpublished results of repeated calibrations, we have also found standard deviations in $K'_{Fe'AL}$ and/or $\beta'_{Fe'AL}$ between log 0.5 and log 1 for D.

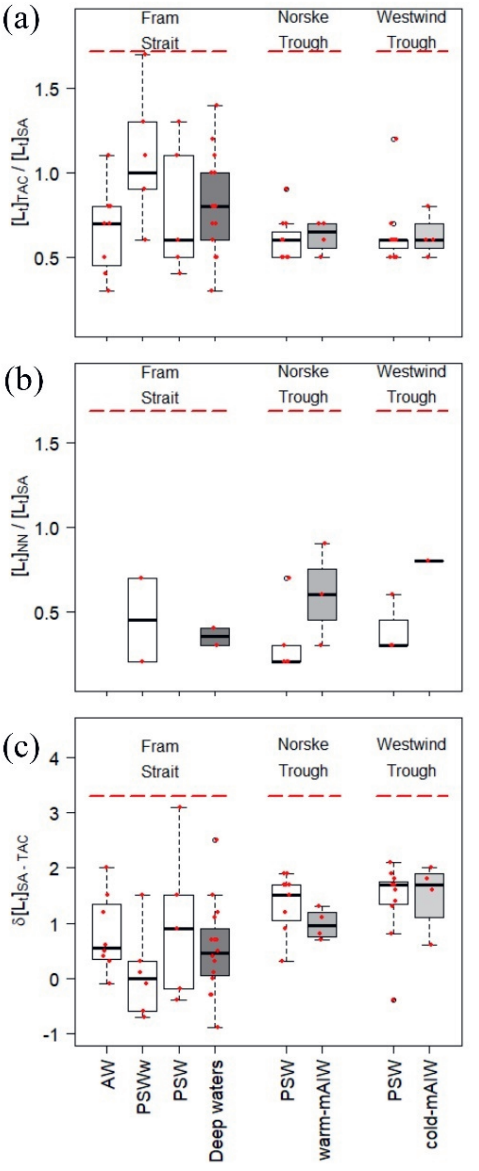

Figure 4-3. Boxplot showing the difference in ligand concentrations obtained by TAC, SA and NN, $[L_t]_{TAC}$, $[L_t]_{SA}$ and $[L_t]_{NN}$, respectively. a) the absolute difference in concentrations $[L_t]_{TAC}$ - $[L_t]_{SA}$ (nM eq. Fe), the relative ratio of b) $[L_t]_{TAC}$ / $[L_t]_{SA}$ and c) $[L_t]_{NN}$ / $[L_t]_{SA}$. The details of the boxplot are described in Figure caption 5-2.

In addition, uncertainties can emanate during the interpretation of titration data. The competition between AL and the natural ligands determines log $K_{Fe'L}^{cond}$ obtained where Fe additions filled the natural ligand sites, forming the curved part of the titration. The number of data points in the curved part hardly affects the calculation of [L_t], but a lack of data points here propagates high standard deviation in the estimation of log $K_{Fe'L}^{cond}$. This causes a high standard deviation in log $K_{Fe'L}^{cond}$ in relatively saturated natural organic ligands. In the linear part of the titration, the number of data points affects both the values of [L_t] and log $K_{Fe'L}^{cond}$. (Gerringa et al., 2014). Therefore, in our data we expect larger errors in $K_{Fe'L}^{cond}$ estimated by SA and NN because these methods had fewer data points in the range of 0-1.5 nM added Fe (steps of 0.5 versus 0.2 nM Fe added). Indeed, larger error in estimation of log $K_{Fe'L}^{cond}$(SA) and log $K_{Fe'L}^{cond}$(NN) relative to log $K_{Fe'L}^{cond}$(TAC) were observed (https://doi.org/10.25850/nioz/7b.b.7). Moreover, the sensitivity, which transforms the peak current (nA) into Fe concentration (nM), is obtained also from the slope of the linear part of the titration (Hudson et al., 2003). At high [L_t] it is possible that the linear part is not reached yet, and the titration curve is not truly linear, introducing an error in the estimation of S and [L_t]. The nonlinear Langmuir approach should compensate for this source of error in the data (Gerringa et al., 2014; Hudson et al., 2003; Turoczy et al., 1997).

The quality of the titration curves is given by the standard deviation of [L_t] and log $K_{Fe'L}^{cond}$. The variation of duplicate scans, especially in the first few points and at the high end of the titration could have large impact on the quality of the titration curves, adding uncertainties in the [L_t] and log $K_{Fe'L}^{cond}$, respectively. The zero Fe addition was done and measured twice to ensure that the measurement was not influenced by unconditioned cell. The variation of duplicate scans at low Fe addition could go up to 50%. The zero Fe addition was different from the blank only in a few samples containing near saturated ligands. The variation of duplicate scans at the high end of the titration affects the linear part of the titration curve, and thus the determination of [L_t], log $K_{Fe'L}^{cond}$ and S. Therefore, the highest point

Fe addition was done twice and measured with duplicate scans. At the highest Fe addition, the difference between duplicate scans was sometimes quite large, i.e. outliers were more than 20% different from the linear stretch (between 2 and 6 nM additions).

Other sources of uncertainty might come from the nature of the ligands. The heterogeneity of binding sites of large humic type molecules induces uncertainty depending on the saturation of the natural ligands with Fe. In this case, DFe concentration influences the outcome of the titration together with the detection window (Gledhill and Gerringa, 2017). Overall, the following discussion is limited to the above-mentioned uncertainties and the assumptions used on the calculations.

4.1 One-ligand model

The different detection windows reflect the ability of the methods to detect ligands (Gledhill and Gerringa, 2017) that are characterized by a range of log $\alpha_{Fe'L}$. The detection windows of the SA, NN and TAC methods overlap (log $Dw_{(SA)}$ = 0 – 1.6; log $Dw_{(NN)}$ and log $Dw_{(TAC)}$ = 1.4 – 3. 4). Nevertheless, the resulting median values for log $\alpha_{Fe'L}$ from the natural samples differ one order of magnitude between methods (SA: 1.2 – 3.5; TAC: 1.3 – 4.8; NN: 0.2 - 1.9; Table 2). Having the lowest Dw, the SA method detected ligands with log $\alpha_{Fe'L}$ values in between the other two methods (Figure 5-4e), and always had the highest [L_t] (Figure 5-2b), whereas log $K^{cond}_{Fe'L}$ obtained from each method varied for SA: log $K^{cond}_{Fe'L}$ 10 – 12.4, NN: log $K^{cond}_{Fe'L}$ 9.2 – 11.8 and TAC: log $K^{cond}_{Fe'L}$ 11.9 - 13.9 (https://doi.org/10.25850/nioz/7b.b.7). The three methods thus appear to detect different ligand pools in the same samples. However, considering an error of ±0.5 - 1 due to uncertainties in calibration of the AL, NN and SA could have detected the same ligand group, albeit with different concentrations. With TAC we might have detected a different and stronger ligand group, compared to the results of the other two methods.

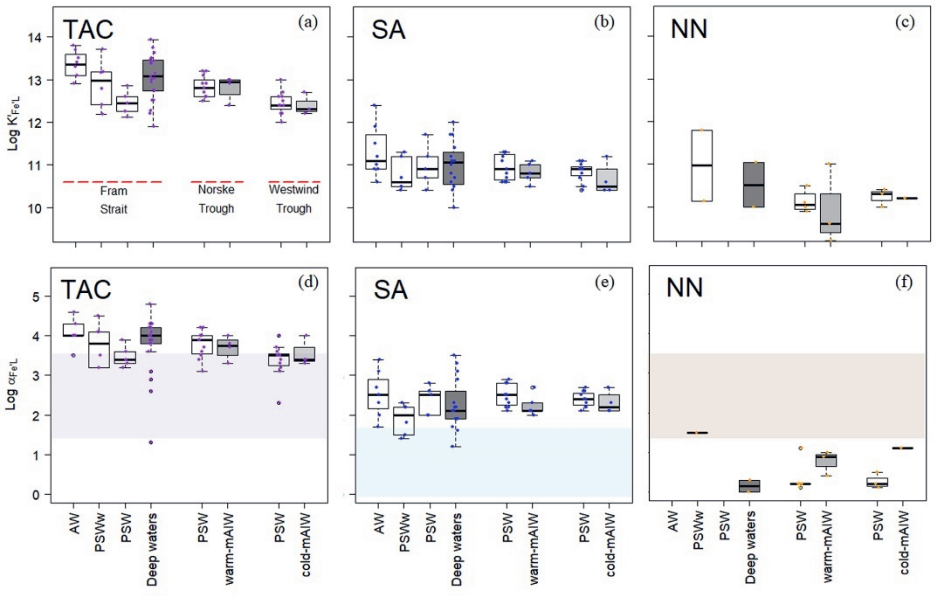

Figure 4-4. Boxplot of the conditional stability constants (log $K^{cond}_{Fe'L}$, a,b,c) and side reaction coefficients (log $\alpha_{Fe'L}$, d,e,f) from three different methods using TAC, SA and NN as the AL. The shades in d,e and f indicate the detection window (log Dw) for each method. The details of the boxplot are described in Figure 5-2.

Many of the log $\alpha_{Fe'L}$ values were above the upper limit of Dw for data using the TAC and SA methods (Figures 5-4d and 5-4e), which agrees with reported data using the same analytical procedures (Buck et al., 2015; Gerringa et al., 2015). Buck et al. (2015) reported a range of log $\alpha_{Fe'L}$ from 2.5 to 3.5 (in their Figure 5-4c) with log D = 1.8, whereas Gerringa et al. (2015) reported log $\alpha_{Fe'L}$ values that varied from ~ 3.0 to 4.0 (in their Figure 4) with log D = 2.4. Observations of log $\alpha_{Fe'L}$ above log Dw are relatively common (Caprara et al., 2016), which can be explained by the titration process. During a titration with Fe, [L´] decreases as the binding sites get filled with Fe, and consequently decreases the capacity of natural ligands to bind Fe ($\alpha_{Fe'L}$=[L′]*$K^{cond}_{Fe'L}$), whereas the capacity of AL ($\alpha_{Fe'AL}$) is assumed to be constant (Gledhill and Gerringa, 2017). The equivalence point of the titration is the point at which $\alpha_{Fe'L}$ = D. If during the titration,

the $\alpha_{Fe'L}$ crosses Dw, then values of $\alpha_{Fe'L}$ can be estimated. However, if the curve is not evenly weighted (i.e. more titration points lie below D_w than above as is usually the case), then the estimate may be biased. Furthermore, if $\alpha_{Fe'L}$ is below Dw, then the data must be treated with care, since the values of log $\alpha_{Fe'L}$ became even lower with the Fe additions during the estimation. This is the case for almost all results obtained with NN and possibly arises as result of the lower sensitivity of the NN method, since these impacts both on the detection limit and the precision of the method. In practice this means that D_w for NN is likely to be narrower than that for SA and TAC and that NN could underestimate log $K^{cond}_{Fe'L\,(NN)}$ using the CLE-AdCSV metal titration approach.

The median value of $\delta[L_t]_{SA\text{-}TAC}$ in PSW in western Fram Strait was 0.9 nM eq. Fe, whereas $\delta[L_t]_{SA\text{-}TAC}$ in PSW on the shelf increased to 1.5 nM eq. Fe and 1.7 nM eq. Fe, respectively, in the Norske Trough and in the Westwind Trough (Figure 5-3c). According to Laglera et al. (2011), the TAC method cannot detect part of the HS, and the NN method not sufficiently sensitive enough to elucidate stronger HS binding sites at nanomolar Fe concentrations in seawater. No consensus exists however on the underestimation of the HS ligands by the TAC method (Batchelli et al., 2010; Dulaquais et al., 2018; Gerringa et al., 2007; Slagter et al., 2017). Slagter et al. (2019) concluded that the TAC method can detect HS ligands when these ligands are either present at high concentrations or of a specific chemical composition. This could explain the lower $[L_t]$ obtained with the TAC and NN methods compared to the SA method, and may even support the above reasoning using D. Since HS are heterogenous - with a distribution of ligand sites- HS does not therefore itself fit into 'one group' of ligands as determined by CLE-CSV. Moreover, the observable heterogeneity of ligand binding sites in samples is reduced at a higher detection window, thus a group of binding sites can be missed by an AL with a higher detection window (Gledhill and Gerringa, 2017). As such, the presence of HS as part of the ligand pool, can to some extent explain the difference in results between the methods. The PSW-flow via the TPD from the Arctic likely transfers HS ligands (Laglera et al., 2019a; Slagter

et al., 2019). Approximately 62% of the Fe-binding ligands are humics in the TPD flow path in the Arctic (Sukekava et al., 2018), and thus $[L_t]_{TAC}$ is probably underestimated for the NN method, the influence of HS on the results obtained were only for measurements at high NN concentrations when HS possibly cannot compete with NN (Laglera et al., 2011). However, NN ([NN] = 5 µM; log D = 2.9) has successfully been used to assess DFe speciation in Antarctic sea ice (Genovese et al., 2018; Lannuzel et al., 2015).

The $[L_t]_{TAC}$ and $[L_t]_{SA}$ capture the same trend of increasing concentrations from Fram Strait to Norske Trough and Westwind Trough (Figures 5-2a and 2b ; SI Figure 5-2a) with a fairly constant ratio of $[L_t]_{TAC}$ over $[L_t]_{SA}$ in PSW (median $[L_t]_{TAC}/[L_t]_{SA}$ = 0.6; Figure 5-3b). The absolute differences, $\delta[L_t]_{SA\text{-}TAC,}$ varied in Fram Strait, where the HS influence possibly also varied, because the PSW-flow in western Fram Strait likely contains Arctic HS ligands. This suggests that HS play a role in the different results by the TAC and SA methods, however, the constant ratio ~0.6 suggests a systematic offset between two methods, similar to the earlier studies (Buck et al., 2016; Slagter et al., 2019). Buck et al. (2016) concluded that TAC measurements from Gerringa et al. (2015) determined roughly half the ligand concentrations measured by the 25 µM SA method (Buck et al., 2012) at the BATS station in the Western Atlantic near Bermuda. Comparing the TAC and 25 µM SA methods, Slagter et al. (2019) found a ratio of 0.6 in the Arctic Ocean as well, remarkably both in and outside the influence of the HS-rich TPD. It must be noted that the 25 µM SA method is different in concentration and equilibration time from the SA method used in our study, indicating the offset likely appears irrespective to the used analytical procedure. In addition, even though a ratio near 0.6 is often found, the offset is irregular in Fram Strait outside PSW as we find ratios varying between 0.6 and 1 (Figure 5-3b). Thus, the question remains, does the TAC method underestimate the ligand concentration because it cannot detect part of the ligands or does SA method overestimate the ligand concentration?

An offset caused by HS should result in varying ratios of $[L_t]_{TAC}/[L_t]_{SA}$ with a varying relative amount of HS, as shown in the value of $\delta[L_t]_{SA\text{-}TAC}$.

However, no relationship between HS and $[L_t]_{TAC}/[L_t]_{SA}$ was observed in a previous study (Slagter et al., 2019) and we also did not see difference between the ratio of $[L_t]_{TAC}/[L_t]_{SA}$ in HS-rich PSW compared to HS-poor AW (Figure 5-3b). Therefore, the difference between TAC and SA cannot solely be ascribed to their respective abilities to detect ligand groups in HS.

To conclude, the method with the highest detection window, i.e. TAC can detect a strong ligand group, and possibly misses weaker ligand groups, which were detected by the method with a lower detection window, SA. In contrast, despite having D_w similar to TAC, The use of NN results in both a lower $[L_t]$ and log $K^{cond}_{Fe'L}$. The application of multiple methods as suggested by Buck et al. (2012) thus requires careful consideration. Nevertheless, our results showed that the one ligand model captured a similar trend in $[L_t]$ for all three AL, and $[L_t]$ increased from Fram Strait to the Norske Trough to the Westwind Trough (Figure 5-2).

4.2 Two-ligand model

A one and a two-ligand model were fitted in the same dataset. The one-ligand model gives an overall bulk result of what is present to facilitate the comparison of all samples. The two-ligand model worked only in a few samples where two ligand groups were different enough to be distinguished. Even though the two-ligand model did not work in some samples, this does not mean that the diversity is less, only that the diversity obscures that two groups can be detected.

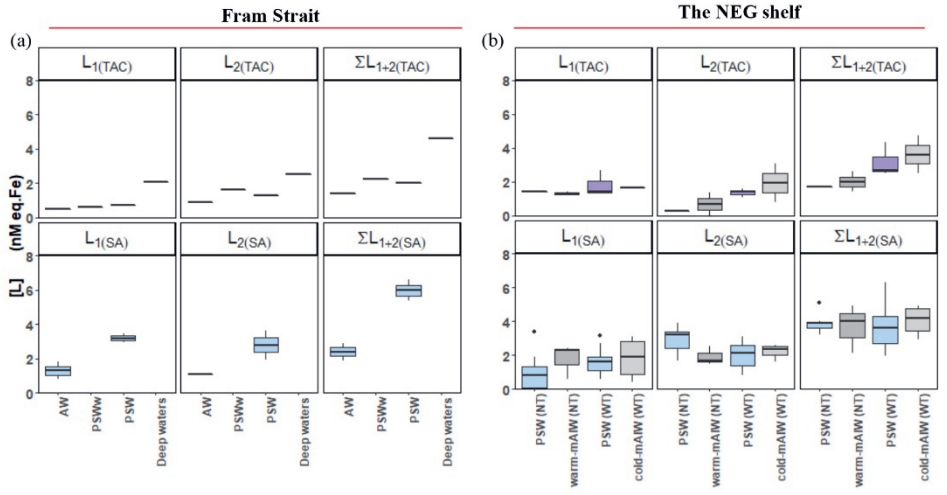

Figure 4-5. Boxplot of the results from a two-ligand model: ligand concentrations of the strong ligand group [L_1], and the relatively weak ligand group [L_2], together with the sum of [L_1] and [L_2] from samples a) from Fram Strait and b) from the northeast Greenland shelf. The details of the boxplot are described in Figure 2.

A strong and progressively weaker ligand group was distinguished (Figures 5-6a and 5-6b) by the methods using TAC and SA as AL. Distinguishing two ligand groups is possible when ligands are distinct enough, although this depends on data quality and interpretation. The number of data points in a titration determines the quality of the interpretation whereas the different pH of the analyses and the different saturation with Fe of the ligand are complicating the interpretation (Gledhill and Gerringa, 2017; Ye et al, 2020). Assuming that two ligand groups exist, [L_t], log $K^{cond}_{Fe'L}$ and log $\alpha_{Fe'L}$ in the one-ligand model represent a mixture of ligand groups (Figures 5-4a, 5-4b and 5-4c) probably with a continuum binding strength from strong to weak ligands (Buffle et al., 2007; Bundy et al., 2014). The range of log $K^{cond}_{Fe'L}$ that has been reported spans up to five orders of magnitude from 9 to 14 and covers samples from the coastal to the open ocean (Gledhill and Buck (2012);and Hassler et al. (2017) in their Tables 1). In this study the distinction of two ligand groups was possible in results from the TAC and SA methods. The conditional stability constants of the L_1 and L_2 ligand group obtained from each AL method are quite distinct and only for SA there is a slight overlap between

the strong and weak log $K^{cond}_{Fe'L}$ values (log $K'_{1(TAC)}$ = 11.6 – 14 and log $K'_{2(TAC)}$ =11.1 – 11.7; log $K'_{1(SA)}$ = 11.3 – 13.8 and log $K'_{2(SA)}$ = 10.5 – 11.2; Figures 5-6a and 5-6b; https://doi.org/10.25850/nioz/7b.b.7). The log $K'_{1(TAC)}$ is overlapping with log $K'_{1(SA)}$. In addition, the log $K'_{2(TAC)}$ is in between log $K'_{1(SA)}$ and log $K'_{2(SA)}$, suggesting that the L_2 ligands detected by the TAC method are also detected by the SA method. Results from the NN method could not be resolved in two ligand groups in any of samples analyzed. To the best of our knowledge, the detection of two ligand groups from samples analyzed using NN as the AL, has never been reported (Boye et al., 2001; Genovese et al., 2018; Lannuzel et al., 2015).

There is a significant correlation between $\sum L_{1+2}$ and [L_t] from the TAC and SA methods (p-value<0.05; SI Figure 2b and 2c). The SA method can resolve two ligands in more samples than the TAC method, especially for samples from the shelf. The SA method has a lower D, and therefore it should be better equipped to detect the weaker L_2 ligand group.

Given the many sources of uncertainties mentioned above, the error of the D is probably bigger than assumed, reducing likewise the precision of [L_t] and foremost log $K^{cond}_{Fe'L}$ values. The composition of ligands as well as the heterogeneity of binding sites add an unknown error. The use of multiple methods did not simply resolve this issue. Our data shows that the ligand pool may contain two ligand groups or better stated two groups of binding sites.

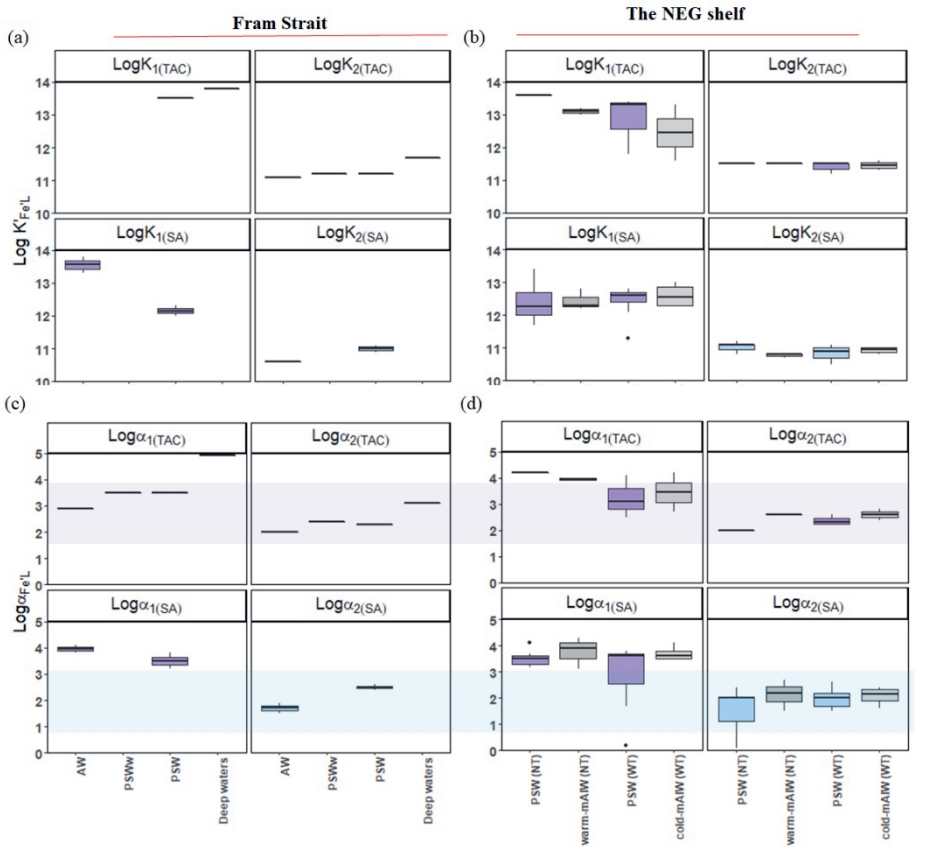

Figure 4-6. Boxplot of the results from a two-ligand model: the conditional stability constants of the relatively strong (log K′$_1$) and weak ligand groups (log K′$_2$) from samples a) from Fram Strait and b) from the northeast Greenland shelf; side reaction coefficients of the relatively strong (log α_1) and weak ligand groups (log α_2) from samples c) from Fram Strait and d) from the northeast Greenland shelf. The application of TAC and SA are indicated in subscribed letters. The shades in c and d indicate the detection window (log Dw) for each method. The details of the boxplot are described in Figure 42.

4.3 Environmental implications of Fe speciation: consequences for Fe transport

Apart from possible method specific bias, similar trends in increasing $[L_t]_{TAC}$, $[L_t]_{NN}$ and $[L_t]_{SA}$ from Fram Strait to the Norske Trough and

Westwind Trough may reflect a spatial and temporal differences in $[L_t]$ in each biogeochemical province as described by Ardiningsih et al. (2020). It is reassuring that this trend is observed regardless of the used AL. The samples from Fram Strait have higher ratios of $[L_t]_{TAC}/[L_t]_{SA}$. This might be explained by a different composition of the ligand pool, compared to the shelf. However, as shown above, a distinction in the L_1-type and L_2-type ligands was not possible in Fram Strait. In deep waters of Fram Strait, $[L_t]_{TAC}$ is almost equal to $[L_t]_{SA}$ in near-seafloor samples (stations 7 and 14, SI Figure 5-3), whereas at intermediate depth (~400 – 600 m, stations 14 and 26, SI Figure 5-3) $[L_t]_{TAC}$ is even higher than $[L_t]_{SA}$. Biogeochemical and physical processes may alter the nature of Fe-binding ligands, changing the composition of the existing ligand groups, i.e. decomposition of sinking organic matter and vertical mixing in the water column (Tani et al., 2003). As speculated above, the alteration of ligand characteristics in the water column may explain the large variations of the ratios of $[L_t]_{TAC}/[L_t]_{SA}$ in PSWw (Figure 5-3b). Overall, specific groups of ligands may not be detected by one method, whereas it is detected by the other, influencing the $[L_t]_{TAC}/[L_t]_{SA}$ ratio.

Seawater on the shelf has a $[L_t]_{TAC}/[L_t]_{SA}$ ratio of 0.5-0.6, and surface waters (>100 m) in PSW in Fram Strait, show a similar ratio. These similarities may be indicative of a similar composition of the ligand pool in PSW. Bundy et al. (2014) suggested that water mass-specific in situ production of ligands is responsible for the increase in strong ligands in surface waters, whereas ligands from terrestrial origin mainly contributed to a weaker ligand group in surface waters. Ardiningsih et al. (2020) suggested that Fe-binding ligands in surface waters of the western Fram Strait mostly originated from surface microbial activity, with potential addition of HS ligands from the Arctic Ocean via the TPD-flow. In the shelf region, microbial processes seem to be the main source of ligands with possible addition of HS or exo-polymeric substances (EPS) produced *in situ* (Burkhardt et al., 2014; Calace et al., 2001; Decho and Gutierrez, 2017; Laglera et al., 2019b; Laglera and van den Berg, 2009; Poorvin et al., 2011). Moreover, EPS that are excreted by microbes, are expected to

be present abundantly (Decho and Gutierrez, 2017; Hassler et al., 2011), especially in regions with sea ice-coverage (Genovese et al., 2018; Krembs et al., 2002; Lannuzel et al., 2015; Lin and Twining, 2012) such as surface waters over the northeast Greenland shelf. Thus, a mixture of ligand groups is expected in PSW, as confirmed by the distinction of two ligand groups in PSW of the western Fram Strait (by the SA method and only 4 samples by the TAC method) and over the shelf (by the SA and TAC methods) (Figure 5-5b)

The concentrations of excess ligand [L´] increased from Fram Strait to the Norske Trough and Westwind Trough (SI Figure 5-4), indicating that ligands became less saturated. This increase is not only seen by TAC (Ardiningsih et al., 2020), but is here also confirmed by the SA method. The results of the two-ligand model have shown that the ligand pool contained the relatively weak ligand group, with a low complexation capacity despite its high concentration. Therefore, even though [L´] is available and provides binding sites for Fe, the low affinity of these ligands for Fe binding implies these ligands are relatively ineffective in preventing Fe scavenging and precipitation. Any additional Fe source to the seawater will effectively not result in more DFe, but rather in more Fe precipitation along with adsorption on sinking particles, thus capping DFe in seawater at the concentration range defined by the effective binding affinity (the product of [L´]* K'_{FeL}) of the natural ligands. This was previously postulated by Ardiningsih et al. (2020) based solely on the TAC method to explain how ligand characteristics were crucial in controlling DFe export from the 79N Glacier terminus into Fram Strait. The use of the SA method provided a wider view in resolving the L_2 ligands, a relatively weak ligand group.

5. Conclusions

The assessment of TAC, SA and NN as AL with their specific detection windows in CLE-AdCSV titrations resulted in different ligand characteristics. The values of log $K^{cond}_{Fe'L}$ and log $\alpha_{\mathrm{Fe'L}}$ obtained from the SA method (log $K^{cond}_{Fe'L}$ 10 – 12.4; log $\alpha_{\mathrm{Fe'L}}$ 1.2 – 3.5) fell in between the other

two methods (TAC: log $K^{cond}_{Fe'L}$ 11.9 - 13.9, log $\alpha_{Fe'L}$ 1.3 – 4.8 and NN: log $K^{cond}_{Fe'L}$ 9.2 – 11.8; log $\alpha_{Fe'L}$ 0.2 - 1.9). Hence, we cannot be sure that the ligands detected by the SA method are chemically similar to the ones detected by TAC and NN. The standard deviation of titration results, published by our group and others, generally considers only the fit of the data to the Langmuir isotherm, and not the underlying uncertainty of the precision of D of the ALs. Taking the uncertainty in D into account the interpretation is hampered by relatively large standard deviations generated by CLE-AdCSV titrations.

Our results showed that the SA and TAC methods detected ligands above or at the upper end of its Dw, whereas NN below its Dw. The results do not reflect the application of a broad detection window by the three ALs which are probably due to uncertainties propagated from the calibration of ALs, the titration procedures and the nature of ligands (i.e composition of ligands and the heterogeneity of binding sites). The inability of TAC and NN to detect part of HS, is a probable explanation for the lower $[L_t]_{TAC}$ and $[L_t]_{NN}$ compared to $[L_t]_{SA}$ in this study.

Our data from Fram Strait, where $[L_t]_{TAC}/[L_t]_{SA}$ changes without relation to Arctic outflow of HS, provides an indication that other ligand groups than humics interfere with the detection efficiency of the AL. Other ligand groups also seem to be detected to a different extent by the TAC and SA methods. The constant ratios of $[L_t]_{TAC}/[L_t]_{SA}$ ~0.5 – 0.6 observed for the shelf region versus the variable ratios of $[L_t]_{TAC}/[L_t]_{SA}$ in Fram Strait requires future research looking at the method specific bias in detecting specific types of Fe-binding ligands.

The similar trend of increasing $[L_t]$ from Fram Strait to Norske Trough and Westwind Trough was captured by all three methods. This trend most likely reflects the spatial and temporal variability of Fe-binding ligands in the sampling region. The SA method is more suitable for the distinction of a relatively weak ligand group given that the detection window of SA is lower than TAC. The distinction of two ligand groups by both the TAC and SA methods provides information on the composition of Fe-binding

ligands, particularly in PSW of western Fram Strait and in PSW over the shelf.

Supplementary Information (SI)

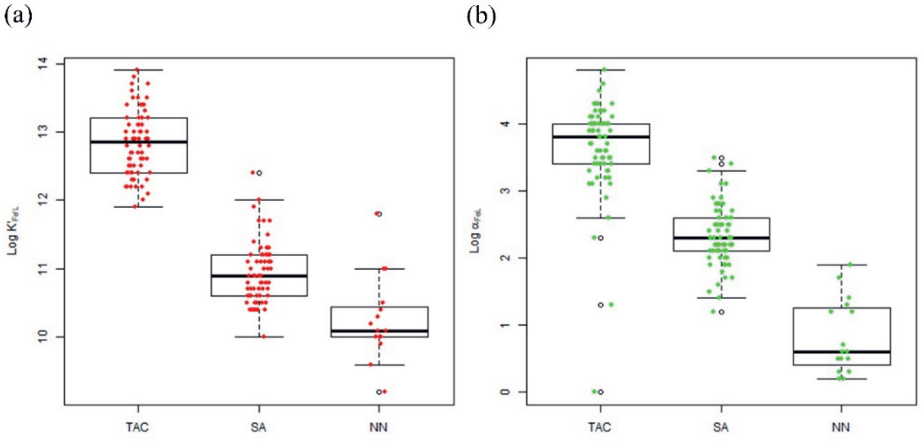

SI Figure 4-1. Boxplot of the values of log $K^{cond}_{Fe'L}$ (a) and log $\alpha_{Fe'L}$ (b) according to the one-ligand model from overall samples analyzed using the TAC, SA and NN.

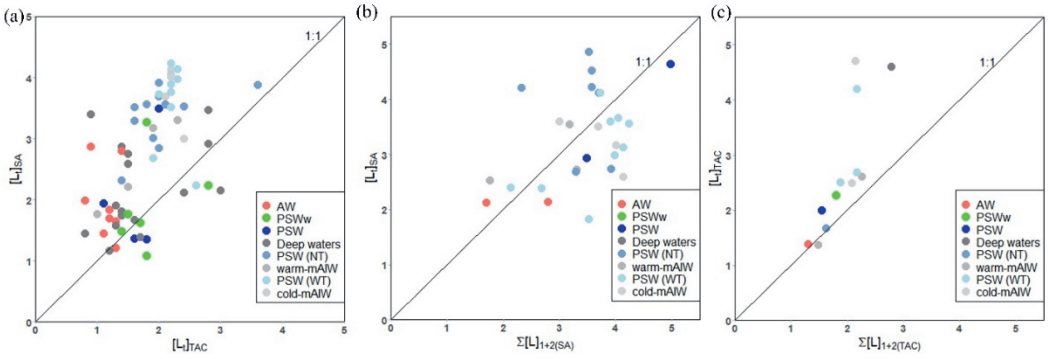

SI Figure 4-2. Comparison between ligand concentrations (a) $[L_1]_{TAC}$ versus $[L_1]_{SA}$ according to the one-ligand model. (b) $[L_1]_{SA}$ versus $\sum L_{1+2(SA)}$, the sum of the relatively strong and weak ligand groups $[L_1]_{SA}$, $[L_2]_{SA}$, obtained using SA according to the two-ligand model. (c) $[L_1]_{TAC}$ versus $\sum L_{1+2(TAC)}$, the sum of the relatively strong and weak ligand groups $[L_1]_{TAC}$, $[L_2]_{TAC}$, obtained using TAC according to the two-ligand model. The diagonal line indicates the 1:1 ratio. Figures were made using the software package R.

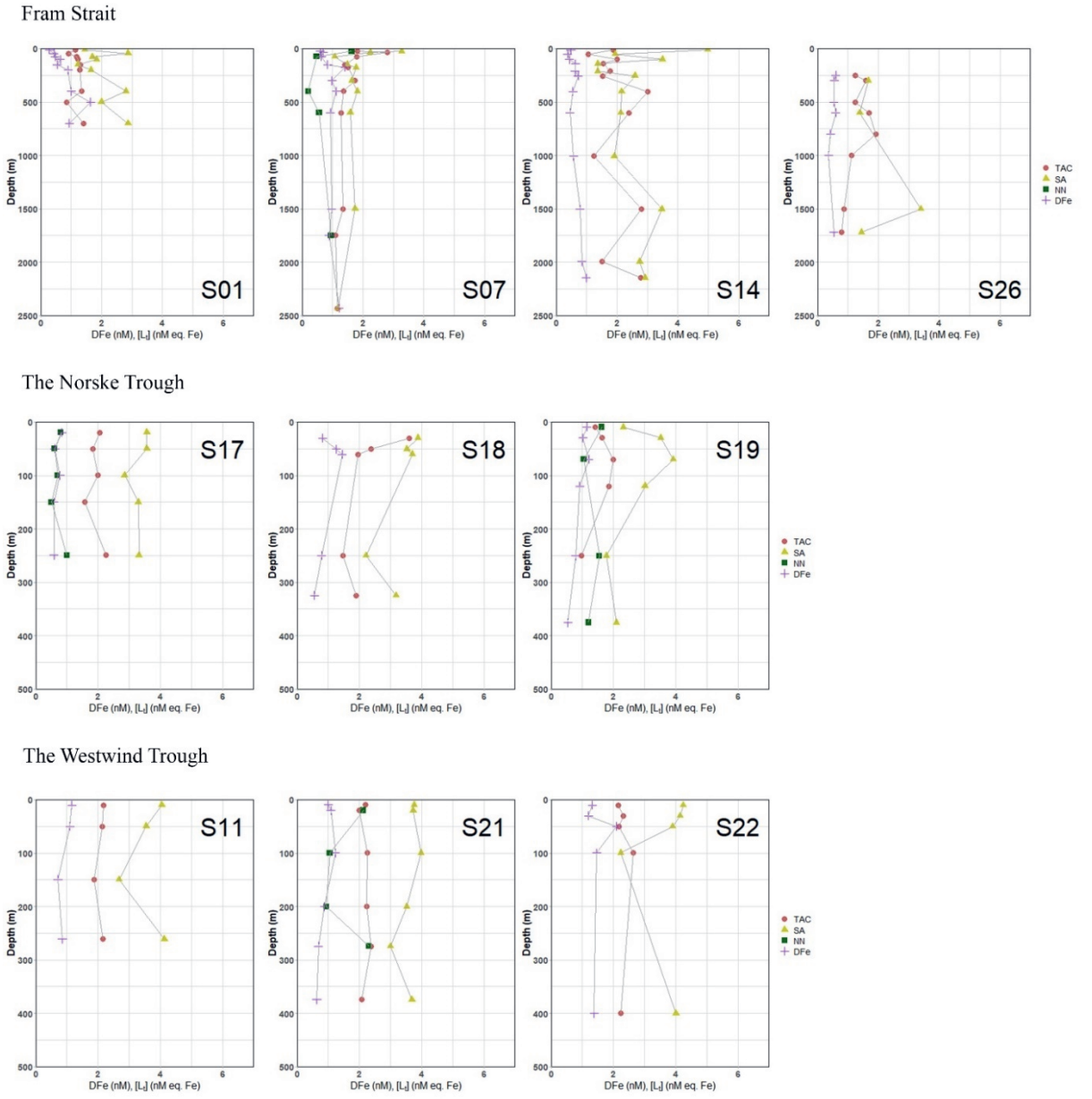

SI Figure 4-3. The depth profiles of dissolved-Fe (DFe) and total ligand concentrations [L_t] of three different methods using different added ligands (TAC, SA and NN) for each station in Fram Strait and over the Northeast Greenland shelf. Station numbers are indicated at the bottom right of each figure. Figures were made using the software package R.

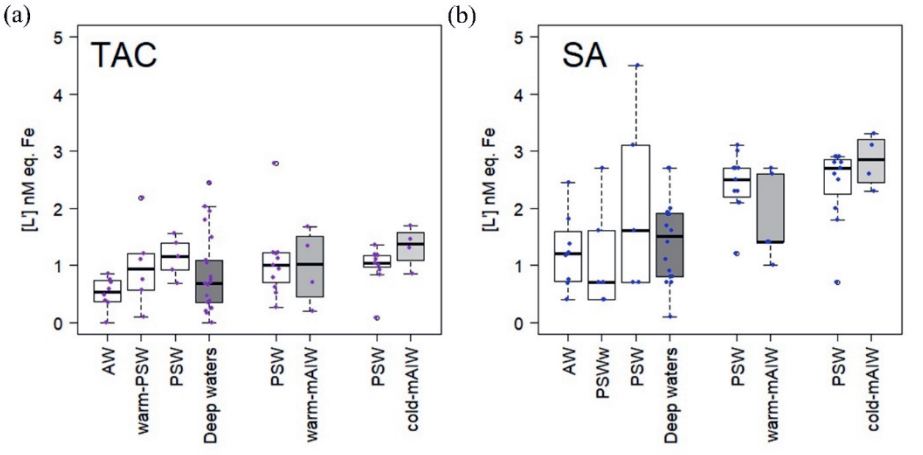

SI Figure 4-4. Boxplot of excess ligand concentrations ([L´]) the TAC (a) and SA (b) methods according to the one-ligand model. The added ligand used is indicated at the top left of each figure. The calculation was done using the script written in R software. The details of the boxplot are described in Figure 5-2.

Acknowledgments

The authors would like to acknowledge Captain Schwarze and his crew of the RV Polarstern, as well as chief scientist Torsten Kanzow and all other participants, for their effort and support during sample collection. Patrick Laan and Stephan Krisch are acknowledged for analyzing DFe. We are grateful for the help of Mathijs van Manen and Hans Slagter during sample analysis. IA was financed by Indonesia Endowment Fund for Education (LPDP), and KZ was financed by a scholarship from the China Scholarship Council.

Chapter 6

Fe-binding organic ligands in coastal and frontal regions of the western Antarctic Peninsula

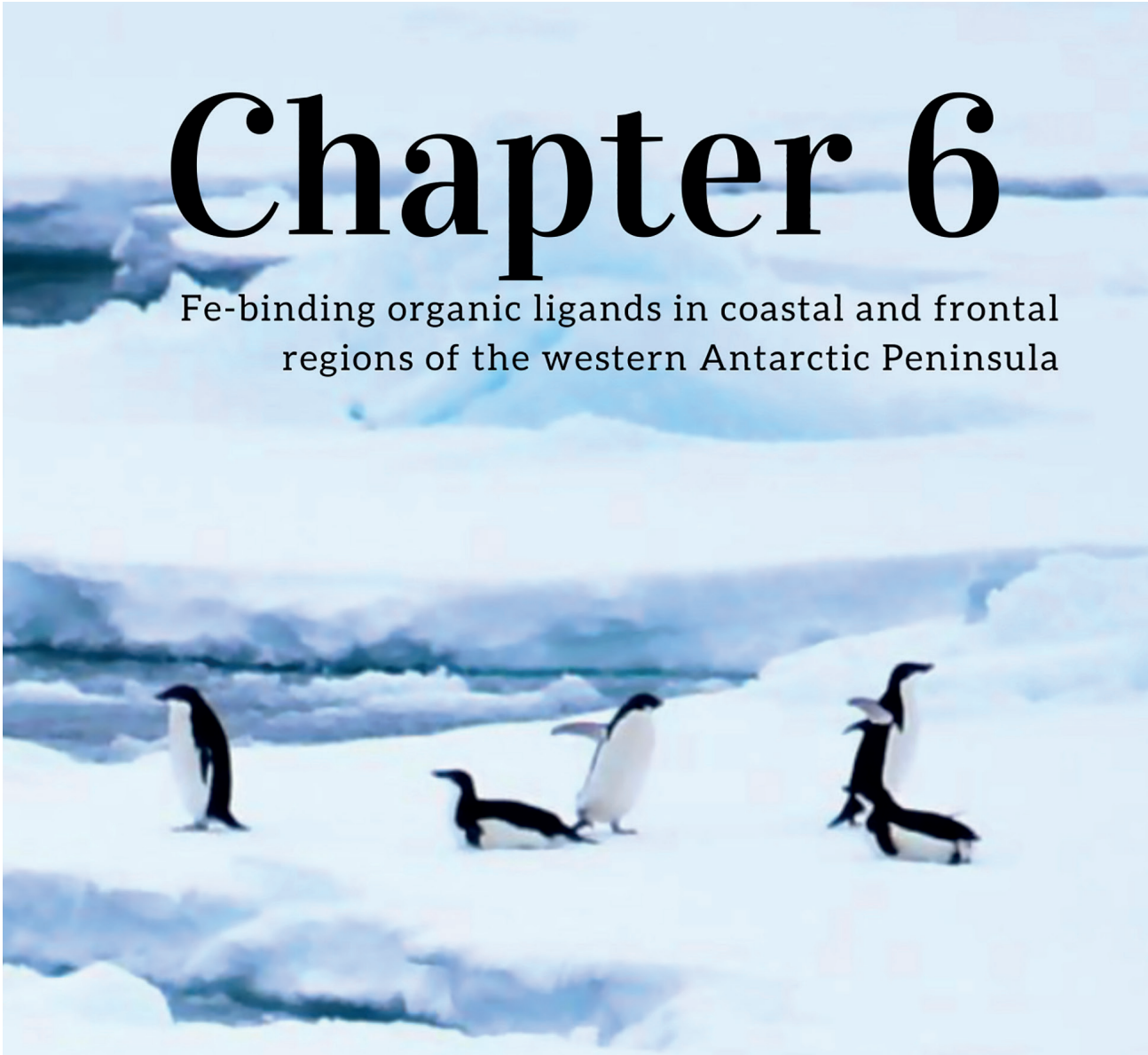

Indah Ardiningsih, Kyyas Seyitmuhammedov, Sylvia G. Sander, Claudine H. Stirling, Gert-Jan Reichart, Kevin R. Arrigo, Loes J. A. Gerringa, Rob Middag

Ardiningsih et al., In press, Biogeosciences.

Abstract

Organic ligands are a key factor determining the availability of dissolved iron (DFe) in the high nutrient low chlorophyll (HNLC) areas of the Southern Ocean. In this study, organic speciation of Fe is investigated along a natural gradient of the western Antarctic Peninsula, from an ice-covered shelf to the open ocean. An electrochemical approach, competitive ligand exchange - adsorptive cathodic stripping voltammetry (CLE-AdCSV) was applied. Our results indicated that organic ligands in the surface water on the shelf are associated with ice-algal exudates, possibly combined with melting of sea-ice. Organic ligands in the deeper shelf water are supplied via resuspension of slope or shelf sediments. Further offshore, organic ligands are most likely related to the development of phytoplankton blooms in open ocean waters. On the shelf, total ligand concentrations ($[L_t]$) were between 1.2 nM eq. Fe and 6.4 nM eq. Fe. The organic ligands offshore ranged between 1.0 and 3.0 nM eq. Fe. The southern boundary of the Antarctic Circumpolar Current (SB ACC) separated the organic ligands on the shelf from bloom-associated ligands offshore. Overall, organic ligand concentrations always exceeded DFe concentration (excess ligand concentration, $[L']$ = 0.8 - 5.0 nM eq. Fe). The $[L']$ made up to 80% of $[L_t]$, suggesting that any additional Fe input can be stabilized in the dissolved form via organic complexation. The denser modified Circumpolar Deep Water (mCDW) on the shelf showed the highest complexation capacity of Fe ($\alpha_{Fe'L}$; the product of $[L']$ and conditional binding strength of ligands, $K_{Fe'L}^{cond}$). Since Fe is also supplied by shelf sediments and glacial discharge, the high complexation capacity over the shelf can keep Fe dissolved and available for local primary productivity later in the season, upon sea ice melting.

1. Introduction

The Southern Ocean is a High Nutrient Low Chlorophyll (HNLC; e.g. Sunda et al., 1989) region where the phytoplankton biomass is relatively low despite high ambient macronutrient concentrations, i.e. nitrogen (N), phosphorus (P) and silicon (Si) (e.g. Martin et al., 1991; Schoffman et al., 2016). The generally limited availability of light and the micronutrient iron (Fe) prevents phytoplankton from depleting P and N in the vast majority of HNLC areas (de Baar, 1990; de Baar et al., 2005; Martin et al., 1991; Viljoen et al., 2018). Indeed, Fe regulates the dynamics of primary production as it is involved in various cellular processes (Schoffman et al., 2016; Sunda, 1989). In the HNLC Southern Ocean, the availability of Fe has a direct impact on the early spring phytoplankton bloom, and thus on primary productivity (Moore et al., 2013). The Fe limitation in the Southern Ocean could thus have a direct effect on the amount of atmospheric CO_2 sequestration (Arrigo et al., 2008a; Le Quéré et al., 2016; Raven et al., 1999) to the deep ocean via the biological pump (De La Rocha, 2006; Lam et al., 2011). Accordingly, the availability of Fe in the Southern Ocean is not only important for sustaining the food web, but also has a substantial impact on global climate (Henley et al., 2019 and references therein).

The low solubility of Fe in seawater, coupled with low atmospheric and terrestrial input of Fe, result in the scarcity of dissolved-Fe (DFe) in the Southern Ocean. In oxygenated seawater, Fe is mainly present in its oxidized form, Fe(III), predominantly as Fe(III)oxy-hydroxide species. These species tend to undergo further hydrolysis (Liu and Millero, 2002) and are thereby removed from the water column by scavenging or precipitation processes. Organic Fe-binding ligands greatly elevate Fe solubility in seawater (Kuma et al., 1996) by stabilizing Fe in Fe-ligand complexes, and thus allowing Fe to remain longer in the water column. Moreover, Fe bound to organic ligands appears to be bioavailable to marine phytoplankton (Hassler et al., 2020; Maldonado et al., 2005; Rijkenberg et al., 2008a). As such, organic ligands are a key component of Fe chemistry and bioavailability, notably in HNLC regions, as illustrated

by Lauderdale et al. (2020). These authors showed, with an idealized biogeochemical model of the ocean, that the interaction between microbial ligand production and binding of Fe by these ligands functions as a positive feedback to maintain the DFe standing stock in the oceans.

Different ligand types exist with characteristics (*i.e* binding strength) often being defined by their origin. The characteristics of organic ligands can be measured by the competition against well-characterized artificial ligands with known stability constants. Analysis is done using an electrochemical technique, competitive ligand exchange (CLE) - adsorptive cathodic stripping voltammetry (AdCSV). The application of AdCSV gives the total concentration ($[L_t]$) and conditional binding strength ($K^{cond}_{Fe'L}$) of the dissolved organic ligands but does not provide information on the identity of ligands. Despite identities of Fe-binding ligands are still largely unknown, $[L_t]$ and $K^{cond}_{Fe'L}$ obtained from CLE-AdCSV measurement, together with ancillary data, can be used to infer the potential sources of these organic ligands. The organic ligands in seawater either have a terrestrial or marine source. The terrestrial-sourced ligands supply from lithogenic inputs within the boundary region between land and sea (i.e coastal seas and estuaries) (Buck and Bruland, 2007; Batchelli et al., 2010; Kondo et al., 2007; Buck et al., 2007; Bundy et al., 2015; Gerringa et al., 2007; Laglera and van den Berg, 2009). The organic ligands with marine source come from *in situ* biological activities, being either actively produced or passively generated through microbial activity.

Laboratory studies have documented the active production of Fe-binging ligands under Fe-limited conditions (Boiteau et al., 2013; Boiteau et al., 2016; Butler, 2005). Several types of siderophores, low-molecular-weight organic compounds which have strong affinity to Fe, are produced by mixed marine bacteria communities under Fe stress (Butler, 2005), suggesting that high ligand concentrations are related to a mechanism of Fe acquisition in an Fe-limited environment. These compounds have also been extracted (Boiteau et al., 2016; Macrellis et al., 2001; Velasquez et al., 2011) or identified (Mawji et al., 2008; Velasquez et al., 2016) in field samples. However, they generally occur at picomolar levels (Boiteau et al.,

2019) and are a small contributor to the total ligand pool. Other ligand types, such as polysaccharide compounds, are passively generated in situ from microbial excretion and grazing (Laglera et al., 2019b; Sato et al., 2007). The polysaccharides, such as exo-polymeric substances (EPS), are excreted abundantly by a large number of microbial cells, especially in surface water covered by sea-ice (Lannuzel et al., 2015; Norman et al., 2015). Although EPS are relatively labile macromolecules, they can be present in up to micromolar concentrations in seawater, showing the potential to outcompete stronger binding siderophores (Hassler et al., 2017). In addition, humic or humic-like substances (HS) from various origins constitute another type of ligand (Krachler et al., 2015; Laglera et al., 2019a; Whitby et al., 2020). Typically, HS are derived from remineralization and degradation of organic matter (Burkhardt et al., 2014). Terrestrial input of organic matter can supply HS to estuarine and coastal areas, whereas sediment resuspension and upwelling often supply HS to the continental shelf (Buck et al., 2017; Gerringa et al., 2008). HS have also shown to be part of Fe binding ligands in biologically refractory deep ocean dissolved organic matter (rDOM) with low Fe-bioavailability. However, photodegradation of rDOM was shown to increase the Fe bioavailability making Fe bound to such substances an important source in HNLC areas where upwelling plays a role (Hassler et al., 2020; Laglera et al., 2019a; Lauderdale et al., 2020; Whitby et al., 2020).

The Bellingshausen Sea along the western Antarctic Peninsula (WAP) region has a distinct natural DFe gradient (Moffat et al., 2018; Sherrell et al., 2018). The hydrography is strongly influenced by the dynamics of shelf-ocean water exchange. The shoreward intrusion of Circumpolar Deep Water (CDW) provides macronutrients to the shelf region, whereas offshore-flowing waters supply the micronutrients Fe and Mn to the open ocean from local sources (De Jong et al., 2015; Sherrell et al., 2018), such as glacial meltwater, sediments, and upwelling. The shelf sea of the WAP is a biologically-rich marine ecosystem in the Southern Ocean. The abundance, community composition and trophic structure of marine primary producers are directly impacted by the changing ice conditions and longer periods of open water due to climate change (Turner et al.,

2013). Moreover, rapid increases in anthropogenic CO_2 has enhanced the air-sea CO_2 fluxes, decreasing the bulk seawater pH, resulting in ocean acidification (Mikaloff Fletcher et al., 2006), which alters the physicochemical properties of seawater and impacts the organic complexation of Fe (Ye et al., 2020). As the WAP has undergone significant warming (Turner et al., 2020), the changes in ice conditions will influence the supply of Fe and organic ligands, shaping the net primary production in this region. Understanding the sources and distribution of organic ligands provides important information on DFe availability, which is a fundamental step towards understanding the impact of warming of the Antarctic region on primary productivity in the Southern Ocean.

In this study, surface waters were sampled in a region of mixing between shelf-influenced waters and HNLC waters in the Bellingshausen Sea along the WAP. The CLE-AdCSV technique was used to quantify the total concentrations and conditional stability constants of Fe-binding ligands. These parameters were used to examine the distribution and identify the potential sources of organic ligands from ice covered shelf waters to the open ocean of the Antarctic zone.

2. Material and methods

2.1 Sample collection

Samples were collected onboard the research vessel Nathaniel B. Palmer (Cruise NBP1409) during the austral spring between 31 October and 21 November 2014 in the Bellingshausen Sea, west of the Antarctic Peninsula (Figure 6-1). Water samples were obtained from the surface to maximum 600 m depth at five stations along a transect extending from Adelaide Island on the shelf out into the Bellingshausen Sea in a northwest direction (Figure 6-1). St. A(70) and B(72) are situated near the shore in the shelf sea, St. C(96) is located at the continental shelf break, and St. D(84) and E(90) are located offshore over deep waters. Hereafter, the

alphabetical scheme of the station number will be used, being station A is the closest station to the coast and station E is the furthest station from the coast.

Hydrographic parameters were measured using a conventional conductivity-temperature-depth (CTD) rosette equipped with a fluorometer (WET Labs ECOAFL/FL) and an oxygen sensor (SBE-43). Seawater samples for DFe and Fe-binding ligands in this study were obtained using 12 L GO-FLO bottles attached to a Kevlar® wire. Seawater samples were filtered over 0.2 μm filters (cellulose acetate, Satroban 300, Sartorius®) into pre-cleaned sample bottles inside a trace metal clean van. Sample bottles were pre-cleaned following a three-step cleaning protocol for trace element sample bottles (Middag et al., 2009).

Filtered seawater samples for Fe-binding ligand analysis were collected into acid-cleaned 500 mL low density polyethylene (LDPE, Nalgene) bottles and stored at -20ºC immediately after collection. For DFe analysis, filtered seawater was collected into acid-cleaned 60 mL LDPE (Nalgene), and acidified to a pH of 1.8 with concentrated quartz-distilled hydrochloric acid (HCl) to give a final concentration of 0.024 M HCl. Filtered samples for macronutrient concentration analysis were stored at -20ºC (for N samples) and at 4ºC (for Si samples).

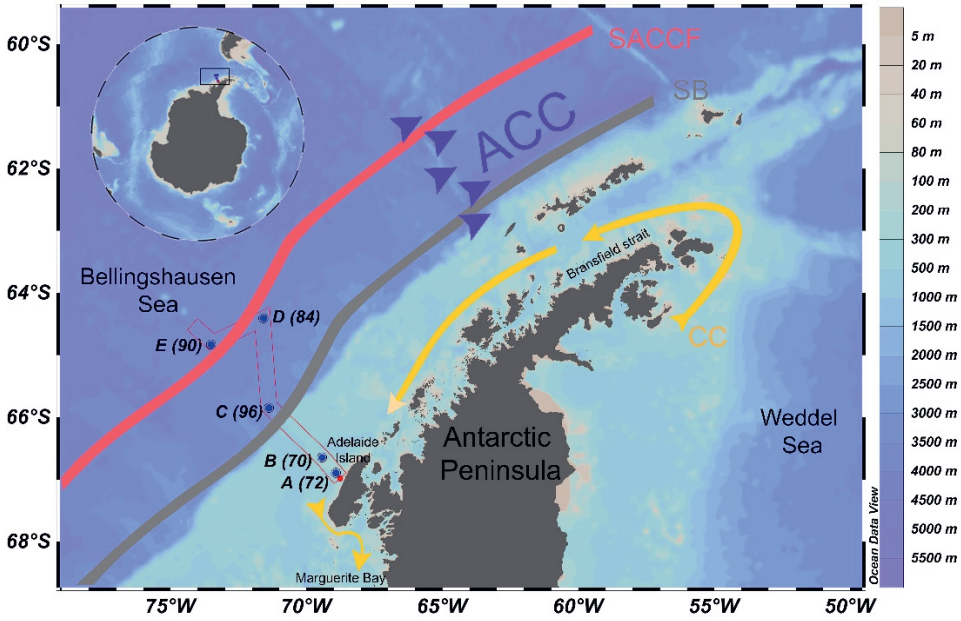

Figure 5-1. Map of the sampling sites along our study transect near the Western Antarctic Peninsula. The stations are indicated by blue dots and station numbers. The Antarctic Circumpolar Current (ACC) is indicated by purple arrows. The Coastal Current (CC) is indicated by a yellow arrow. The Southern Boundary (SB) of ACC Front is indicated by the grey line. The southern ACC front (SACCF) is indicated by the red line. The details ACC flow along the transect is described by Arrigo et al. (2017).

2.2 Analysis of DFe and nutrients

The DFe analysis is described in detail by Seyitmuhammedov et al. (in review). In short, the DFe analysis was conducted using high-resolution inductively coupled plasma mass spectrometry (HR-ICP-MS) using a Thermo Fisher Element XR instrument at NIOZ, the Netherlands and using an Amtek Nu Attom instrument at University of Otago, New Zealand. Samples were UV-oxidized and pre-concentrated using an automated seaFAST system (SC-4 DX seaFAST pico; ESI) equipped with Nobias-PA1 chelate resin. The quantification was done via standard additions. The recovery of the resin was ~100% and was verified in every analytical run by comparison between the slope of the seawater calibration

curve and the eluent acid calibration curve after (Biller et al., 2012). Accuracy and reproducibility were monitored by regular measurements of the reference materials SAFe D1 and GEOTRACES South Pacific (GSP) seawater, and an in-house reference seawater sample, North Atlantic Deep Water (NADW). Results for DFe analyses of reference samples were 0.722 ± 0.008 nM (n = 3; NIOZ) and 0.729 ± 0.018 nM (n = 6; U. Otago) for SAFe D1 2013 (consensus value = 0.69 ± 0.04 nM) and 0.155 ± 0.045 nM (n = 13) for GSP 2019 consensus values.The average overall method blank (seaFAST and ICP-MS), determined by repeatedly measuring acidified ultrapure water in every analytical run as a sample, was 0.05 ± 0.02 nM (n = 21). Macronutrients (N and Si) were analyzed simultaneously with a discrete autoanalyzer TRAACS 800 (Technicon) in the shore-based laboratory at NIOZ.

2.3 Analysis of Fe-binding ligands

Samples were thawed in the dark and vigorously shaken prior to further treatment. Electrochemical analysis CLE-AdCSV with salicylaldoxime (SA) as a competing added ligand (Abualhaija and van den Berg, 2014) was used. In short, the voltammetric system consisted of a BioAnalytical System (BASi) controlled growth mercury electrode connected to an Epsilon 2 analyzer (BASi). The voltammetric system was controlled using ECDsoft interface software. The electrodes in the voltammetric stand included a standard Hg drop working electrode, a platinum wire counter electrode, and a double-junction Ag/AgCl reference electrode (3M KCl).

For the titration, 10 mL sample aliquots were added to 12 pre-conditioned Teflon (Fluorinated Ethylene Propylene (FEP), Savillex) vials and buffered to seawater a pH of 8.2 with 0.1 M ammonium-borate buffer. The sample aliquots were titrated with Fe from 0 to 10 nM (with a 0.5 nM interval from 0 to 3 nM; and with a 2 nM interval from 4 to 10 nM Fe) and vials without Fe addition were prepared twice. Then, the competing ligand, SA, was added at a final concentration of 5 µM. The mixture was left to equilibrate for at least 8 hours or typically overnight (Abualhaija and van den Berg, 2014). Before analysis, the Teflon vials for titration were pre-

conditioned at least three times with seawater containing SA and the intended Fe addition. For each titration point, duplicate scans were done in the same Teflon vial as voltammetric cell.

2.4 Calculation of Fe speciation

Ligand parameters, [L_t] and $K^{cond}_{Fe'L}$, were obtained by fitting the data from the CLE-AdCSV titration into a non-linear Langmuir model. One- and a two-ligand models were applied, assuming one ligand and two ligand groups existed, respectively. The R software package was used for data fitting (Gerringa et al., 2014). The [L_t] reported in nM eq. Fe and the conditional stability constant values are reported as log $K^{cond}_{Fe'L}$.

The values of [L_t], log $K^{cond}_{Fe'L}$, and DFe were used to calculate the concentration of natural unbound ligands, the excess ligands concentration [L´], and the side reaction coefficient of ligands ($\alpha_{Fe'L}$; the product of [L´] and $K^{cond}_{Fe'L}$, Gledhill and Gerringa (2017). The prime symbol (´) in excess ligand concentrations denotes the free ligands not bound to Fe, whereas the prime symbol after Fe denotes the inorganic fraction of Fe. The value of $\alpha_{Fe'L}$ is presented as a logarithmic value (log $\alpha_{Fe'L}$) and referred to as complexation capacity.

The value of the inorganic Fe side reaction coefficient ($\alpha_{Fe'}$) was determined using the hydrolysis constants of Liu and Millero (1999) at S=36 and at pH of the analysis (pH=8.2). Hence, the value of log $\alpha_{Fe\text{-inorganic}}$ =10.4 was used in the calculation for Fe speciation. The conditional stability constant of SA (log $K^{cond}_{Fe'(SA)}$ = 5.94) used in this study is based on the calibration of SA against diethylenetriaminepentaacetic acid by Gerringa et al., (in review).

3. Results

3.1 Hydrography

Water masses were identified by plotting the Conservative Temperature (Θ) versus the Absolute Salinity (S_A) (Tomczak and Godfrey, 2003) as generated by the freeware ODV (Schlitzer, 2018) from CTD data (Figure 6-2a). The water mass description follows the definitions of Klinck et al. (2004) and Smith et al. (1999). A detailed description of hydrographic features of the WAP was described elsewhere (Klinck et al., 2004; Moffat and Meredith, 2018; Smith et al., 1999) and briefly summarized here.

Two distinct horizontal currents exist in the study area: The Coastal Current (CC) and the Antarctic Circumpolar Current (ACC) (Figure 6-1). In the vicinity of the WAP, the ACC is a large strong eastward flowing current bordering the outer continental shelf. The CC is a strong but narrow southwesterly flowing current that is forced by freshwater discharge and wind over the shelf (Grotov et al., 1998; Moffat and Meredith, 2018). The CC flows along the coast of the WAP from Bransfield Strait to Marguerite Bay (Figure 6-1). Our sampling stations are located along a transect that is perpendicular to the prevailing currents. A number of oceanographic fronts exist along the ACC (Orsi et al., 1995). Two fronts intersect our sampling transect, namely the southern ACC Front and the southern boundary (SB) of the ACC. These two fronts are present oceanward from the shelf (Figure 6-1), usually about 50 – 200 km apart. Although their positions vary, these fronts remain approximately parallel with the continental shelf break along the WAP (Moffat and Meredith, 2018).

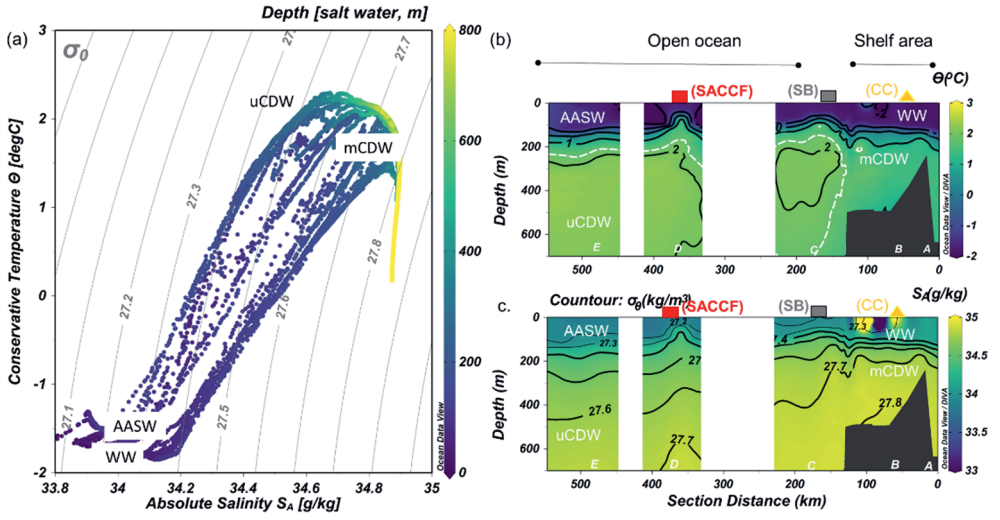

Figure 5-2. (a) Diagram of absolute salinity (S_A) versus conservative temperature (Θ) with isopycnal lines and colors denoting depth in m. The distribution along the transect shown in Figure 6-1 of (b) Θ and (c) S_A with density (σ_θ) as contours. The approximate boundary between uCDW and mCDW is marked with white-dashed line in Figure 6-2(b). The values of Θ and S_A were generated by ODV software from CTD data.

During the austral spring sampling period, Winter Water (WW; Θ < -1.8 °C and S_A ~34.1) still existed in the upper 100 m at stations in the shelf sea (Figures 6-2b and 6-2c). In spring, Antarctic Surface Water (AASW) forms that has a higher temperature (-1.5 – 1°C) and a lower salinity (33.0 < S_A< 33.7) than WW (Orsi et al., 1995; Tomczak and Godfrey, 2003). During sampling, AASW was present at stations outside the shelf region (St. D, E and C; Figures 6-2b and 6-2c). The position of the SB marks the southern terminus of water with CDW properties. From the shelf break toward the open ocean, upper Circumpolar Deep Water (uCDW) existed at 300 m depth, characterized by Θ_{max} = 2°C and a maximum of S_A ~34.7. Near the WAP, the Antarctic Slope Front is missing (Klinck et al., 2004; Moffat and Meredith, 2018); hence, there is no barrier in the outer shelf region (Klinck et al., 2004). As a consequence, the shelf region is directly affected by the presence of the SB, resulting in subsurface intrusion of uCDW onto the continental shelf. This water mass is modified into cooler and less saline water, referred to as modified CDW (mCDW) (Hofmann et

al., 1998), and was present at stations 70 and 72 below 200 m. Ocean eddies, modulated by wind forcing and interaction with the slope, are responsible for the transport of uCDW from the ACC into the inner shelf region. Intrusion of uCDW displaces shelf water, allowing a heat flux to the shelf area that triggers the melting of floating ice shelves. Melting of the glacial ice produces buoyant northward (offshore) flowing surface water that maintains the continuation of offshore-onshore water mass exchange (Klinck et al., 2004; Moffat and Meredith, 2018), although it did not seem to occur along our transect.

The ice-coverage diminished with increasing distance from the shore, with stations near-shore (St. A and B) having sea ice concentrations of 100%, and falling to 60% at the shelf break (St. C). The ice-cover dropped to 20% at St. D offshore, whereas St. E was ice free.

3.2 Fe speciation

Stations located in the continental shelf (St. A and B) generally had higher [L_t] and DFe than stations sampled offshore (St. C, D and E; Figures 6-3a and 6-3b). At the shelf stations, [L_t] varied from 1.23 to 6.43 nM eq. Fe and high [L_t] (>2 nM) was present below 200 m in mCDW (Figure 6-3a). In particular, at St. A nearest to the shore, [L_t] was higher than 2.5 nM eq. Fe at the surface and reached up to 6.43 nM eq. Fe at 400 m close to the sediment.

Concentrations of DFe were <0.6 nM (0.29 - 0.52 nM) in the upper 100 m, but >1 nM (1.11 to 2.26 nM) at depths below 200 m near the sediment (Figure 6-3b). Further offshore towards the open ocean (St. C, D and E), [L_t] varied from 1.07 to 3.09 nM eq. Fe (Figure 6-3a), whereas DFe concentrations ranged from <0.05 and 0.47 nM (Figure 6-3b). At the shelf break, approximately where the SB was located, [L_t] was relatively low (St. C; Figure 6-3a). Low DFe was observed in the upper 200 m offshore, reaching the lowest concentration (<0.05 nM) at St. E farthest from the shelf (Figure 6-3b).

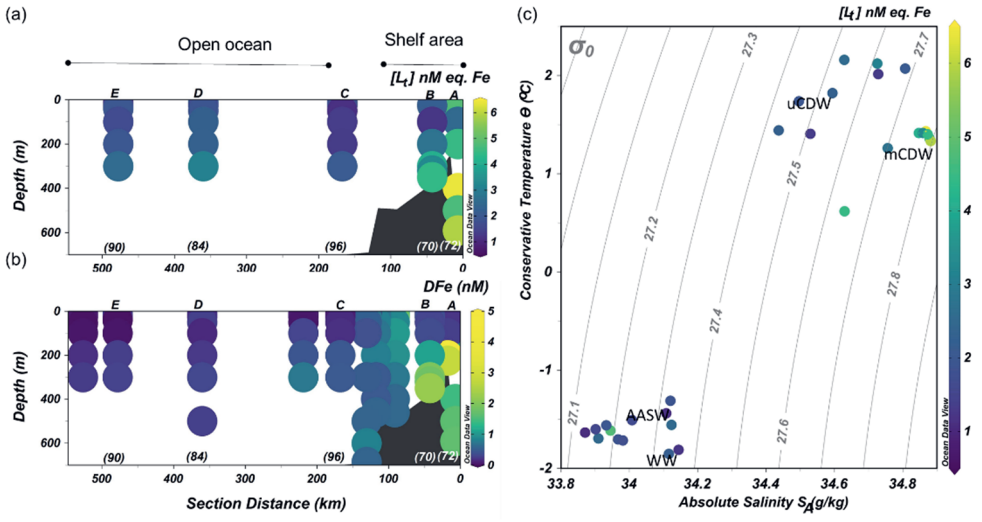

Figure 5-3. The distribution along the transect shown in Figure 6-1 of (a) the concentrations of total Fe-binding ligand [L_t] and (b) concentrations of dissolved-Fe (DFe, data from Seyitmuhammedov et al.,(in review); and (c) a Θ-S_A diagram with colors denoting the values of [L_t]. The alphabetical (above) and numerical (below) indication in (a) and (b) point to the stations. DFe data is not in linear-scale for clarity.

Two ligand groups were distinguished only in two samples in open ocean waters, both collected at St. E (at 40 and 300 m). The measured conditional stability constant for the stronger L_1 ligands and the progressively weaker L_2 ligands were distinct, and the values did not overlap. At 40 m, log K_1 = 12.4±1.1 and log K_2 = 10±1.1, whereas at 300 m, log K_1 = 11.3±0.6 and log K_2 =10.4±0.7. However, the uncertainty for the ligand concentrations was relatively large for the two-ligand model, L_1 (0.66±1.81 and 1.58±4.29 nM eq. Fe, at 40 and 300 m, respectively) and L_2 (1.10±4.32 and 1.34±3.74 nM eq. Fe, at 40 and 300 m, respectively), which implies that the one-ligand model fit the data better. Therefore, results of data fitting with the two-ligand model will not be presented.

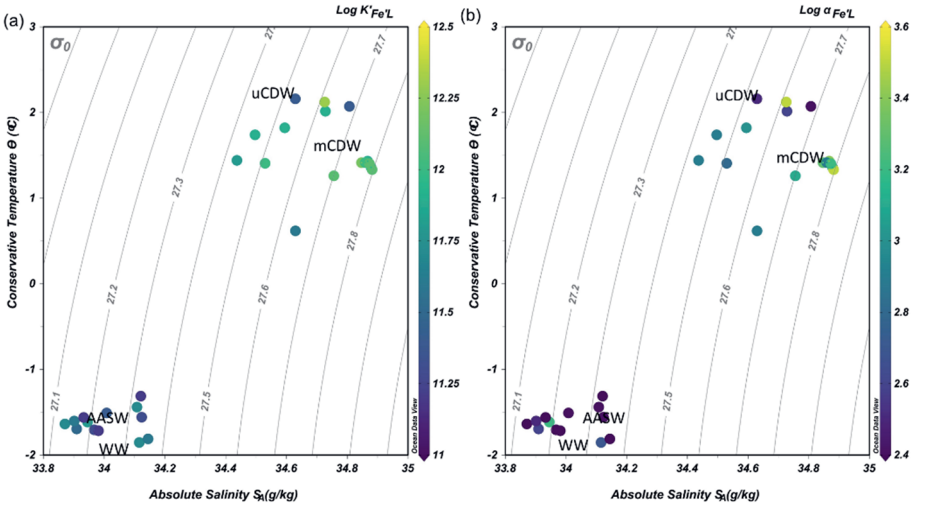

Figure 5-4. (a) The binding strength, log $K^{cond}_{Fe'L}$ and (b) complexation capacity, log $\alpha_{Fe'L}$ plotted in a Θ-S_A diagram. The color scale indicates the values of log $K^{cond}_{Fe'L}$ and log $\alpha_{Fe'L}$.

The values of log $K^{cond}_{Fe'L}$ varied within one order of magnitude between 11.1 and 12.3 (Figure 6-4a). The lower log $K^{cond}_{Fe'L}$ in AASW coincided with the lowest log $\alpha_{Fe'L}$ (AASW: mean log $\alpha_{Fe'L}$ = 2.6±0.3, N=13; Figure 6-4b). The largest log $K^{cond}_{Fe'L}$ and log $\alpha_{Fe'L}$ was measured in shelf waters, particularly in mCDW (mean log $\alpha_{Fe'L}$ =3.4±0.2, N=8; Figure 6-4b). The overall decreasing trend of log $K^{cond}_{Fe'L}$ and log $\alpha_{Fe'}$ was observed from mCDW, uCDW to AASW.

Ligands were always present in excess of DFe, with [L′] ranging from 0.75 to 4.98 nM eq. Fe. High excess ligand concentrations (>2 nM eq. Fe) were observed close to shore (St. A) declining towards the shelf break and reaching the lowest [L′] at St. C near the shelf break (Figure 6-5a). Further offshore (St. D and E), [L′] remains fairly constant at 1 – 2 nM eq. of Fe.

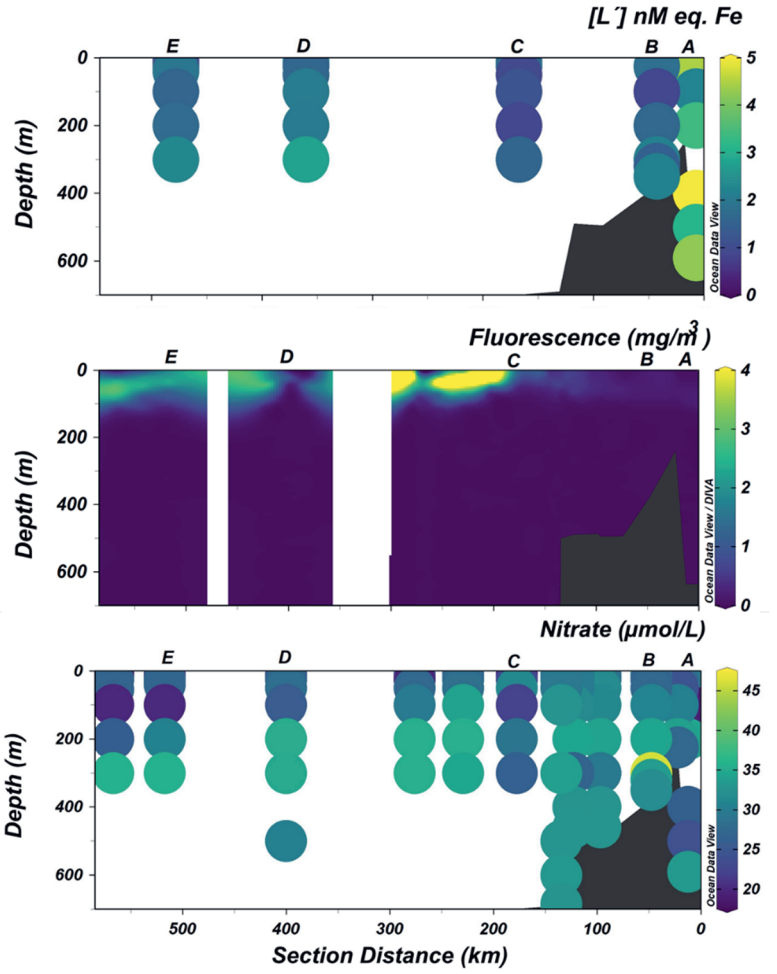

Figure 5-5. The distribution along the transect shown in Figure 6-1 of (a) excess ligand concentrations [L´], (b) Fluorescence, and (c) Nitrate. In the deeper than 100m where normally phytoplankton concentrations are really low. The calibration equation that is used to convert Volts in fluorescence to chl-a concentration in units of 'mg/m^3' creates negative values for the fluorescence when there is basically no chl-a. Thus, the negative values are basically 0 mg/m^3.

4. Discussion

The ligand concentrations measured during our study (1.07 – 6.43 nM eq. Fe; Figure 6-3a) are consistent with the broad range of Fe-binding

ligand concentrations measured in DFe speciation studies in the Southern Ocean (Boye et al., 2001; Lin and Twining, 2012; Nolting et al., 1998; Thuróczy et al., 2011b). Previously reported [L_t] in the Southern Ocean varies from 0.5 – 1.84 nM eq. Fe in the Atlantic sector (Thuróczy et al., 2011b), 2.2 to 12.3 nM eq. Fe in the Pacific sector (Nolting et al., 1998), and 0.44 – 1.61 nM eq. Fe in the Indian sector (Gerringa et al., 2008). The [L_t] in Antarctic polynyas ranges between 0.3 – 1.6 nM eq. Fe (Gerringa et al., 2019; Thuróczy et al., 2012), whereas in regions with sea ice-coverage, [L_t] in underlying water is relatively high, with values of 4.9 – 9.6 nM eq. Fe and up to 72.1 nM eq. Fe within the sea ice (Genovese et al., 2018; Lannuzel et al., 2015).

4.1 Fe-binding ligands along the transect from the shelf to the open ocean

The high sea ice cover on the continental shelf obstructs the light penetration into the water column, inhibiting the development of an early spring bloom. Therefore, bloom generated ligands are less likely to be found. However, microbial excretion from sea-ice algae and bacteria within and just beneath the sea-ice release EPS, which can form Fe-binding ligands (Genovese et al., 2018; Hassler et al., 2017; Lannuzel et al., 2015; Norman et al., 2015). The planktonic community in spring is dominated by diatoms and haptophytes (*Phaeocystis antarctica*) (Arrigo et al., 2017; Joy-Warren et al., 2019). According to Lannuzel et al. (2015), the omnipresence of tube dwelling diatoms (*Berkelaya* sp.) attached via EPS to the bottom of the sea-ice was responsible for relatively high [L_t] in under-ice seawater, indicating that EPS could elevate seawater [L_t] in areas of sea-ice cover. In addition, a laboratory study has shown that cultured *P. antarctica* appears to excrete EPS in relatively high concentrations (Norman et al., 2015), with similar binding strength (log $K^{cond}_{Fe'L}$ 11.5 – 12) to those measured in this study (log $K^{cond}_{Fe'L}$ 11.1 – 12.3). At the ice-covered shelf stations, the high [L_t] in the upper water column implies that ice algae exudates are a source of Fe-binding ligands (St. A and B; Figure 6-3a).

Further from the coast, EPS from phytoplankton likely provide an additional surface source of ligands.

High [L_t] (>2.75 nM eq. Fe) was observed in mCDW (Figure 6-3c) with a narrow range of log $K^{cond}_{Fe'L}$ (11.1 - 11.9; Figure 6-4a), which suggests similar chemical characteristics and a common origin. Given that uCDW at the shelf break has [L_t] lower than 2.5 nM eq. Fe and relatively low DFe concentrations, the high [L_t] in mCDW appears to be supplied by the shelf sediments. Upwelling and contact with the sediment of uCDW presumably results in the resuspension of organic matter and pore water from the sediment, supplying ligands and DFe to the water column. Indeed, ligand input in the proximity of sediments was previously observed in upwelling regions over the continental shelf or in coastal areas (Buck et al., 2017; Gerringa et al., 2008). Subsequent upwelling processes may transport the ligands to the upper water column, including rDOM. Moreover, intrusion of uCDW also provides heat (Smith et al., 1999), which may cause glacial and sea ice melt. The melting of sea ice (i.e. first year pack ice) supplies ligands to surrounding seawater (Genovese et al., 2018), whereas glacial ice is not expected to contribute organic ligands. The estimated flux of [L_t] from melting pack ice in spring can reach up micromolar levels per square meter of pack-ice per day (Genovese et al., 2018), showing the significance of the sea-ice melt contribution to the ligand pool. Overall, the high [L_t] in the shelf region (Figure 6-3a) can be explained by several ligand sources associated with sea-ice, including the melting of sea-ice, as well as sediment resuspension and upwelling.

At the continental shelf break (St. C) in the vicinity of the SB, the lowest [L_t] was found in the upper 200 m of the water column. The presence of the SB is noticeable by the increased upward tilt of the isopycnals (Figure 6-2a) (Klinck et al., 2004; Orsi et al., 1995). Here the ACC interacts with the continental slope (Orsi et al., 1995), propagating ocean eddies that subsequently cause cross-shelf water intrusion (Moffat and Meredith, 2018). The subsurface intrusion of uCDW and its associated turbulence may cause vertical water mass mixing at the proximate location of the SB. The little ice-cover at the shelf break compared to the inner shelf

allows more light penetration, triggering a bloom, as indicated by fluorescence maximum observed at St. C (Figure 6-5b). The bloom and its related microbial activities could release Fe-binding ligands. However, given the consistently low and constant distribution of [L_t] at the shelf break, it seems that mixing determines the distribution and net concentrations of ligands (Figure 6-3a) and microbial species composition. Different microbial species have different rates of organic ligand production, and different microbial species may produce different type of organic ligands (Norman et al., 2015). The influence of mixing on ligands and microbial species composition is confirmed by the relatively constant distribution of DFe and macronutrients (i.e. nitrate; Figure 6-5c) at the same station, indicating that prominent mixing at the shelf break indeed is the major factor governing the distribution of ligands, DFe and nutrients.

Further oceanward from the shelf break, [L_t] was >1 nM eq. of Fe (St. D and E; Figure 6-3a), probably related to the spring bloom at this location. Satellite-based data (Arrigo et al., 2017), showed that open water formed one month earlier offshore than near-shore (St. A and B), implying that the melting of sea ice offshore (St. D and E) occurred preceding and during our occupation. The melting of sea ice released nutrients and micronutrients such as Fe (Lannuzel et al., 2016; Sherrell et al., 2018), which together with the availability of light stimulated the spring bloom. Such a bloom in turn is a source of Fe-binding ligands in the upper water column (Boye et al., 2001; Croot et al., 2004; Gerringa et al., 2019; Gledhill and Buck, 2012). Arrigo et al. (2017) reported that a bloom in its early stages was observed underneath variable sea ice cover seaward from the shelf break. Indeed, the fluorescence maxima observed in the upper 100 m at the offshore stations (St. D and E; Figure 6-5b) concurred with depletion of DFe and drawdown of macronutrients (N and Si), illustrating the presence of a bloom. Siderophores are expected to be produced upon Fe depletion by marine microbes as a strategy to acquire Fe (Buck et al., 2010; Butler, 2005; Mawji et al., 2008; Velasquez et al., 2011). Similarly, as detailed above for the shelf stations, the exudation of EPS from diatoms and haptophytes could be an important addition to the organic ligand pool. Moreover, polysaccharide ligands will be released by microbial cells

during the bloom as well as via grazing (Laglera et al., 2019b; Sato et al., 2007) and viral lysis (Poorvin et al., 2011; Slagter et al., 2016). Additionally, the ratios of labile particulate Fe to labile particulate Mn (0.27 ± 0.49; Seyitmuhammedov et al. (in review) indicate that Fe has a biogenic origin in the offshore waters (Twining et al., 2004). Therefore, we suggest that the origin of [L_t] offshore was, next to the melting of sea ice, the result of *in situ* production of organic ligands during the bloom and passive generation from microbial processes associated with the bloom.

The lowest concentrations of DFe (<0.05 nM) were observed at St. D and E and were a result of both biological uptake and limited supply. This area most likely represent Fe-limited conditions as indicated by declining Si* (Si*= [Si] – [N]) values and high ratios of [nitrate]/DFe (Figures 6-6a and 6-6b). The value of Si* serves as a proxy for Fe limitation, where Fe stress leads to preferential drawdown of Si compared to N by diatoms in surface water (Takeda, 1998). A negative Si* indicates Fe limiting conditions, assuming that Si and N are required in a 1:1 ratio by diatoms (Brzezinski et al., 2002). In our dataset, although there were no negative values for Si*, some Si* values at the open ocean stations were close to 0. Our data indicates that although there is no Fe-limitation yet during our sampling period, Fe limitation could potentially occur later in the season. Typically, organic ligands excreted under Fe-limited conditions have strong affinity for Fe (Maldonado et al., 2005; Mawji et al., 2008), i.e. a high log $K_{Fe'L}^{cond}$ (>12). However, a relatively low log $K_{Fe'L}^{cond}$ is observed in AASW relative to deeper uCDW and mCDW (Figure 6-4a). This indicates that in offshore AASW where Fe limitation is expected, the contribution of siderophores is modest. Indeed, recent studies showed that only <10% of Fe is complexed by siderophores (Boiteau et al., 2019; Bundy et al., 2018), suggesting that the binding strength of the overall ligand pool is not always a good indicator of the presence of particular ligand group if multiple ligand sources are present. Moreover, in the presence of light, organic ligands can undergo photo-degradation (Hassler et al., 2020), and thus the chemical structure can be altered into a slightly weaker ligand type (Barbeau et al., 2001; Powell and Wilson-Finelli, 2003). Mopper et al.

(2015) suggested that the absorption of solar radiation by chromophoric dissolved organic matter as part of the ligand pool. These chromophoric compounds are commonly produced by sea ice algae (Norman et al., 2011), leading to the photochemical transformation of these compounds. These photo-oxidative processes can thus also explain the shift in log $K^{cond}_{Fe'L}$ in the AASW to lower values compared to deeper uCDW and mCDW.

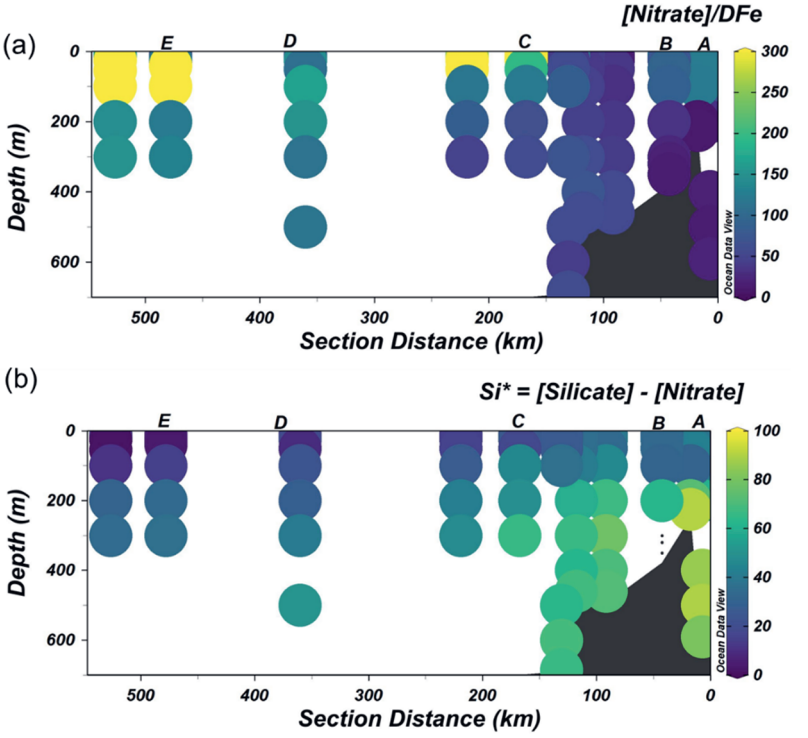

Figure 5-6. The distribution of Si(a) and the ratio of [Nitrate]/DFe (b) along the transect shown in Figure 6-1.*

The presence of the SACCF and SB fronts affects bloom conditions. As shown by Arrigo et al. (2017), high chlorophyll-a concentrations were observed in surface waters in between the SB and SACCF, which suggest the distribution of phytoplankton biomass is affected by physical processes in the area. The SB also appears to mark the boundary between offshore organic ligands that result from a combination of the earlier sea ice melt

and *in situ* production and/or generation associated with offshore blooms, and organic ligands on the shelf that result from a combination of ice-algae exudation, sea-ice melt, and sediment resuspension. In the region near the SB at the shelf break, water mass mixing due to the baroclinically unstable water column seems to have caused consistent distributions of [L_t] (Figure 6-3a). Further offshore, ligands are most likely associated with the bloom, but the distribution of ligands is also affected by enhanced vertical mixing and intensified currents proximal to the area of the fronts. Solar radiation enhances stratification and drives the formation of the spring bloom whereas deep mixing can both hinder as well as stimulate bloom formation based on the balance between availability of light and nutrients (Arrigo et al., 2017). It thus seems likely that the balance between mixing and stratification results in variable [L_t] in the area around the SACCF (St. D and E; Figure 6-3a).

4.2 Implications for primary productivity

In general, we found [L´] >0.75 nM eq. Fe (Figure 6-5a), which accounts for approximately 80% of [L_t]. This implies that at least 80% of total ligands measured are available to bind Fe, although the total complexation capacity of ligands is also determined by its log $K^{cond}_{Fe'L}$. The highest complexation capacity log $\alpha_{Fe'L}$ was found in mCDW on the shelf (Figure 6-4b), and concurred with the highest concentrations of DFe in mCDW (Figure 6-3b and Figures 6-4b). The high complexation capacity of ligands on the shelf increases the potential of organic ligands to stabilize additional Fe input to the shelf waters (Gerringa et al., 2019; Lannuzel et al., 2015; Thuróczy et al., 2012) and lengthen the residence time of DFe (Gerringa et al., 2015). A longer residence time has a positive feedback on the development of local primary productivity upon sea ice melting (Arrigo et al., 2017), supplying DFe to primary producers on the shelf, which were dominated by *Phaeocystis* Antarctica during our sampling period (Joy-Warren et al., 2019). Moreover, the results of oxygen isotope ($^{18}O/^{16}O$, conventionally reported into delta-notation as $\delta^{18}O$; Seyitmuhammedov et al. (in review) analysis showed $\delta^{18}O$ values ranged

from -0.56 – 0.06 ‰ with estimated fractions of sea-ice meltwater (-1.9 – 1.1 %) and meteoric meltwater (precipitation and glacial;0.3 – 3.9 %). Based on those results of oxygen isotope analysis, meltwater associated with runoff and glacial discharge is present in the upper 200 m of the shelf, and probably is a source of particulate and dissolved Fe that will increase under continued climate change. However, whether Fe in particulate form will partition into the dissolved pool via ligand driven dissolution of Fe, also depends on the fraction of labile particulate Fe. In addition, local primary productivity not only relies on the DFe input from, for example, meltwater and glacial debris (Klunder et al., 2011; Lannuzel et al., 2016), but probably also on the input of Co and Mn (Middag et al., 2013; Saito et al., 2010; Wu et al., 2019) as these elements showed co-limitation in the Southern Ocean (Middag et al., 2013; Saito et al., 2008).

Besides affecting the shelf conditions, ice melt also produces buoyant northward-flowing surface water, which may facilitate DFe transport from the shelf to the open ocean, supplying DFe for primary production offshore, but this effect was not noticeable in the transport data for this specific transect. However, the conditions along the WAP are not homogenous and elevated Fe (ranged from 0.08 – 4.88 nM for DFe and 0.16-85.42 nM for total-dissolvable; (Seyitmuhammedov et al., in review) concentrations northeast of our transect were observed in the upper 100 m, suggesting that some of the observed ligands might have been transported south-westerly with the CC. This high DFe stabilized by organic ligands will probably be transported further to the southwest where a coastal polynya is commonly observed in Marguerite Bay (Arrigo et al., 2015). Such transport would supply DFe to the highly productive Marguerite Bay polynya and fuel phytoplankton blooms in these ice-free waters but could also be partly transported offshore in the region southwest of our transect. However, the relative amount of DFe bound to organic ligands can vary, and is also strongly influenced by the continued change in environmental conditions due to global warming (Slagter et al., 2017; Ye et al., 2020), making it likely such a transport of DFe to the southwest or offshore will change as well.

Global warming has caused glaciers to retreat and induced significant loss of sea-ice, particularly in the Antarctic Peninsula area (Henley et al., 2019; Stammerjohn et al., 2012; Turner et al., 2020). The sea ice extent over the southern Bellingshausen Sea, has decreased in recent decades, creating open water and lengthening the ice-free season (Turner et al., 2013). This results in increased solar irradiance and enhanced stratification (Henley et al., 2019), which can lead to an alteration of the phytoplankton community structure. As previously reported, variable light conditions favor the growth of *Phaeocystis antarctica* over diatoms (Alderkamp et al., 2012; Joy-Warren et al., 2019). In contrast, smaller-cell diatoms are better adapted to increased sea surface temperature (Schofield et al., 2017). Changes in planktonic community composition affect net primary production and overall carbon drawdown, which lead to further alteration of the food web and carbon cycling (Alderkamp et al., 2012; Arrigo et al., 1999; Joy-Warren et al., 2019; Schofield et al., 2017). These and other ongoing changes in the food web will also affect production of dissolved organic carbon (DOC) and thus ligands as they form a fraction of the DOC pool (Gledhill and Buck, 2012; Whitby et al., 2020). Generally, one expects that increased DOC production would lead to more ligands, but the binding strength depends on which molecules are formed (Gledhill and Buck, 2012; Hassler et al., 2017). Additionally, intensified light exposure alters log $K^{cond}_{Fe'L}$ by photo-oxidative processes, possibly reducing the complexation capacity and binding strength for Fe (Barbeau et al., 2001; Mopper et al., 2015; Powell and Wilson-Finelli, 2003) as well as the bioavailability (Hassler et al., 2020). Furthermore, complexation capacity is affected by pH, implying that ongoing ocean acidification also influences the speciation of Fe (Ye et al., 2020). The melting of black sea-ice entrapped with sediment potentially releases organic ligands (Genovese et al., 2018). Organic ligands from microbial excretions are expected to be abundant on the base of sea ice (Norman et al., 2015), although the fluctuation rate (decrease or increase) under on-going changes cannot be confirmed without further experiment. Overall, the continued sea-ice melt and glacial retreat can be expected to increase the supply of Fe (Lannuzel et al., 2016), other micronutrients (Co, Mn, etc.),

and Fe-binding ligands (Lin and Twining, 2012), but the consequences for their complexation capacity and overall bio-availability of Fe remain elusive. If DFe becomes progressively more available in the Southern Ocean, phytoplankton growth could increase until another process becomes limiting, such as the availability of another micronutrient or macronutrient. Many uncertainties remain, but the changing environmental conditions of the WAP due to climate change will affect marine biogeochemical cycles and influence productivity beyond the Southern Ocean as the Southern Ocean is an important hub in ocean circulation and its waters eventually supply nutrients to other regions (e.g. Middag et al. (2020).

5. Summary

Our results indicate that organic Fe-binding ligands in surface water on the continental shelf of the WAP are associated with ice-algal exudates and addition of ligands from melting sea ice. In the water column close to the continental slope and shelf sediments, resuspension of sediment followed by upwelling processes appears to be another source of ligands. From the continental shelf-break oceanward, sources of Fe-binding ligands are likely related to offshore phytoplankton blooms, either actively produced during the bloom, or passively generated by microbial processes associated with the bloom. The distribution of ligands is affected by the two major fronts in the region, the SACCF and SB. The SB along the shelf break not only marks the boundary between the shelf and open ocean, but also marks the border between organic ligands associated with the bloom offshore and organic ligands on the shelf originating from sea-ice and sediment related sources, such as ice-algae exudation, sea-ice melt, and sediment resuspension. Overall, excess ligands comprised up to 80% of the total ligand concentrations, implying the potential to solubilize additional Fe input. The ligands in denser mCDW on the shelf have a higher complexation capacity for Fe, and are thus capable of increasing the residence time of Fe as DFe and fuel local primary production later in the season upon ice melt.

Acknowledgements

The authors would like to thank the captain and his crew of the R/VIB N. B. Palmer, as well as Anne-Carlijn Alderkamp and all other participants, for their efforts and support. Our colleagues in the nutrients lab at NIOZ are acknowledged for analyzing nutrients. IA was financed by Indonesia Endowment Fund for Education (LPDP), and KS received a scholarship from the University of Otago. KRA was funded by a grant from the National Science Foundation Office of Polar Programs (ANT-1063592). The IAEA is grateful to the Government of the Principality of Monaco for the support provided to its Environment Laboratories.

Chapter 7

Synthesis

Organic speciation of iron (Fe) in seawater has gained much attention over the last decades, as it provides additional insight into the biogeochemical cycle of Fe. Natural ligands influence many aspects of the Fe cycle (*i.e* Fe input, scavenging, remineralization, sedimentation, and biological uptake). Organic Fe-binding ligands are a key factor controlling mobility and bioavailability of Fe in the ocean, as organic ligands enable Fe to remain in the dissolved form. Rapid environmental changes due to global warming influence the input and removal of both Fe and organic ligands. Such environmental changes vary between regions, leading to the supply of ligands in different quantities and/or characteristics (*i.e* conditional binding strength). The conditional binding strength ($K^{cond}_{Fe'L}$) and the available binding sites (concentration of 'free' ligands, [L´]) determine the complexation capacity of organic ligands ($\alpha_{Fe'L}$). The complexation capacity can set the threshold of dissolved-Fe (DFe) in seawater, which could affect the export of DFe further away from its sources. To understand the impact of global warming on the Fe cycle, the role of organic ligands needs to be better constrained. This study quantifies the total concentration ([L_t]) and $K^{cond}_{Fe'L}$ of Fe-binding ligands. These parameters can be used to infer the potential sources of the measured organic ligands. The results of this study add valuable information on the role Fe binding ligands in oceanic regions, where the impact of global warming is severe, such as in the Arctic and Antarctic regions.

Besides the polar regions, there is also limited knowledge on DFe speciation in seas and oceans that are affected by local processes and seasonal variability, such as seasonal intrusion of low-nutrient (oligotrophic) oceanic water onto the shelf. Therefore, this study also investigated DFe speciation in the Hauraki gulf of the North Island, New Zealand. This subtropical region is subjected to distinct temporal variability with seasonal oligotrophic conditions. In addition, a laboratory study was conducted in sub-tropical water to investigate Fe-binding ligand production by marine bacteria in the presence of phytoplankton.

1. The major findings, its implications and contribution to the field

1.1 Laboratory experiment on ligands production

Despite many challenges encountered in the laboratory experiments on the production of ligands in cultures of natural bacteria and phytoplankton, we concluded that physical interaction between phytoplankton and bacteria is somewhat counterproductive, whereas chemical interaction can benefit phytoplankton growth. The 'low'-Fe treatment in the culture did not have a measurable effect on the growth rate, however, it affects photosynthetic performance. Within the ambient DFe concentration (>1 nM) in the culture media, the production of strong Fe-binding ligands did not seem to be stimulated as the incubation progressed. This study attempted to examine the growth of phytoplankton with less interference (without bacteria) from natural bacteria. However, it was challenging to eliminate natural bacteria from seawater by filtration. A better separation setup (i.e. seawater that is both filtered and autoclaved to produce sterilize seawater, Button et al. (1993)) might be helpful to get more reliable results.

1.2 DFe speciation in subtropical waters

This research reported the first observations of the total concentration and conditional stability constant of Fe-binding ligands in the Hauraki Gulf within two consecutive years, autumn 2015 and 2016. The high concentrations of organic ligands enabled relatively high DFe to persist on the shelf and consequently, the export of DFe from the shelf to the open ocean, where Fe can be an important driver of primary productivity. This potential DFe export is linked to the dynamics of ligand production in shelf regions where notably microbial remineralization plays an important role. Furthermore, the intrusion of oceanic water onto the shelf affects the distribution of both [L_t] and DFe in surface water. This study illustrates that changes in [L´] can be a good indicator to observe differences in Fe input, if DFe input is not coinciding with any ligand sources. The

complexation capacity of organic ligands remains high and in the same order of magnitude between water masses, and along the transect from the shore to the open ocean. This result indicates that ligands with a high complexation capacity are expected to be found throughout the water column. These ligands likely play a critical role to maintain the ocean DFe inventory, as previously suggested (Hassler et al., 2020; Whitby et al., 2020).

1.3 DFe speciation in Fram Strait and the Northeast Greenland shelf regions

Based on the characteristic of Fe-binding ligands, three different biogeochemical provinces were distinguished: Fram strait, the Westwind Trough and the Norske Trough. This research provided a connection to previous studies on Fe-binding ligands in the north Atlantic and Arctic regions. The results confirmed the hypothesis that the concentration of organic ligands decreases southward from the Arctic Ocean.

The results reveal that the competing strength of organic ligands regulate the export of DFe from the largest glacier of northeast Greenland. A high concentration of organic ligands, yet with relatively weak binding strength, was found at the vicinity of the glacier terminus and in the Norske Trough. These ligands competed less efficient against scavenging and precipitation, relative to the stronger ligands present elsewhere in Norske Trough and Fram Strait, resulting into less than expected export of DFe into Fram Strait (Krisch et al., 2021). This illustrates the controlling factor of Fe binding organic ligands on the mobility of Fe in seawater. Although rapid environmental changes due to global warming will cause increased gross Fe supply by increased river runoff and glacial melt, this study showed that it is the combination of available binding sites and binding strength, i.e. the complexation capacity, of organic ligands that regulates DFe transport and the DFe distribution in Fram Strait.

1.4 Comparison study of voltammetric methods

Various sources of ligands existed in Fram Strait and the Northeast Greenland region, comprising a ligand pool with high heterogeneity, and most likely including humic substances. Since humic substances can form a large part of the ligand pool and are known to be underestimated by the analytical methods used in Chapter 4, the results of the TAC based application of CLE-AdCSV needed to be compared with other CLE-AdCSV applications (Laglera et al., 2019b; Slagter et al., 2019). Three different added ligands (AL) were used: (2-thiazolylazo)-p-cresol (TAC), salicylaldoxime (SA) and 1-nitroso-2-napthol (NN), each with their specific detection window.

Data interpretation using a one-ligand model resulted in organic ligand concentrations of $[L_t]_{SA} > [L_t]_{TAC} > [L_t]_{NN}$; with the mean log $K^{cond}_{Fe'L}$ being the highest for TAC > SA > NN. The differences are only partly explained by the detection windows employed, and are probably due to uncertainties propagated from the calibration and the over or underestimation of specific ligand groups within the heterogeneity of the natural organic ligand pool. The SA method seemed to be most suitable, since it could detect a relatively weak ligand group, missed by the other applications, due to its lower detection window compared to the TAC and NN methods. However, this study revealed that the estimated contribution of different ligand groups differs between the TAC and SA methods. Thus, probably ligand groups other than humic substances interfere with the detection efficiency of the ALs.

1.5 DFe speciation in the Antarctic Ocean

Concentrations and characteristics of organic Fe-binding ligands were investigated along a natural gradient of the western Antarctic Peninsula, from ice covered shelf waters to the open ocean of the Antarctic Zone. The hydrographic setting in this region was strongly influenced by the sea ice cover and the presence of two major hydrographic fronts, the Southern Antarctic Circumpolar Current Front (SACCF) and the Southern

Boundary (SB). The different hydrographic regions hosted different concentrations, binding strengths and complexation capacities of Fe-binding ligands. The presence of fronts affected the distribution of ligands. Under sea ice cover near the coast, organic ligand production was associated with ice-associated algae. Sediment-water interaction and resuspension resulted in high concentrations of Fe and ligands in upwelling deep waters over the continental slope. Towards the open ocean, phytoplankton blooms depleted nutrients and iron, while actively or passively producing organic ligands.

The presence of these fronts along the shelf break not only marks the boundary between the shelf and open ocean, but also marks the border between shelf derived ligands and bloom-associated ligands offshore.

Organic ligand concentrations always exceeded DFe concentrations, as commonly observed in other ocean regions, but interestingly, excess ligand concentrations in this region were remarkably high, comprising up to 80% of the total ligand concentration. Particularly, the high excess ligand concentrations were observed in the open ocean region, where DFe was relatively low. Since Fe was also supplied by shelf sediments and glacial discharge, and organic ligands on the shelf had relatively high complexation capacity, any additional Fe input can potentially be stabilized in dissolved form via organic complexation. Thus, we postulate that in this region organic complexation increases the residence time of Fe as DFe and will make Fe available for local primary productivity later in the season, upon sea ice melting.

2. Recommendation for future work

The improvement of current voltammetric techniques and the development of new methods to characterize organic ligands with more advanced technologies (e.g.(Boiteau et al., 2013; Boiteau et al., 2016) will continue to expand our knowledge in this field. This thesis helps to expand our current understanding on the concentration, distribution and characteristics of Fe-binding ligands in different ocean regions with

distinct environmental circumstances. Our study area in the Fram strait and the Northeast Greenland shelf, the Western Antarctic Peninsula, as well as the Hauraki Gulf, all have distinct hydrographic settings. The study areas in the high latitude oceans are particularly susceptible to changes in climate, and our results help provide a basic overview that is needed to predict the consequences of climate change on the Fe biogeochemical cycle in the globally important high latitude oceans. Furthermore, the findings of this study lead to the comparison study on voltammetric methods can contribute to the development of improved voltammetric methods to study Fe speciation in seawater. Recommendations for future research are outlined below.

- Microbial remineralization likely plays an important role in ligand production. Typically, organic ligands produced from remineralization processes are particularly stable from degradation and have longer residence times in the water column. These organic ligands can maintain the deep ocean DFe inventory in the deep ocean, however, there is not much information about the chemical structure of these ligands. Future research into the chemical structure would be very welcome. This information will also give insight in the contribution of these organic ligands to the total ligand pool in the deep ocean.
- In ocean regions with seasonal hydrographic changes (*i.e.* our study area in the Hauraki Gulf), higher temporal resolution data is required to get a better idea about the seasonal variability of DFe speciation.
- To understand the consequences of global warming in the Arctic and sub-Arctic Oceans for the biogeochemical cycle of Fe, the changes in the biogeochemical cycle of the ligands need to be understood as well. Especially in areas where organic ligands as well as DFe concentrations are influenced by glacial systems, we need to investigate the temporal variability in DFe speciation. Future studies to examine whether differences in Fe-binding ligand characteristics exist between different types of glacier systems (*i.e.* continental ice sheet glacier, marine versus land terminating glaciers) would also be

a very valuable addition to understand Fe cycling in the ocean near such glacier systems.

- With ongoing climate change, environmental controls on DFe speciation could become more important. For example, recent work showed the importance of pH on organic Fe speciation (Ye et al., 2020; Zhu et al., 2021) where the marine pH is changing due to rising atmospheric CO_2. Therefore, future research to investigate the environmental controls on organic ligands is required.
- From the comparison of voltammetric methods, we found a constant ratio (~0.5 – 0.6) between total ligand concentrations obtained by the TAC and SA methods. In previous comparisons between TAC and another application of SA, this was observed in contrasting environments such as the open Atlantic Ocean (Buck et al., 2016) and the Arctic Ocean with high humic influences (Slagter et al., 2019). This result warrants future research into specific bias for specific Fe-binding ligands by different methods. Furthermore, it is challenging to identify more than one ligand group. The SA method is able to identify two ligand groups more often, than the TAC and NN methods. The underlying reasons for this are as of yet not clear. Finally, a large error is propagated during data interpretation, making a comparison between log $K^{cond}_{Fe'L}$ values obtained from different voltammetric techniques difficult. Overall, method improvements as well as a better understanding of the results of various methods are obviously needed. The results of chapter 4 of this thesis, already stimulated further research in which model ligands were measured using three applications (Gerringa et al., in review). Considering that each method has its drawbacks, future experiments to develop quality control procedures are essential to put the existing DFe speciation data in the same framework and make reliable data comparison possible.

Although it is difficult to relate a natural ligand group to a specific conditional stability constant value, the $K^{cond}_{Fe'L}$ in the Fram Strait and the northeast Greenland samples were relatively low and might be indicative

of terrestrial humic substances. Therefore, it would be interesting to measure/characterize actual humic compounds in the same samples.

NEDERLANDSE SAMENVATTING

De opwarming van de aarde door klimaatsverandering heeft grote invloed op de cyclus van sporenelementen in de oceaan. Een van deze sporenelementen is ijzer (Fe). Het is een essentieel micro-nutriënt voor al het leven op aarde en is belangrijk voor onder andere de primaire productie, oftewel fotosynthese door planten zoals algen in de oceaan. Opgelost ijzer (DFe) is aanwezig in nanomolaire (10^{-9} mol) concentraties, vanwege de slechte oplosbaarheid in zeewater en het gebrek aan bronnen van Fe in de open oceaan. Als gevolg hiervan kan DFe beperkend worden voor primaire producenten in regio's zoals de Zuidelijke Oceaan. Fe-beperking is ook bekend als seizoensgebonden fenomeen in andere oceaanregio's, zoals de Noord-Atlantische Oceaan.

De biogeochemische cyclus van Fe in de oceaan bestaat uit een complexe interactie tussen Fe toevoer, biologische opname, 'scavenging' (adsorptie aan zinkende deeltjes), remineralisatie en sedimentatie. Natuurlijke organische liganden – een mengsel van organische moleculen met een hoge affiniteit voor Fe – beïnvloeden elk van deze aspecten in de cyclus. Hoewel concentraties van DFe in de oceaan sterk afhankelijk zijn van de balans tussen aan- en afvoer, bepalen natuurlijke Fe-bindende organische liganden de maximaal mogelijke DFe-concentraties in de oceaan. De aanwezigheid van natuurlijke organische liganden verhoogt de oplosbaarheid van Fe in zeewater door de vorming van opgeloste organische Fe-ligandcomplexen. Organische liganden verlengen de verblijftijd van Fe in de waterkolom als DFe, waardoor potentieel transport met oceaanstromingen kan plaatsvinden en de kans op opname door primaire producenten toeneemt.

Opgeloste organische Fe-bindende liganden maken deel uit van opgelost organisch materiaal (DOM) en zijn slecht gekarakteriseerd (Gledhill et al., 2012; Hassler et al., 2017; Laglera et al., 2019). Karakterisering van organische liganden in zeewater is een hele uitdaging, aangezien deze liganden een onbekende samenstelling hebben, chemisch divers van aard zijn en doorgaans in bijzonder lage concentraties aanwezig zijn. De huidige kennis over de identiteit van liganden definieert een breed scala aan Fe-bindende liganden, van laagmoleculaire tot macromoleculaire

verbindingen. De oorsprong kan zowel marien als terrestrisch zijn. De organische liganden van mariene oorsprong zijn afkomstig van lokale biologische processen. Deze biologisch geproduceerde liganden omvatten twee groepen. Eén groep wordt actief geproduceerd door mariene microben als een strategie om Fe te verkrijgen, ze bestaan uit relatief kleine moleculen en worden sideroforen genoemd. De andere groep wordt passief gegenereerd via microbiële afbraak van organisch materiaal, cel uitscheiding, begrazing en virale lysis. Deze stoffen bestaan uit onder andere uit polysachariden. Lithogene inbreng in het grensgebied tussen land en zee (kustzeeën en estuaria) leveren liganden van terrestrische oorsprong. Deze liganden bestaan grotendeels uit macromoleculaire humusstoffen. Resuspensie van sediment op de zeebodem kan ook een bron zijn van organische liganden. In de Zuidelijke Oceaan en de Noordelijke IJszee vormt het smelten van zee-ijs en landijs een extra bron van organische liganden.

Aangezien opgeloste organische Fe-vormen in zeewater domineren, is kennis van organische Fe-bindende liganden een cruciaal onderdeel van de Fe-biogeochemie. Vooral het begrijpen van de processen die vorming en afbraak van natuurlijke organische liganden beheersen, is van fundamenteel belang om de invloed van de opwarming van de aarde op de Fe-cyclus te kunnen interpreteren en voorspellen. Door een gebrek aan data en kennis omtrent de liganden en gerelateerde processen is het niet mogelijk de effecten van wereldwijde klimaatverandering op de biogeochemische cyclus van Fe volledig te beoordelen. In dit proefschrift is daarom een koppeling gemaakt tussen de omgeving waar monsters genomen zijn en de daar heersende processen, met de data, te weten: de totale concentratie opgeloste organische ligand ([Lt]) en de conditionele stabiliteitsconstante ($K^{cond}_{Fe'L}$) van Fe met de natuurlijke organische liganden. De $K^{cond}_{Fe'L}$ wordt ook wel de bindingssterkte van organische liganden genoemd, hogere waarden komen overeen met een sterkere binding tussen Fe en het ligand. De distributie van [Lt] en $K^{cond}_{Fe'L}$ maakt onderzoek naar potentiële bronnen mogelijk. Bovendien geven deze parameters inzicht in de beschikbaarheid en mobiliteit van DFe op locaties die kwetsbaar zijn

voor klimaatverandering. Daarnaast zijn in dit proefschrift ook organische liganden onderzocht in de subtropische wateren voor de kust van Nieuw-Zeeland om seizoensmatige variatie te onderzoeken.

In dit proefschrift wordt gebruik gemaakt van een elektrochemische benadering, genaamd "competitive ligand exchange – adsorptive cathodic stripping voltammetry" (CLE-AdCSV). De CLE-AdCSV is een indirecte methode om [Lt] en $K_{Fe'L}^{cond}$ te bepalen, en geeft geen informatie over de chemische structuur van de organische liganden. Dergelijke methodes gebruiken de concurrentie voor Fe tussen een bekend toegevoegd ligand (AL) en natuurlijke organische liganden, waarbij een elektro-actief complex wordt gevormd, Fe(AL)x. De gevormde Fe(AL)x-complexen kunnen worden gemeten aan het oppervlak van een hangende kwikdruppelelektrode met behulp van voltammetrie.

Er zijn meerdere gevestigde CLE-AdCSV-technieken die zich onderscheiden door toepassing van verschillende AL's en condities zoals pH, concentratie van AL en equilibratie tijd. De meest gebruikte AL's zijn 2-(2-thiazolylazo)-p-cresol (TAC), salicylaldoxime (SA) en 1-nitroso-2-naptol (NN). Een voordeel van CLE-AdCSV is dat er geen voorbehandeling, zoals een concentratie stap of verwijdering van de zeewatermatrix (het zeezout), nodig is. De methode heeft echter wel zijn beperkingen bij het interpreteren van de gegevens, want de bepaling van de waardes van [Lt] en $K_{Fe'L}^{cond}$ uit de CLE-AdCSV-analyse is niet eenvoudig. Bovendien kan de toepassing van de bovengenoemde verschillende AL's resulteren in verschillende uitkomsten. Daarom is een vergelijkend onderzoek uitgevoerd naar de toepassing van verschillende AL's op de CLE-AdCSV analyse met TAC, SA en NN.

Dit proefschrift rapporteert de parameters [Lt] en $K_{Fe'L}^{cond}$ van Fe-bindende liganden in subtropische wateren en de twee poolgebieden, aangevuld met een laboratoriumstudie. De resultaten en de implicaties van het onderzoek worden beschreven in de verschillende hoofdstukken en hieronder samengevat.

1. Laboratoriumexperiment naar het onderlinge effect van diatomeeën en bacteriën op organische Fe-bindende liganden

In dit hoofdstuk wordt onderzocht hoe fytoplankton en bacteriën op elkaar inwerken om de meest efficiënte Fe-opname te bereiken bij gebrek aan DFe. Dit experiment is gedaan door diatomeeën en mariene bacteriën samen te kweken in zeewater onder condities met laag DFe en met hoog DFe. Een dialysemembraan is gebruikt om de diatomeeën fysiek te scheiden van mariene bacteriën om te testen of direct cel contact of de afwezigheid hiervan tussen bacteriën en diatomeeën effect heeft op de productie en eigenschappen van de opgeloste Fe-bindende organisch liganden. Het zeewater dat voor het kweken is gebruikt, was bemonsterd voor de kust van het Otago Schiereiland (Nieuw-Zeeland), een gebied waar zowel sub-tropisch als sub-antarctisch water wordt aangetroffen.

Uit de experimenten bleek dat fysieke interactie tussen diatomeeën en bacteriën enigszins contraproductief is, terwijl de chemische interactie de groei van fytoplankton ten goede kan komen. Met de aanwezige DFe (>1 nM) in de kweekmedia leek de productie van sterke Fe-bindende liganden niet te worden gestimuleerd tijdens het experiment. Het bleek ook een uitdaging te zijn om natuurlijke bacteriën door filtratie uit zeewater te verwijderen. Om betrouwbaardere resultaten te krijgen in toekomstige studies, raden we aan om het zeewatermedium zowel te filteren als te autoclaveren om steriel zeewater te verkrijgen voordat het incubatie-experiment begint.

2. Fe-bindende organische liganden in de subtropische wateren van de Hauraki Golf, Nieuw-Zeeland.

De Haraki Golf is een half ingesloten ‘shelf’-zee ten noordoosten van de metropool Auckland in Nieuw-Zeeland. Een kust zee is relatief ondiep en bevindt zich op het continentale plat.

De Hauraki Golf bestaat tijdens de lente uit een productief ecosysteem, en wordt onderworpen aan oligotrofe (voedingsstoffen arm) omstandigheden afhankelijk van de seizoenen. Deze seizoensgebonden veranderingen worden veroorzaakt door de veranderingen in de watercirculatie in deze kust zee, die een verschuiving in de gemeenschapssamenstelling van het ecosysteem veroorzaken. Het gebied dient als een natuurlijk laboratorium om Fe-bindende organische liganden te bestuderen in een zeer variabel systeem, waar veranderingen van het microbiële ecosysteem de aard van de liganden mogelijk beïnvloedt. In dit studiegebied was [Lt] relatief hoog (~ 2,5 tot 7,5 nM eq. Fe) dicht bij de kust. De hoge [Lt] maakte een relatief hoge DFe nabij de kust mogelijk, en bijgevolg een verhoogde potentiële export van DFe naar de open oceaan, waar Fe een belangrijke aanjager van primaire productie kan zijn. Deze potentiële DFe-export is gekoppeld aan de dynamiek van de productie van liganden, waarbij met name microbiële remineralisatie een belangrijke rol speelt. Bovendien is de kust zee onderhevig aan het periodiek binnendringen van water uit de oceaan tijdens de overgang tussen de seizoenen. Hoewel het effect van het binnendringen van water uit de open oceaan op de verdeling van zowel [Lt] als DFe nabij het oppervlak nog steeds onduidelijk is, kunnen onze observaties tijdens twee opeenvolgende jaren worden gebruikt als een startpunt om de variabiliteit in de biogeochemische Fe-cyclus en Fe-bindende organische liganden verder te onderzoeken.

3. Fram Straat en de kust zee ten noordoosten van Groenland.

De Fram Straat is een diepe zeestraat en een belangrijk knooppunt voor de uitwisseling van warmte en watermassa tussen de Noordelijke IJszee en de Noordse zeeën (Groenlandzee, Noorse Zee en IJslandse Zee). In de buurt van de Fram Straat eindigt de grootste gletsjer van noordoost Groenland. De voortdurende

veranderingen in de Noordelijke IJszee en subarctische wateren beïnvloeden de biogeochemische cyclus van Fe onder meer door het effect op de bronnen van Fe-bindende organische liganden. Het studiegebied biedt een ideale setting om de invloed van diverse bronnen van organische liganden op de toevoer en het transport van DFe te onderzoeken.

De belangrijkste conclusie uit deze studie is dat de bindingssterkte van organische liganden de export van DFe van de grootste gletsjer van noordoost Groenland reguleert. De Fe-bindende organische liganden in de buurt van het eindpunt van de gletsjer worden gekarakteriseerd door weliswaar een hoge [Lt] (tot ~3 nmol eq. Fe), maar ook door een relatief zwakke bindingssterkte. Deze relatief zwakke liganden concurreren minder efficiënt tegen adsorptie aan deeltjes en precipitatie, vergeleken met de sterkere liganden elders in de 'shelf' zee en in de Fram Straat. Hierdoor was de uitvoer van DFe naar de Fram Straat veel minder dan in eerste instantie was aangenomen (Krisch et al., 2021) en illustreert de controlerende factor van Fe-bindende organische liganden op de mobiliteit van Fe in zeewater. Hoewel snelle veranderingen in het milieu door het broeikaseffect zullen leiden tot een grotere bruto Fe-toevoer via rivieren en smeltende gletsjers, heeft deze studie aangetoond dat het de combinatie van beschikbare bindingsplaatsen en bindingssterkte, de complexeringscapaciteit, van organische liganden is die het DFe-transport reguleert in de Fram Straat.

4. Vergelijkende studie van de voltammetrische methodes

Drie verschillende AL's zijn vergeleken: TAC, SA en NN. Elk van deze AL's heeft een specifiek detectie-venster. De berekening volgens de Langmuir isotherm waarin aangenomen werd dat er één natuurlijk ligand werd getitreerd, resulteerde in [Lt]SA > [Lt]TAC > [Lt]NN; waarbij log $K^{cond}_{Fe'L}$ gemiddeld de hoogste waarde had volgens TAC > SA > NN. De SA-methode leek het meest geschikt,

omdat deze een relatief zwakke ligandgroep kon detecteren die door de andere toepassingen werd gemist. Dit wordt vermoedelijk veroorzaakt door het lagere detectievenster (de zwakkere binding) van SA in vergelijking met de TAC- en NN-methodes. De verschillen worden echter slechts gedeeltelijk verklaard door de detectievensters en zijn waarschijnlijk te wijten aan onzekerheden die voortkomen uit de kalibratie van de methodes en de over- of onderschatting van specifieke ligandgroepen binnen de heterogeniteit van de natuurlijke organische liganden. Deze studie onthulde dat de geschatte bijdrage van verschillende ligandgroepen verschilt tussen de methodes. De verschillende ligandgroepen die in onze monsters aanwezig waren, interfereren dus met de detectie-efficiëntie van de AL's. Er is verder onderzoek nodig om dit uit te zoeken en om een vergelijk mogelijk te maken tussen de gepubliceerde data verkregen met de afzonderlijke AL's.

5. Het westelijke Antarctische Schiereiland.

In de wateren die grenzen aan het westelijke Antarctische schiereiland werden concentraties en kenmerken van organische Fe-bindende liganden onderzocht langs een gradiënt van de met ijs bedekte 'shelf' zee naar de open oceaan. De hydrografische ligging in deze regio werd sterk beïnvloed door de zee-ijsbedekking en de aanwezigheid van twee grote hydrografische fronten: het 'Southern Antarctic Circumpolar Current Front' (SACCF) en de 'Southern Boundary' (SB). De hierdoor gevormde hydrografische regio's bevatten verschillende concentraties, bindingssterkten en complexeringscapaciteiten van organische Fe-bindende liganden. Onder de zee-ijsbedekking nabij de kust was de productie van organische liganden gekoppeld aan in zee-ijs groeiende algen. De interactie tussen sediment en water en resuspensie van bodem deeltjes resulteerden in hoge concentraties van zowel DFe als liganden in oceaanwater dat uit de diepe oceaan omhoog komt over de continentale helling. Richting de open oceaan bloeiden de algen

(fytoplankton) met steeds minder voedingsstoffen en ijzer, terwijl ze actief of passief organische liganden produceerden. De aanwezigheid van fronten beïnvloedde de verdeling van de liganden en markeerde de grens tussen op het continentale plat geproduceerde liganden en de algenbloei-geassocieerde liganden.

Concentraties van organische liganden waren altijd hoger dan DFe-concentraties. In de open oceaan, waar DFe relatief laag was, werden grote verschillen tussen [Lt] en DFe waargenomen, en bestond er dus een grote overmaat aan liganden. Aangezien Fe ook werd aangeleverd vanuit de sedimenten en via het smelten van gletsjers, en bovendien de organische liganden op het continentale plat een relatief hoge complexeringscapaciteit hadden, kan elke extra Fe-toevoer gestabiliseerd worden door organische liganden. We postuleren dus dat in deze regio de binding met organische liganden de verblijftijd van Fe als DFe verhoogt. Hierdoor zal DFe later in het seizoen, na het smelten van het zee ijs, waarschijnlijk beschikbaar zijn voor lokale primaire productie.

Voor het onderzoek beschreven in dit proefschrift zijn de concentratie, distributie en kenmerken van Fe-bindende liganden bepaald in verschillende oceaanregio's met verschillende omgevingsomstandigheden. Deze waardevolle dataset vergroot onze huidige kennis over de wereldwijde verspreiding van DFe en de Fe-bindende organische liganden. De studiegebieden in de Fram Straat en ten noordoosten van Groenland, het Westelijk Antarctisch Schiereiland en de Hauraki Golf hebben allemaal verschillende hydrografische condities. De studiegebieden in de oceanen op hoge breedtegraden zijn bijzonder gevoelig voor klimaatveranderingen, en onze resultaten helpen het fundamentele overzicht te bieden dat nodig is om de gevolgen van klimaatverandering op de biogeochemische cyclus van Fe in deze wereldwijd belangrijke oceanen te voorspellen. Bovendien tonen onze bevindingen aan dat er meer onderzoek nodig is om de efficiëntie van de verschillende toepassingen van voltammetrische methodes te onderzoeken en dat het aan

te raden is om betere methodes te ontwikkelen om de Fe-bindende organische liganden in zeewater te bestuderen.


RINGKASAN
BASAHA
INDONESIA

Pemanasan global menyebabkan perubahan lingkungan yang sangat cepat. Perubahan ini sangat berpengaruh pada siklus unsur logam renik (konsentrasi rendah) di lautan, salah satunya adalah besi (Fe), yang merupakan logam berat essensial bagi miko-organisme laut. Secara kimia, Fe memiliki tingkat kelarutan yang sangat rendah di dalam air laut, selain itu, pasokan Fe di laut sangat terbatas. Akibatnya, Fe terlarut (DFe) menjadi faktor penentu produktivitas di beberapa wilayah lautan lepas, seperti di Samudra sekitar Kutub Selatan. Beberapa penelitian juga telah melaporkan adanya 'keterbatasan DFe' di Samudra Atlantik Utara.

Siklus biogeokimia Fe di laut melibatkan interaksi kompleks antara proses – proses yang melibatkan Fe di perairan laut, antara lain: jumlah pasokan Fe yang masuk ke perairan laut, penggunaan Fe dalam aktivitas biologi di zona eufotik, proses adsoprsi oleh partikel, remineralisasi, dan sedimentasi. Proses – proses tersebut sangat mempengaruhi konsentrasi Fe dalam air laut, dengan ambang batas DFe dalam air laut sangat tergantung oleh keberadaan ligan organik pengikat besi.

Ligan organik pengikat besi merupakan kumpulan dari senyawa organik yang mempunyai afinitas tinggi terhadap Fe. Keberadaan ligan alami ini dapat meningkatkan kelarutan Fe dalam air laut dengan pembentukan Fe-ligan organik kompleks yang mudah larut, dan dapat melindungi Fe dari hidrolisis dan koagulasi yang menyebabkan pengendapan. Pembentukan senyawa kompleks ini dapat meningkatkan waktu tinggal Fe di perairan, sehingga potensi Fe memiliki potensi yang lebih tinggi untuk terlibat dalam aktivitas biologi mikroba laut.

Komposisi dari ligan pengikat Fe ini tidak banyak diketahui, biasanya terdapat di dalam air laut dengan konsentrasi rendah, sehingga karakterisasi dari struktur molekul campuran organik ini menjadi cukup sulit. Walaupun begitu, beberapa penelitian terkini telah berhasil mengidentifikasi beberapa molekul organik yang diduga sebagai bagian dari ligan pengikat Fe. Dari penelitian – penelitian tersebut, ligan pengikat Fe secara umum dikategorikan menjadi kelompok molekul organik yang memiliki berat molekul rendah (seperti siderofor), hingga kelompok makromolekul (seperti senyawa humus dan polisakarida). Karakteristik

dari kelompok molekul ini berbeda – beda, biasanya ditentukan oleh asal – usul dari kelompok molekul tersebut.

Ligan pengikat besi di lautan dapat berasal dari daratan, ataupun di produksi langsung dari aktivitas biologi mikroba laut. Sebagai contoh, beberapan jenis microba laut secara aktif memproduksi senyawa yang disebut siderofor sebagai suatu strategi untuk mendapatkan zat Fe dari air laut. Ligan pengikat Fe juga dapat dihasilkan secara pasif dari degradasi senyawa organik oleh mikroba serta ekskresi dari sel mikroba yang ada di lautan. Biasanya ligan pengikat Fe yang dihasilkan secara pasif (contoh: polisakarida) memiliki konsentrasi yang lebih tinggi dibandingkan dengan ligan pengikat Fe yang dihasilkan secara aktif (contoh: siderofor). Namun. dilihat dari karakteristik kekuatan ikatannya dengan Fe, secara umum, ligan sejenis siderofor memiliki ikatan yang lebih kuat dibandingkan dengan ligan dari senyawa polisakarida. Senyawa organik yang berasal dari daratan biasanya dipasok ke lautan melalui pesisir dan muara sungai. Pasokan senyawa organik dari daratan ke lautan ini merupakan salah satu sumber ligan pengikat Fe, biasanya berjenis senyawa humus.

Spesies Fe organik mendominasi DFe dalam air laut, sehingga spesies ini menjadi bagian yang penting dalam siklus biogeokimia Fe di lautan. Pemahaman yang lebih komprehensif tentang spesies Fe organik ini sangatlah penting untuk mengetahui dampak pemanasan global pada siklus Fe. Sayangnya tidak banyak data scientifik yang mengedepankan pembahasan tentang spesies Fe organik ini, sehingga dampak perubahan iklim pada siklus biogeokimia Fe tidak dapat dievaluasi secara mendetail. Oleh karenanya, studi ini berfokus pada analisa ligan pengikat Fe, sebagai factor penentu utama spesi Fe organik. Studi ini mengukur konsentrasi dan karakteristik ligand pengikat Fe, yaitu konsentrasi total ([Lt]) dan konstanta stabilitas ($K_{Fe'L}^{cond}$) ligan. Konstanta stabilitas ligan, $K_{Fe'L}^{cond}$ juga dikenal sebagai kekuatan ikat ligan organik terhadap Fe, biasanya ditunjukkan dengan satuan logaritmik, log $K_{Fe'L}^{cond}$. Penentuan [Lt] dan $K_{Fe'L}^{cond}$ dapat digunakan untuk mengetahui distribusi dan memperkirakan darimana ligan organik ini berasal. Dengan adanya data tentang senyawa kompleks Fe-ligan, ketersediaan DFe dan mobilitasnya di lautan dapat

dipelajari dengan lebih detail, terutama di daerah perairan yang sangat rentan terhadap perubahan iklim, seperti daerah kutub utara dan selatan. Selain daerah kutub tersebut, data mengenai organik ligan juga dikumpulkan dari perairan yang memiliki variabilitas tinggi saat terjadi perubahan musim. sebagai contoh, daerah perairan subtropis di Selandia Baru. Hasil – hasil dari studi ini dapat memberikan gambaran bagaimana distribusi organik ligan di daerah perairan subtropis yang memiliki variabilitas tinggi, atau daerah perairan lain yang memiliki kesamaan musim.

Penelitian ini menggunakan pendekatan elektrokimia, *competitive ligand exchange - adsorptive cathodic stripping voltametry* (CLE-AdCSV). CLE-AdCSV adalah metode tidak langsung untuk menentukan sifat termodinamika ligan organik, seperti [Lt] dan $K_{Fe'L}^{cond}$. Penentuan [Lt] dan $K_{Fe'L}^{cond}$ dengan metode elektrokimia tersebut dapat dilakukan dengan mentitrasi sampel dengan Fe untuk menjenuhkan ligan organik alami yang ada dalam sampel. Ligan tambahan (added ligand, AL) yang diketahui karakteristiknya bersaing dengan ligan alami untuk mendapatkan Fe, dan terbentuk senyawa kompleks elektroaktif, Fe(AL)x, yang dapat terdeposisi pada elektroda merkuri dengan voltase negatif. Selanjutnya Fe pada Fe(AL)x direduksi, dan arus listrik reduksinya dapat diukur. Sinyal listrik terukur dari setiap titik titrasi digunakan untuk menghitung [Lt] dan $K_{Fe'L}^{cond}$ secara bersamaan dengan menerapkan transformasi isoterm. [Lt] yang diperoleh dilaporkan dalam nM ekivalen Fe (nM eq. Fe) dan nilai $K_{Fe'L}^{cond}$ dalam M^{-1}, dinyatakan sebagai nilai lognya, log $K_{Fe'L}^{cond}$.

Ada empat teknik CLE-AdCSV yang umum digunakan untuk pengukuran spesiasi Fe dalam air laut. Teknik ini menggunakan AL dan kondisi titrasi yang berbeda (pH, konsentrasi AL dan waktu ekuilibrasi). AL yang digunakan adalah 2-(2-thiazolylazo)-p-cresol (TAC), salisylaldoxime (SA), 1-nitroso-2-napthol (NN) dan 2,3-dihydroxynaphthalen (DHN). Metode CLE-AdCSV menggunakan TAC dan SA sebagai AL adalah metode yang paling banyak digunakan dalam analisis CLE-AdCSV. Metode CLE-AdCSV adalah metode yang relatif sederhana, yang dapat memberikan hasil analisa akurat adanya gugus aktif

untuk mengikat Fe dalam ligan organik. Perlakuan sampel, seperti pra-konsentrasi atau penghilangan matriks air laut, tidak diperlukan dalam metode ini. Namun, perlu dicatat bahwa metode tersebut memiliki keterbatasan ketika menafsirkan data. Penentuan [Lt] dan $K_{Fe'L}^{cond}$ dari analisis CLE-AdCSV cukup rumit, dan penerapan AL berbeda dapat menghasilkan interpretasi data spesiasi yang sedikit berbeda. Oleh karena itu, studi ini melakukan studi perbandingan dengan analisis menggunakan AL yang berbeda namun menganalisa sampel yang sama. AL yang dipilih yaitu (TAC, SA dan NN). Perbandingan ini bertujuan untuk mengetahui pengaruh penggunaan AL yang berbeda terhadap hasil analisis spesiasi Fe.

Secara keseluruhan, studi ini melaporkan parameter termodinamis [L_t] and $K_{Fe'L}^{cond}$ dari ligan organik pengikat Fe dalam sampel air laut yang diambil dari beberapa kawasan perairan subtropis dan kutub, serta dari kultur di laboratorium. Beberapa kawasan perairan yang menjadi studi area antara lain: Teluk Hauraki yang berada di timur laut Selandia Baru, Fram Strait di kawasan laut Arktik, dan Laut Bellingshausen di semenanjung Antartika bagian barat. Hasil dan implikasi dari studi ini diringkas dibawah ini:

1. **Eksperimen laboratorium dengan mengkulturkan diatom dan bakteri dalam media yang sama.**

   Eksperimen ini dilakukan untuk mengetahui interaksi antara diatom dan bakteri untuk mendapatkan Fe secara efisien, terlebih saat terjadi defisiensi Fe di sekitar habitatnya. Dua perlakuan berbeda dilakukan pada kultur media, antara lain (1) kultur tanpa penambahan Fe dalam medianya, disebut kultur dengan Fe-rendah; dan (2) kultur dengan tambahan Fe dalam medianya, disebut kultur dengan Fe-tinggi. Membran dialisis digunakan untuk memisahkan diatom dan bakteri secara fisik, tujuannya untuk menguji apaka kontak sel langsung antara diatom dan bakteri diperlukan untuk memproduksi ligand dan untuk pertumbuhan diatom. Experimen ini menggunakan media air laut, yang diambil dari lepas pantai

semenanjung Otago (Selandia Baru). Semenanjung ini merupakan daerah subtropis, dimana air berasal dari daerah tropis dan daerah kutub.

Dari hasil eksperimen ini dapat disimpulkan bahwa interaksi fisik dari diatom dan bakteri terbukti kontraproduktif, yaitu membuat pertumbuhan diatom menjadi lambat. Sedangkan interaksi kimia dapat menguntungkan pertumbuhan diatom. Ligand dengan afinitas tinggi terhadap Fe nampaknya tidak diproduksi secara aktif oleh diatom pada kultur dengan konsentrasi DFe lebih besar dari 1 nM. Penelitian ini bertujuan untuk mengkaji pertumbuhan diatom dengan adanya bakteri, baik dengan kontak langsung ataupun tidak langsung, namun, sangat sulit untuk meminimalisir keberadaan bakteri di dalam medium kultur, terlebih hanya dengan pemisahan melalui penyaringan. Untuk mendapatkan hasil dengan presisi tinggi, sebaiknya penyaringan beserta autoklaf dilakukan pada media air laut untuk mendapatkan air laut dengan jumlah bakteri seminimal mungkin.

2. Studi spesiasi DFe di perairan subtropis Teluk Hauraki, Selandia Baru.

Teluk Hauraki adalah laut semi tertutup yang terletak di hilir kota metropolitan Auckland di Selandia Baru. Teluk ini memiliki ekosistem yang sangat produktif di musim semi, dan mengalami kondisi oligotropik musiman. Perubahan arah angin saat pergantian musim menyebabkan perubahan sirkulasi air di teluk ini, yaitu, air dari laut lepas secara berkala masuk ke dalam laut dangkal (zona neritik). Perubahan tersebut dapat menyebabkan pergeseran komposisi mikroba di perairan ini. Pergeseran komposisi mikroba akan sangat berpengaruh pada spesiasi Fe. Sehingga teluk ini dapat digunakan sebagai laboratotium alami untuk mempelajari spesiasi Fe di perairan yang mengalami variasi musiman.

Hasil studi menunjukkan bahwa [Lt] relatif tinggi (~2,5 sampai 7,5 nM eq. Fe), terutama di daerah laut dangkal. Keberadaan [Lt] dalam konsentrasi tinggi memungkinkan DFe berada dalam konsentrasi yang cukup tinggi pula. Tingginya konsentrasi DFe di laut dangkal berpotensi untuk meningkatkan pasokan Fe ke laut lepas. Pasokan Fe ke laut lepas ini sangat penting untuk produktivitas primer.

Dari rentang nilai log $K^{cond}_{Fe'L}$, didukung dengan data sekunder seperti *apparent oxygen utilization* (AOU), dapat diketahui bahwa remineralisasi mikroba merupakan proses yang mendominasi dinamika ligan di zona neritik. Pengaruh intrusi air laut ke zona neritik terhadap distribusi [Lt] dan DFe masih belum dapat diobservasi dengan jelas. Walaupun begitu, observasi pada studi ini dapat dijadikan titik awal untuk mengkaji lebih lanjut mengenai fluktuasi DFe pada saat pergantian musim. Penelitian ini merupakan penelitian pertama yang melaporkan kondisi spesiasi Fe dan beberapa logam berat pada saat pergantian musim panas ke musim gugur, dalam dua tahun berturut-turut.

3. Studi Spesiasi DFe di Selat Fram dan dangkalan timu laut Greenland.

Selat Fram adalah selat yang terletak diantara Pulau Greenland dan Pulai Svalbard. Selat ini menjadi pintu gerbang utama pertukaran panas dan masa air antara Samudra Arktik dan Laut Nordik (Laut Greenland, Laut Norwegia, dan Laut Islandia). Ligan – ligan yang di produksi di kawasan Arktik dapat terbawa oleh arus laut, melewati Selat Fram. Perubahan yang terjadi di kawasan Arktik akan sangat mempengaruh produksi ligan di kawasan tersebut, serta akan berpengaruh pada distribusi dan karakteristik ligan organik di Selat Fram Strait. Selain itu, Gletser terbesar di daerah timur laut Pulau Greenland, 79N Gletser, bermuara langsung ke Selat Fram. Gletser ini diperkiraan juga dapat

memasok ligan organik pengikat Fe ke Selat Fram. Selat Fram dan daerah dangkalan di timur laut Greenland merupakan kawasan perairan yang ideal untuk observasi pengaruh beragam sumber ligan organik pengikat Fe, terhadap distribusi dan karakteristik ligan.

Studi ligan organik pengikat Fe di selat Fram menunjukkan bahwa kekuatan ikatan ligan dan Fe sangat berpengaruh terhadap eksport DFe dari Gletser 79N ke Selat Fram. Ligan dengan konsentrasi tinggi tinggi ([Lt] hingga mencapai ~3 nmol eq. Fe) banyak ditemukan di sekitar mulut gletser, namun dengan kekuatan ikatan yang relatif lemah,. Ligan yang berkekuatan ikat relatif lemah ini tidak dapat berikatan dengan Fe secara efisien, sehingga, Fe akan cenderung berikatan dengan partikel, kemudian mengendap bersama partikel tersebut. Hasil observasi ini menunjukkan bahwa ligan memiliki peranan yang sangat penting dalam mobilitas Fe. Dengan adanya pemanasan global, kondisi lingkungan akan berubah dengan cepat, adanya peningkatan pencairan gletser diprediksikan akan meningkatkan pasokan Fe dan ligan. Namun, penelitian ini menunjukkan bahwa kombinasi antara ketersediaan gugus aktif serta kekuatan ikatan ligan~~d~~, akan sangat mempengaruhi seberapa besar Fe dari gletser akan berpindah ke laut lepas. Dengan kata lain, ligan organik ~~akan~~ sangat mempengaruhi distribusi DFe di selat Fram. (Selengkapnya dapat dibaca: https://doi.org/10.1016/j.marchem.2020.103815).

4. Studi spesiasi DFe di sepanjang Semenanjung Antartika barat

Pada studi ini, konsentrasi dan karakteristik ligan organik pengikat Fe diobservasi di sekitar semenanjung barat Antartika. Pengambilan sampel dilakukan sepanjang gradien dari dangkalan dengan permukaan yang tertutup es hingga ke laut lepas tanpa adanya lapisan es di permukaan. Hidrografi di wilayah ini sangat dipengaruhi lapisan es, serta keberadaan beberapa oseanografik

front, antara lain *Front* Arus Circumpolar Antartika Selatan (SACCF) dan *Front* Batas Selatan (SB).

Menariknya, pada kondisi hidrografi yang berbeda ditemukan konsentrasi dan kekuatan pengikatan, serta kapasitas kompleksasi ligan yang berbeda – beda pula. Pada permukaan yang tertutup es, di daerah dangkalan di dekat pantai, ligan nampaknya berasal dari aktivitas biologis ganggang laut di bawah lapisan es. Interaksi antara sedimen dengan lapisan air di atasnya menyebabkan resuspensi dasar sedimen, menghasilkan konsentrasi DFe dan ligan yang tinggi di dasar laut dangkalan. Di laut lepas, produktivitas fitoplankton menyebabkan penurunan konsentrasi nutrient (nitrat, fosfat dll) serta Fe. Di sisi lain, produktivatas fitoplankton ini secara aktif atau pasif dapat menghasilkan ligan organik. Keberadaan oseanografik *front* di sekitar area pengambilan sampel sangat mempengaruhi distribusi ligan. Selain itu adanya SB, nampaknya menandai antara ligan yang berasal dari daerah dangkalan di dekat pantai dan ligan yang berasal dari laut lepas.

Konsentrasi ligan organik selalu melebihi konsentrasi DFe. Sementara itu, konsentrasi ligan 'bebas' yang tinggi diamati di wilayah laut terbuka, di mana DFe relatif rendah. Karena Fe juga disuplai oleh sedimen dan lelehan gletser, ligan organik di kawasan dangkalan memiliki kapasitas kompleksasi yang relatif tinggi. Dengan kapasitas kompleksasi yang tinggi, adanya suplai Fe yang masuk ke perairan kemungkinan besar akan distabilkan melalui kompleksasi organik dalam bentuk DFe. Dengan demikian, DFe akan bertahan lebih lama di perairan, dan dapat digunakan sebagai pasokan DFe saat produktifitas fitoplankton memuncak, terlebih setelah lapisan es di permukaan mencair. (Selengkapnya dapat dibaca di: https://doi.org/10.5194/bg-2020-357).

5. Studi perbandingan metode voltametri untuk spesiasi DFe

Studi ini membandingkan tiga AL yang berbeda, yaitu TAC, SA dan NN. Masing-masing AL ini memiliki rentang deteksi tertentu. Interpretasi data menggunakan model satu ligan menghasilkan konsentrasi ligan organik [Lt]SA > [Lt]TAC >[Lt] NN; dengan rata-rata log $K_{Fe'L}^{cond}$ TAC > SA > NN. Metode SA tampaknya menjadi AL yang paling sesuai untuk mendeteksi ligan pada sampel dari daerah ini, karena dengan SA sebagai AL, metode ini dapat mendeteksi gugus ligan yang relatif lemah, bahkan ligan – ligan yang tidak dapat terdeteksi oleh AL lain (TAC dan NN). Hal ini dikarenakan metode SA memiliki rentang deteksi yang lebih rendang dibanding rentang deteksi metode TAC dan NN. Namun, perbedaan hasil dari ketiga penggunaan AL diatas, hanya dapat dijelaskan secara parsial oleh perbedaan pengaruh deteksi. Perbedaan hasil spesiasi dengan menggunakan AL yang berbeda juga dapat disebabkan oleh error atau ketidakpastian pada saat kalibrasi masing–masing AL. Selain itu, heterogenitas ligan alami atau perbedaan komposisi jenis/kelompok ligan yang ada di dalam sampel juga dapat mempengaruhi pendeteksiannya dengan AL yang berbeda. Penelitian ini menunjukkan bahwa kontribusi kelompok ligan tertentu mempengaruhi hasil dari analisa dengan menggunakan AL yang berbeda. Dengan kata lain, kelompok ligan tertentu dapat mempengaruhi efisiensi pendeteksian ligan dengan metode TAC, SA atau NN. Studi lebih lanjut diperlukan pada efisiensi deteksi masing-masing AL. (Selengkapnya dapat dibaca: 10.3389/fmars.2020.609379).

Singkatnya, penelitian ini melaporkan konsentrasi, distribusi, dan karakteristik ligan pengikat Fe di wilayah laut yang berbeda dengan keadaan lingkungan yang berbeda, yang dapat menambahkan/memperluas data tentang spesiasi Fe secara global. Daerah penelitian di selat Fram dan dangkalan timur laut Greenland, Semenanjung Antartika Barat, serta Teluk Hauraki, semuanya memiliki pengaturan hidrografi yang berbeda. Area studi di lautan lintang tinggi sangat rentan terhadap perubahan iklim,

dan hasil penelitian membantu memberikan gambaran mendasar yang diperlukan untuk memprediksi konsekuensi perubahan iklim pada siklus biogeokimia Fe di lautan di daerah kutub. Selanjutnya, temuan dari studi perbandingan metode voltametri menunjukkan perlunya pengembangan metode yang lebih baik untuk mempelajari spesiasi Fe dalam air laut.

REFERENCES

Abualhaija, M.M. and van den Berg, C.M.G., 2014. Chemical speciation of iron in seawater using catalytic cathodic stripping voltammetry with ligand competition against salicylaldoxime. Marine Chemistry, 164: 60-74.

Abualhaija, M.M., Whitby, H. and van den Berg, C.M.G., 2015. Competition between copper and iron for humic ligands in estuarine waters. Marine Chemistry, 172: 46-56.

Achterberg, E.P., Steigenberger, S., Marsay, C.M., LeMoigne, F.A.C., Painter, S.C., Baker, A.R., Connelly, D.P., Moore, C.M., Tagliabue, A. and Tanhua, T., 2018. Iron Biogeochemistry in the High Latitude North Atlantic Ocean. Scientific Reports, 8(1): 1283.

Adly, C.L., Tremblay, J.-E., Powell, R.T., Armstrong, E., Peers, G. and Price, N.M., 2015. Response of heterotrophic bacteria in a mesoscale iron enrichment in the northeast subarctic Pacific Ocean. Limnology and Oceanography, 60(1): 136-148.

Aguilar-Islas, A.M., Séguret, M.J.M., Rember, R., Buck, K.N., Proctor, P., Mordy, C.W. and Kachel, N.B., 2016. Temporal variability of reactive iron over the Gulf of Alaska shelf. Deep Sea Research Part II: Topical Studies in Oceanography, 132: 90-106.

Aguirre, J.D., Bollard-Breen, B., Cameron, M., Constantine, R., Duffy, C.A.J., Dunphy, B., Hart, K., Hewitt, J.E., Jarvis, R.M., Jeffs, A., Kahui-McConnell, R., Kawharu, M., Liggins, L., Lohrer, A.M., Middleton, I., Oldman, J., Sewell, M.A., Smith, A.N.H., Thomas, D.B., Tuckey, B., Vaughan, M. and Wilson, R., 2016. Loved to pieces: Toward the sustainable management of the Waitematā Harbour and Hauraki Gulf. Regional Studies in Marine Science, 8: 220-233.

Alderkamp, A.-C., Kulk, G., Buma, A.G.J., Visser, R.J.W., Van Dijken, G.L., Mills, M.M. and Arrigo, K.R., 2012. The effect of iron limitation on the photophysiology of phaeocystis antarctica (prymnesiophyceae) and fragilariopsis cylindrus (bacillariophyceae) under dynamic irradiance. Journal of Phycology, 48(1): 45-59.

Amin, S.A., Green, D.H., Gärdes, A., Romano, A., Trimble, L. and Carrano, C.J., 2012a. Siderophore-mediated iron uptake in two clades of Marinobacter spp. associated with phytoplankton: The role of light. BioMetals, 25(1): 181-192.

Amin, S.A., Parker, M.S. and Armbrust, E.V., 2012b. Interactions between Diatoms and Bacteria. Microbiology and Molecular Biology Reviews, 76(3): 667-684.

Apte, S.C., Gardner, M.J. and Ravenscroft, J.E., 1988. An evaluation of voltammetric titration procedures for the determination of trace metal complexation in natural waters by use of computers simulation. Analytica Chimica Acta, 212: 1-21.

Ardiningsih, I., Krisch, S., Lodeiro, P., Reichart, G.-J., Achterberg, E.P., Gledhill, M., Middag, R. and Gerringa, L.J.A., 2020. Natural Fe-binding organic ligands in Fram Strait and over the northeast Greenland shelf. Marine Chemistry, 224: 103815.

Arrigo, K.R., Robinson, D.H., Worthen, D.L., Dunbar, R.B., DiTullio, G.R., VanWoert, M. and Lizotte, M.P., 1999. Phytoplankton Community Structure and the Drawdown of Nutrients and CO2 in the Southern Ocean. Science, 283(5400): 365-367.

Arrigo, K.R., van Dijken, G. and Long, M., 2008a. Coastal Southern Ocean: A strong anthropogenic CO2 sink. Geophysical Research Letters, 35(21): 0094-8276.

Arrigo, K.R., van Dijken, G. and Pabi, S., 2008b. Impact of a shrinking Arctic ice cover on marine primary production. Geophysical Research Letters, 35(19).

Arrigo, K.R., van Dijken, G.L., Alderkamp, A.-C., Erickson, Z.K., Lewis, K.M., Lowry, K.E., Joy-Warren, H.L., Middag, R., Nash-Arrigo, J.E., Selz, V. and van de Poll, W., 2017. Early Spring Phytoplankton Dynamics in the Western Antarctic Peninsula. Journal of Geophysical Research: Oceans, 122(12): 9350-9369.

Arrigo, K.R., van Dijken, G.L. and Strong, A.L., 2015. Environmental controls of marine productivity hot spots around Antarctica. Journal of Geophysical Research: Oceans, 120(8): 5545-5565.

Baltar, F., Gutiérrez-Rodríguez, A., Meyer, M., Skudelny, I., Sander, S., Thomson, B., Nodder, S., Middag, R. and Morales, S.E., 2018. Specific Effect of Trace Metals on Marine Heterotrophic Microbial Activity and Diversity: Key Role of Iron and Zinc and Hydrocarbon-Degrading Bacteria. Frontiers in Microbiology, 9(3190).

Baltar, F., Stuck, E., Morales, S. and Currie, K., 2015. Bacterioplankton carbon cycling along the Subtropical Frontal Zone off New Zealand. Progress in Oceanography, 135: 168-175.

Barbeau, K., Rue, E.L., Bruland, K.W. and Butler, A., 2001. Photochemical cycling of iron in the surface ocean mediated by microbial iron(iii)-binding ligands. Nature, 413(6854): 409-413.

Batchelli, S., Muller, F.L.L., Chang, K.-C. and Lee, C.-L., 2010. Evidence for Strong but Dynamic Iron−Humic Colloidal Associations in Humic-Rich Coastal Waters. Environmental Science & Technology, 44(22): 8485-8490.

Benner, R., Pakulski, J.D., Mccarthy, M., Hedges, J.I. and Hatcher, P.G., 1992. Bulk Chemical Characteristics of Dissolved Organic Matter in the Ocean. Science, 255(5051): 1561-1564.

Bennett, S.A., Achterberg, E.P., Connelly, D.P., Statham, P.J., Fones, G.R. and German, C.R., 2008. The distribution and stabilisation of dissolved Fe in deep-sea hydrothermal plumes. Earth and Planetary Science Letters, 270(3): 157-167.

Beszczynska-Möller, A., Fahrbach, E., Schauer, U. and Hansen, E., 2012. Variability in Atlantic water temperature and transport at the entrance to the Arctic Ocean, 1997–2010. ICES Journal of Marine Science, 69(5): 852-863.

Bidle, K.D. and Azam, F., 1999. Accelerated dissolution of diatom silica by marine bacterial assemblages. Nature, 397(6719): 508-512.

Biller, D.V. and Bruland, K.W., 2012. Analysis of Mn, Fe, Co, Ni, Cu, Zn, Cd, and Pb in seawater using the Nobias-chelate PA1 resin and magnetic sector inductively coupled plasma mass spectrometry (ICP-MS). Marine Chemistry, 130: 12-20.

Boiteau, R.M., Fitzsimmons, J.N., Repeta, D.J. and Boyle, E.A., 2013. Detection of iron ligands in seawater and marine cyanobacteria cultures by high-performance liquid chromatography-inductively coupled plasma-mass spectrometry. Analytical Chemistry, 85(9): 4357-4362.

Boiteau, R.M., Mende, D.R., Hawco, N.J., McIlvin, M.R., Fitzsimmons, J.N., Saito, M.A., Sedwick, P.N., DeLong, E.F. and Repeta, D.J., 2016. Siderophore-based microbial adaptations to iron scarcity across the eastern Pacific Ocean. Proceedings of the National Academy of Sciences of the United States of America, 113(50): 14237-14242.

Boiteau, R.M. and Repeta, D.J., 2015. An extended siderophore suite from Synechococcus sp. PCC 7002 revealed by LC-ICPMS-ESIMS. Metallomics, 7(5): 877-84.

Boiteau, R.M., Till, C.P., Coale, T.H., Fitzsimmons, J.N., Bruland, K.W. and Repeta, D.J., 2019. Patterns of iron and siderophore distributions across the California Current System. 64(1): 376-389.

Bourke, R.H., Newton, J.L., Paquette, R.G. and Tunnicliffe, M.D., 1987. Circulation and water masses of the East Greenland shelf. Journal of Geophysical Research: Oceans, 92(C7): 6729-6740.

Boxberg, F., 2017. Anthropogenic input of heavy metals to near-coastal sediment depocenters in the eastern North Sea and the Hauraki Gulf in historical times, Universität Bremen.

Boyd, P., Ibisanmi, E., Sander, S., Hunter, K. and Jackson, G., 2010a. Remineralization of upper ocean particles: Implications for iron biogeochemistry. Limnology and Oceanography, 55(3): 1271-1288.

Boyd, P.W., 2013. Ocean Iron Cycle, Surface Ocean-Lower Atmosphere Processes, pp. 161-179.

Boyd, P.W. and Ellwood, M.J., 2010b. The biogeochemical cycle of iron in the ocean. Nature Geosci, 3(10): 675-682.

Boyd, P.W., Watson, A.J., Law, C.S., Abraham, E.R., Trull, T., Murdoch, R., Bakker, D.C.E., Bowie, A.R., Buesseler, K.O., Chang, H., Charette, M., Croot, P., Downing, K., Frew, R., Gall, M., Hadfield, M., Hall, J., Harvey, M., Jameson, G., LaRoche, J., Liddicoat, M., Ling, R., Maldonado, M.T., McKay, R.M., Nodder, S., Pickmere, S., Pridmore, R., Rintoul, S., Safi, K., Sutton, P., Strzepek, R., Tanneberger, K., Turner, S., Waite, A. and Zeldis, J., 2000. A mesoscale phytoplankton bloom in the polar Southern Ocean stimulated by iron fertilization. Nature, 407: 695.

Boye, M., Aldrich, A., van den Berg, C.M.G., de Jong, J.T.M., Nirmaier, H., Veldhuis, M., Timmermans, K.R. and de Baar, H.J.W., 2006. The chemical speciation of iron in the north-east Atlantic Ocean. Deep-Sea Research Part I-Oceanographic Research Papers, 53(4): 667-683.

Boye, M., Nishioka, J., Croot, P., Laan, P., Timmermans, K.R., Strass, V.H., Takeda, S. and de Baar, H.J.W., 2010. Significant portion of dissolved organic Fe complexes in fact is Fe colloids. Marine Chemistry, 122(1): 20-27.

Boye, M., van den Berg, C.M.G., de Jong, J.T.M., Leach, H., Croot, P. and de Baar, H.J.W., 2001. Organic complexation of iron in the Southern Ocean. Deep-Sea Research Part I-Oceanographic Research Papers, 48(6): 1477-1497.

Boyle, E.A., Edmond, J.M. and Sholkovitz, E.R., 1977. The mechanism of iron removal in estuaries. Geochimica et Cosmochimica Acta, 41(9): 1313-1324.

Bruland, K.W., Donat, J.R. and Hutchins, D.A., 1991. Interactive influences of bioactive trace metals on biological production in oceanic waters. Limnology and Oceanography, 36(8): 1555-1577.

Bruland, K.W., Middag, R. and Lohan, M.C., 2014. 8.2 - Controls of Trace Metals in Seawater. In: H.D. Holland and K.K. Turekian (Editors), Treatise on Geochemistry (Second Edition). Elsevier, Oxford, pp. 19-51.

Brzezinski, M.A., Pride, C.J., Franck, V.M., Sigman, D.M., Sarmiento, J.L., Matsumoto, K., Gruber, N., Rau, G.H. and Coale, K.H., 2002. A switch from Si(OH)4 to NO3− depletion in the glacial Southern Ocean. Geophysical Research Letters, 29(12): 5-1-5-4.

Buck, K.N. and Bruland, K.W., 2007a. The physicochemical speciation of dissolved iron in the Bering Sea, Alaska. Limnology and Oceanography, 52(5): 1800-1808.

Buck, K.N., Gerringa, L.J.A. and Rijkenberg, M.J.A., 2016. An Intercomparison of Dissolved Iron Speciation at the Bermuda Atlantic Time-series Study (BATS) Site: Results from GEOTRACES Crossover Station A. Frontiers in Marine Science, 3(262).

Buck, K.N., Lohan, M.C., Berger, C.J.M. and Bruland, K.W., 2007b. Dissolved iron speciation in two distinct river plumes and an estuary: Implications for riverine iron supply. Limnology and Oceanography, 52(2): 843-855.

Buck, K.N., Moffett, J., Barbeau, K.A., Bundy, R.M., Kondo, Y. and Wu, J., 2012. The organic complexation of iron and copper: an intercomparison of competitive ligand exchange-adsorptive cathodic stripping voltammetry (CLE-ACSV) techniques. Limnology and Oceanography: Methods, 10(7): 496-515.

Buck, K.N., Sedwick, P.N., Sohst, B. and Carlson, C.A., 2017. Organic complexation of iron in the eastern tropical South Pacific: Results from US GEOTRACES Eastern Pacific Zonal Transect (GEOTRACES cruise GP16). Marine Chemistry, 201: 229 - 251.

Buck, K.N., Selph, K.E. and Barbeau, K.A., 2010. Iron-binding ligand production and copper speciation in an incubation experiment of Antarctic Peninsula shelf waters from the Bransfield Strait, Southern Ocean. Marine Chemistry, 122(1-4): 148-159.

Buck, K.N., Sohst, B. and Sedwick, P.N., 2015. The organic complexation of dissolved iron along the U.S. GEOTRACES (GA03) North Atlantic Section. Deep Sea Research Part II: Topical Studies in Oceanography, 116: 152-165.

Budéus, G., Schneider, W. and Kattner, G., 1997. Distribution and exchange of water masses in the Northeast Water polynya (Greenland Sea). Journal of Marine Systems, 10(1): 123-138.

Buffle, J., Zhang, Z. and Startchev, K., 2007. Metal Flux and Dynamic Speciation at (Bio)interfaces. Part I: Critical Evaluation and Compilation of Physicochemical Parameters for Complexes with Simple Ligands and Fulvic/Humic Substances. Environmental Science & Technology, 41(22): 7609-7620.

Bundy, R.M., Abdulla, H.A.N., Hatcher, P.G., Biller, D.V., Buck, K.N. and Barbeau, K.A., 2015. Iron-binding ligands and humic substances in the San Francisco Bay estuary and estuarine-influenced shelf regions of coastal California. Marine Chemistry, 173: 183-194.

Bundy, R.M., Biller, D.V., Buck, K.N., Bruland, K.W. and Barbeau, K.A., 2014. Distinct pools of dissolved iron-binding ligands in the surface and benthic boundary layer of the California Current. Limnology and Oceanography, 59(3): 769-787.

Bundy, R.M., Boiteau, R.M., McLean, C., Turk-Kubo, K.A., McIlvin, M.R., Saito, M.A., Van Mooy, B.A.S. and Repeta, D.J., 2018. Distinct Siderophores Contribute to Iron Cycling in the Mesopelagic at Station ALOHA. Frontiers in Marine Science, 5: 61.

Bundy, R.M., Jiang, M., Carter, M. and Barbeau, K.A., 2016. Iron-binding ligands in the Southern California current system: Mechanistic studies. Frontiers in Marine Science, 3(MAR).

Burkhardt, B.G., Watkins-Brandt, K.S., Defforey, D., Paytan, A. and White, A.E., 2014. Remineralization of phytoplankton-derived organic matter by natural populations of heterotrophic bacteria. Marine Chemistry, 163: 1-9.

Butler, A., 2005. Marine siderophores and microbial iron mobilization. Biometals, 18(4): 369-374.

Button, D.K., Schut, F., Quang, P., Martin, R. and Robertson, B.R., 1993. Viability and Isolation of Marine Bacteria by Dilution Culture: Theory, Procedures, and Initial Results. Applied and Environmental Microbiology, 59(3): 881-891.

Byrne, R.H., Kump, L. and Cantrell, K., 1988. The influence of temperature and pH on trace metal speciation in seawater. Marine Chemistry, 25(2): 163-181.

Calace, N., Castrovinci, D., Maresca, V., Petronio, B.M., Pietroletti, M. and Scardala, S., 2001. Aquatic humic substances in pack ice-seawater-sediment system. International Journal of Environmental Analytical Chemistry, 79(4): 315-329.

Calleja, M.L., Al-Otaibi, N. and Morán, X.A.G., 2019. Dissolved organic carbon contribution to oxygen respiration in the central Red Sea. Scientific Reports, 9(1): 4690.

Caprara, S., Buck, K.N., Gerringa, L.J., Rijkenberg, M.J. and Monticelli, D., 2016. A compilation of iron speciation data for open oceanic waters. Frontiers in Marine Science, 3: 221.

Cauwet, G., 1994. HTCO method for dissolved organic carbon analysis in seawater: influence of catalyst on blank estimation. Marine Chemistry, 47(1): 55-64.

Chang, F.H., Zeldis, J., Gall, M. and Hall, J., 2003. Seasonal and spatial variation of phytoplankton assemblages, biomass and cell size from spring to summer across the north-eastern New Zealand continental shelf. Journal of Plankton Research, 25(7): 737-758.

Cherkasheva, A., Bracher, A., Melsheimer, C., Köberle, C., Gerdes, R., Nöthig, E.M., Bauerfeind, E. and Boetius, A., 2014. Influence of the physical environment on polar phytoplankton blooms: A case study in the Fram Strait. Journal of Marine Systems, 132: 196-207.

Chiswell, S.M., Bostock, H.C., Sutton, P.J.H. and Williams, M.J.M., 2015. Physical oceanography of the deep seas around New Zealand: a review. New Zealand Journal of Marine and Freshwater Research, 49(2): 286-317.

Croot, P.L., Andersson, K., Öztürk, M. and Turner, D.R., 2004. The distribution and speciation of iron along 6°E in the Southern Ocean. Deep Sea Research Part II: Topical Studies in Oceanography, 51(22): 2857-2879.

Croot, P.L. and Johansson, M., 2000. Determination of Iron Speciation by Cathodic Stripping Voltammetry in Seawater Using the Competing Ligand 2-(2-Thiazolylazo)-p-cresol (TAC). Electroanalysis, 12(8): 565-576.

Cullen, J.T., Bergquist, B.A. and Moffett, J.W., 2006. Thermodynamic characterization of the partitioning of iron between soluble and colloidal species in the Atlantic Ocean. Marine Chemistry, 98(2): 295-303.

Cutter, G., Andersson, P. , Codispoti, L. , Croot, P. François, R. , Lohan, M. C. , Obata, H. and Rutgers v. d. Loeff, M. , 2010. Sampling and Sample-handling Protocols for GEOTRACES Cruises.

Cutter, G.A. and Bruland, K.W., 2012. Rapid and noncontaminating sampling system for trace elements in global ocean surveys. Limnology and Oceanography: Methods, 10(6): 425-436.

de Baar, H.J., 1990. On iron limitation of the Southern Ocean : experimental observations in the Weddell and Scotia Seas. Marine Ecol. Prog. Ser., 65: 105-122.

de Baar, H.J., Boyd, P.W., Coale, K.H., Landry, M.R., Tsuda, A., Assmy, P., Bakker, D.C., Bozec, Y., Barber, R.T. and Brzezinski, M.A., 2005. Synthesis of iron fertilization experiments: from the iron age in the age of enlightenment. Journal of Geophysical Research: Oceans, 110(C9).

De Jong, J.T.M., Stammerjohn, S.E., Ackley, S.F., Tison, J.L., Mattielli, N. and Schoemann, V., 2015. Sources and fluxes of dissolved iron in the Bellingshausen Sea (West Antarctica): The importance of sea ice, icebergs and the continental margin. Marine Chemistry, 177: 518-535.

De La Rocha, C., 2006. 8.4 - The Biological Pump, The oceans and marine geochemistry. Elsevier, Oxford, pp. 83.

De Serrano, L.O., Camper, A.K. and Richards, A.M., 2016. An overview of siderophores for iron acquisition in microorganisms living in the extreme. BioMetals, 29(4): 551-571.

Decho, A.W. and Gutierrez, T., 2017. Microbial Extracellular Polymeric Substances (EPSs) in Ocean Systems. Frontiers in Microbiology, 8(922).

Duarte, C.M., Regaudie-de-Gioux, A., Arrieta, J.M., Delgado-Huertas, A. and Agustí, S., 2013. The oligotrophic ocean is heterotrophic.

Ducklow, H. and Kirchman, D., 2000. Bacterial Production and Biomass in the Oceans.

Dulaquais, G., Waeles, M., Gerringa, L.J., Middag, R., Rijkenberg, M.J. and Riso, R., 2018. The biogeochemistry of electroactive humic substances and its connection to iron chemistry in the North East Atlantic and the Western Mediterranean Sea. Journal of Geophysical Research: Oceans, 123(8): 5481-5499.

Ekwurzel, B., Schlosser, P., Mortlock, R.A., Fairbanks, R.G. and Swift, J.H., 2001. River runoff, sea ice meltwater, and Pacific water distribution and mean residence times in the Arctic Ocean. Journal of Geophysical Research: Oceans, 106(C5): 9075-9092.

Field, C.B., Behrenfeld, M.J., Randerson, J.T. and Falkowski, P., 1998. Primary Production of the Biosphere: Integrating Terrestrial and Oceanic Components. Science, 281(5374): 237-240.

Filella, M. and Town, R.M., 2000. Determination of metal ion binding parameters for humic substances: part 1. Application of a simple calculation method for extraction of meaningful parameters from reverse pulse polarograms. Journal of electroanalytical chemistry, 485(1): 21-33.

Fischer, A.C., Kroon, J.J., Verburg, T.G., Teunissen, T. and Wolterbeek, H.T., 2007. On the relevance of iron adsorption to container materials in small-volume experiments on iron marine chemistry: 55Fe-aided assessment of capacity, affinity and kinetics. Marine Chemistry, 107(4): 533-546.

Fitzsimmons, J.N., Bundy, R.M., Al-Subiai, S.N., Barbeau, K.A. and Boyle, E.A., 2015. The composition of dissolved iron in the dusty surface ocean: An exploration using size-fractionated iron-binding ligands. Marine Chemistry, 173: 125-135.

Fuqua, C. and Greenberg, E.P., 2002. Listening in on bacteria: acyl-homoserine lactone signalling. Nature Reviews Molecular Cell Biology, 3: 685.

Gall, M. and Zeldis, J., 2011. Phytoplankton biomass and primary production responses to physico-chemical forcing across the northeastern New Zealand continental shelf. Continental Shelf Research, 31(17): 1799-1810.

Gascard, J.-C., Festy, J., le Goff, H., Weber, M., Bruemmer, B., Offermann, M., Doble, M., Wadhams, P., Forsberg, R., Hanson, S., Skourup, H., Gerland, S., Nicolaus, M., Metaxian, J.-P., Grangeon, J., Haapala, J., Rinne, E., Haas, C., Wegener, A., Heygster, G., Jakobson, E., Palo, T., Wilkinson, J., Kaleschke, L., Claffey, K., Elder, B. and Bottenheim, J., 2008. Exploring Arctic Transpolar Drift During Dramatic Sea Ice Retreat. Eos, Transactions American Geophysical Union, 89(3): 21-22.

Geider, R.J. and La Roche, J., 1994. The role of iron in phytoplankton photosynthesis, and the potential for iron-limitation of primary productivity in the sea. Photosynthesis research, 39(3): 275-301.

Genovese, C., Grotti, M., Pittaluga, J., Ardini, F., Janssens, J., Wuttig, K., Moreau, S. and Lannuzel, D., 2018. Influence of organic complexation on dissolved iron distribution in East Antarctic pack ice. Marine Chemistry, 203: 28-37.

Gerringa, L., Laan, P., Arrigo, K., van Dijken, G. and Alderkamp, A.-C., 2019. The organic complexation of iron in the Ross sea. Marine Chemistry: 103672.

Gerringa, L.J., Rijkenberg, M.J., Thuróczy, C.-E. and Maas, L.R., 2014. A critical look at the calculation of the binding characteristics and concentration of iron complexing ligands in seawater with suggested improvements. Environmental Chemistry, 11(2): 114-136.

Gerringa, L.J.A., Blain, S., Laan, P., Sarthou, G., Veldhuis, M.J.W., Brussaard, C.P.D., Viollier, E. and Timmermans, K.R., 2008. Fe-binding dissolved organic ligands near the Kerguelen Archipelago in the Southern Ocean (Indian sector). Deep Sea Research Part II: Topical Studies in Oceanography, 55(5): 606-621.

Gerringa, L.J.A., Gledhill, M., Ardiningsih, I., Muntjewerf, N. and Laglera, L., in review. Comparing CLE-AdCSV applications using SA and TAC to determine the Fe binding characteristics of model ligands in seawater. Biogeosciences.

Gerringa, L.J.A., Rijkenberg, M.J.A., Bown, J., Margolin, A.R., Laan, P. and de Baar, H.J.W., 2016. Fe-Binding Dissolved Organic Ligands in the Oxic and Suboxic Waters of the Black Sea. 3(84).

Gerringa, L.J.A., Rijkenberg, M.J.A., Schoemann, V., Laan, P. and de Baar, H.J.W., 2015. Organic complexation of iron in the West Atlantic Ocean. Marine Chemistry, 177: 434-446.

Gerringa, L.J.A., Rijkenberg, M.J.A., Wolterbeek, H.T., Verburg, T.G., Boye, M. and de Baar, H.J.W., 2007. Kinetic study reveals weak Fe-binding ligand, which affects the solubility of Fe in the Scheldt estuary. Marine Chemistry, 103(1): 30-45.

Gledhill, M., Achterberg, E.P., Li, K., Mohamed, K.N. and Rijkenberg, M.J.A., 2015. Influence of ocean acidification on the complexation of iron and copper by organic ligands in estuarine waters. Marine Chemistry, 177: 421-433.

Gledhill, M. and Buck, K., 2012. The organic complexation of iron in the marine environment: A review. Frontiers in Microbiology, 3: 69.

Gledhill, M. and Gerringa, L.J.A., 2017. The Effect of Metal Concentration on the Parameters Derived from Complexometric Titrations of Trace Elements in Seawater—A Model Study. Frontiers in Marine Science, 4: 254.

Gledhill, M., McCormack, P., Ussher, S., Achterberg, E.P., Mantoura, R.F.C. and Worsfold, P.J., 2004. Production of siderophore type chelates by mixed bacterioplankton populations in nutrient enriched seawater incubations. Marine Chemistry, 88(1-2): 75-83.

Gledhill, M. and van den Berg, C.M.G., 1994. Determination of complexation of iron(III) with natural organic complexing ligands in seawater using cathodic stripping voltammetry. Marine Chemistry, 47(1): 41-54.

Gordienko, P.A. and Laktionov, A.F., 1969. Section 3.3 - Circulation and physics of the Arctic basin waters. In: A.L. Gordon and F.W.G. Baker (Editors), Oceanography. Pergamon, pp. 94-112.

Granger, J. and Price, N.M., 1999. The importance of siderophores in iron nutrition of heterotrophic marine bacteria. 44(3): 541-555.

Greig, M.J., 1990. Circulation in the Hauraki Gulf, New Zealand. New Zealand Journal of Marine and Freshwater Research, 24(1): 141-150.

Grotov, A.S., Nechaev, D.A., Panteleev, G.G. and Yaremchuk, M.I., 1998. Large scale circulation in the Bellingshausen and Amundsen seas as a variational inverse of climatological data. Journal of Geophysical Research: Oceans, 103(C6): 13011-13022.

Gustafsson, J.P., 2012. The chemical speciation program visual MINTEQ version 3.0.

Hans-Peter, G. and Meinhard, S., 2007. Interactions of planktonic algae and bacteria: effects on algal growth and organic matter dynamics. Aquatic Microbial Ecology, 47(2): 163-176.

Hassler, C., Cabanes, D., Blanco-Ameijeiras, S., Sander, S.G. and Benner, R., 2020. Importance of refractory ligands and their photodegradation for iron oceanic inventories and cycling. Marine and Freshwater Research, 71(3): 311-320.

Hassler, C.S., Alasonati, E., Mancuso Nichols, C.A. and Slaveykova, V.I., 2011. Exopolysaccharides produced by bacteria isolated from the pelagic Southern Ocean — Role in Fe binding, chemical reactivity, and bioavailability. Marine Chemistry, 123(1–4): 88-98.

Hassler, C.S., Norman, L., Nichols, C.A.M., Clementson, L.A., Robinson, C., Schoemann, V., Watson, R.J. and Doblin, M.A., 2015. Iron associated with exopolymeric substances is highly bioavailable to oceanic phytoplankton. Marine Chemistry, 173: 136-147.

Hassler, C.S., van den Berg, C.M.G. and Boyd, P.W., 2017. Toward a Regional Classification to Provide a More Inclusive Examination of the Ocean Biogeochemistry of Iron-Binding Ligands. Frontiers in Marine Science, 4: 19.

Hawkes, J.A., Connelly, D.P., Gledhill, M. and Achterberg, E.P., 2013. The stabilisation and transportation of dissolved iron from high temperature hydrothermal vent systems. Earth and Planetary Science Letters, 375: 280-290.

Henley, S.F., Schofield, O.M., Hendry, K.R., Schloss, I.R., Steinberg, D.K., Moffat, C., Peck, L.S., Costa, D.P., Bakker, D.C.E., Hughes, C., Rozema, P.D., Ducklow, H.W., Abele, D., Stefels, J., Van Leeuwe, M.A., Brussaard, C.P.D., Buma, A.G.J., Kohut, J., Sahade, R., Friedlaender, A.S., Stammerjohn, S.E., Venables, H.J. and Meredith, M.P., 2019. Variability and change in the west Antarctic

Peninsula marine system: Research priorities and opportunities. Progress in Oceanography, 173: 208-237.

Hoagland, K.D., Rosowski, J.R., Gretz, M.R. and Roemer, S.C., 1993. Diatom extracellular polymeric substances: function, fine structure, chemistry, and physiology. Journal of phycology, 29(5): 537-566.

Hofmann, E.E. and Klinck, J.M., 1998. Thermohaline variability of the waters overlying the west Antarctic Peninsula continental shelf. Ocean, Ice, and Atmosphere: Interactions at the Antarctic Continental Margin, Antarct. Res. Ser, 75: 67-81.

Hogle, S.L., Bundy, R.M., Blanton, J.M., Allen, E.E. and Barbeau, K.A., 2016. Copiotrophic marine bacteria are associated with strong iron-binding ligand production during phytoplankton blooms. Limnology and Oceanography Letters, 1(1): 36-43.

Hopkinson, B.M. and Morel, F.M.M., 2009. The role of siderophores in iron acquisition by photosynthetic marine microorganisms. BioMetals, 22(4): 659-669.

Hopwood, M.J., Carroll, D., Browning, T.J., Meire, L., Mortensen, J., Krisch, S. and Achterberg, E.P., 2018. Non-linear response of summertime marine productivity to increased meltwater discharge around Greenland. Nature Communications, 9(1): 3256.

Hudson, R.J.M., Covault, D.T. and Morel, F.M.M., 1992. Investigations of iron coordination and redox reactions in seawater using 59Fe radiometry and ion-pair solvent extraction of amphiphilic iron complexes. Marine Chemistry, 38(3): 209-235.

Hudson, R.J.M., Rue, E.L. and Bruland, K.W., 2003. Modeling Complexometric Titrations of Natural Water Samples. Environmental Science & Technology, 37(8): 1553-1562.

Hunter, K.A. and Boyd, P.W., 2007. Iron-binding ligands and their role in the ocean biogeochemistry of iron. 4(4): 221-232.

Hutchins, D.A. and Bruland, K.W., 1998. Iron-limited diatom growth and Si:N uptake ratios in a coastal upwelling regime. Nature, 393(6685): 561-564.

Ibisanmi, E., Sander, S.G., Boyd, P.W., Bowie, A.R. and Hunter, K.A., 2011. Vertical distributions of iron-(III) complexing ligands in the Southern Ocean. Deep Sea Research Part II: Topical Studies in Oceanography, 58(21–22): 2113-2125.

IPCC, 2014. Climate Change 2014: Synthesis Report. Contribution of Working Groups I, II and III to the Fifth Assessment Report of the Intergovernmental Panel on Climate Change [Core Writing Team, R.K. Pachauri and L.A. Meyer (eds.)]. (IPCC, Geneva, Switzerland,): 151 pp.

Jensen, L.T., Wyatt, N.J., Landing, W.M. and Fitzsimmons, J.N., 2020. Assessment of the stability, sorption, and exchangeability of marine dissolved and colloidal metals. Marine Chemistry, 220: 103754.

Johnson, K.S., Gordon, R.M. and Coale, K.H., 1997. What controls dissolved iron concentrations in the world ocean? Marine Chemistry, 57(3): 137-161.

Joy-Warren, H.L., van Dijken, G.L., Alderkamp, A.-C., Leventer, A., Lewis, K.M., Selz, V., Lowry, K.E., van de Poll, W. and Arrigo, K.R., 2019. Light Is the Primary Driver of Early Season Phytoplankton Production Along the Western Antarctic Peninsula. Journal of Geophysical Research: Oceans, 124(11): 7375-7399.

Kanzow, T., 2017. The Expedition PS100 of the Research Vessel POLARSTERN to the Fram Strait in 2016. 1866-3192.

Karen, E.S. and Gerhard, J.H., 1999. Production of exopolymer particles by marine bacterioplankton under contrasting turbulence conditions. Marine Ecology Progress Series, 189: 9-16.

King, A.L., Buck, K.N. and Barbeau, K.A., 2012. Quasi-Lagrangian drifter studies of iron speciation and cycling off Point Conception, California. Marine Chemistry, 128-129: 1-12.

Kinsey, J.D., Kieber, D.J. and Neale, P.J., 2016. Effects of iron limitation and UV radiation on Phaeocystis antarctica growth and dimethylsulfoniopropionate, dimethylsulfoxide and acrylate concentrations. Environmental Chemistry, 13(2): 195-211.

Kleint, C., 2016. The speciation and organic complexation of iron (Fe) and copper (Cu) in different marine hydrothermal vent systems, Doctoral dissertation, University of Bremen, Germany.

Kleint, C., Hawkes, J.A., Sander, S.G. and Koschinsky, A., 2016. Voltammetric Investigation of Hydrothermal Iron Speciation. Frontiers in Marine Science, 3(75).

Klinck, J.M., Hofmann, E.E., Beardsley, R.C., Salihoglu, B. and Howard, S., 2004. Water-mass properties and circulation on the west Antarctic Peninsula Continental Shelf in Austral Fall and Winter 2001. Deep Sea Research Part II: Topical Studies in Oceanography, 51(17): 1925-1946.

Klunder, M.B., Bauch, D., Laan, P., de Baar, H.J.W., Van Heuven, S. and Ober, S., 2012. Dissolved iron in the Arctic shelf seas and surface waters of the central Arctic Ocean: Impact of Arctic river water and ice-melt. Journal of Geophysical Research: Oceans, 117(C1).

Klunder, M.B., Laan, P., Middag, R., De Baar, H.J.W. and van Ooijen, J.C., 2011. Dissolved iron in the Southern Ocean (Atlantic sector). Deep Sea Research Part II: Topical Studies in Oceanography, 58(25): 2678-2694.

Kondo, Y., Takeda, S. and Furuya, K., 2007. Distribution and speciation of dissolved iron in the Sulu Sea and its adjacent waters. Deep Sea Research Part II: Topical Studies in Oceanography, 54(1): 60-80.

Krachler, R., Krachler, R.F., Wallner, G., Hann, S., Laux, M., Cervantes Recalde, M.F., Jirsa, F., Neubauer, E., von der Kammer, F., Hofmann, T. and Keppler, B.K., 2015. River-derived humic substances as iron chelators in seawater. Marine Chemistry, 174: 85-93.

Krembs, C., Eicken, H., Junge, K. and Deming, J.W., 2002. High concentrations of exopolymeric substances in Arctic winter sea ice: implications for the polar ocean carbon cycle and cryoprotection of diatoms. Deep Sea Research Part I: Oceanographic Research Papers, 49(12): 2163-2181.

Krisch, S., Browning, T.J., Graeve, M., Ludwichowski, K.-U., Lodeiro, P., Hopwood, M.J., Roig, S., Yong, J.-C., Kanzow, T. and Achterberg, E.P., 2020. The influence of Arctic Fe and Atlantic fixed N on summertime primary production in Fram Strait, North Greenland Sea. Scientific Reports, 10(1): 15230.

Krisch, S., Hopwood, M.J., Schaffer, J., Al-Hashem, A., Höfer, J., Rutgers van der Loeff, M.M., Conway, T.M., Summers, B.A., Lodeiro, P., Ardiningsih, I., Steffens, T. and Achterberg, E.P., 2021. The 79°N Glacier cavity modulates subglacial iron export to the NE Greenland Shelf. Nature Communications, 12(1): 3030.

Kuma, K., Nishioka, J. and Matsunaga, K., 1996. Controls on iron(III) hydroxide solubility in seawater: The influence of pH and natural organic chelators. Limnology and Oceanography, 41(3): 396-407.

Laglera, L.M., Battaglia, G. and van den Berg, C.M.G., 2007. Determination of humic substances in natural waters by cathodic stripping voltammetry of their complexes with iron. Analytica Chimica Acta, 599(1): 58-66.

Laglera, L.M., Battaglia, G. and van den Berg, C.M.G., 2011. Effect of humic substances on the iron speciation in natural waters by CLE/CSV. Marine Chemistry, 127(1): 134-143.

Laglera, L.M. and Filella, M., 2015. The relevance of ligand exchange kinetics in the measurement of iron speciation by CLE–AdCSV in seawater. Marine Chemistry, 173: 100-113.

Laglera, L.M., Sukekava, C.F., Slagter, H.A., Downes, J., Aparicio-Gonzalez, A. and Gerringa, L.J., 2019a. First Quantification of the Controlling Role of Humic Substances in the Transport of Iron Across the Surface of the Arctic Ocean. Environmental science & technology, 53(22): 13136-13145.

Laglera, L.M., Tovar-Sanchez, A., Sukekava, C.F., Naik, H., Naqvi, S.W.A. and Wolf-Gladrow, D.A., 2019b. Iron organic speciation during the LOHAFEX experiment: Iron ligands release under biomass control by copepod grazing. Journal of Marine Systems, 207: 103151.

Laglera, L.M. and van den Berg, C.M.G., 2009. Evidence for geochemical control of iron by humic substances in seawater. Limnology and Oceanography, 54(2): 610-619.

Lam, P.J., Doney, S.C. and Bishop, J.K.B., 2011. The dynamic ocean biological pump: Insights from a global compilation of particulate organic carbon, CaCO3, and opal concentration profiles from the mesopelagic. Global Biogeochemical Cycles, 25: 3.

Lannuzel, D., Grotti, M., Abelmoschi, M.L. and van der Merwe, P., 2015. Organic ligands control the concentrations of dissolved iron in Antarctic sea ice. Marine Chemistry, 174: 120-130.

Lannuzel, D., Vancoppenolle, M., van der Merwe, P., de Jong, J.T.M., Meiners, K.M., Grotti, M., Nishioka, J. and Schoemann, V., 2016. Iron in sea ice: Review and new insights. Elem. Sci. Anth., 4.

Lauderdale, J.M., Braakman, R., Forget, G., Dutkiewicz, S. and Follows, M.J., 2020. Microbial feedbacks optimize ocean iron availability. Proceedings of the National Academy of Sciences, 117(9): 4842-4849.

Laukert, G., Frank, M., Bauch, D., Hathorne, E.C., Rabe, B., von Appen, W.-J., Wegner, C., Zieringer, M. and Kassens, H., 2017. Ocean circulation and freshwater pathways in the Arctic Mediterranean based on a combined Nd isotope, REE and oxygen isotope section across Fram Strait. Geochimica et Cosmochimica Acta, 202: 285-309.

Le Quéré, C., Andrew, R.M., Canadell, J.G., Sitch, S., Korsbakken, J.I., Peters, G.P., Manning, A.C., Boden, T.A., Tans, P.P., Houghton, R.A., Keeling, R.F., Alin, S., Andrews, O.D., Anthoni, P., Barbero, L., Bopp, L., Chevallier, F., Chini, L.P., Ciais, P., Currie, K., Delire, C., Doney, S.C., Friedlingstein, P., Gkritzalis, T., Harris, I., Hauck, J., Haverd, V., Hoppema, M., Klein Goldewijk, K., Jain,

A.K., Kato, E., Körtzinger, A., Landschützer, P., Lefèvre, N., Lenton, A., Lienert, S., Lombardozzi, D., Melton, J.R., Metzl, N., Millero, F., Monteiro, P.M.S., Munro, D.R., Nabel, J.E.M.S., Nakaoka, S., O'Brien, K., Olsen, A., Omar, A.M., Ono, T., Pierrot, D., Poulter, B., Rödenbeck, C., Salisbury, J., Schuster, U., Schwinger, J., Séférian, R., Skjelvan, I., Stocker, B.D., Sutton, A.J., Takahashi, T., Tian, H., Tilbrook, B., van der Laan-Luijkx, I.T., van der Werf, G.R., Viovy, N., Walker, A.P., Wiltshire, A.J. and Zaehle, S., 2016. Global Carbon Budget 2016. Earth Syst. Sci. Data, 8(2): 605-649.

Lelong, A., Bucciarelli, E., Hégaret, H. and Soudant, P., 2013. Iron and copper limitations differently affect growth rates and photosynthetic and physiological parameters of the marine diatom Pseudo-nitzschia delicatissima. Limnology and Oceanography, 58(2): 613-623.

Lin, H. and Twining, B.S., 2012. Chemical speciation of iron in Antarctic waters surrounding free-drifting icebergs. Marine Chemistry, 128-129: 81-91.

Lippiatt, S.M., Lohan, M.C. and Bruland, K.W., 2010. The distribution of reactive iron in northern Gulf of Alaska coastal waters. Marine Chemistry, 121(1): 187-199.

Lis, H., Shaked, Y., Kranzler, C., Keren, N. and Morel, F.M., 2015. Iron bioavailability to phytoplankton: an empirical approach. The ISME journal, 9(4): 1003-1013.

Liu, X. and Millero, F.J., 1999. The solubility of iron hydroxide in sodium chloride solutions. Geochimica et Cosmochimica Acta, 63(19): 3487-3497.

Liu, X. and Millero, F.J., 2002. The solubility of iron in seawater. Marine Chemistry, 77(1): 43-54.

Lodeiro, P., Rey-Castro, C., David, C., Achterberg, E.P., Puy, J. and Gledhill, M., 2020. Acid-base properties of dissolved organic matter extracted from the marine environment. Science of The Total Environment, 729: 138437.

Lohan, M.C., Buck, K.N. and Sander, S.G., 2015. Organic ligands - A key control on trace metal biogeochemistry in the oceans. Marine Chemistry, 173: 1-2.

Longnecker, K., Kido Soule, M.C. and Kujawinski, E.B., 2015. Dissolved organic matter produced by Thalassiosira pseudonana. Marine Chemistry, 168: 114-123.

Macrellis, H.M., Trick, C.G., Rue, E.L., Smith, G. and Bruland, K.W., 2001. Collection and detection of natural iron-binding ligands from seawater. Marine Chemistry, 76(3): 175-187.

Mahmood, A., Abualhaija, M.M., van den Berg, C.M.G. and Sander, S.G., 2015. Organic speciation of dissolved iron in estuarine and coastal waters at multiple analytical windows. Marine Chemistry, 177: 706-719.

Maldonado, M.T. and Price, N.M., 1999. Utilization of iron bound to strong organic ligands by plankton communities in the subarctic Pacific Ocean. Deep Sea Research Part II: Topical Studies in Oceanography, 46(11-12): 2447-2473.

Maldonado, M.T., Strzepek, R.F., Sander, S. and Boyd, P.W., 2005. Acquisition of iron bound to strong organic complexes, with different Fe binding groups and photochemical reactivities, by plankton communities in Fe-limited subantarctic waters. Global Biogeochemical Cycles, 19: 4.

Marañón, E., Behrenfeld, M.J., González, N., Mouriño, B. and Zubkov, M.V., 2003. High variability of primary production in oligotrophic waters of the Atlantic Ocean: uncoupling from phytoplankton biomass and size structure. Marine Ecology Progress Series, 257: 1-11.

Martin, J.H., 1990. Glacial-interglacial CO2 change: The iron hypothesis. Paleoceanography, 5(1): 1-13.

Martin, J.H. and Fitzwater, S.E., 1988. Iron deficiency limits phytoplankton growth in the north-east Pacific subarctic. Nature, 331(6154): 341-343.

Martin, J.H., Gordon, M. and Fitzwater, S.E., 1991. The case for iron. Limnology and Oceanography, 36(8): 1793-1802.

Mawji, E., Gledhill, M., Milton, J.A., Tarran, G.A., Ussher, S., Thompson, A., Wolff, G.A., Worsfold, P.J. and Achterberg, E.P., 2008. Hydroxamate Siderophores: Occurrence and Importance in the Atlantic Ocean. Environmental Science & Technology, 42(23): 8675-8680.

Mawji, E., Gledhill, M., Milton, J.A., Zubkov, M.V., Thompson, A., Wolff, G.A. and Achterberg, E.P., 2011. Production of siderophore type chelates in Atlantic Ocean waters enriched with different carbon and nitrogen sources. Marine Chemistry, 124(1–4): 90-99.

McKay, R.M.L., Wilhelm, S.W., Hall, J., Hutchins, D.A., Al-Rshaidat, M.M.D., Mioni, C.E., Pickmere, S., Porta, D. and Boyd, P.W., 2005. Impact of phytoplankton on the biogeochemical cycling of iron in subantarctic waters southeast of New Zealand during FeCycle. Global Biogeochemical Cycles, 19(4).

Measures, C.I., 1999. The role of entrained sediments in sea ice in the distribution of aluminium and iron in the surface waters of the Arctic Ocean. Marine Chemistry, 68(1): 59-70.

Meier, W.N., Hovelsrud, G.K., van Oort, B.E.H., Key, J.R., Kovacs, K.M., Michel, C., Haas, C., Granskog, M.A., Gerland, S., Perovich, D.K., Makshtas, A. and Reist, J.D., 2014. Arctic sea ice in transformation: A review of recent observed changes and impacts on biology and human activity. Reviews of Geophysics, 52(3): 185-217.

Middag, R., De Baar, H., Laan, P. and Bakker, K., 2009. Dissolved aluminium and the silicon cycle in the Arctic Ocean. Marine Chemistry, 115(3-4): 176-195.

Middag, R., de Baar, H.J.W., Bruland, K.W. and van Heuven, S.M.A.C., 2020. The Distribution of Nickel in the West-Atlantic Ocean, Its Relationship With Phosphate and a Comparison to Cadmium and Zinc. Frontiers in Marine Science, 7: 105.

Middag, R., de Baar, H.J.W., Klunder, M.B. and Laan, P., 2013. Fluxes of dissolved aluminum and manganese to the Weddell Sea and indications for manganese co-limitation. Limnology and Oceanography, 58(1): 287-300.

Mikaloff Fletcher, S., Gruber, N., Jacobson, A.R., Doney, S., Dutkiewicz, S., Gerber, M., Follows, M., Joos, F., Lindsay, K. and Menemenlis, D., 2006. Inverse estimates of anthropogenic CO2 uptake, transport, and storage by the ocean. Global biogeochemical cycles, 20: 2.

Miller, L.A. and Bruland, K.W., 1997. Competitive equilibration techniques for determining transition metal speciation in natural waters: Evaluation using model data. Analytica Chimica Acta, 343(3): 161-181.

Millero, F.J., 1998. Solubility of Fe(III) in seawater. Earth and Planetary Science Letters, 154(1-4): 323-329.

Millero, F.J., Huang, F. and Laferiere, A.L., 2002. The solubility of oxygen in the major sea salts and their mixtures at 25°C. Geochimica et Cosmochimica Acta, 66(13): 2349-2359.

Millero, F.J., Yao, W. and Aicher, J., 1995. The speciation of Fe(II) and Fe(III) in natural waters. Marine Chemistry, 50(1): 21-39.

Moffat, C. and Meredith, M., 2018. Shelf-ocean exchange and hydrography west of the Antarctic Peninsula: a review. Philosophical Transactions of the Royal Society A: Mathematical, Physical and Engineering Sciences, 376(2122): 20170164.

Mohamed, K.N., Steigenberger, S., Nielsdottir, M.C., Gledhill, M. and Achterberg, E.P., 2011. Dissolved iron(III) speciation in the high latitude North Atlantic Ocean. Deep Sea Research Part I: Oceanographic Research Papers, 58(11): 1049-1059.

Moore, C.M., Mills, M.M., Arrigo, K.R., Berman-Frank, I., Bopp, L., Boyd, P.W., Galbraith, E.D., Geider, R.J., Guieu, C., Jaccard, S.L., Jickells, T.D., La Roche, J., Lenton, T.M., Mahowald, N.M., Maranon, E., Marinov, I., Moore, J.K., Nakatsuka, T., Oschlies, A., Saito, M.A., Thingstad, T.F., Tsuda, A. and Ulloa, O., 2013. Processes and patterns of oceanic nutrient limitation. Nature Geosci, 6(9): 701-710.

Mopper, K., Kieber, D.J. and Stubbins, A., 2015. Chapter 8 - Marine Photochemistry of Organic Matter: Processes and Impacts. In: D.A. Hansell and C.A. Carlson (Editors), Biogeochemistry of Marine Dissolved Organic Matter (Second Edition). Academic Press, Boston, pp. 389-450.

Morel, F.M.M. and Price, N.M., 2003. The Biogeochemical Cycles of Trace Metals in the Oceans. 300(5621): 944-947.

Nelson, D.M., Tréguer, P., Brzezinski, M.A., Leynaert, A. and Quéguiner, B., 1995. Production and dissolution of biogenic silica in the ocean: Revised global estimates, comparison with regional data and relationship to biogenic sedimentation. Global Biogeochemical Cycles, 9(3): 359-372.

Nielsdóttir, M.C., Moore, C.M., Sanders, R., Hinz, D.J. and Achterberg, E.P., 2009. Iron limitation of the postbloom phytoplankton communities in the Iceland Basin. Global Biogeochemical Cycles, 23(3).

Nolting, R.F., Gerringa, L.J.A., Swagerman, M.J.W., Timmermans, K.R. and de Baar, H.J.W., 1998. Fe (III) speciation in the high nutrient, low chlorophyll Pacific region of the Southern Ocean. Marine Chemistry, 62(3): 335-352.

Norman, L., Thomas, D.N., Stedmon, C.A., Granskog, M.A., Papadimitriou, S., Krapp, R.H., Meiners, K.M., Lannuzel, D., van der Merwe, P. and Dieckmann, G.S., 2011. The characteristics of dissolved organic matter (DOM) and chromophoric dissolved organic matter (CDOM) in Antarctic sea ice. Deep Sea Research Part II: Topical Studies in Oceanography, 58(9-10): 1075-1091.

Norman, L., Worms, I.A.M., Angles, E., Bowie, A.R., Nichols, C.M., Ninh Pham, A., Slaveykova, V.I., Townsend, A.T., David Waite, T. and Hassler, C.S., 2015. The role of bacterial and algal exopolymeric substances in iron chemistry. Marine Chemistry, 173: 148-161.

Omanović, D., Garnier, C. and Pižeta, I., 2015. ProMCC: An all-in-one tool for trace metal complexation studies. Marine Chemistry, 173: 25-39.

Orellana, M.V., Lessard, E.J., Dycus, E., Chin, W.-C., Foy, M.S. and Verdugo, P., 2003. Tracing the source and fate of biopolymers in seawater: application of an immunological technique. Marine chemistry, 83(1-2): 89-99.

Orsi, A.H., Whitworth, T. and Nowlin, W.D., 1995. On the meridional extent and fronts of the Antarctic Circumpolar Current. Deep Sea Research Part I: Oceanographic Research Papers, 42(5): 641-673.

Pakulski, J.D. and Benner, R., 1994. Abundance and distribution of carbohydrates in the ocean. Limnology and Oceanography, 39(4): 930-940.

Paris, R. and Desboeufs, K.V., 2013. Effect of atmospheric organic complexation on iron-bearing dust solubility. Atmospheric Chemistry and Physics, 13: 4895-4905.

Parsons, T.M., Y.; Lalli, C., 1984. A Manual of Chemical and Biological Methods for Seawater Analysis. Pergamon Press, Oxford.

Paul, C., Barofsky, A., Vidoudez, C. and Pohnert, G., 2009. Diatom exudates influence metabolism and cell growth of co-cultured diatom species. Marine Ecology Progress Series, 389: 61-70.

Paulsen, M.L., Nielsen, S.E.B., Müller, O., Møller, E.F., Stedmon, C.A., Juul-Pedersen, T., Markager, S., Sejr, M.K., Delgado Huertas, A., Larsen, A. and Middelboe, M., 2017. Carbon Bioavailability in a High Arctic Fjord Influenced by Glacial Meltwater, NE Greenland. Frontiers in Marine Science, 4(176).

Pizeta, I., Sander, S.G., Hudson, R.J.M., Omanovic, D., Baars, O., Barbeau, K.A., Buck, K.N., Bundy, R.M., Carrasco, G., Croot, P.L., Garnier, C., Gerringa, L.J.A., Gledhill, M., Hirose, K., Kondo, Y., Laglera, L.M., Nuester, J., Rijkenberg, M.J.A., Takeda, S., Twining, B.S. and Wells, M., 2015. Interpretation of complexometric titration data: An intercomparison of methods for estimating models of trace metal complexation by natural organic ligands. Marine Chemistry, 173: 3-24.

Poorvin, L., Sander, S.G., Velasquez, I., Ibisanmi, E., LeCleir, G.R. and Wilhelm, S.W., 2011. A comparison of Fe bioavailability and binding of a catecholate siderophore with virus-mediated lysates from the marine bacterium Vibrio alginolyticus PWH3a. Journal of Experimental Marine Biology and Ecology, 399(1): 43-47.

Porter, K.G. and Feig, Y.S., 1980. The use of DAPI for identifying and counting aquatic microflora1. 25(5): 943-948.

Poulson-Ellestad, K.L., Jones, C.M., Roy, J., Viant, M.R., Fernández, F.M., Kubanek, J. and Nunn, B.L., 2014. Metabolomics and proteomics reveal impacts of chemically mediated competition on marine plankton. Proceedings of the National Academy of Sciences, 111(24): 9009-9014.

Powell, R.T. and Wilson-Finelli, A., 2003. Photochemical degradation of organic iron complexing ligands in seawater. Aquatic Sciences, 65(4): 367-374.

R Development Core Team, R., 2011. R: A language and environment for statistical computing. R foundation for statistical computing, Vienna, Austria.

Raven, J.A. and Falkowski, P.G., 1999. Oceanic sinks for atmospheric CO2. Plant, Cell & Environment, 22(6): 741-755.

Richter, M.E., von Appen, W.J. and Wekerle, C., 2018. Does the East Greenland Current exist in the northern Fram Strait? Ocean Sci., 14(5): 1147-1165.

Rijkenberg, M.J., Gerringa, L.J., Timmermans, K.R., Fischer, A.C., Kroon, K.J., Buma, A.G., Wolterbeek, B.T. and de Baar, H.J., 2008a. Enhancement of the reactive iron pool by marine diatoms. Marine Chemistry, 109(1-2): 29-44.

Rijkenberg, M.J.A., Powell, C.F., Dall'Osto, M., Nielsdottir, M.C., Patey, M.D., Hill, P.G., Baker, A.R., Jickells, T.D., Harrison, R.M. and Achterberg, E.P., 2008b. Changes in iron speciation following a Saharan dust event in the tropical North Atlantic Ocean. Marine Chemistry, 110(1): 56-67.

Rijkenberg, M.J.A., Slagter, H.A., Rutgers van der Loeff, M., van Ooijen, J. and Gerringa, L.J.A., 2018. Dissolved Fe in the Deep and Upper Arctic Ocean With a Focus on Fe Limitation in the Nansen Basin. 5(88).

Robinson, C., 2019. Microbial Respiration, the Engine of Ocean Deoxygenation. Frontiers in Marine Science, 5(533).

Rudels, B., Björk, G., Nilsson, J., Winsor, P., Lake, I. and Nohr, C., 2005. The interaction between waters from the Arctic Ocean and the Nordic Seas north of Fram Strait and along the East Greenland Current: results from the Arctic Ocean-02 Oden expedition. Journal of Marine Systems, 55(1): 1-30.

Rudels, B., Korhonen, M., Schauer, U., Pisarev, S., Rabe, B. and Wisotzki, A., 2015. Circulation and transformation of Atlantic water in the Eurasian Basin and the contribution of the Fram Strait inflow branch to the Arctic Ocean heat budget. Progress in Oceanography, 132: 128-152.

Rue, E.L. and Bruland, K.W., 1995. Complexation of iron(III) by natural organic ligands in the Central North Pacific as determined by a new competitive ligand equilibration/adsorptive cathodic stripping voltammetric method. Marine Chemistry, 50(1): 117-138.

Rue, E.L. and Bruland, K.W., 1997. The role of organic complexation on ambient iron chemistry in the equatorial Pacific Ocean and the response of a mesoscale iron addition experiment. Limnology and Oceanography, 42(5): 901-910.

Ružić, I., 1982. Theoretical aspects of the direct titration of natural waters and its information yield for trace metal speciation. Analytica Chimica Acta, 140(1): 99-113.

Ryan-Keogh, T.J., Macey, A.I., Nielsdóttir, M.C., Lucas, M.I., Steigenberger, S.S., Stinchcombe, M.C., Achterberg, E.P., Bibby, T.S. and Moore, C.M., 2013. Spatial and temporal development of phytoplankton iron stress in relation to bloom dynamics in the high-latitude North Atlantic Ocean. Limnology and Oceanography, 58(2): 533-545.

Ryan-Keogh, T.J., Thomalla, S.J., Mtshali, T.N., van Horsten, N.R. and Little, H.J., 2018. Seasonal development of iron limitation in the sub-Antarctic zone. Biogeosciences, 15(14): 4647-4660.

Saito, M., Goepfert, T., Noble, A., Bertrand, E., Sedwick, P.N. and DiTullio, G.R., 2010. A Seasonal Study of Dissolved Cobalt in the Ross Sea, Antarctica: Micronutrient Behavior, Absence of Scavenging, and Relationships with Zd, Cd, and P. Biogeosciences, 7(12).

Saito, M.A. and Goepfert, T.J., 2008. Zinc-cobalt colimitation of Phaeocystis antarctica. Limnology and Oceanography, 53(1): 266-275.

Sander, S.G., Hunter, K.A., Harms, H. and Wells, M., 2011a. Numerical Approach to Speciation and Estimation of Parameters Used in Modeling Trace Metal Bioavailability. Environmental Science & Technology, 45(15): 6388-6395.

Sander, S.G. and Koschinsky, A., 2011b. Metal flux from hydrothermal vents increased by organic complexation. Nature Geoscience, 4: 145.

Sander, S.G., Tian, F., Ibisanmi, E.B., Currie, K.I., Hunter, K.A. and Frew, R.D., 2015. Spatial and seasonal variations of iron speciation in surface waters of the Subantarctic front and the Otago Continental Shelf. Marine Chemistry, 173: 114-124.

Sato, M., Takeda, S. and Furuya, K., 2007. Iron regeneration and organic iron(III)-binding ligand production during in situ zooplankton grazing experiment. Marine Chemistry, 106(3): 471-488.

Schaffer, J., von Appen, W.-J., Dodd, P.A., Hofstede, C., Mayer, C., de Steur, L. and Kanzow, T., 2017. Warm water pathways toward Nioghalvfjerdsfjorden Glacier, Northeast Greenland. Journal of Geophysical Research: Oceans, 122(5): 4004-4020.

Schlitzer, R., 2018. Ocean Data View. odv.awi.de.

Schoffman, H., Lis, H., Shaked, Y. and Keren, N., 2016. Iron–Nutrient Interactions within Phytoplankton. Frontiers in Plant Science, 7: 1223.

Schofield, O., Saba, G., Coleman, K., Carvalho, F., Couto, N., Ducklow, H., Finkel, Z., Irwin, A., Kahl, A., Miles, T., Montes-Hugo, M., Stammerjohn, S. and Waite, N., 2017. Decadal variability in coastal phytoplankton community composition in a changing West Antarctic Peninsula. Deep Sea Research Part I: Oceanographic Research Papers, 124: 42-54.

Schuur, E.A.G., McGuire, A.D., Schädel, C., Grosse, G., Harden, J.W., Hayes, D.J., Hugelius, G., Koven, C.D., Kuhry, P., Lawrence, D.M., Natali, S.M., Olefeldt, D., Romanovsky, V.E., Schaefer, K., Turetsky, M.R., Treat, C.C. and Vonk, J.E., 2015. Climate change and the permafrost carbon feedback. Nature, 520: 171.

Sedwick, P.N., DiTullio, G.R. and Mackey, D.J., 2000. Iron and manganese in the Ross Sea, Antarctica: seasonal iron limitation in Antarctic shelf waters. Journal of Geophysical Research: Oceans, 105(C5): 11321-11336.

Seyitmuhammedov, K., 2020. Biogeochemical cycling of trace metals in the shelf regions: importance of cross-shelf exchange, University of Otago, Dunedin.

Seyitmuhammedov, K., Stirling, C.H., Reid, M.R., van Hale, R., Laan, P., Arrigo, K.R., van Dijken, G., Alderkamp, A.-C. and Middag, R., in review. The distribution of Fe across the shelf of the Western Antarctic Peninsula at the start of the phytoplankton growing season. Marine Chemistry.

Sharples, J., 1997. Cross-shelf intrusion of subtropical water into the coastal zone of northeast New Zealand. Continental Shelf Research, 17(7): 835-857.

Sharples, J. and Zeldis, J.R., 2019. Variability of internal tide energy, mixing and nitrate fluxes in response to changes in stratification on the northeast New Zealand continental shelf. New Zealand Journal of Marine and Freshwater Research: 1-18.

Sherrell, R.M., Annett, A.L., Fitzsimmons, J.N., Roccanova, V.J. and Meredith, M.P., 2018. A shallow bathtub ring of local sedimentary iron input maintains the Palmer Deep biological hotspot on the West Antarctic Peninsula shelf. Philosophical Transactions of the Royal Society A: Mathematical, Physical and Engineering Sciences, 376(2122): 20170171.

Shi, X., Wei, L., Hong, Q., Liu, L., Wang, Y., Shi, X., Ye, Y. and Cai, P., 2019. Large benthic fluxes of dissolved iron in China coastal seas revealed by 224Ra/228Th disequilibria. Geochimica et Cosmochimica Acta, 260: 49-61.

Slagter, H.A., Gerringa, L.J.A. and Brussaard, C.P.D., 2016. Phytoplankton Virus Production Negatively Affected by Iron Limitation. Frontiers in Marine Science, 3: 156

Slagter, H.A., Laglera, L.M., Sukekava, C. and Gerringa, L.J.A., 2019. Fe-binding Organic Ligands in the Humic-Rich TransPolar Drift in the Surface Arctic Ocean using Multiple Voltammetric Methods. Journal of Geophysical Research: Oceans, 124(3): 1491-1508.

Slagter, H.A., Reader, H.E., Rijkenberg, M.J.A., Rutgers van der Loeff, M., de Baar, H.J.W. and Gerringa, L.J.A., 2017. Organic Fe speciation in the Eurasian Basins of the Arctic Ocean and its relation to terrestrial DOM. Marine Chemistry, 197: 11-25.

Smith, D.A., Hofmann, E.E., Klinck, J.M. and Lascara, C.M., 1999. Hydrography and circulation of the West Antarctic Peninsula Continental Shelf. Deep Sea Research Part I: Oceanographic Research Papers, 46(6): 925-949.

Smith Jr., W.O., Baumann, M.E.M., Wilson, D.L. and Aletsee, L., 1987. Phytoplankton biomass and productivity in the marginal ice zone of the Fram Strait during summer 1984. 92(C7): 6777-6786.

Soria-Dengg, S., Reissbrodt, R. and Horstmann, U., 2001. Siderophores in marine coastal waters and their relevance for iron uptake by phytoplankton: Experiments with the diatom Phaeodactylum tricornutum. Marine Ecology Progress Series, 220: 73-82.

Stammerjohn, S., Massom, R., Rind, D. and Martinson, D., 2012. Regions of rapid sea ice change: An inter-hemispheric seasonal comparison. Geophysical Research Letters, 39(6).

Su, H., Yang, R., Li, Y. and Wang, X., 2018. Influence of humic substances on iron distribution in the East China Sea. Chemosphere, 204: 450-462.

Su, H., Yang, R., Zhang, A. and Li, Y., 2015. Dissolved iron distribution and organic complexation in the coastal waters of the East China Sea. Marine Chemistry, 173: 208-221.

Suggett, D.J., Moore, C.M., Hickman, A.E. and Geider, R.J., 2009. Interpretation of fast repetition rate (FRR) fluorescence: signatures of phytoplankton community structure versus physiological state. Marine Ecology Progress Series, 376: 1-19.

Sukekava, C., Downes, J., Slagter, H.A., Gerringa, L.J.A. and Laglera, L.M., 2018. Determination of the contribution of humic substances to iron complexation in seawater by catalytic cathodic stripping voltammetry. Talanta, 189: 359-364.

Sunda, W., 2012. Feedback Interactions between Trace Metal Nutrients and Phytoplankton in the Ocean. Frontiers in Microbiology, 3(204).

Sunda, W.G., 1989. Trace metal interactions with marine phytoplankton. Biological Oceanography, 6(5-6): 411-442.

Sunda, W.G. and Huntsman, S.A., 1995. Iron uptake and growth limitation in oceanic and coastal phytoplankton. Marine Chemistry, 50(1): 189-206.

Sutton, P.J.H., 2003. The Southland Current: A subantarctic current. New Zealand Journal of Marine and Freshwater Research, 37(3): 645-652.

Swift, J.H. and Aagaard, K., 1981. Seasonal transitions and water mass formation in the Iceland and Greenland seas. Deep Sea Research Part A. Oceanographic Research Papers, 28(10): 1107-1129.

Takeda, S., 1998. Influence of iron availability on nutrient consumption ratio of diatoms in oceanic waters. Nature, 393(6687): 774-777.

Tani, H., Nishioka, J., Kuma, K., Takata, H., Yamashita, Y., Tanoue, E. and Midorikawa, T., 2003. Iron(III) hydroxide solubility and humic-type fluorescent organic matter in the deep water column of the Okhotsk Sea and the northwestern North

Pacific Ocean. Deep Sea Research Part I: Oceanographic Research Papers, 50(9): 1063-1078.

Teetor, P., 2011. R Cookbook. O'Reilly Media, Inc.

Thingstad, T.F., Skjoldal, E.F. and Bohne, R.A., 1993. Phosphorus cycling and algal-bacterial competition in Sandsfjord, western Norway. Marine Ecology Progress Series, 99(3): 239-259.

Thuróczy, C.-E., Alderkamp, A.-C., Laan, P., Gerringa, L.J.A., Mills, M.M., Van Dijken, G.L., De Baar, H.J.W. and Arrigo, K.R., 2012. Key role of organic complexation of iron in sustaining phytoplankton blooms in the Pine Island and Amundsen Polynyas (Southern Ocean). Deep Sea Research Part II: Topical Studies in Oceanography, 71-76: 49-60.

Thuróczy, C.-E., Gerringa, L.J.A., Klunder, M., Laan, P., Le Guitton, M. and de Baar, H.J.W., 2011a. Distinct trends in the speciation of iron between the shallow shelf seas and the deep basins of the Arctic Ocean. 116(C10).

Thuróczy, C.E., Gerringa, L.J.A., Klunder, M.B., Laan, P. and de Baar, H.J.W., 2011b. Observation of consistent trends in the organic complexation of dissolved iron in the Atlantic sector of the Southern Ocean. Deep Sea Research Part II: Topical Studies in Oceanography, 58(25): 2695-2706.

Thuróczy, C.E., Gerringa, L.J.A., Klunder, M.B., Middag, R., Laan, P., Timmermans, K.R. and de Baar, H.J.W., 2010. Speciation of Fe in the Eastern North Atlantic Ocean. Deep Sea Research Part I: Oceanographic Research Papers, 57(11): 1444-1453.

Timmermans, K.R., Van Der Wagt, B., Veldhuis, M.J.W., Maatman, A. and De Baar, H.J.W., 2005. Physiological responses of three species of marine pico-phytoplankton to ammonium, phosphate, iron and light limitation. Journal of Sea Research, 53(1-2 SPEC. ISS.): 109-120.

Tomczak, M. and Godfrey, J., 2003. Regional oceanography: An introduction. Daya Publishing House, Daya, New Delhi, xi+390p pp.

Topp, R. and Johnson, M., 1997. Winter intensification and water mass evolution from yearlong current meters in the Northeast Water Polynya. Journal of Marine Systems, 10(1): 157-173.

Tsilinsky, V.S. and Finenko, Z.Z.J.R.J.o.M.B., 2018. The Spatial Variability of the Fluorescent Characteristics of Phytoplankton in the Black Sea. 44(1): 1-7.

Turner, D.R. and Hunter, K.A., 2001. The biogeochemistry of iron in seawater, 6. Wiley Chichester, UK.

Turner, J., Maksym, T., Phillips, T., Marshall, G.J. and Meredith, M.P., 2013. The impact of changes in sea ice advance on the large winter warming on the western Antarctic Peninsula. International Journal of Climatology, 33(4): 852-861.

Turner, J., Marshall, G.J., Clem, K., Colwell, S., Phillips, T. and Lu, H., 2020. Antarctic temperature variability and change from station data. International Journal of Climatology, 40(6): 2986-3007.

Turoczy, N.J. and Sherwood, J.E., 1997. Modification of the van den Berg/Ruzic method for the investigation of complexation parameters of natural waters. Analytica Chimica Acta, 354(1-3): 15-21.

Twining, B.S., Baines, S.B. and Fisher, N.S., 2004. Element stoichiometries of individual plankton cells collected during the Southern Ocean Iron Experiment (SOFeX). Limnology and Oceanography, 49(6): 2115-2128.

van den Berg, C.M.G., 1982. Determination of copper complexation with natural organic ligands in seawater by equilibration with MnO2 I. Theory. Marine Chemistry, 11(4): 307-322.

van den Berg, C.M.G., 1995. Evidence for organic complexation of iron in seawater. Marine Chemistry, 50(1): 139-157.

van den Berg, C.M.G., 2006. Chemical speciation of iron in seawater by cathodic stripping voltammetry with dihydroxynaphthalene. Analytical Chemistry, 78(1): 156-163.

van den Berg, C.M.G., Nimmo, M., Daly, P. and Turner, D.R., 1990. Effects of the detection window on the determination of organic copper speciation in estuarine waters. Analytica Chimica Acta, 232: 149-159.

Velasquez, I., Nunn, B.L., Ibisanmi, E., Goodlett, D.R., Hunter, K.A. and Sander, S.G., 2011. Detection of hydroxamate siderophores in coastal and Sub-Antarctic waters off the South Eastern Coast of New Zealand. Marine Chemistry, 126(1-4): 97-107.

Velasquez, I.B., Ibisanmi, E., Maas, E.W., Boyd, P.W., Nodder, S. and Sander, S.G., 2016. Ferrioxamine siderophores detected amongst iron binding ligands produced during the remineralization of marine particles. Frontiers in Marine Science, 3: 172.

Viljoen, J.J., Philibert, R., Van Horsten, N., Mtshali, T., Roychoudhury, A.N., Thomalla, S. and Fietz, S., 2018. Phytoplankton response in growth, photophysiology and community structure to iron and light in the Polar Frontal Zone and Antarctic waters. Deep Sea Research Part I: Oceanographic Research Papers, 141: 118-129.

Völker, C. and Tagliabue, A., 2015. Modeling organic iron-binding ligands in a three-dimensional biogeochemical ocean model. Marine Chemistry, 173: 67-77.

Vraspir, J.M. and Butler, A., 2009. Chemistry of marine ligands and siderophores. Annual Review of Marine Science, 1: 43-63.

Wagener, T., Pulido-Villena, E. and Guieu, C., 2008. Dust iron dissolution in seawater: Results from a one-year time-series in the Mediterranean Sea. Geophysical Research Letters, 35(16).

Welschmeyer, N.A., 1994. Fluorometric analysis of chlorophyll a in the presence of chlorophyll b and pheopigments. 39(8): 1985-1992.

Whitby, H., Planquette, H., Cassar, N., Bucciarelli, E., Osburn, C.L., Janssen, D.J., Cullen, J.T., González, A.G., Völker, C. and Sarthou, G., 2020. A call for refining the role of humic-like substances in the oceanic iron cycle. Scientific reports, 10(1): 6144-6144.

Wood, A.M., 2005. Measuring growth rates in microalgal cultures. Algal Culture Techniques: 269-285.

Wu, J., Boyle, E., Sunda, W. and Wen, L.-S., 2001. Soluble and Colloidal Iron in the Oligotrophic North Atlantic and North Pacific. Science, 293(5531): 847-849.

Wu, M., McCain, J.S.P., Rowland, E., Middag, R., Sandgren, M., Allen, A.E. and Bertrand, E.M., 2019. Manganese and iron deficiency in Southern Ocean Phaeocystis antarctica populations revealed through taxon-specific protein indicators. Nature communications, 10(1): 1-10.

Xing, W., Huang, W.-m., Li, D.-h. and Liu, Y.-d., 2007. Effects of Iron on Growth, Pigment Content, Photosystem II Efficiency, and Siderophores Production of Microcystis aeruginosa and Microcystis wesenbergii. Current Microbiology, 55(2): 94-98.

Ye, Y., Völker, C. and Gledhill, M., 2020. Exploring the Iron-Binding Potential of the Ocean Using a Combined pH and DOC Parameterization. Global Biogeochemical Cycles, 34(6): e2019GB006425.

Yokoi, K. and van den Berg, C.M.G., 1992. The determination of iron in seawater using catalytic cathodic stripping voltammetry. Electroanalysis, 4(1): 65-69.

Zeldis, J. and Smith, S., 1999. Water, salt and nutrient budgets for Hauraki Gulf, New Zealand. Smith, SV; Crossland, CJ Australasian Estuarine Systems: Carbon, Nitrogen and Phosphorus Fluxes. LOICZ Reports & Studies(12).

Zeldis, J.R., 2004. New and remineralised nutrient supply and ecosystem metabolism on the northeastern New Zealand continental shelf. Continental Shelf Research, 24(4): 563-581.

Zeldis, J.R., Walters, R.A., Greig, M.J.N. and Image, K., 2004. Circulation over the northeastern New Zealand continental slope, shelf and adjacent Hauraki Gulf, during spring and summer. Continental Shelf Research, 24(4): 543-561.

Zeldis, J.R. and Willis, K.J., 2015. Biogeographic and trophic drivers of mesozooplankton distribution on the northeast continental shelf and in Hauraki Gulf, New Zealand. New Zealand Journal of Marine and Freshwater Research, 49(1): 69-86.

Zhu, K., Hopwood, M.J., Groenenberg, J.E., Engel, A., Achterberg, E.P. and Gledhill, M., 2021. Influence of pH and Dissolved Organic Matter on Iron Speciation and Apparent Iron Solubility in the Peruvian Shelf and Slope Region. Environmental Science & Technology, 55(13): 9372-9383.

Zigah, P.K., McNichol, A.P., Xu, L., Johnson, C., Santinelli, C., Karl, D.M. and Repeta, D.J., 2017. Allochthonous sources and dynamic cycling of ocean dissolved organic carbon revealed by carbon isotopes. Geophysical Research Letters, 44(5): 2407-2415.

Zitoun, R., 2019. Copper speciation in different marine ecosystems around New Zealand, University of Otago, Dunedin.


BIOGRAPHY

About the author

Indah Ardiningsih was born in Pasuruan, East Java, Indonesia. She was raised in a village surrounded by paddy and sugarcane fields. The village is a little further from the ocean, although the whole country is surrounded by the sea. One day in her youth, she watched a documentary movie on how trace amount of organic mercury (Hg) from fish has a lethal effect on the human and animal nerve systems. This documentary movie motivated her to study chemical speciation for her bachelor's degree at the University of Brawijaya, Indonesia. Her final BSc project focused on the development of a quick method to detect different chromium species in rivers and estuary, where she experienced a great adventure floating on the boat to take water samples. Her passion for studying trace metal led her to join the research team on the monitoring of trace metal levels in an artificial lake in the industrial area in Mokpo, South Korea. She joined the International Environmental Research Center, United Nation University – Gwangju Institute of Science and Technology, as an intern student. After the internship, she continued to join the team on the monitoring project in the Mekong River in Vietnam, where finally she studied Hg speciation. Following this project, she had the opportunity to pursue a master's study in the same university, where she investigated Hg speciation in the Hydrothermal vent field. The more she dives into the metal speciation world, the more she realizes how little she knows; she decided to dive

deeper into the metal speciation world. In 2016, she started her Ph.D. at the Department of Chemistry, University of Otago, New Zealand, under the supervision of Rob Middag and Sylvia Sander. Her research focused on the organic speciation of Fe in seawater, with the study area on the Antarctic and sub-antarctic regions. Following the transfer of both supervisors to Europe, she continued her Ph.D. study at Royal Netherland Institute for Sea Research (NIOZ) in 2017. She carried on her PhD project on Fe speciation in seawater under supervision of Rob Middag and Loes Gerringa.

List of publications

- Ardiningsih, I., Krisch, S., Lodeiro, P., Reichart, G.-J., Achterberg, E.P., Gledhill, M., Middag, R. and Gerringa, L.J.A., 2020. Natural Fe-binding organic ligands in Fram Strait and over the northeast Greenland shelf. Marine Chemistry, 224: 103815.
- Ardiningsih, I., Zhu, K., Lodeiro, P., Gledhill, M., Reichart, G.-J., Achterberg, E.P., Middag, R. and Gerringa, L.J.A., 2021. Iron Speciation in Fram Strait and Over the Northeast Greenland Shelf: An Inter-Comparison Study of Voltammetric Methods. Frontiers in Marine Science, 7(1203).
- Ardiningsih, K. Seyitmuhammedov, S. G. Sander, C. H. Stirling, G.J. Reichart, K. R. Arrigo, L. J. A. Gerringa, and R. Middag. In review.“Sources of Fe-binding organic ligands in surface waters of the western Antarctic Peninsula”. In press, Biogeosciences
- Krisch, S., Hopwood, M.J., Schaffer, J., Al-Hashem, A., Höfer, J., Rutgers van der Loeff, M.M., Conway, T.M., Summers, B.A., Lodeiro, P., Ardiningsih, I., Steffens, T. and Achterberg, E.P., 2021. The 79°N Glacier cavity modulates subglacial iron export to the NE Greenland Shelf. Nature Communications, 12(1): 3030.
- Gerringa, L. J. A., Gledhill, M., Ardiningsih, I., Muntjewerf N., Laglera L. M. “Comparing CLE-AdCSV applications using SA and TAC to determine the Fe binding characteristics of model ligands in seawater”. In review, Biogeosciences

ACKNOWLEDGEMENTS

I would like to express my sincere gratitude to my supervisors, Loes Gerringa and Rob Middag, who supervised me to the completion of this work with patience. This work would not have been possible without their motivation, guidance, and technical expertise. I thank Loes for her kindness, and endless support during my stay in the Netherlands, not only for the scientific works. Thank you for the simple, yet delicious food recipe, too. Thank you for everything that I can't mention one by one. I am also very grateful to Rob, who offered me the great opportunity to start my PhD in New Zealand. This opportunity has opened many doors to the more adventurous and priceless experiences from the southern hemisphere to the northern hemisphere. I recall the joke during one of our online meetings, "you guys are not born with functional brain, you train your brain". Uyeah, I am glad and proud to have you as one of my brain trainers, Rob!

My PhD transfer from New Zealand to the Netherlands would not have been smooth without the help of my promotor, Gert-Jan Reichart, thank you. I greatly thank Sylvia Sander who first introduced me to the field of voltammetry and iron speciation. I am very grateful for having Claudine Stirling as my primary supervisor before my PhD transfer to the Netherlands.

I would like to thank the reading committee. Anita Buma, Hannah Whitby, Karline Soetaert, Luis Laglera, Jack Middelburg, thank you for reading our work. I am also grateful from the help from Martha, Eric, Kechen, Stephan, Mark, Pablo, thank you for your positive feedbacks and support.

I really appreciated the help of trace metal team, Patrick Laan and Bas van der Wagt, and all OCS members for creating the good atmosphere in our department. Jan-Berend, Geert-Jan, Furu; also, Rick and Peter, you guys indirectly helped me to find my office in the first few weeks at NIOZ since meeting you were a good sign that I was on the right floor and corridor in the building. Thank you to my officemates, Niels and Laurent; Laura Korte, and Femke - my office neighbor, thank you for your companionship and nice chat during teatime. Karel, Sharyn and Jan – thank you to keep our office corridor alive; Sharyn, I could not have wish

for a better cabinmate, you are the best! I am also very thankful to Hans van Haren, I enjoyed your insightful knowledge on – every single topic we come to discuss whether it relates to science or not. I would also like to thank, Meta, Daniella, Claudia – a small talk before or after trip to freezer somehow filled my NIOZ memories. Peter-Roy, thank you to let me put some frozen samples in the small freezer, on the corner.

To all OCS PhD, thank you for all of your companionship. Thank you to Hans, Ulrike, Evelyne, Sofia, Esme, Sabine, Linda, Siham, Ros, Coral, Kristin, Nora, Elodie, Laura, Szabine, Louise. I won't forget the good time I spent with all of you. To my favorite allies, the trace metal boys :))), Mathijs van Manen and Hung-an 'Stanley' Tian, who helped me from the day-1 of my PhD journey at NIOZ. Thank you for everything! I want to send my gratitude to the other members of FePhyrusII, Erin Bertrand, Charlotte Eich and Corrina Brussarrd, Sven Pont and Sven Ober. I give many thanks to my Potvis friends, especially Rachel and Kim, who have made my last few days at Potvis joyful, you two are the witness that I had 'full Potvis experience'.

My colleagues in New Zealand, I am forever grateful to have the opportunity to know them and to be part of the Waterworld research group. Thank you to Evelyn Armstrong, Malcolm Reid, Judith Murdoch, Abida Mahmood, Shopie Gangl, Matt Druce, Geraldus Listiono, Ejin George. Also, thank you to Rebecca Zitoun, who helped me with voltammetry when I was a new come in the voltammetry world. I am happy to be your colleagues once again at NIOZ.

I also acknowledge, Charlotte Middag and Taran Jenkins, for helping me during my maternity period in the Netherlands. To my Indonesian friends in Dunedin (New Zealand) and the Netherlands; yes, all of you! Thank you! Mba Dewi, thanks for all the 'javanese' humor :))).

Finally, I thank to family, for giving me energy to finish this thesis. Umik, who left the world before I could show her how cute the penguin and polar bear I drew. Aurum and her daddy, thanks to bear with me ☺.

The end is just the beginning –

T.S. Eliot